



Development of New Oligofluorene- functionalised Truxene Analogues

Submitted by

Neil Thomson

2013

A thesis submitted to the Department of Pure and Applied Chemistry,
University of Strathclyde, Glasgow, in fulfilment of the regulations for
the Degree of Doctor of Philosophy.

This thesis is the result of the author's original research. It has been composed by the author and has not been previously submitted for examination which has led to the award of a degree.

The copyright of this thesis belongs to the author under the terms of the United Kingdom Copyright Acts as qualified by University of Strathclyde Regulation 3.50. Due acknowledgement must always be made of the use of any material contained in, or derived from, this thesis.

Signed:

Date:

Acknowledgements

First and foremost I would like to thank Professor Peter Skabara for the fantastic opportunity to conduct my PhD within his research group, as well as his support and guidance over the past 3 years.

I would also like to thank Dr Alexander Kanibolotsky and Dr Neil Findlay for their guidance and help within the lab and also the production of this thesis. The Skabara group has been an enjoyable place to work over the past 3 years and that is thanks to the past and present members of the group. I would like to thank Joe Cameron in particular for running the DFT calculations presented in chapter 2.

I would like to acknowledge the help that Craig Irvine, Patricia Keating and Denise Gilmore have given me in the areas of NMR, Mass Spectroscopy and Elemental Analysis respectively.

My PhD project could not have taken place without the support of my industrial sponsors, Cambridge Display Technology, who provided both funding and guidance over the course of my degree, especially Dr Jeremy Burroughes, Dr Richard Wilson and Dr Natasha Conway for providing me with excellent advice and feedback.

I am very lucky to have such a supportive group of friends and family who have been excited for me when my studies were going well, and provided me with encouragement when I felt I was struggling with tougher hurdles. In particular I would like to thank my fellow chemists Kevin and Paul. You both were always keen to hear how my experiments were progressing and help me troubleshoot some of the trickier problems I encountered, as long as it didn't distract us from whatever sport we were watching at the time of course.

Finally I would like to thank my wife, Heather, for her patience and support. You have happily listened to me ramble about the highs and lows during my PhD and been there to provide either a gentle prod or a forceful kick to help me keep the reactions going and the writing flowing. Thank you.

Abbreviations

2D	two dimensional
3D	three dimensional
a.u.	arbitrary units
Ac	acetyl
ASE	amplified spontaneous emission
BLA	bond length alternation
BHJ	bulk hetero-junction
BODIPY	boron-dipyrromethene
Bu	butyl
calcd	calculated
cm	centimetre
CT	charge transfer
CV	cyclic voltammetry
d	doublet
dd	doublet of doublets
DDQ	dichlorodicyanoquinone
DFB	distributed feedback
DFT	density functional theory
DME	dimethoxyethane
DMF	dimethylformamide
DMSO	dimethyl sulfoxide
E_g	band gap
EL	electroluminescent
eq	equivalents
Et	ethyl
ETL	electron transport layer
eV	electronvolt
Fc	ferrocene
Fc ⁺	ferrocenium
g	gram

h	hours
Hex	hexyl
HOMO	highest occupied molecular orbital
HTL	hole transport layer
Hz	hertz
kW	killowatt
l	litre
LDA	lithium diisopropylamide
LUMO	lowest unoccupied molecular orbital
m	multiplet
M	molar
MALDI-TOF	matrix assisted laser desorption ionisation-time of flight
Me	methyl
MeCN	acetonitrile
MHz	megahertz
mg	milligram
mins	minutes
ml	millilitre
mm	millimetre
mmol	millimole
mol	mole
MS	mass spectrometry
mV	millivolts
n-BuLi	n-butyllithium
nm	nanometre
NMR	nuclear magnetic resonance
OFETs	organic field effect transistors
OLED	organic light emitting diodes
OPVs	organic photovoltaics
Ph	phenyl

PCMB	(1-(3-methoxycarbonyl) propyl-1-phenyl[6,6]C ₆₁)
Pd(PPh ₃) ₄	tetrakis(triphenylphosphine) palladium(0)
PEDOT	poly (3,4-ethylenedioxy)thiophene
PLQY	photoluminescence quantum yield
PPV	poly (p-phenylenevinylene)
Pr	propyl
PSS	polystyrene-sulfonate
P3HT	poly(3-hexyl thiophene)
q	quartet
rt	room temperature
s	second/singlet
t	triplet
TBAF	tetrabutyl ammonium fluoride
TEG	triethylene glycol
THF	tetrahydrofuran
TLC	thin layer chromatography
Ts	tosyl
UV	ultraviolet
V	volt
vis	visible
vs	versus
W	Watt

Greek

π	pi bonding orbital
α	first position on heterocycle
β	second position on heterocycle
ΔE	difference between energy levels
δ	chemical shift
ϵ	dielectric constant / molar extinction coefficient
λ	wavelength

λ_{max}	maximum absorption wavelength
μ	charge transport mobility
ω	terminal position of heterocycle

Abstract

Interest in conjugated materials continues to increase as various types of new electronic devices based on organic semiconductors have been developed, some of which are now found in the marketplace. Many of these materials are either small molecules or polymers, both of which have their own advantages and drawbacks. Oligomers are macromolecules which can be envisioned as midway between small molecules and polymers, containing the advantages of both. In addition, while polymers are limited to one dimensional conjugated chains, oligomers have the potential to contain conjugated chains spanning over 2 dimensions, which makes their development of keen interest to those conducting research in the field of organic semiconductors.

Chapter 1 details the development of organic semiconducting materials and explores their applications in devices, as well as discussing the development of star-shaped oligomers, and in particular those based around the truxene moiety.

Chapters 2, 3 and 4 then present new oligofluorene-functionalised truxene analogues. Chapter 2 discusses the synthesis and optical and electrochemical properties of perfluorenehexylthiophene end capped oligofluorene-functionalised truxenes. The importance of the position of the perfluorohexyl chain on the thiophene was investigated by the synthesis of structural isomers and comparing the optical and electrochemical properties, demonstrating that the steric effects of the chain alter the degree of planarity within the molecules. In Chapter 3, attempts to synthesise oligofluorenes substituted with triethylene glycol (TEG) chains are discussed, as well as the synthesis of **T1POLAR**, an analogue of the parent **T1** molecule where the fluorene moieties are substituted with TEG chains. The optical and electrochemical properties of **T1POLAR** are also presented. Attempts to introduce primary alkyl

amines at the terminal position of oligofluorene functionalised truxenes are then presented in Chapter 4.

Contained within chapter 5 are the procedures for synthesis of compounds presented in chapters 2, 3 and 4.

Contents

1	Introduction.....	1
1.1	Band Theory	2
1.2	Organic Semiconductors	3
1.3	Applications of organic semiconductors	8
	a) Organic Field Effect Transistors.....	9
	b) Organic Photovoltaics.....	12
	c) Organic Light Emitting Diodes	16
	d) Organic Lasers.....	30
1.4	Fabrication Techniques.....	33
1.5	Fluorenes	36
1.6	Star-Shaped Oligomers	41
1.7	Truxene.....	47
2	Perfluorohexylthiophene end capped oligofluorene - functionalised truxenes.....	56
2.1	Introduction.....	57
2.2	Synthesis.....	58
2.3	Results and Discussion	68
2.4	Conclusions and Future Work	76
3	Tri(ethylene glycol) substituted oligofluorene-functionalised truxenes	79
3.1	Introduction.....	80
3.2	Synthesis.....	83
3.3	Results and Discussion	94
3.4	Conclusions and Future work.....	100
4	Attempted formation of alkyl amine end capped oligofluorene- functionalised truxenes.....	102
4.1	Introduction.....	103
4.2	Synthesis.....	104
4.3	Results and Discussion	110
4.4	Conclusions and Future Work	111

5 Experimental.....	113
6 References	188

List of Figures

Figure 1.1 Formation of bands as the number of MOs increase.	3
Figure 1.2 Examples of common conjugated polymers.....	4
Figure 1.3 Diagram of effects contributing to band gap.....	4
Figure 1.4 Aromatic (1.1) and quinoidal (1.2) structures of poly(p-phenylene).	5
Figure 1.5 Two resonance structures of poly(isothianaphthalene).....	6
Figure 1.6 Structure of polyacetylene.	6
Figure 1.7 Doping of polyacetylene to form a bipolaron.....	8
Figure 1.8 Diagram of an OFET.....	9
Figure 1.9 Ethynyl-alkyl-silyl-functionalised pentacene.	11
Figure 1.10 Examples of alkyl-group functionalisation of oligothiophene.	11
Figure 1.11 Regioregular poly(alkylthiophene).	12
Figure 1.12 Diagram of an OPV.	12
Figure 1.13 Creation of an excited state in an OPV.	13
Figure 1.14 Bi-phasic and BHJ active layers.....	14
Figure 1.15 (1-(3-Methoxycarbonyl) propyl-1-phenyl[6,6]C61) (PCBM).	15
Figure 1.16 Poly(3-hexylthiophene) (P3HT) and poly(3-hexylselenophene) (P3HS).	15
Figure 1.17 Potential energy diagram of excitation to and relaxation from an excited state.....	17
Figure 1.18 Potential energy diagram showing intersystem crossing and phosphorescence.....	18
Figure 1.19 Structure of poly(1,4-phenylene vinylene).	20
Figure 1.20 Diagram of a sandwich type OLED device.....	20
Figure 1.21 Structures of Rubrene and PEB.	21
Figure 1.22 Structure of PFO-DBT5.	21
Figure 1.23 Structure of (Alq3).....	23

Figure 1.24 2-(4-Biphenyl)-5-(4-tert-butylphenyl)-1,3,4-oxadiazol (butyl PBD).....	24
Figure 1.25 A 1,3,4-oxadiazole-containing dendrimer.....	25
Figure 1.26 poly(phenyl quinoxaline) (PPQ).....	25
Figure 1.27 Energy level diagram of the interfaces in an OLED device.	26
Figure 1.28 Perfluorinated materials used as ECHB layers.....	27
Figure 1.29 (PFON+(CH ₃) ₃ I--PBD), a water soluble polymer.....	27
Figure 1.30 Arylamine based hole transport small molecules.	28
Figure 1.31 Spiro-fluorene based hole transport material.....	29
Figure 1.32 Aryl-amine based hole transport starburst compounds. ...	29
Figure 1.33 Star-shaped hole transport materials.	30
Figure 1.34 Illustration of stimulated emission.	31
Figure 1.35 Light amplification in a laser.	31
Figure 1.36 Diagram of a DFB laser.	33
Figure 1.37 Polar/non-polar and fluoruous/non-fluoruous scales.....	36
Figure 1.38 9H-Fluorene and Fluorenone.....	37
Figure 1.39 Homopolymers of alkylated fluorene.....	38
Figure 1.40 Oligo(fluorenes) with branched alkyl chains.	39
Figure 1.41 Structure of poly(alkylidene fluorenes).	40
Figure 1.42 Poly(fluorene-co-pentacenes).	41
Figure 1.43 Geometry of Boron and Carbon.	42
Figure 1.44 Possible functionalisation of benzene to afford 2D cores... 43	
Figure 1.45 Functionalisation of thiophene and triazine to afford 2D cores.	43
Figure 1.46 Divergent approach.	43
Figure 1.47 Incomplete reaction in the divergent approach.	44
Figure 1.48 Convergent approach.	45
Figure 1.49 Incomplete reaction in the convergent approach.	45
Figure 1.50 Labelled truxene.....	47
Figure 1.51 Substituted and functionalised truxene.....	48

Figure 1.52 Oligo(thiophene)-functionalised truxenes.	48
Figure 1.53 syn-Trialkyl truxene.	49
Figure 1.54 Oligo(phenylene)-functionalised truxenes.	49
Figure 1.55 Substituted BODIPY arms.	51
Figure 1.56 Bridged truxenes.	52
Figure 1.57 Phenyl-truxene dendrimer.	53
Figure 1.58 Tr-TPA3 and Tr-TPA9 HTL materials.	54
Figure 1.59 Hexaphenylamine-functionalised truxene 1.52	54
Figure 2.1 Normalised absorbance of TX-YFTh materials in solution (CH ₂ Cl ₂ , 1 x10 ⁻⁶ M).	68
Figure 2.2 Normalised emission of TX-YFTh materials materials in solution (CH ₂ Cl ₂ , 5 x10 ⁻⁷ M).	70
Figure 2.3 Plot of absorbance vs integral of emission.	71
Figure 2.4 Oxidation (left) and reduction (right) waves from cyclic voltammetry of T1-3FTh in dichloromethane, electrolyte 0.1 M Bu ₄ NPF ₆ , glassy carbon electrode, scan rate 100 mVs ⁻¹	72
Figure 2.5 Oxidation (left) and reduction (right) waves from cyclic voltammetry of T1-4FTh in tetrahydrofuran, electrolyte 0.1 M Bu ₄ NPF ₆ , glassy carbon electrode, scan rate 100 mVs ⁻¹	72
Figure 2.6 Oxidation (left) and reduction (right) waves from cyclic voltammetry of T4-4FTh in 1:1 acetonitrile/benzene, electrolyte 0.1 M Bu ₄ NPF ₆ , glassy carbon electrode, scan rate 100 mVs ⁻¹	73
Figure 2.7 HOMO-1 (bottom, left), HOMO (bottom, right), LUMO (top, left) and LUMO+1 (top, right) of T1-3FTh . Coloured regions indicate the different phases within the molecular orbitals.	74
Figure 2.8 HOMO-1 (bottom, left), HOMO (bottom, right), LUMO (top, left) and LUMO+1 (top, right) of T1-4FTh . Coloured regions indicate the different phases within the molecular orbitals.	75
Figure 3.1 Examples of covalent polar fluorenes.	80
Figure 3.2 Fluorene with ionic side chains with varying counterions. .	81
Figure 3.3 Structure of SPF _x ^{TEG}	82

Figure 3.4 Interaction of TEG chains within the lithium intermediate.	95
Figure 3.5 Interaction of TEG chains with palladium.	95
Figure 3.6 Catalytic cycle of Suzuki-Miyaura coupling.....	96
Figure 3.7 Absorption spectrum of T1POLAR materials in solution (CH ₂ Cl ₂ , 1 x10 ⁻⁶ M).....	97
Figure 3.8 Emission spectrum of T1POLAR materials in solution (CH ₂ Cl ₂ , 5 x10 ⁻⁷ M).....	98
Figure 3.9 Oxidation (left) and reduction (right) waves from cyclic voltammetry of T1POLAR in dichloromethane, electrolyte 0.1 M Bu ₄ NPF ₆ , glassy carbon working electrode, scan rate 100 mVs ⁻¹	99
Figure 4.1 Structure of T3 and T4	103
Figure 4.2 Structure of poly(allyl amine).....	104
Figure 4.3 Catalytic cycle of Buchwald-Hartwig amination.	110

List of Schemes

Scheme 1.1 Reversible functionalisation of pentacene.....	10
Scheme 1.2 Suzuki-Miyaura and Kumada reaction routes to oligofluorenes.	37
Scheme 1.3 Yamamoto reaction route to polyfluorene.	38
Scheme 1.4 Phenyl core synthesis from ketone.	46
Scheme 1.5 Phenyl core synthesis from Diels alder reactions.	46
Scheme 1.6 Synthesis of spirofluorene-substituted truxene 1.49	50
Scheme 2.1 Synthesis and functionalization of truxene core.....	59
Scheme 2.2 Functionalization of fluorene.....	59
Scheme 2.3 Synthesis of oligofluorene arms.....	60
Scheme 2.4 Coupling of oligofluorene arms to truxene core.	61
Scheme 2.5 Preparation of compound 2.14	62
Scheme 2.6 Attempted coupling of perfluorohexyl thiophene to T2Br . 62	
Scheme 2.7 Synthesis of thiophene-fluorene arm for 3-isomer.....	63
Scheme 2.8 Synthesis of thiophene-fluorene arm for 4-isomer.....	65

Scheme 2.9 Coupling of arms to truxene core.....	66
Scheme 2.10 Synthesis of T4-4FTh	67
Scheme 2.11 Semi-pefluoroalkylation of fluorene.	77
Scheme 2.12 Functionalisation of semiperfluoroalkyl-fluorene.....	78
Scheme 2.13 Coupling of semiperfluoroalkyl-fluorene.	78
Scheme 3.1 Preparation of TEGOTs, 3.6	83
Scheme 3.2 Unsuccessful alkylation of fluorene with TEG chains.	83
Scheme 3.3 Successful alkylation of fluorene with TEG chains.	84
Scheme 3.4 Alkylation of 2,7-dibromofluorene with TEG chains.	84
Scheme 3.5 Unsuccessful alkylation of truxene with TEG chains.....	85
Scheme 3.6 Preparation of 3.11	86
Scheme 3.7 Investigation of side products formed during the preparation of 3.14	86
Scheme 3.8 Attempted synthesis of 3.15 <i>via</i> Li-halogen exchange of 3.13	87
Scheme 3.9 Synthesis of compound 3.14	88
Scheme 3.10 Suzuki-Miyaura cross-coupling of 3.14 with 3.8	88
Scheme 3.11 General conditions for attempted preparation of bifluorene 3.17	88
Scheme 3.12 Iodination of diTEG-fluorene.	90
Scheme 3.13 Attempted coupling of 3.14 with 3.19	91
Scheme 3.14 Successful preparation of bifluorene 3.20	91
Scheme 3.15 Attempted synthesis of 3.17 by Kumada coupling.....	92
Scheme 3.16 Preparation of T1POLAR	93
Scheme 3.17 Unsuccessful preparation of T2POLAR	94
Scheme 3.18 Proposed further reactions to explain poor yields of TEG alkylated fluorenes.	101
Scheme 4.1 Initially proposed synthesis of T3N	105
Scheme 4.2 Synthesis of compound 4.9	107
Scheme 4.3 Attempted coupling of 4.9 with T3Br	108
Scheme 4.4 Attempted synthesis of compound 4.12	109

Scheme 4.5 Attempted synthesis of compound 4.13	110
Scheme 4.6 Proposed formylation of T3	112

List of Tables

Table 2.1 Absorbance Data for TX-^yFTh and TX materials.....	69
Table 2.2 Emission Data for TX-^yFTh and TX materials.....	70
Table 2.3 Electrochemical Data for TX-^yFTh and TX	73
Table 3.1 Conditions for Scheme 3.11.....	89
Table 3.2 Optical Data for T1_{POLAR}	98
Table 3.3 Electrochemical data for T1_{POLAR}	99

1 Introduction

1.1 Band Theory

Conductivity is determined by the electronic structure of a material.¹ In a single atom the electrons are divided into atomic orbitals depending on their energies. In molecules the molecular orbitals (MOs) are formed by the linear combination of atomic orbitals (LCAO). The MO of highest energy which is filled by two electrons is known as the highest occupied molecular orbital (HOMO), and the orbital of lowest energy which is unoccupied is known as the lowest unoccupied molecular orbital (LUMO). The energy difference between the HOMO and LUMO levels is known as the HOMO-LUMO gap (E_g), and is defined as the energy required to promote one electron from the HOMO to the LUMO.¹ In the solid state molecules become closely aligned and molecular orbitals begin to overlap.¹ As the number of molecules present increases, the molecular orbitals become more densely packed, with the energy between each MO becoming significantly less, eventually forming a band. The band of occupied orbitals is known as the valence band, and the conduction band is made up of unoccupied orbitals (Figure 1.1). The distance between the top of the valence and bottom of the conduction band is known as the band gap. The smaller the band gap, the less energy is required to promote an electron into the conduction band, and hence, the greater the ability to act as a conductor.¹

In materials where the band gap is very large, electrons are not promoted to the conduction band and the materials act as insulators.¹ In materials where the band gap is small electrons are readily promoted to the conduction band, which results in an unpaired electron in the conduction band. The 'hole' that is left behind is available for another electron to move into, which itself leaves behind a hole. The electron and the electron hole are free to move throughout the material, and the material acts as a semiconductor. Both the movement of electrons and holes contribute to the conductivity of materials.¹

Semiconductors are materials that can be conductors or insulators. Unlike conductors, the band gap is not small enough for electrons to be readily promoted to the conduction band for the material to be conductive. However, since the band gap is significantly smaller than that of an insulator, an increase in energy, for example by the absorption of a photon, leads to a sufficient promotion of electrons into the conduction band to allow the material to become a conductor.

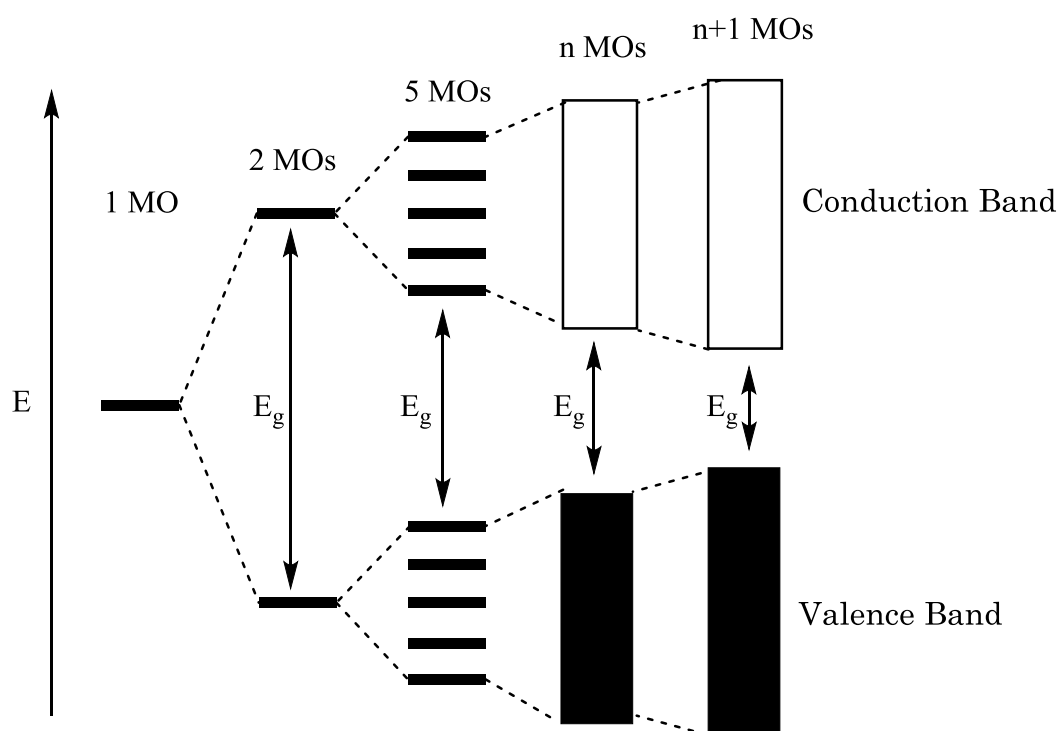


Figure 1.1 Formation of bands as the number of MOs increase.

1.2 Organic Semiconductors

Conjugated small molecules, oligomers and polymers have also been shown to yield semiconductor properties.² These are compounds that have alternating C-C single and multiple (double and/or triple) bonds, which in the case of oligomers and polymers, extends along the repeating unit backbone. Electrons in adjacent p-orbitals overlap and are said to be

delocalised, and since polymers are made up of many repeating units, the electrons are assumed to be delocalised over the entire backbone chain.

The simplest polymer case is poly(acetylene), which is also the exception as, other than substituted acetylene repeat units, all other polymers accomplish the conjugation through the backbone by incorporating conjugated carbocyclic and heterocyclic compounds. Some common examples include poly(thiophene), poly(fluorene) and poly(phenylene vinylene) (Figure 1.2).

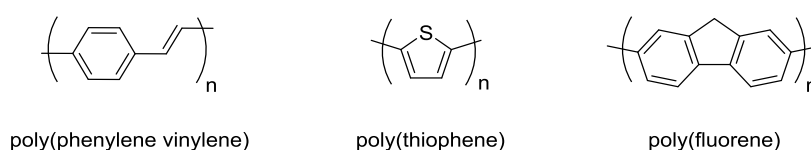


Figure 1.2 Examples of common conjugated polymers.

The semiconducting nature of these conjugated materials lies in the different electronic and structural states that can occur and the different energies attributed to these states. The difference in energy between states gives rise to a band gap for the material, and the factors that determine the energy states are shown in Figure 1.3. The band gap can then be considered to be the sum of these factors (equation 1).³

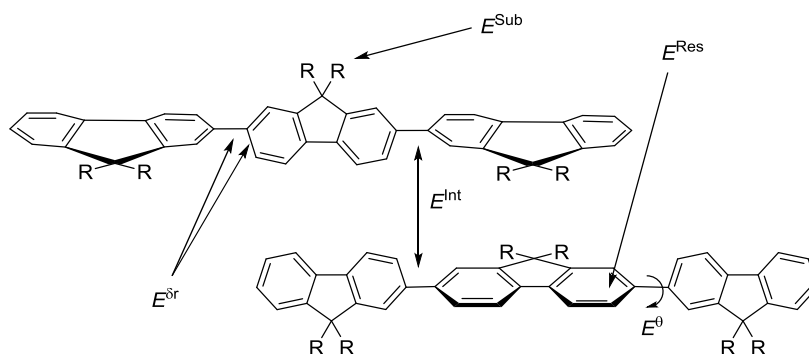


Figure 1.3 Diagram of effects contributing to band gap.

$$E_g = E^{\delta r} + E^{\theta} + E^{\text{Res}} + E^{\text{Sub}} + E^{\text{Int}}$$

Equation 1

- a) $E^{\delta r}$ - the effect of bond length alternation (BLA). The BLA can be decreased by contribution to the electronic structure from quinoid resonance form, which will lead to a decrease in the band gap (Figure 1.4).

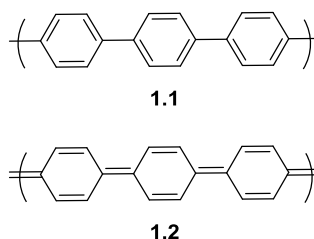


Figure 1.4 Aromatic (1.1) and quinoidal (1.2) structures of poly(p-phenylene).

By fixing the geometry of neutral poly(p-phenylene) to one of undoped (aromatic, main contribution to 1.1) and 50 % n-doped (quinoid, main contribution to 1.2) it has been shown through computational studies that the HOMO-LUMO gap is smaller for the quinoid form.⁴

- b) E^{θ} - the dihedral angle between repeating units. Due to the requirement of p-orbital overlap for conjugation, increasing the angle between repeat units lessens the p-orbital overlap, breaking the effective conjugation length and widening the HOMO-LUMO gap.
- c) E^{Res} - resonance effects from within the monomer units. This can be explained using poly(isothianaphthalene) as an example (Figure 1.5).⁵

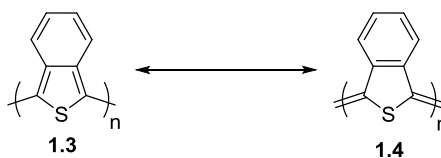


Figure 1.5 Two resonance structures of poly(isothianaphthalene).

Here the stabilisation effect of aromaticity in the thiophene unit in structure **1.3** is in competition from the stabilisation effect of aromaticity in the benzene unit in structure **1.4**. Since the stabilisation energy of benzene is greater than that of thiophene, the band gap of poly(isothianaphthalene) is narrower than that of polythiophene.⁵

- d) E^{Sub} - substituent effects. Electronic effects from substituents on the cyclic unit can alter the electron density across the backbone, altering the band gap.
- e) E^{nt} - effects of interchain interactions. The way molecules pack into a condensed state can allow for π - π interactions, which can affect the HOMO-LUMO gap.

The band gaps of conjugated polymers are similar to those of inorganic semiconductors, and so, like for other semiconductors, assistance is required for the polymer to conduct. This is generally achieved by doping the material.⁵ In 1977, Hideki Shirakawa, Alan MacDiarmid and Alan Heeger published a paper on the conductivity of a doped thin film of poly(acetylene).⁶

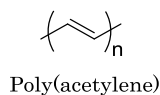


Figure 1.6 Structure of polyacetylene.

This report has led to numerous other publications of doped conjugated small molecules and polymers, forming the basis for the field of organic

electronics which has grown substantially in the past few decades. In 2000, for both their original and continual contribution to this field, Shirakawa, MacDiarmid and Heeger were awarded the Nobel Prize in Chemistry.

In inorganic semiconductors, doping is generally done by the introduction of another semiconductor impurity.¹ For example, the doping of a pure sample of silicon, a group 14 element with 4 valence electrons, with a group 15 element with 5 valence electrons, such as phosphorus, leads to extra valence electrons, which are easily promoted into the conduction band. The material is said to be n-doped and extra unpaired electrons will be able to move into other empty orbitals in the conduction band, thus enabling a 'flow' of electrons through the material. If, on the other hand, a group 13 element such as aluminium, which has 3 valence electrons, was used to dope silicon, a 'hole' would appear in the valence band, which other electrons would be free to move into, themselves leaving behind a hole. This is known as p-doping and would again lead to a 'flow' of electrons through the material and as such lead to electrical conduction.

The 'doping' of organic materials is done in a different way. By reduction or oxidation, either chemically or electrochemically, an electron can be either injected or removed from the material, leading to *n*- or *p*-doping.⁴

In the case of poly(acetylene) (Figure 1.7), two electrons can be removed from the polymer (**1.5a**) to afford two radical cations (polarons) (**1.5b**).⁷ The radicals annihilate to leave two cations (**1.5c**), which are also known as a bipolarons.

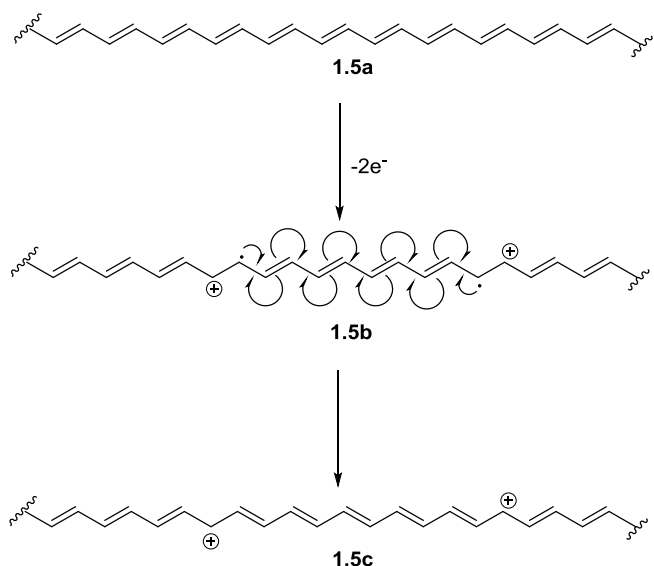


Figure 1.7 Doping of polyacetylene to form a bipolaron.

These charges are now free to move along the polymer chain, and so the polymer becomes conducting.⁷

1.3 Applications of organic semiconductors

From the perspective of device fabrication, there are many potential advantages that organic semiconductors have over inorganic semiconductors. Conjugated organic materials, including small molecules, oligomers and polymers, tend to have high solubility in many common organic solvents, allowing for a range of fabrication methods such as inkjet printing,⁸ spincoating,⁹ and nanolithography.¹⁰ These materials are often made from low cost starting compounds and are readily reproducible. In the solid state (and in films), the materials are often flexible, which opens up new applications for devices. Currently, the main disadvantage is the poorer performance of devices made from organic materials in comparison to inorganic based devices. The main applications for conjugated organic materials includes:

- a) Organic Field Effect Transistors (OFETs)

- b) Organic Photovoltaics (OPVs)
- c) Organic Light Emitting Diodes (OLEDs)
- d) Organic Lasers

a) Organic Field Effect Transistors

Field Effect Transistors are often used as switches and amplifiers in electronic equipment. A diagram of the cross section of a simple OFET is shown below (Figure 1.8).

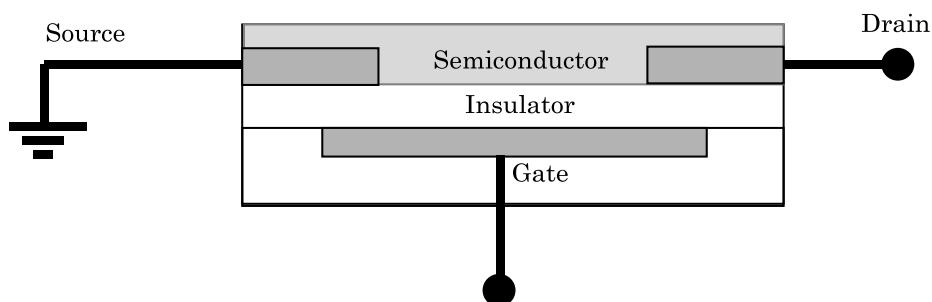
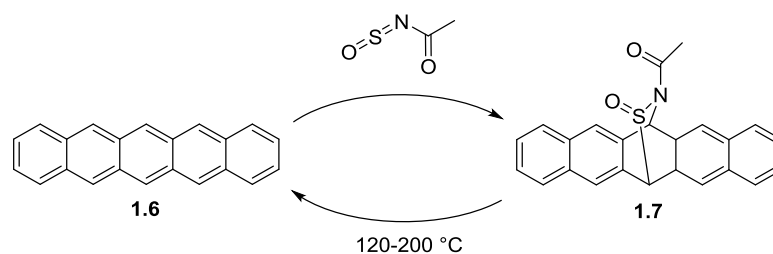


Figure 1.8 Diagram of an OFET.

A semiconducting material, which in the case of OFETs would be a conductive organic small molecule or polymer, is applied on top of a dielectric, between two electrodes. The dielectric itself is applied atop a gate electrode.¹¹ When no potential difference is applied to the gate electrode no current is observed across the OFET, which is said to be in an 'off' state. If there is a potential difference applied to the gate electrode (positive for n-type or negative for p-type semiconductors), this will create an electric field across the dielectric, altering the conductive ability of the semiconductor by causing charges to accumulate at the semiconductor/dielectric interface.¹² This can be envisioned as altering the resistance of the semiconductor, thus affecting the source-drain current. Since the voltage of the gate electrode can be controlled, this gives the ability to finely tune the drain current of the transistor. While there has been relatively less development of n-type organic

semiconductors, there is a wealth of publications on p-type semiconductors including those based on acene and thiophene materials.¹³⁻¹⁶

High charge-carrier mobility is the most desirable property for organic materials for applications in OFETs, which can be enhanced by more efficient π - π stacking between molecules in the bulk material. Therefore small molecules have been widely applied in OFETs, such as pentacene, **1.6**, which has exhibited a charge-carrier mobility of $5 \text{ cm}^2\text{V}^{-1}\text{s}^{-1}$ as a polycrystalline material.¹⁴ Due to its poor solubility the fabrication of a thin film must be done by vacuum deposition. However, Afzali *et al.* from IBM were able to functionalise pentacene with a *N*-sulfinylacetamide in a Diels-Alder reaction, greatly increasing its solubility, allowing a thin film to be cast by solution processing (Scheme 1.1).¹⁷ By exposing the compound to elevated temperatures the elimination by a retro-Diels-Alder reaction afforded the pentacene thin film, albeit with a poorer charge-carrier mobility of $0.89 \text{ cm}^2\text{V}^{-1}\text{s}^{-1}$.



Scheme 1.1 Reversible functionalisation of pentacene.

Direct introduction of solubilising, flexible alkyl side chains can perturb the π - π stacking of the pentacene units in a film, which would result in a negative effect on the charge-carrier mobility of the bulk material. However, by using inflexible spacer groups such as ethynyl moieties between the pentacene and a range of silyl alkyl chains, an enhanced solubility of the pentacene compounds is obtained while allowing for

optimal π - π interactions, affording mobilities of up to $0.4 \text{ cm}^2\text{V}^{-1}\text{s}^{-1}$.^{15, 18} Recently, by appropriate modification of dielectric surfaces, mobilities of around $1.0 \text{ cm}^2\text{V}^{-1}\text{s}^{-1}$ have been achieved.¹⁹⁻²¹

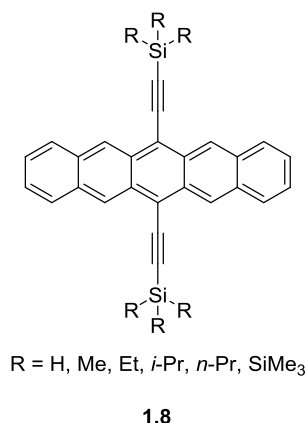


Figure 1.9 Ethynyl-alkyl-silyl-functionalised pentacene.

Oligo- and polythiophenes have also been intensively studied for applications in OFETs. Oligothiophenes are poorly soluble, and so alkyl chains are again required to improve solubility, both to allow synthesis of the oligomers and also for solution processing. This can be achieved by end group (α , ω) or side group (β) functionalisation. Interestingly, end group functionalisation has been shown to improve π - π stacking over that of the unfunctionalised thiophene, with the alkyl chains promoting the face to face assembling of the oligothiophenes.²²

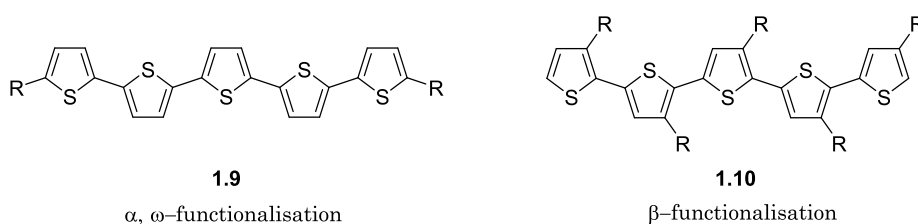


Figure 1.10 Examples of alkyl-group functionalisation of oligothiophene.

The regioregularity of polythiophene is an area of interest due to the fact that head-to-head coupling will result in a large dihedral angle between thiophene units because of the steric hindrance contributed by the alkyl chains. However, it has been demonstrated that regioregular poly(alkylthiophene)s are partially crystalline and form lamellar structures to maximise π - π interactions.²³

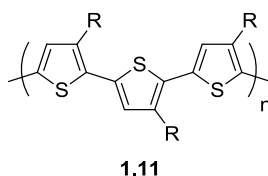


Figure 1.11 Regioregular poly(alkylthiophene).

b) Organic Photovoltaics

Photovoltaic's (PVs), which are popularly known as solar cells, are devices that produce an electric current from energy collected from light incident upon the device, a diagram of which is shown below (Figure 1.12):

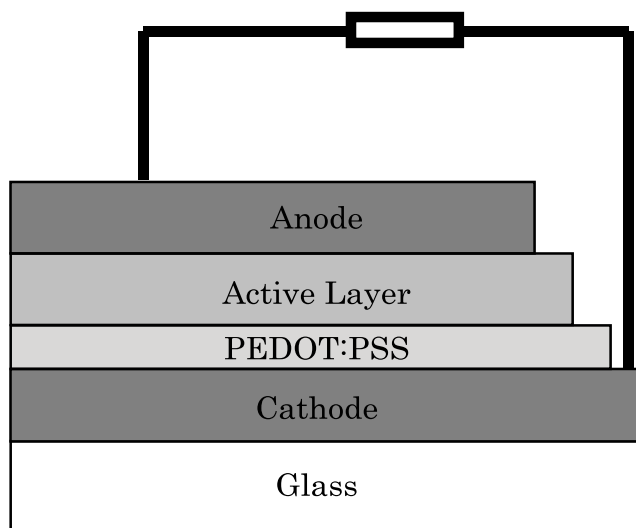


Figure 1.12 Diagram of an OPV.

An active layer is sandwiched between two electrodes, commonly aluminium for the anode and indium tin oxide for the cathode. Indium tin

oxide is often selected due to its transparency. The active layer is a mixture of two materials, one an electron donor and the other an electron acceptor. The device operates when light is incident upon the active layer (hence the need for a transparent electrode).²⁴ Incident light produces an excited state within the donor material, promoting an electron into the conduction band and creating an exciton (Figure 1.13). The exciton can then migrate to the donor-acceptor interface where, due to charge transfer, the excited electron will transfer to the acceptor material. The radical anion now present in the acceptor material, and the radical cation left in the donor material, will move towards the opposing electrodes, affording a current. PEDOT:PSS is often used in OPVs to improve the surface quality of the cathode as well as acting as a hole extraction layer, which increases the efficiency of the device,²⁵ and also improves the thermal annealing of devices.²⁶

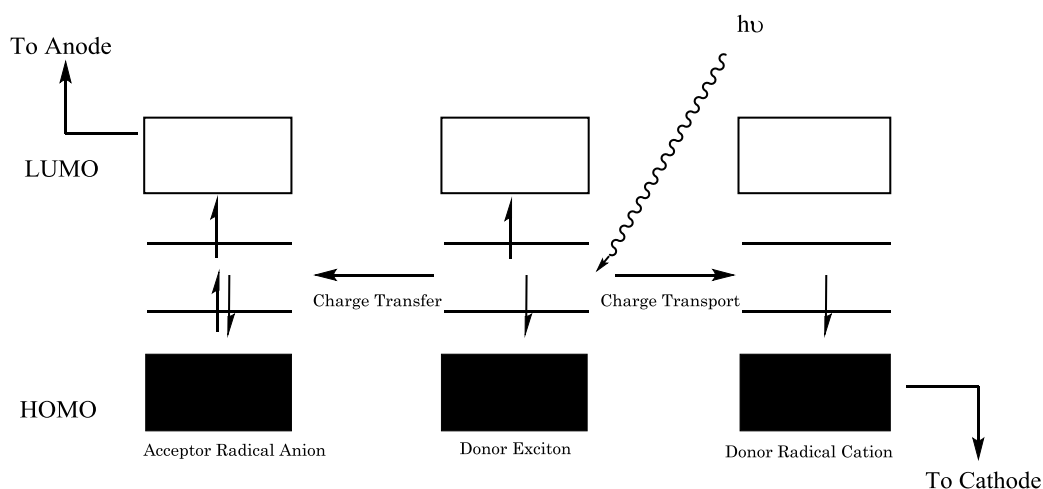


Figure 1.13 Creation of an excited state in an OPV.

Originally, organic photovoltaic devices employed a biphasic active layer (Figure 1.14), where a thin film of donor material was cast on top of the cathode, to which an acceptor material was then cast.²⁷ One limitation to the efficiency of such devices was annihilation of excitons before reaching the bilayer interface, and so only excited states created close to the

interface would exist long enough to charge transfer across the interface. In 1995 a device employing a bulk heterojunction (BHJ) (Figure 1.14), where the donor and acceptor material were blended together and cast as a single layer, was reported.²⁸

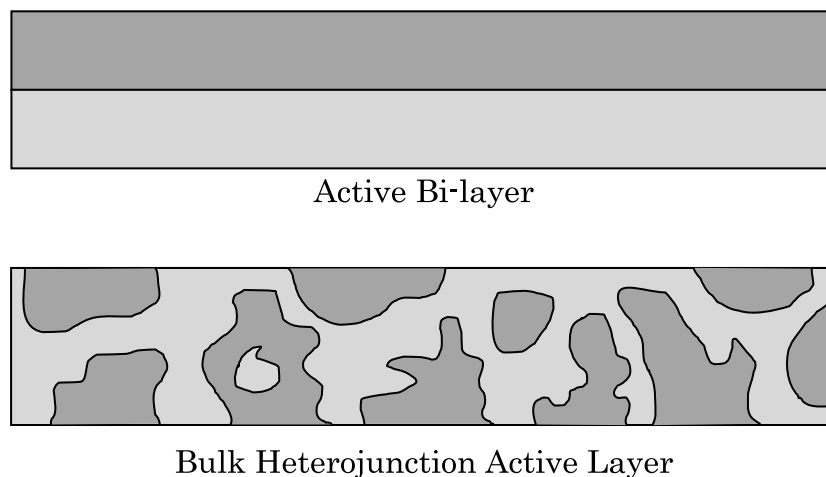


Figure 1.14 Bi-phasic and BHJ active layers.

By mixing the donor and acceptor material in this way the effective interface area is greatly increased, which increases the probability that an exciton will reach an interface before it annihilates, and has led to BHJ device performances showing significant improvements in performance over bilayer devices. This mixing of the materials results in both materials having contact with either electrode, and therefore both electrodes must be carefully selected such that their work functions are different enough that they will induce charge transport towards the desired electrode.²⁹

Materials selected for use in OPVs have the prerequisite that they must have affinities for opposing charges i.e. one material must be an electron donor and the other an electron acceptor. Buckminsterfullerenes have been identified as excellent electron acceptors,³⁰ and in 1992 photoinduced electron transfer to a film of C60 from a polymer film in a

bi-phasic layer system was reported.³¹ Since that report, fullerenes have been the most common material used as acceptors in OPVs, and their performance has yet to be surpassed.³² One limitation to using C60 in a film is its poor solubility and its ability to crystallise over time. This crystallisation can be retarded by functionalising the macrostructure, as demonstrated by Wudl *et al.* who synthesised (1-(3-methoxycarbonyl) propyl-1-phenyl[6,6]C₆₁) (PCBM) (Figure 1.15), which has been widely used as an acceptor material.³³

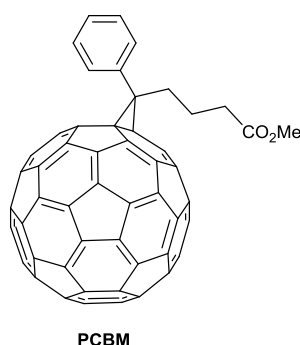


Figure 1.15 (1-(3-Methoxycarbonyl) propyl-1-phenyl[6,6]C₆₁) (PCBM).

Materials for use as electron donors have centred around electron-rich polymers such as poly(3-hexylthiophene) (P3HT) and poly(3-hexylselenophene) (P3HS).^{34, 35} OPVs based on P3HT and PCBM bulk heterojunctions are widely reported with efficiencies often around the 5% mark.³⁶ However, studies on this mixture have shown that choice of casting solvent,³⁷ external solvent annealing,^{38, 39} and thermal annealing can all have an effect on the efficiency of the resulting device.^{40, 41}

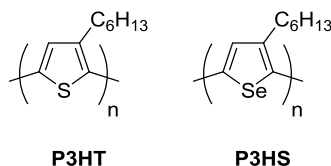


Figure 1.16 Poly(3-hexylthiophene) (P3HT) and poly(3-hexylselenophene) (P3HS).

Many other polymers and copolymers have also been investigated including materials based on benzo[1,2-b:4,5-b']dithiophene,⁴² thieno[3,4-b]thiophene,⁴³ and fluorene units.⁴⁴ Recent examples of donor materials are focused on electron rich fused heterocycles such as naphthodithiophene,⁴⁵ dithieno[3, 2-b:2', 3'-d]thiophene,⁴⁶ 5, 10-dihydroindolo[3, 2-b] indole,⁴⁷ and benzothiadiazole.⁴⁸

c) Organic Light Emitting Diodes

Organic electroluminescent (EL) devices are based upon the emissive properties of conjugated polymers. In this case, when a potential difference is applied to the material, the recombination of electrons and holes within one molecule will produce an excited state.⁴⁹ In an OLED, luminescence (light which is emitted from a material where no heat has been applied) is produced by the relaxation of a molecule from its excited state within the material. The release of energy from that molecule is in the form of photons.⁵⁰

When a molecule is excited, for example by absorption of a photon, its molecular energy is increased, resulting in an electron being promoted to a vacant molecular orbital of higher energy.^{1, 49} The molecule is said to be in an excited electronic state. Frequently, the absorption of energy is such that the molecule is excited into an upper vibrational level of the excited state, and will undergo radiationless decay and fall into lower vibrational level (Figure 1.17). This is commonly caused by collisions with neighbouring molecules. However, when the molecule is in the lowest vibrational level of the excited state, surrounding molecules may not be able to accept the larger energy required to allow the molecules to fall to the ground state. In order to relax into the ground state the molecule must emit the excess energy in the form of a photon. This is known as fluorescence.¹

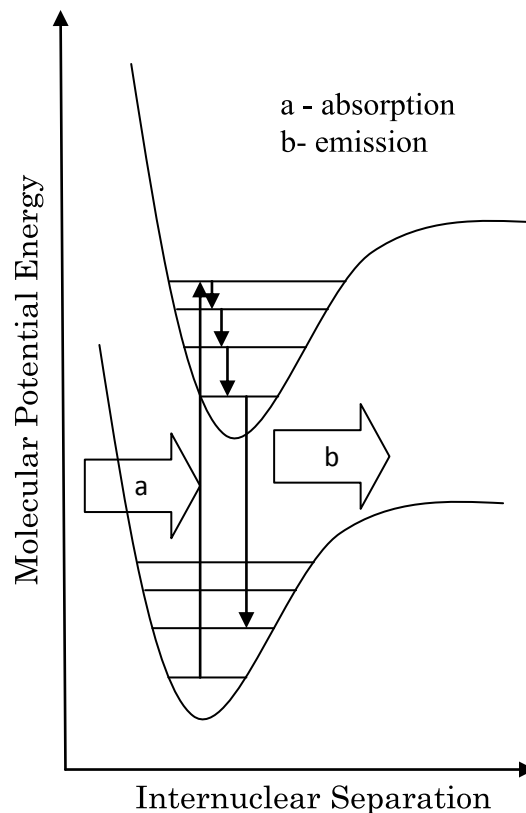


Figure 1.17 Potential energy diagram of excitation to and relaxation from an excited state.

Since energy has already been expelled in vibrational transitions, the emitted photon will have less energy, and therefore a longer wavelength, than that of the photon which was absorbed. This difference in wavelength between the absorbed and emitted light is known as the Stokes' shift.¹ Fluorescence can be quantified by the quantum efficiency, Φ , which is a ratio of photons absorbed by a molecule to photons emitted.

When an electron is promoted to a molecular orbital of higher energy, it retains its spin and is still paired with the electron it formally shared an orbital with.¹ However, as it relaxes through the vibrational levels of the excited state, under certain conditions the electron spin may change, and the molecule will exist in a different excited state. The conditions for this

phenomenon are usually met by spin orbit coupling.¹ The state in which electrons remained paired is known as a singlet state, and when unpaired as a triplet state. This transition occurs when the singlet and triplet molecular geometries are the same, indicated on the molecular potential energy diagram at the point where the curves for each state intersect (Figure 1.18). The transition between singlet and triplet states is known as intersystem crossing and is spin forbidden. After intersystem crossing takes place, the triplet excited state starts to relax *via* vibration until the molecule is in the lowest vibrational energy level of the triplet excited state.

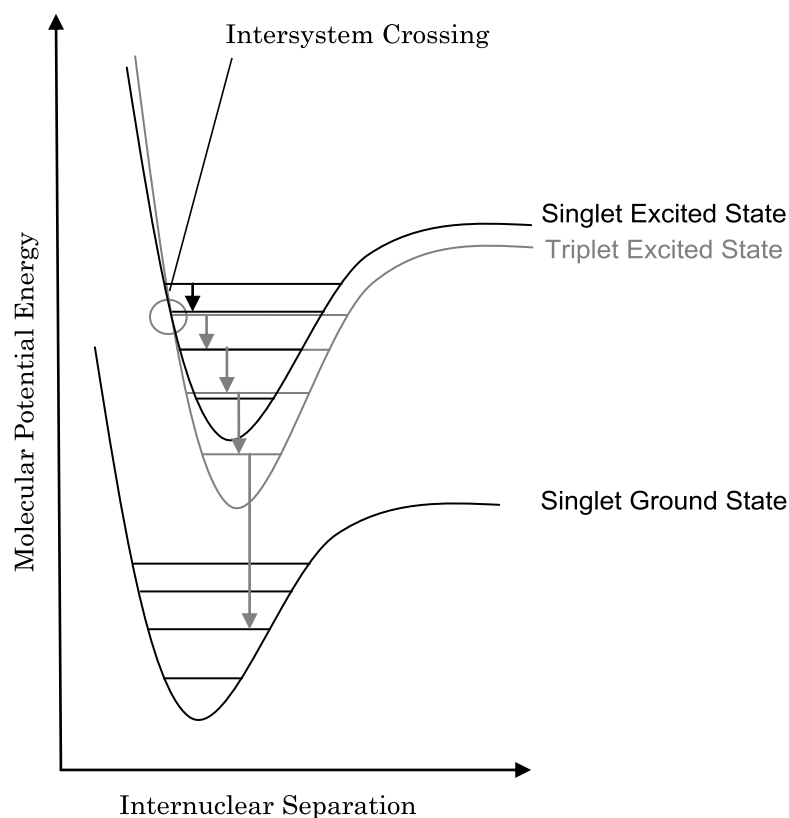


Figure 1.18 Potential energy diagram showing intersystem crossing and phosphorescence.

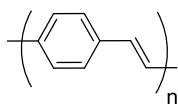
In order to relax to the ground state, molecules must emit a photon, however, as the ground state is also a singlet state, this is spin forbidden.

Intersystem crossing must again take place, which can be facilitated by the same spin orbit coupling that allowed the molecule to become a triplet excited state. As such, emission can still occur, but it is much less intense than that observed for fluorescence. Emission from a triplet state is commonly known as phosphorescence.

In an OLED, the excited states are created by recombination of electrons and holes that are injected into a doped conjugated material by the opposing electrodes. These opposing charges then migrate from molecule to molecule under the influence of a potential difference, and when they combine within a single molecule both triplet and singlet excited states are produced.⁵⁰

Since emission due to phosphorescence is much less intense than fluorescence, the electroluminescence observed is mainly produced from singlet excited states, which are quantified by the internal quantum efficiency, η_{int} , defined as the number of photons emitted per electron injected.^{49, 50} According to Friend *et al.* there are four criteria that must be met in order to achieve efficient luminescence, namely: a good balance of electron and hole currents, efficient capturing of electrons and holes within the emissive layer, strong radiative transitions for singlet electrons, and efficient coupling of these singlet excited states to photon states.⁵¹

Analogously to OPVs, OLED devices consist of layers of thin films sandwiched between two electrodes, again employing a transparent indium tin oxide anode. The first polymer that was found to be electroluminescent, poly(1,4-phenylene vinylene) (PPV), **1.12**, was applied as a thin film sandwiched directly between two electrodes (of which one was transparent) and mounted on glass.⁵² On device operation, light in the green-yellow area of the spectrum was observed.



1.12

Figure 1.19 Structure of poly(1,4-phenylene vinylene).

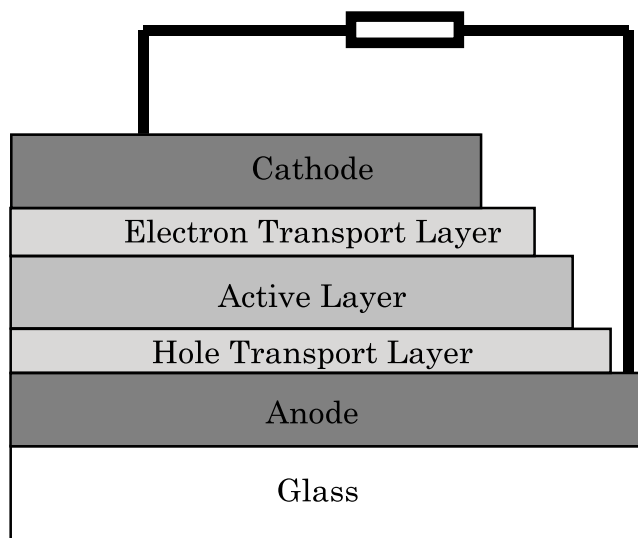


Figure 1.20 Diagram of a sandwich type OLED device.

Since that first publication, a variety of electroluminescent conjugated materials have been published. The colour of light observed from the bulk material is dependent upon the energy of the photons emitted, which is determined by the HOMO-LUMO gap. The ability to finely tune the HOMO-LUMO gap of conjugated compounds affords the possibility to selectively develop a material that will produce light of a certain wavelength.

An application of OLEDs that has received a great deal of interest is that for white lighting due to the potential for large scale, paper thin and flexible light sources. Unlike fluorescent lamps and incandescent bulbs, no heat is generated from OLEDs, which should therefore theoretically provide greater power to light conversion. However, since there are no

examples of white light emitted from a single chromophore it must be produced either from a multilayered devices, or from carefully designed copolymers, where the combination of emitted colours creates white light. In 1995 a white OLED was reported from a multilayered device employing a red, green and blue emitting layers, with brightness comparable to that of a fluorescent lamp.⁵³ Jin *et al.* have demonstrated a single layer device, where rubrene, an orange emitter and 1,4-bis(1,1-diphenyl-2-ethenyl)benzene (PEB), a blue emitter (Figure 1.21), were mixed with polystyrene and deposited from a dichloromethane solution.⁵⁴ Furthermore, by altering the PEB:rubrene ratio the colour of emission could be finely tuned.

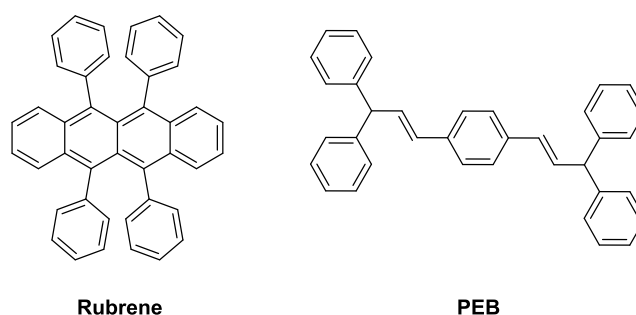


Figure 1.21 Structures of Rubrene and PEB.

Recently, Wang *et al.* reported white emission from a single polymer of 9,9-dioctylfluorene by introducing a low content of 4,7-dithienyl-2,1,3-benzothiadiazole (DBT) into the polymer chain (Figure 1.22).⁵⁵

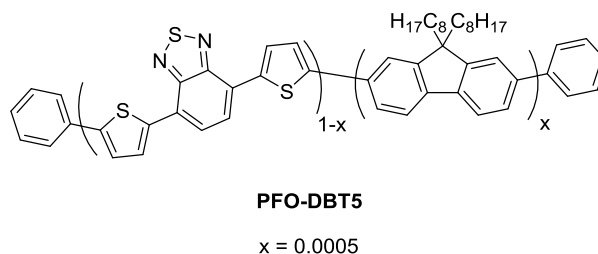


Figure 1.22 Structure of PFO-DBT5.

Further spectroscopic analysis suggested that the excited state of the DBT moiety, relaxation of which produced orange emission, was generated from inter-chain energy transfer from a fluorene moiety. Since there were a far greater number of fluorene units present within the polymer, there was still a significant amount of blue light emitted from the polymer, the mixture of which with orange emission produced the observed white light.

Charge Transport materials

Commonly, in addition to the luminescent layer, two more layers are applied; electron and hole transport layers. These additional materials are used to improve electron and hole transport from the electrodes into the emissive material.

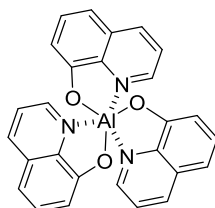
In order for efficient capture of the charge carriers within the emissive layer, electrons and holes must be injected and transported at the same rate.⁵¹ In the event that injection and transport is favoured for one charge carrier over the other (the favoured one becoming the majority charge carrier), some quantity of the majority charge carrier will be extracted by the opposite electrode, resulting in a loss of efficiency. For the PPV device mentioned above, for example, holes are the majority charge carrier.⁵² The injection of electrons into the emissive layer can be increased by the use of a second, electron deficient material in the EL device, placed between the emissive layer and the cathode.⁴⁹ This layer is known as an electron transport layer (ETL). Thus, there will be an increase in charge recombination in the emissive layer, and quenching by the cathode will be significantly reduced.

Selection of a material for an ETL layer is a complex matter. Jenekhe *et al.*⁵⁶ have highlighted some important requirements such as reversible electrochemical reduction, as to inject electrons into the emissive layer,

electrons must first be injected into the ETL from the cathode, suitable LUMO and HOMO values, where the LUMO value facilitates not only electron injection into the emissive layer, but also electron injection from the cathode into the ETL itself (if the difference in value for the LUMO and work function of the cathode is too large this will result in high turn-on and operating voltages), and high electron-mobility such that charge recombination is more likely to occur as far away from the cathode as is possible. The above criteria are similarly important for hole transport materials, where hole injection and hole mobility are the main concern in the hole transport layer (HTL).

Electron transport materials

Since the first publication of an OLED in 1987,⁵⁷ which employed tris(8-hydroxyquinoline) aluminum (Alq₃), **1.13**, (Figure 1.23) as the electroluminescent layer, (Alq₃) has been most commonly used as an ETL layer because of its excellent thin film forming properties and good thermal stability,^{58, 59} as well as improved device efficiencies in comparison to a wide range of other electron transport materials.



1.13

Figure 1.23 Structure of (Alq₃).

The most widely studied class of materials used to date as ETL layers are the oxadiazoles.⁴⁹ By nature, oxadiazoles are electron deficient, and so have poor affinity for holes. 2-(4-Biphenyl)-5-(4-tert-butylphenyl)-1,3,4-oxadiazol (butyl PBD), **1.14** (Figure 1.24), has been applied as an ETL layer in the PPV sandwich device described above. In this case **1.14** was

applied as a solid dispersion in poly(methyl methacrylate), an inert polymer, in order to retard crystallisation.⁶⁰

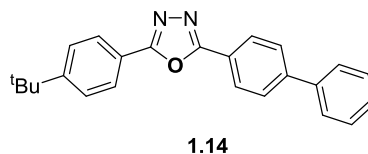


Figure 1.24 2-(4-Biphenyl)-5-(4-tert-butylphenyl)-1,3,4-oxadiazol (butyl PBD).

Comparisons between the PPV devices with and without the ETL layer showed that while the device containing the ETL layer required a larger voltage to produce electroluminescence, the internal quantum efficiency was raised from 0.1 % to 0.8 %.⁶⁰ It has been suggested that branched materials may be able to increase efficiencies to an even greater level than that of devices containing linear molecules within the ETL layer, as the branches will increase the probability that an electron will find an energetically favourable pathway when moving (within the layer) from one molecule to another. An oxadiazole-containing dendrimer, **1.15**, has been synthesised to exploit this effect (Figure 1.25).⁶¹ However, significant improvement was not observed over the butyl PBD, **1.14**.

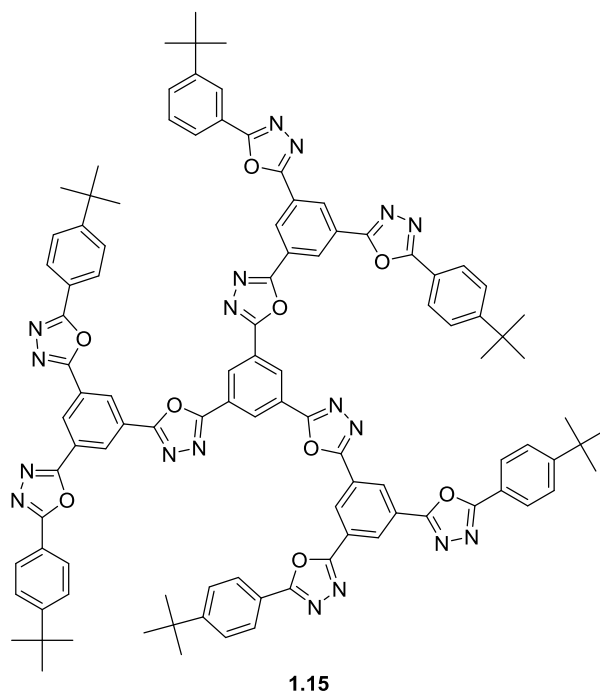


Figure 1.25 A 1,3,4-oxadiazole-containing dendrimer.

Quinoxaline units have also received some interest, including the development of poly(phenylquinoxaline) (PPQ), **1.16** (Figure 1.26).⁶² Here, it is the electron deficiency of the quinoxaline units within the polymer chain that give the polymer an increased affinity for electrons.

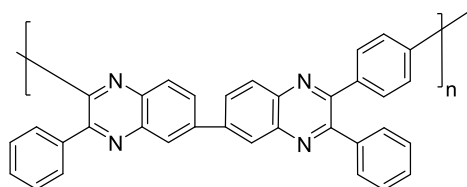


Figure 1.26 poly(phenyl quinoxaline) (PPQ).

A device containing PPQ as the ETL layer was constructed and the luminescence was quantitatively recorded. In comparison with that of a device containing the emissive layer only, the device containing PPQ as an ETL layer showed vastly enhanced luminescence over the single-layer

device, and efficiencies of 0.35 % compared to that of 0.03 % for the single-layer device.⁶²

If a material that is to be applied as an ETL has a HOMO energy level lower than that of the emissive material it is matched with, then the ETL material will retard the passage of holes from the emissive layer, demonstrated in Figure 1.27. The material is said to be an electron conducting/hole blocking (ECHB) material.⁵⁶

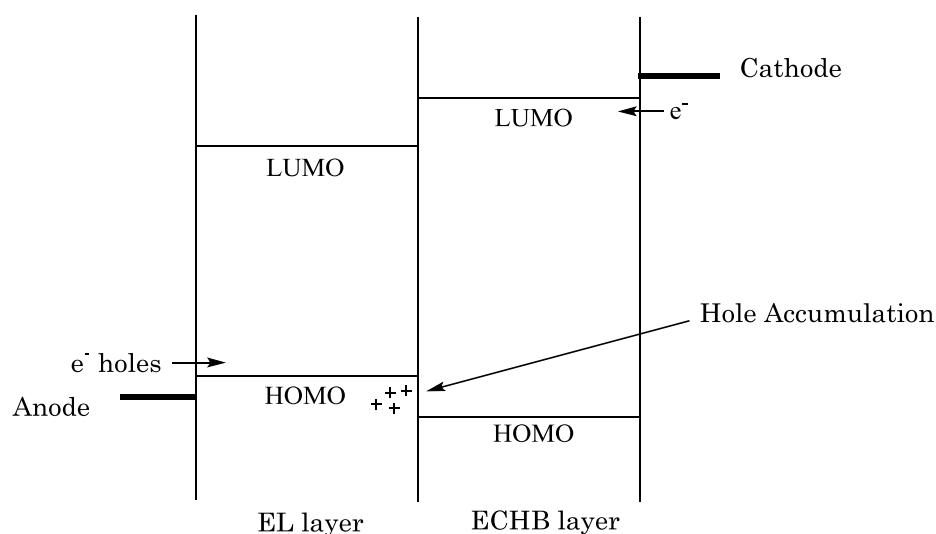


Figure 1.27 Energy level diagram of the interfaces in an OLED device.

With this concept in mind, perfluorinated materials have been proposed as ECHB layers, as the presence of perfluorinated groups leads to low lying HOMO and LUMO levels, as well as thermal and chemical stability due to the presence of strong C-F bonds.⁶³ Devices using these perfluoroalkyl materials (1.17, 1.18, Figure 1.28) were found to have relatively high quantum efficiencies.

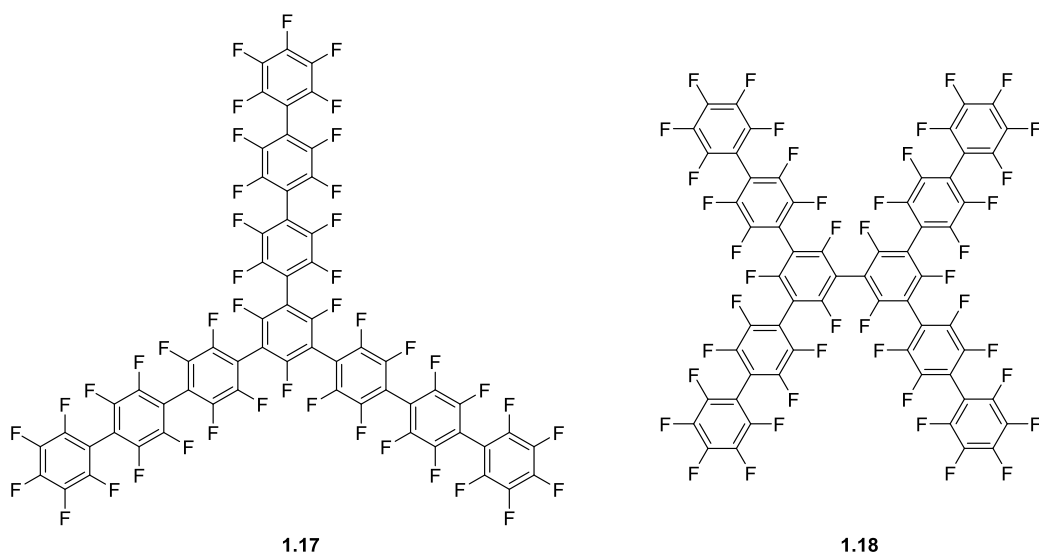


Figure 1.28 Perfluorinated materials used as ECHB layers.

Attempts have also been made to synthesise materials that are soluble in polar organic solvents in order to employ orthogonal processing, such as polymer **1.19** (Figure 1.29), a polymer containing alternating phenylene-oxadiazole-phenylene and fluorene units within the backbone, and polar tetramethylammonium side-chains.⁶⁴

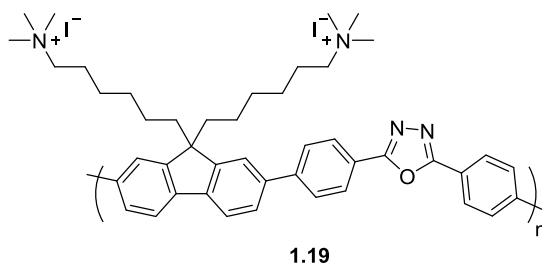


Figure 1.29 (PFON+(CH₃)₃I--PBD), a water soluble polymer.

This polymer is soluble in polar solvents, and can be applied onto a glass substrate from a methanol/water mixture. Devices utilising polymer **1.19** as an ECHB layer with a range of different emissive materials, where the emissive layer was applied from solution in an organic solvent, were shown to have high quantum efficiencies while overcoming the problem of mixing at the ECHB layer/emissive layer interface.

Hole Transport Materials

The vast majority of materials reported with hole transport characteristics contain electron rich arylamine components. Early reports demonstrated *N,N'*-diphenyl-*N,N'*-bis(3-methylphenyl)(1,1'-biphenyl)-4,4'-diamine (TPD) as a suitable material for application as a hole transport layer.⁶⁵ However, due to the low glass transition temperatures, alternatives such as *N,N'*-bis(1-naphthyl)-*N,N'*-diphenyl-1,1'-biphenyl-4,4'-diamine (NPB) and (4,4'-di(*N*-carbazolyl)biphenyl) (CBP), both of which have a greater T_g , have been investigated (Figure 1.30).^{66, 67}

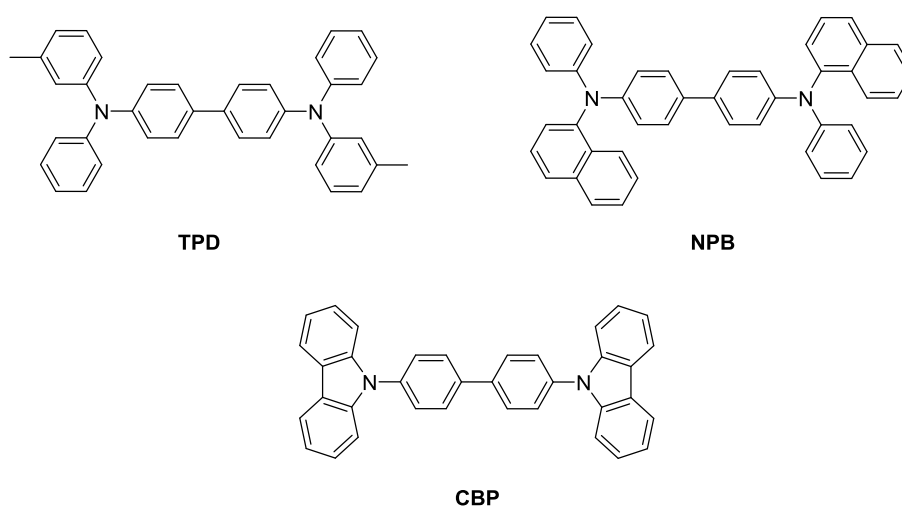
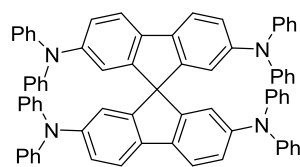


Figure 1.30 Arylamine based hole transport small molecules.

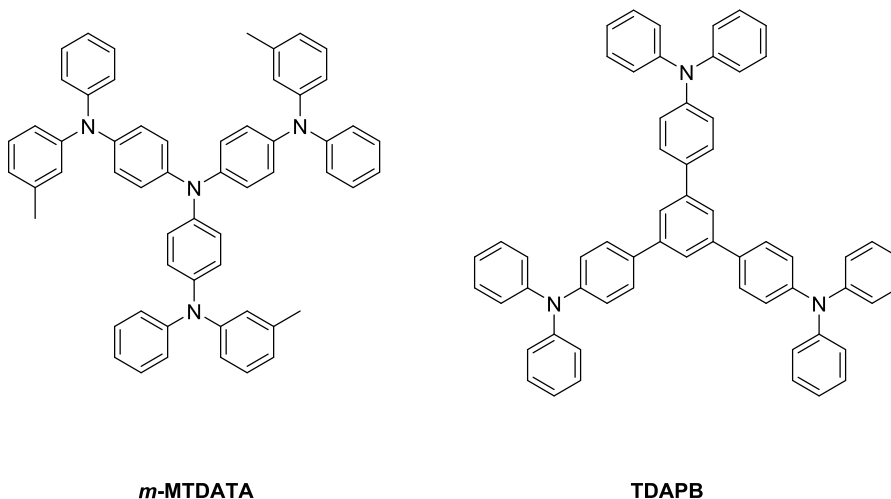
Salbeck *et al.* have reported compounds based on a spiro-fluorene centre, include Spiro-TAD (Figure 1.31), which have been implemented as hole transport layers in both organic transistors as well as OLEDs, and show even greater T_g values than those in Figure 1.30.^{68, 69}



Spiro-TAD

Figure 1.31 Spiro-fluorene based hole transport material..

Starburst compounds are also widely used as hole transporting materials. These compounds generally involve three identical aryl-amine branches bonded to a central amine core, such as 1,3,5-tris[4-(diphenylamino)phenyl]benzene (TDAPB) and 4,4',4''-tris[*N*-(3-methylphenyl)-*N*-phenylamino]triphenylamine (*m*-MTDATA) (Figure 1.32). Such compounds are amorphous in nature with high T_g values and the ability to form good thin films.^{70, 71}



***m*-MTDATA**

TDAPB

Figure 1.32 Aryl-amine based hole transport starburst compounds.

More recently Yang *et al.* have reported a star-shaped oligomer based around a hexakis-fluorenyl-benzene core that was end-capped with either carbazole (HFA-Cz) or diphenyl amine (HFA-Dpa) functionalities (Figure 1.33).⁷² The hexafluorenyl benzene core provides both high thermal stability and excellent solubility to allow solution processing. The authors report efficiencies of devices employing these compounds as HTLs were

increased by 0.5-0.6 % over those employing NPB, and among the highest for devices of similar configuration.

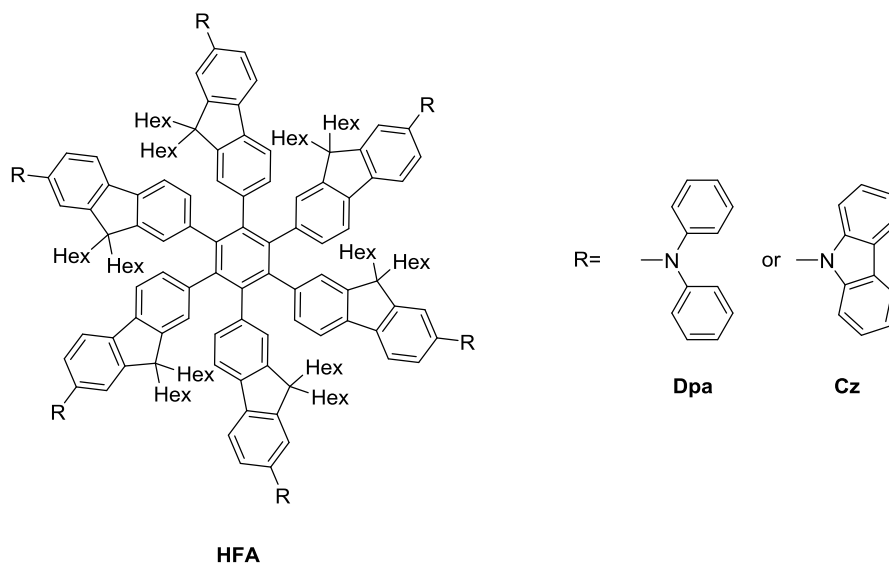


Figure 1.33 Star-shaped hole transport materials.

d) Organic Lasers

Electroluminescent organic materials have also found applications as gain media in lasers. Lasers emit light of a very narrow spectrum, which can be focused onto tight spots, even over long distances. Since the first publication of a laser there has been widespread innovation and lasers are now used in a wide variety of applications including everyday electronic devices such as CD/DVD players, barcode scanners and devices for use in the field of medicine.⁷³

Lasers consist of a material which amplifies light, by way of stimulated emission, in a cavity/resonator which will provide optical feedback. Stimulated emission involves a molecule in an excited state interacting with an electromagnetic wave such that it relaxes to the ground state with the emission of a photon that has the same phase, frequency and direction of the photons of the incident wave. This results in amplification

of the incident wave. This is in contrast to spontaneous emission such as that observed with OLEDs.

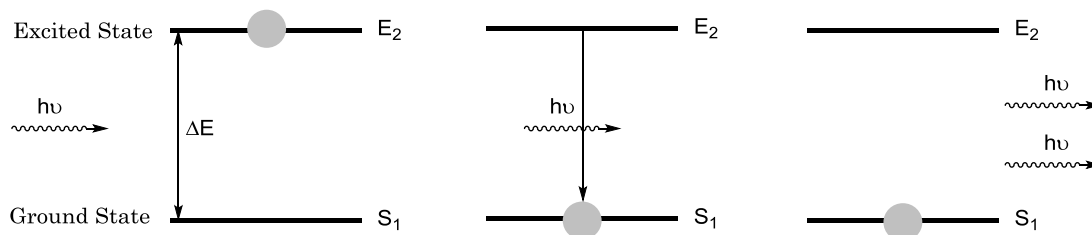


Figure 1.34 Illustration of stimulated emission.

The material relaxing from its excited state is known as the gain material. Laser pumping is the act of exciting the gain material, and the number of molecules in the excited states must be greater than the number of molecules in the ground state in order for stimulated emission to be achieved.⁷⁴

The other required component of a laser is an optical resonator consisting of two mirrors, one of which has high reflective properties and the other partial reflective properties. The gain medium is placed between these mirrors which reflect light from the gain medium back through itself repeatedly, with a portion of the light transmitting through the partially reflective mirror, which is observed as the laser light exiting the device.

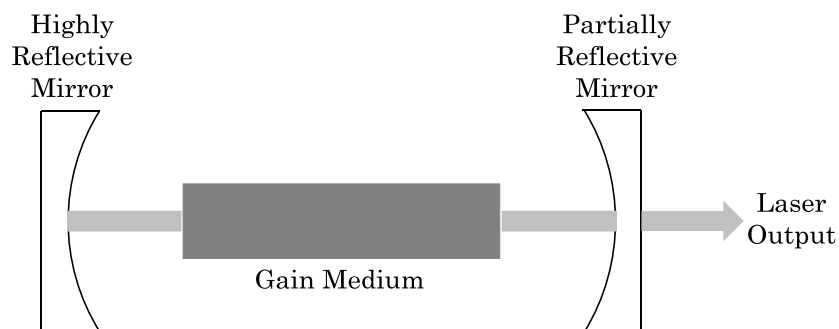


Figure 1.35 Light amplification in a laser.

While anthracene was the first organic compound that received significant focus as a gain medium,⁷⁵ over time other small molecules, polymers (such as poly(phenylene vinylene)s and poly(fluorene)s⁷⁶⁻⁷⁹), dendrimers,⁸⁰ and spiro-compounds have all seen application in organic lasers.⁸¹ Currently, these materials are optically pumped using diodes composing of, for example, gallium nitride. As discussed previously in this chapter, electroluminescence is observed from some organic semiconductors by applying a potential difference across the material. This paves the way for direct electrical pumping of gain material. While this is an attractive goal which could lead to small, battery operated lasers, there are severe limitations to electrical pumping which include short excited state lifetimes and poor gain from transitions due to phosphorescence. One solution is to indirectly pump the gain material with an OLED. However, while spontaneous emission has been achieved in such a way, as demonstrated by Duarte *et al.*,⁸² stimulated emission remains a challenge to be overcome.

Distributed feedback (DFB) lasers are a subset of lasers where the gain materials are applied as a thin film on top of a diffraction grating (Figure 1.36). The grating provides the feedback, and is designed such that the light emitted from the device is of a specific wavelength.⁷⁴ The wavelength of emission supported by a DFB resonator is dependent on the period of corrugation and effective refractive index of the device waveguide. The latter can be affected by manipulation with an organic semiconductor surface.⁷⁴ This has led to applications as bio-sensors, where organic probes are bound to the surface and the change in emission is monitored in the presence of target analytes.⁸³⁻⁸⁶ In order to introduce the probes to the surface of the laser, polyelectrolytes are usually applied on top of the gain materials, to which the probes can then bound to the device.

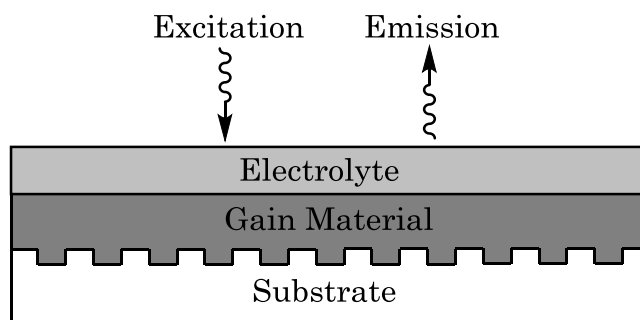


Figure 1.36 Diagram of a DFB laser.

1.4 Fabrication Techniques

Fabrication of functional devices requires application of an organic material as a thin film onto a substrate as part of the manufacturing stage. There are two common types of fabrication for large scale applications: vacuum deposition and solution processing.

Vacuum deposition involves the sublimation of organic materials onto substrates under high vacuum.⁵⁷ This results in well ordered thin films, the thickness of which can be controlled by varying both the sublimation and substrate temperatures and pressure.⁸⁷ However, the utilisation yield of materials (percentage of material used in fabrication that is successfully applied to the device) is as low as 20 %, and the pixelation effect caused by evaporation masks during processing limits large scale and high resolution applications.⁸⁸

Solution processing involves dissolving an organic material into solution, which is applied to a substrate using methods such as inkjet printing and spin coating. During the application the solvent is evaporated, leaving behind a thin film of material. By varying the concentration of solution, and other factors such as the number of drops in inkjet printing and the speed of rotation during spin coating, the thickness of films can be controlled. These methods are more easily scaled up, can be adapted for high-throughput and have lower running costs than vacuum deposition.⁸⁹

One major drawback for solution processing during fabrication of devices involving multiple layers of organic materials is mixing of adjacent layers. While the application of the first layer will be fairly routine, the application of a second layer from a solvent in which the first layer is soluble in will cause material on the surface of the first layer to redissolve.⁸⁹ This results in mixing of materials at the surface interface, rather than the desired bi-layer with a well defined interface. One method used to circumvent this problem is to develop polymers possessing functional units which will allow the polymers to be cross-linked post processing, making them insoluble towards common solvents under ambient conditions.^{90, 91} However, this method can result in undesirable cross-linking, and while some cross-linking can be achieved photochemically, chemically cross-linking polymers can leave impurities, resulting from the cross-linking reaction, within the film.

Another method is orthogonal processing, whereby each material to be solution processed dissolve in a solvent other components of the device are insoluble in. In some instances, materials will have different solubility and so orthogonal processing is readily applicable. Elschner *et al.* have demonstrated fabrication of a multilayer device where the PEDOT:PSS, HTL and emissive layer were spin-coated from solutions of water, THF and methanol respectively.⁹² However, many materials designed for applications in organic semiconductors have very similar solubility. Generally, this derives from the fact that to improve solubility, most conjugated materials are functionalised with linear or branched saturated alkyl chains, which are selected due to their highly stable nature. This affords good solubility in non-polar solvents and poor solubility in solvents which are polar in nature. In order to employ orthogonal processing, materials for different layers within a device will require different side chains in order to change their solubility. In

practice, this requires the solubility of materials to be determined from the outset and synthetic routes designed to afford such materials. This has led to a great deal of interest in ionic and polar materials, which can be spin coated from water/alcohol mixtures.⁹³

One variant of orthogonal processing is the use of fluorinated solvents, which are solvents where a significant proportion of hydrogen atoms are replaced by fluorine atoms. This results in organic compounds having poor solubility, and in some cases being completely insoluble, in fluorinated solvents unless they contain fluorine atoms in their structure. Ober *et al.* conducted a series of tests where the performance of a batch of OFET devices made from P3HT were recorded before and after being submerged in a variety of solvents for 5 minutes.⁹⁴ It was shown that, as expected, the non-polar organic solvents dissolved the P3HT layer, significantly reducing the device performance, while the polar solvents had little effect on device performance. Results also showed that after submerging in perfluoroethers (HFE 7100), the performance of the device was largely unaffected. In addition, the authors also conducted atomic force microscopy of widely used organic semiconducting materials, including poly(9,9-dioctylfluorene) and PEDOT:PSS, before and after submersion in boiling HFE 7100, stating that there was no significant change in morphology and no cracks or pinholes were observed.⁹⁴

An increasing percentage of fluorine content within the molecular structure will generally result in better solubility in fluorinated solvents, however different fluorinated solvents may also have differing polarity, which also must be considered. Curran *et al.*, in conducting extraction studies of fluorinated organic molecules from an organic phase into a fluorous phase, rather than considering polar/non-polar and fluorous/non-fluorous as two one dimensional scales, they should be considered as one two-dimensional scale, as demonstrated in Figure 1.37.⁹⁵

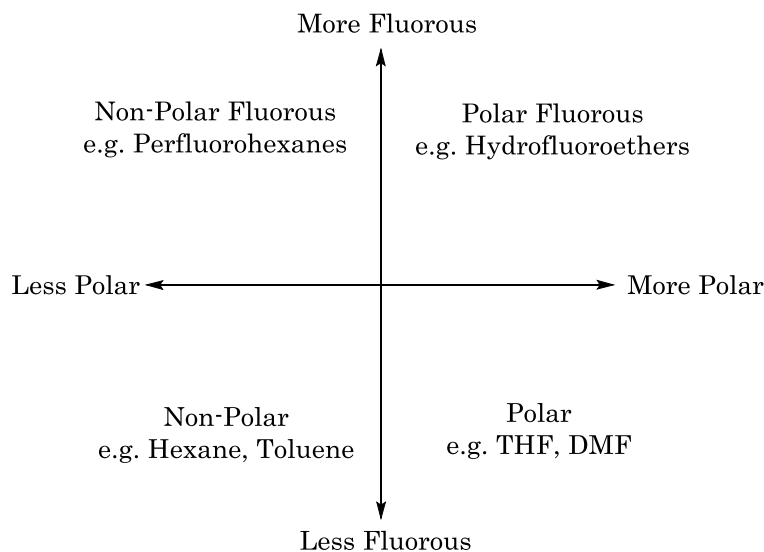


Figure 1.37 Polar/non-polar and fluorous/non-fluorous scales.

Considering fluorous solvents this way allows for selection of appropriate solvents for solution processing. Ober *et al.* have reported the fabrication of blue, red and green OLEDs by spin coating co-polymers containing fluorene units with semiperfluoroalkyl chains, namely **R_fB**, **R_fR** and **R_fG**, from a range of fluorinated solvents.⁹⁶ The authors also reported the fabrication of a multilayered device containing poly(3,4-ethylenedioxythiophene):poly(styrene sulfonate) (PEDOT:PSS) and poly(9,9-dioctylfluorene), which were spin coated from water and *p*-xylene respectively, and **R_fG** and **R_fR**, which were spin coated from two different fluorinated solvents. This demonstrates the wide applicability of fluorinated solvents for solution processing.

1.5 Fluorenes

9H-Fluorene, or more commonly known as simply fluorene, is an aromatic carbocyclic compound containing two benzene rings which are joined with a methylene bridge and an adjacent direct C-C bond. Due to the fused nature of the rings, the compound is planar,⁹⁷ which allows for good

overlap of the π -orbitals of the benzene rings across the direct C-C bond. The potential resonance stabilisation of the fluorenyl anion at the 9-position means that the protons at that position are acidic in nature,⁹⁸ and easily deprotonated by a variety of bases. This allows for a range of functionalisation at the 9 position, which can improve the solubility in a variety of different solvents by the introduction of alkyl or aryl groups. Substitution of the methylene carbon serves to prevent oxidation to fluorenone, **1.21**, which occurs readily due to the increase in conjugation that a carbonyl group would provide.⁹⁹

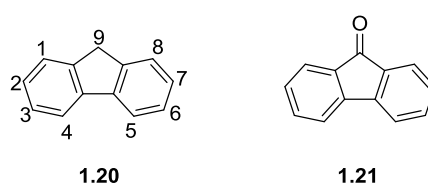
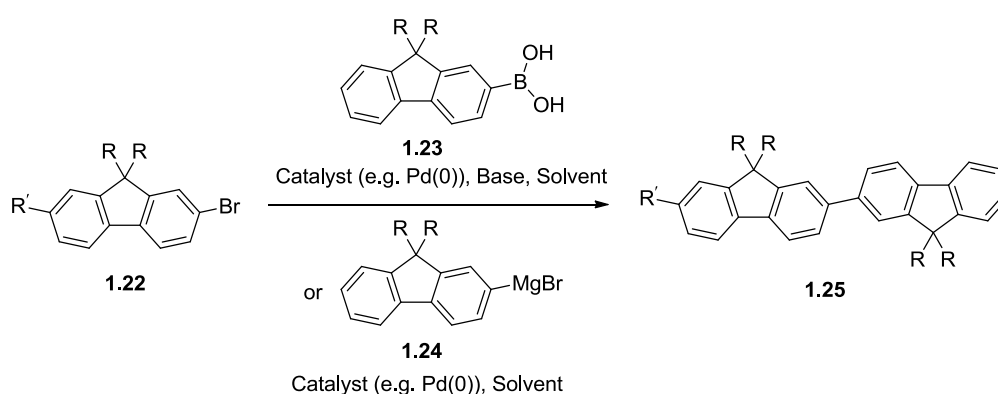
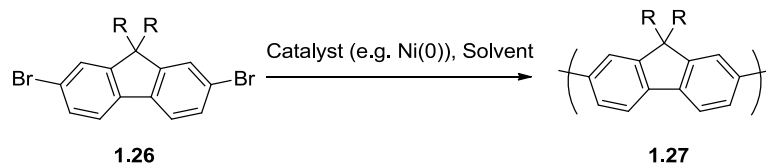


Figure 1.38 9H-Fluorene and Fluorenone.

Oligo- and polyfluorenes can be easily synthesised by joining fluorene units together through the 2- and the 7-positions. Synthesis of oligo- or polyfluorenes is generally achieved using cross coupling reactions; some examples include Suzuki-Miyaura,¹⁰⁰⁻¹⁰² Yamamoto¹⁰²⁻¹⁰⁴ and Kumada¹⁰⁵ reactions (schemes 1.2 and 1.3).



Scheme 1.2 Suzuki-Miyaura and Kumada reaction routes to oligofluorenes.



Scheme 1.3 Yamamoto reaction route to polyfluorene.

The functional group present at the 9-position of the fluorene repeat units will define the solubility of the polymers (Figure 1.39). Alkyl chains at this position can affect the degree of aggregation of polymer chains. Therefore a shorter chain will result in a greater degree of aggregation.

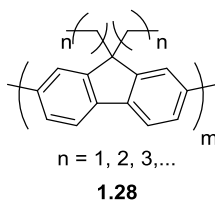


Figure 1.39 Homopolymers of alkylated fluorene.

Poly(dimethylfluorene) and poly(diethylfluorene) are poorly soluble materials,⁹⁹ whereas poly(dihexylfluorene) and poly(dioctylfluorene) are soluble in a range of organic solvents.¹⁰⁶ Oligomers and polymers of fluorene all possess absorption maxima in the UV region, and show emission in the blue region. In oligofluorenes, as the conjugation length increases with more fluorene units, a narrowing of the band gap is observed, resulting in a bathochromic shift for both absorption and emission maxima.⁹⁹ After six repeat units the wavelength of emission, 420-425 nm, is no longer affected by increasing the conjugation length, however it is not until twelve repeat units that the wavelength of absorption, at around 380 nm, is unaffected by conjugation length.⁹⁹

Tsutsui *et al.* have developed oligofluorenes with branched alkyl side chains, F(Pr)5F(MB)2 and F(MB)10F(EH)2 for applications in OFETs

(Figure 1.40), where the use of branched alkyl chains promotes the formation of monodomain glassy-nematic films while resisting crystallisation.¹⁰⁷ Chen *et al.* have also investigated crystallisation of oligofluorenes with chiral alkyl side chains, showing interesting crystallisation properties as chain length increases.¹⁰⁸

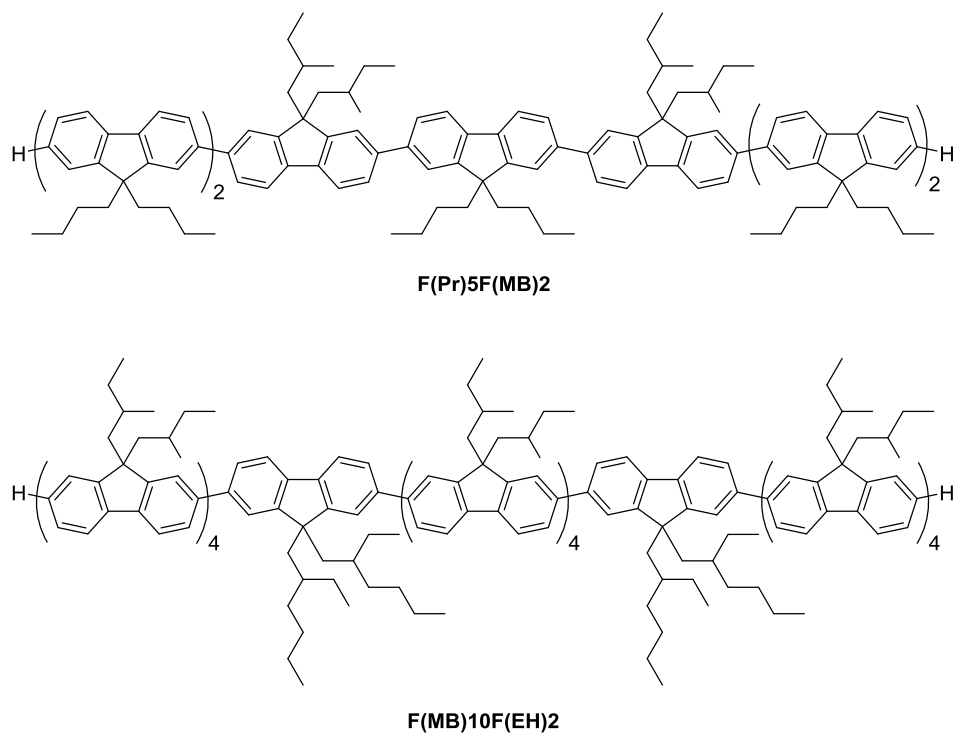


Figure 1.40 Oligo(fluorenes) with branched alkyl chains.

Also for OFET applications Heeney *et al.* have developed poly(fluorenes) with an sp^2 -hybridised carbon atom at the 9-position (Figure 1.41). The alkyl chains attached to the alkyldiene functionality are therefore orientated in-plane with the polymer chain, affording reduced distances between polymer chains in the bulk film and showing charge carrier mobilities up to $2 \times 10^{-3} \text{ cm}^2\text{V}^{-1}\text{s}^{-1}$.¹⁰⁹

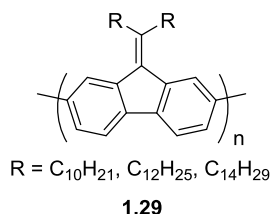


Figure 1.41 Structure of poly(alkylidene fluorenes).

Due to the blue emission observed from poly(fluorenes) there has been significant interest in exploring their applicability as the source of blue light in OLEDs. Coincidentally, the first publication of an OLED utilising a fluorene homopolymer (in this instance poly(9,9-dihexylfluorene) was also the first publication of a blue emitting OLED.¹¹⁰

There is also a wealth of examples employing fluorene units in copolymers. The synthesis of these compounds is made easy by the Suzuki-Miyaura coupling of fluorenyl boronate esters with other halogenated heterocycles, affording alternating fluorene-heterocycle copolymers. The choice of heterocycle will have a bearing on the optical and electrochemical properties of the resulting polymer, and therefore potential applications.

Polymers with alternating fluorene and bithiophene components,⁴⁴ or fluorene and thienothiophenes units,¹¹¹ have been studied for applications in OLEDs,⁴⁴ and OPVs.¹¹¹ Incorporation of such electron-rich heterocycles into the polyfluorene chain leads to a reduction of the band gap. A similar effect is observed with pentacene derivatives to achieve polymers with band gaps between 1.78 and 2.15 eV, as reported by Bao *et al.*, which were investigated as materials for OPVs, with polymer **1.31** showing power conversion efficiencies of 0.68 % (Figure 1.42).¹¹²

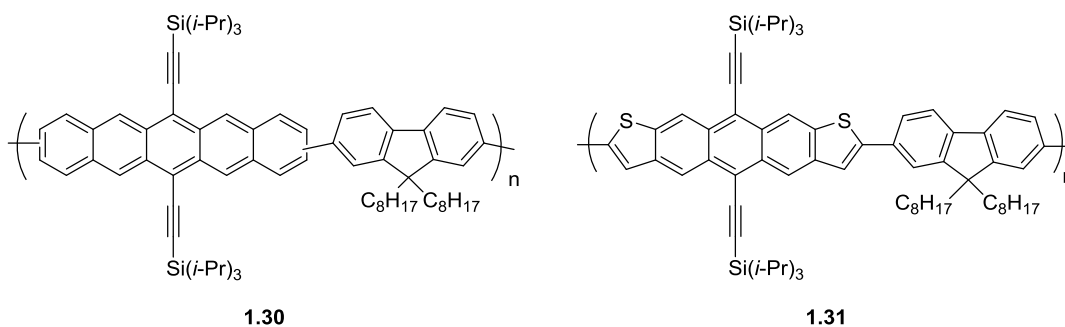


Figure 1.42 Poly(fluorene-co-pentacenes).

Through incorporating electron-deficient heterocycles, such as benzothiadiazole, into the polyfluorene chain a lower LUMO is achieved, therefore resulting in a contraction of the band gap.¹¹³ It has been demonstrated that a fluorene-benzothiadiazole copolymer has improved electron transport properties compared to that of polyfluorene, with potential applications as an ETL.¹¹⁴

1.6 Star-Shaped Oligomers

Oligomers can be envisioned as materials that are midway between small molecules and polymers, offering the best of both worlds. The benefits of small molecules and polymers are often mutually exclusive. For example, while small molecules have precise electronic properties such as HOMO and LUMO levels, polymers, having a range of molecular weights, have less defined electronic properties. However, conjugated small molecules without alkyl chain substituents often have poor solubility due to a high degree of π - π stacking and require more expensive processing techniques such as vacuum deposition, whereas polymers often have far superior solubility and can be processed from a range of low cost techniques e.g. spin coating.

Oligomers are molecules that contain a small, defined number of repeat units. Good solubility can be achieved while retaining precise HOMO and LUMO levels, and high molecular weights provide good thermal stability.

The downside of oligomers comes in the synthetic procedures, which often require many synthetic steps. While purification, including techniques such as recrystallisation, column chromatography or distillation, of intermediate compounds after each individual step affords oligomers with high purity, the synthetic procedures to achieve oligomers are often time consuming.

Linear oligomers, much like polymers, show efficient movement of charge carriers along the conjugated backbone, the plane of which can be considered to be in one directional. An increase in conjugation into other directions provides the opportunity to improve the electronic properties of organic materials in these directions, and could help bridge the gap between linear organic material and metallic behaviour.¹¹⁵

Star-shaped conjugated oligomers are macromolecules where three or more linear oligomers, referred to as arms, are connected by a central core unit. The core unit itself may or may not be conjugated. The geometry of the core, more specifically whether it is planar or not, will dictate whether the star shaped oligomer will be two or three dimensional.¹¹⁶

Simple elements such as boron and carbon can act as core (Figure 1.43). Boron, with trigonal planar geometry, can afford a 2D structure,¹¹⁷ whereas the tetrahedral geometry of a carbon core will afford a 3D structure.¹¹⁸

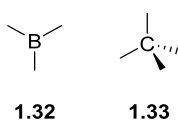


Figure 1.43 Geometry of Boron and Carbon.

Aromatic carbocycles and heterocycles, due to being planar, will afford compounds which are 2D in nature and will take part in the π -conjugated backbone. Common examples include benzene, **1.34**,¹¹⁹⁻¹²¹ which can be functionalised with between 3 and 6 arms (Figure 1.44), thiophene, **1.35**,¹²² and triazine, **1.36** (Figure 1.45).¹²³

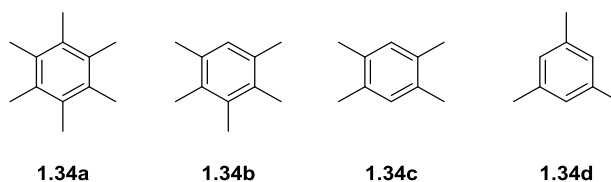


Figure 1.44 Possible functionalisation of benzene to afford 2D cores.

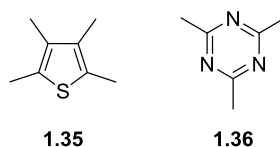


Figure 1.45 Functionalisation of thiophene and triazine to afford 2D cores.

By combining oligomeric arms with various cores, a diverse array of star-shaped oligomers can be achieved. There are two synthetic approaches to the construction of star shaped oligomers; divergent and convergent (Figures 1.46 and 1.47).¹¹⁶

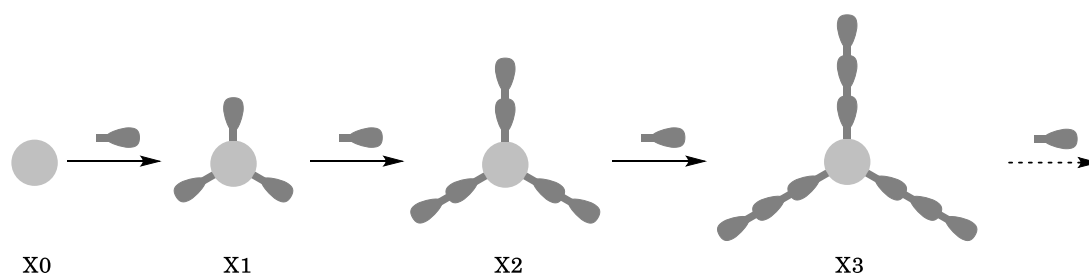


Figure 1.46 Divergent approach.

The divergent approach involves the direct, sequential addition of repeat arm units to the intermediate core structures until the desired arm

length is obtained (Figure 1.47). This involves firstly the coupling of one arm unit to the core, then functionalisation of the terminal points of the arm, followed by coupling of another arm unit. Repetition of these steps will afford star-shaped oligomers of incremental arm length. An advantage of this approach is the requirement for only one arm building block, and the core itself. However, in each case both the coupling of arm units and functionalisation of the terminal points requires a 3 fold reaction; that is, there are 3 reaction sites where a reaction will take place, within the same reaction mixture. The reaction therefore requires to be as near quantitative as possible, as any drop in yield is increased 3 fold (an 80 % yielding reaction will become almost 50 % overall, for example). Another common problem associated with the divergent approach is purification of the desired product and partially reacted by products from the coupling reaction step. While separation is possible for smaller star-shaped oligomers, there is little difference in the properties of the desired product and that of the by-products of incomplete reaction of oligomers of larger arm length. Therefore, for star-shaped oligomers of longer arm length this approach becomes less practical.

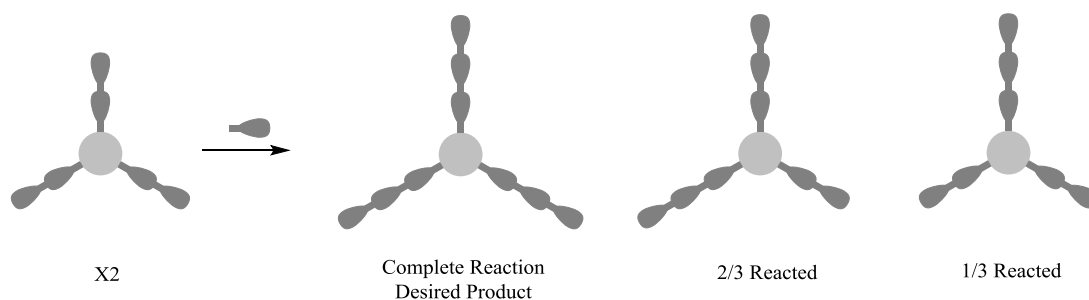


Figure 1.47 Incomplete reaction in the divergent approach.

The convergent approach differs from the divergent approach in that the oligomer arms are first produced in a fashion comparable to that of the synthesis of linear oligomers. Once arms of a desired length have been obtained, these are then coupled to the core (Figure 1.48). While this

approach requires the synthesis of intermediates of differing arm length, and therefore a greater number of synthetic steps, only one 3-fold reaction is required to afford the desired star shaped oligomer.

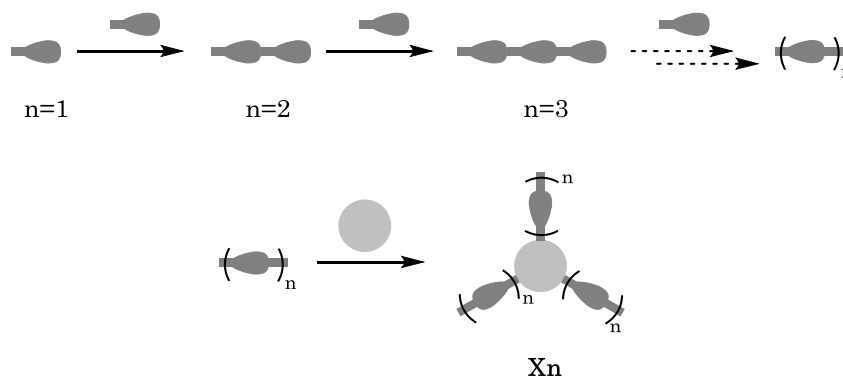


Figure 1.48 Convergent approach.

This approach also circumvents the problem of purification, as the properties of the products from incomplete reaction are sufficiently different to allow for good separation (Figure 1.49).

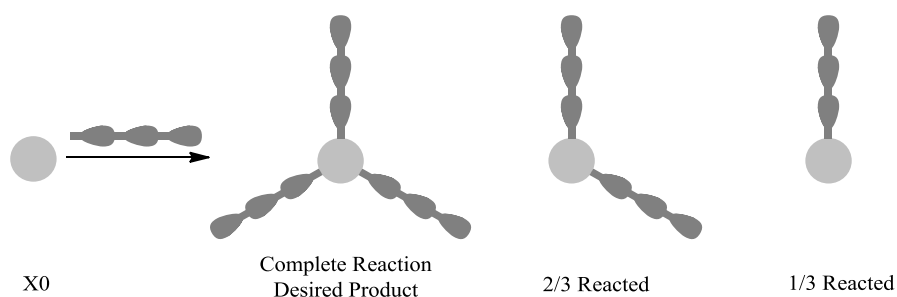
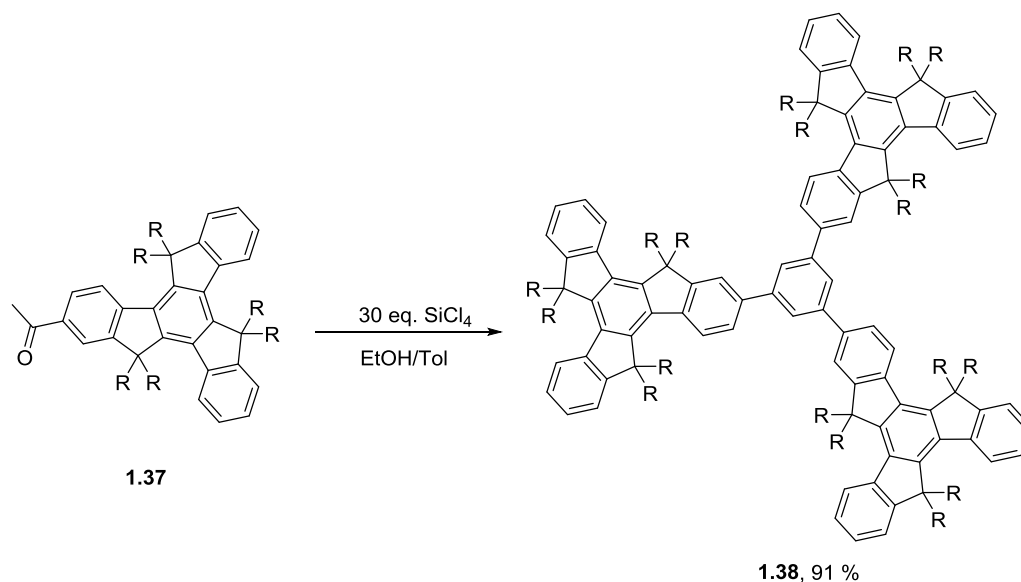


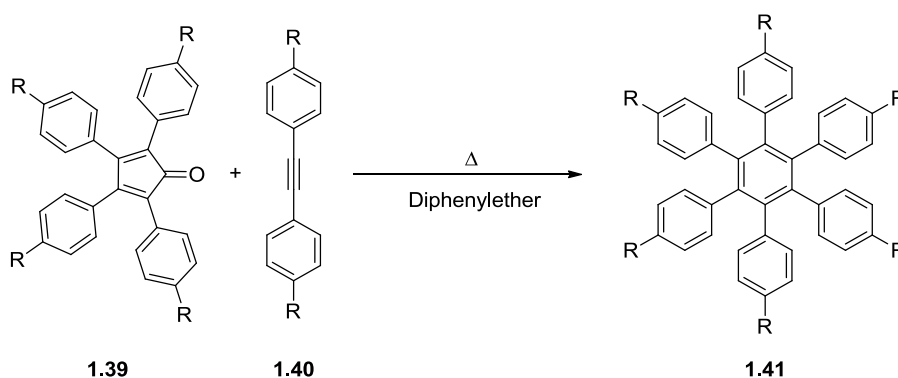
Figure 1.49 Incomplete reaction in the convergent approach.

A variant on the convergent approach is to synthesise oligomeric arms terminated with a functional group, such that these functional groups will react together to afford the core unit. One such example demonstrated by Pei *et al.* is the SiCl_4 mediated trimerisation of truxene units with acetyl functionality, **1.37** to afford a star shaped oligomer with a phenyl core, **1.38** (Scheme 1.4).¹²⁴



Scheme 1.4 Phenyl core synthesis from ketone.

Another technique to afford a phenyl core, as demonstrated by Müllen *et al.*, is the Diels-Alder reaction of tetrasubstituted cyclopentadienones, **1.39**, with disubstituted acetylenes, **1.40** (scheme 1.5).¹²⁵ In this case, by incorporating the same substituent on both the acetylene and cyclopentadienone, a D_6 symmetry can be observed in the star shaped oligomers, **1.41**.



Scheme 1.5 Phenyl core synthesis from Diels Alder reactions.

By implementation of this variant on the convergent approach, star shaped oligomers containing cores that may not be chemically stable

towards the reaction conditions of the steps required to produce oligomers, such as cross-coupling and halogenation, can be synthesised.

1.7 Truxene

10,15-Dihydro-5H-diindeno[1,2-a;1',2'-c]-fluorene, also known as truxene, **1.42** (Figure 1.50), is a heptacyclic polyarene with C_3 symmetry that can be envisaged as three fluorenes, **1.20** (Figure 1.37), which are overlapping.^{126, 127}

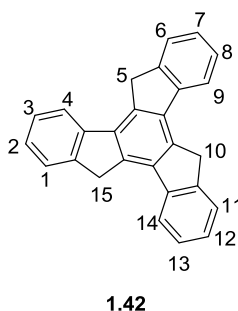


Figure 1.50 Labelled truxene.

It has been used as a starting compound, or a core unit, for larger star-shaped polyarenes such as fullerene fragments and liquid crystalline compounds.^{128, 129} Positions C5, C10 and C15 can be functionalized with a range of substituents, commonly saturated alkyl chains, which can enhance the solubility and processability as well as reduce intermolecular π - π stacking,¹³⁰ but there are also examples of unsaturated alkyl,¹³¹ and phenyl substituents at these positions.¹³² Cross coupling reactions at the C2, C7 and C12 positions is the usual method of attaching ‘arms’ to the core to form the star-shaped oligomers, extending the conjugation length and altering the photophysical properties of the resulting oligomer (Figure 1.51).

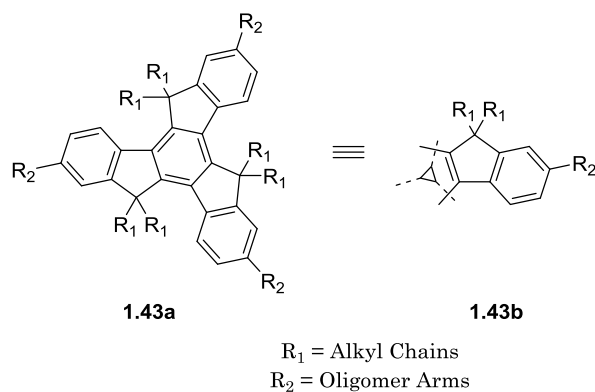


Figure 1.51 Substituted and functionalised truxene.

Pei *et al.* reported compounds of oligothiophene arms with lengths increasing up to 4 thiophene units connected to a central truxene core, synthesised by the divergent approach (Figure 1.52), which have found applications in OFETs.^{126, 133}

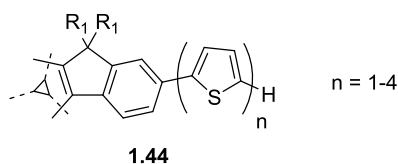


Figure 1.52 Oligo(thiophene)-functionalised truxenes.

The authors reported an increasing red shift in absorption with increasing arm length, which were also red shifted in comparison to their oligo(thiophene) analogues. This difference between the standalone oligomers and those of the oligo(thiophene)-functionalised truxene became less with increasing arm length, and the wavelength of absorption maximum of the quaterthiophene compound was close to that of the corresponding oligothiophene. The authors attributed this result to the extended π -conjugation through the truxene core. ¹H NMR studies of the compounds by the authors showed that, since no change in chemical shift was observed with increasing concentration, the presence of six alkyl chains on the truxene core effectively prevented self-association. This is in contrast to reports by Echavarren *et al.* which demonstrated a change

in chemical shift of the proton at the C14 position with increasing concentration of tri-alkyl truxene compounds.^{134, 135} Interestingly, these reports also demonstrate the selective *syn*-alkylation of truxene at the C5, C10 and C15 positions with a range of alkyl, vinyl and benzyl substituents (Figure 1.53).

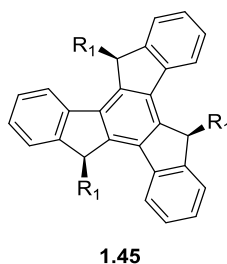


Figure 1.53 *syn*-Trialkyl truxene.

Pei *et al.* have also reported the synthesis of truxene core compounds with oligo(phenylene) arms by what can be considered as a combination of the divergent and convergent approaches (Figure 1.54).¹³⁶

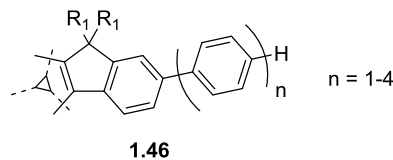
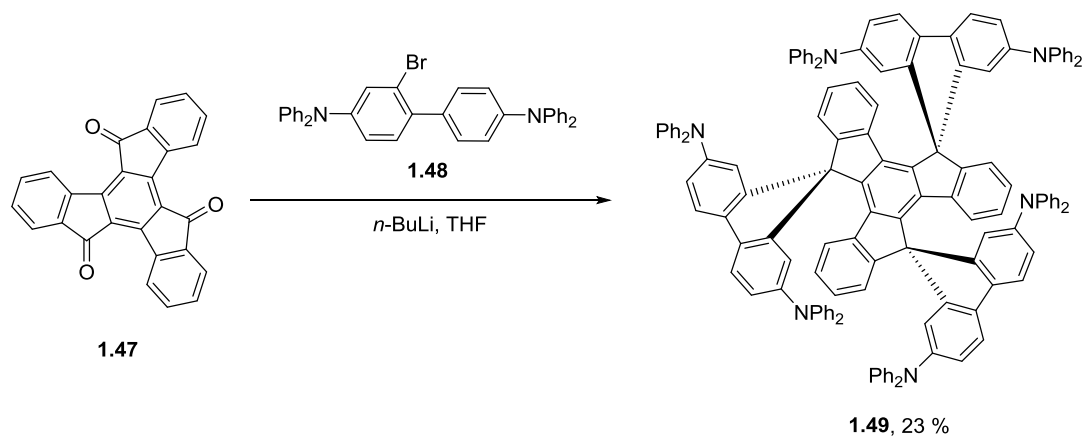


Figure 1.54 Oligo(phenylene)-functionalised truxenes.

Again, as the length of the oligomer arms increases, a red shift was observed in the absorption maximum. The authors reported that a plot of the band gap of the materials against the number of phenyl units in the arms exhibited a trend towards saturation, indicating a point where additional phenyl units would not sufficiently alter the band gap.

A truxene core with diphenylamino functionalised spirofluorenes, synthesised from fluorenone, has been reported, **1.49**. The authors note that the material has hole transport properties, and was successfully

employed as a HTL in an OLED device.¹³⁷ This compound has a very high glass transition temperature and, due to the trispirocyclic core, excellent film forming properties which the authors attribute to the free rotation of the diphenylamino groups.



Scheme 1.6 Synthesis of spirofluorene-substituted truxene **1.49**.

The truxene core can also be substituted with different arms within the one molecule. An example of this has been reported by Ziessel *et al.* who have attached three different difluoroborondipyrromethene (BODIPY) units (Figure 1.55).¹³⁸ Each BODIPY was designed to absorb at either the blue, yellow or green region of the visible spectrum, with the hexabutyltruxene core absorbing in the UV-vis region.

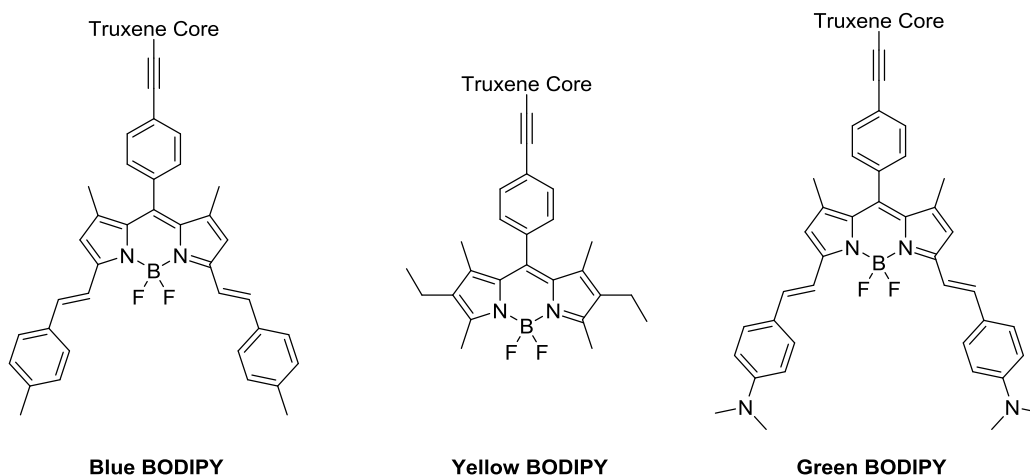


Figure 1.55 Substituted BODIPY arms.

The synthesis was carried out by the sequential cross-coupling reaction of the core with each BODIPY unit to afford a multichromophoric star-shaped oligomer. Emission spectra of the compounds with truxene core and only one of each BODIPY showed a profile consistent with emission from the BODIPY units only in each case, demonstrating efficient transfer from the truxene to the BODIPY moiety. An absorption spectrum of the target compound showed absorption contributions from all three BODIPY units as well as the truxene core, while an emission spectrum showed that emission from the green BODIPY unit dominated over that from the other two BODIPYs, regardless of the excitation wavelength, which is attributed to intramolecular self quenching by the green BODIPY unit.

An example of two truxene units in the same molecule has been reported by Pei *et al.*, employing spirofluorene, ethynylene and vinylene bridges (Figure 1.56).¹³⁹

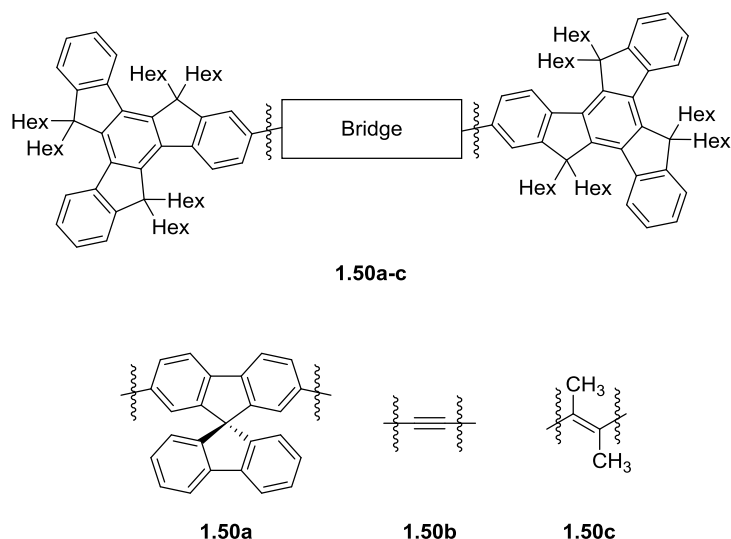


Figure 1.56 Bridged truxenes.

The compound with spirofluorene bridge, **1.50a**, showed very little difference in the emission both in solutions and films, indicating suppression of π - π aggregation due to the nature of the spiro bridge. The other two compounds were red-shifted in comparison to the spiro compound. While the spirofluorene, **1.50a**, and ethynylene bridged, **1.50b**, compounds displayed vibronic structure within the emission spectra, the spectrum of the vinylene bridged compound, **1.50c**, was devoid of any vibronic character, indicating poor π -orbital overlap across the bridge due to the steric hindrance contributed by the methyl groups, which increase the dihedral angle between the vinyl and truxene functionalities. This was supported by the absorbance spectrum of the compound which showed very little difference to that of hexahexyltruxene itself.

Pei *et al.* have also reported a truxene dendrimer linked with trivalent trigonal benzene branching points, **1.51** (Figure 1.57),¹²⁴ as well as dendrimers containing truxene as the nodes, connected with oligo(thienylethynylene)s of increasing length.¹⁴⁰ The absorption spectrum of **1.51** showed little vibronic characteristics in comparison to smaller intermediates which the authors attributed to the lack of

planarity across the phenyl units as a result of the steric hindrance units, leading to a large dihedral angle between the truxenes and phenyl moieties.

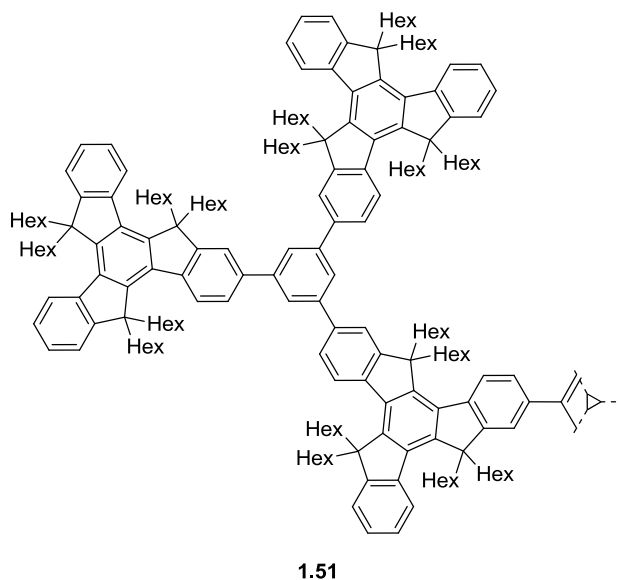


Figure 1.57 Phenyl-truxene dendrimer.

In comparison, the dendrimers containing oligo(thienylethynylene)s bridges between truxene nodes were shown by atomic force microscopy to be highly planar. These compounds were of incredibly high molecular weight (27024 Da for the largest) yet still retained good solubility due to the hexyl chains present on the truxene nodes. The planarity of the compounds decreased with increasing arm length as demonstrated by a trend of increasing Stokes shift and decreasing quantum yield.

Tian *et al.* have reported triphenylamine-based dendrimers with hexabutyltruxene as a core, **Tr-TPA3** and **Tr-TPA9** (Figure 1.58).¹⁴¹ In this instance, the butyl chains, along with the rotation afforded through the triphenylamine moieties, was sufficient for good solubility to form thin films. The authors reported good hole transport properties for the compounds and suggested their use as HTLs in OLEDs.

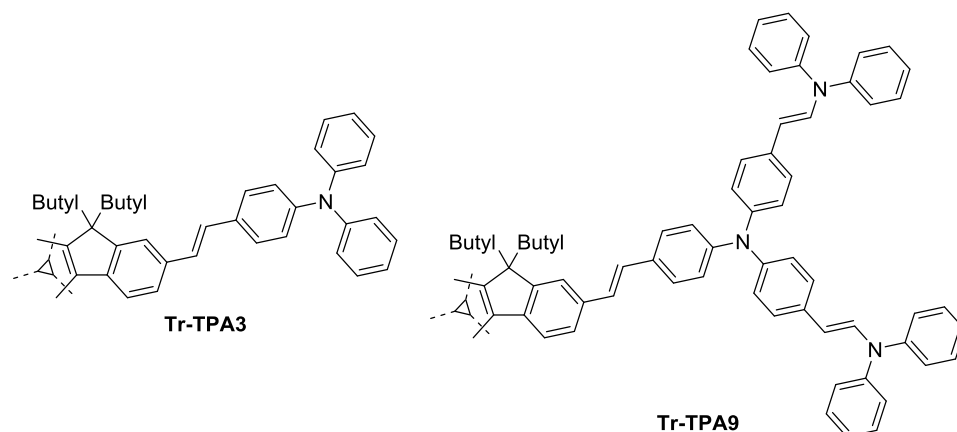


Figure 1.58 **Tr-TPA3** and **Tr-TPA9** HTL materials.

While the vast majority of reports have demonstrated truxene cores with three oligomer arms at the C2, C7 and C12 positions, there are also examples of functionalization at the C3, C8 and C13 positions. A hexahexyltruxene functionalised with six phenyl-carbazole arms has been reported by Huang *et al.*, the synthesis of which involved the coupling of boronate ester arms to a hexabromo truxene, **1.52** (Figure 1.59).¹⁴²

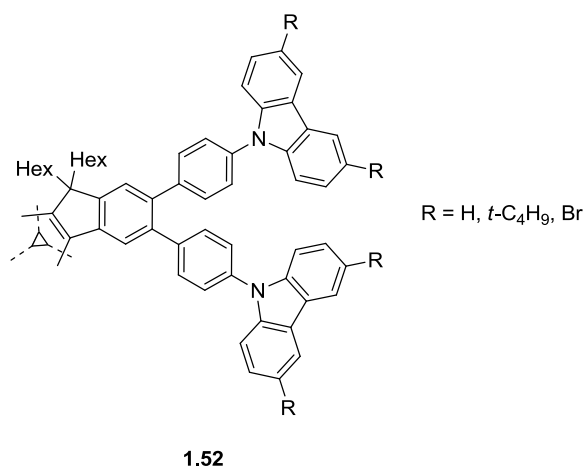


Figure 1.59 Hexaphenylamine-functionalised truxene **1.52**.

The authors reported the good solubility of both the butyl substituted and non-substituted oligomers of **1.52**, suggesting that the arrangement of six 4-(carbazolyl)phenyl moieties within the molecules prevents π - π stacking.

The absence of any vibronic feature within the absorption spectra of the oligomers supports this argument. The authors also reported the successful twelve-fold bromination by treatment with *N*-bromosuccinimide, suggesting that the oligomer would be suitable as a core for even larger oligomers with twelve arms.

2 Perfluorohexylthiophene end capped oligofluorene - functionalised truxenes.

2.1 Introduction

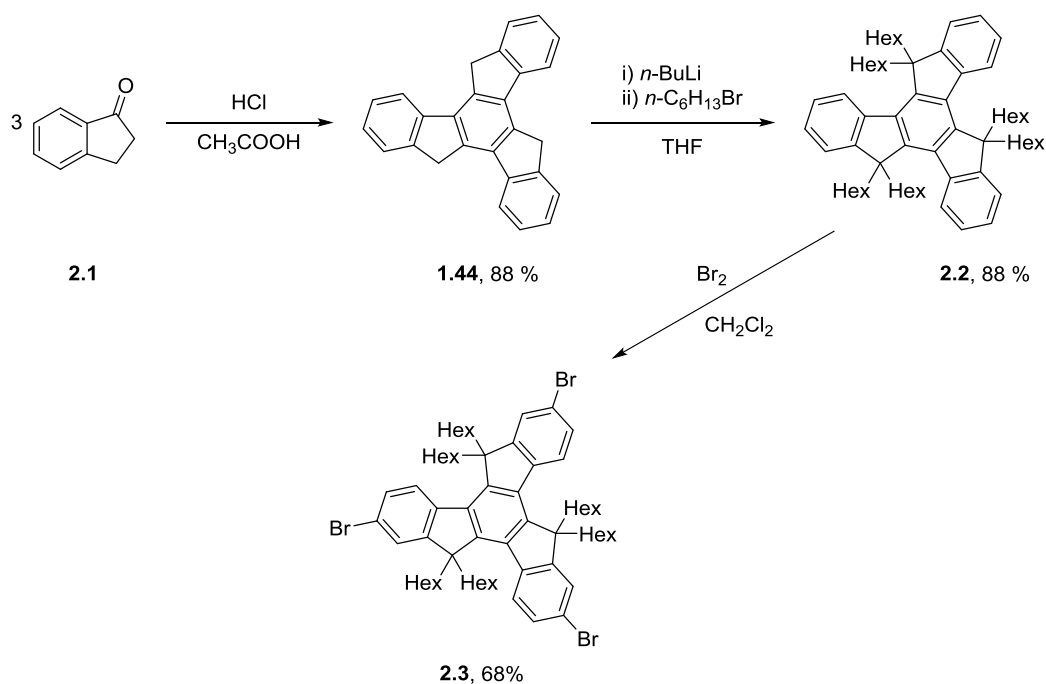
The properties of oligomers and polymers can be affected by the substituents attached to the hetero- and carbocycles that make up the conjugated backbone.¹⁴³ These substituents, such as alkyl chains or other functional groups, can donate or withdraw electron density from the conjugated backbone, for example by inductive effects, altering the HOMO/LUMO values of the conjugated system, and subsequently, the band gap. Perfluoroalkyl chains are one type of substituent that can be attached to the repeat unit of the backbone, where the high percentage of fluorine present gives rise to a large electron-withdrawing effect,¹⁴⁴ pulling electron density away from the conjugated backbone and altering the electronic properties of the polymer. One synthetic challenge associated with perfluoroalkyl halides is that they are not suitable alkylating reagents for S_N2 type reactions, which makes attaching these types of chains to the repeat unit of an oligomer or polymer difficult without the use of a spacer group, such as an ethylene linker. However, employing spacer groups can lessen the inductive effect of the chain, which must be taken into consideration.¹⁴⁵ Due to the widespread use of poly(thiophenes) such as P3HT, analogous poly(perfluoroalkylthiophenes) have received some interest due to the ability to affect certain properties of the polymer, such as the electrochemistry and stability, as well as the improved chemical resistance and thermal stability that replacing alkyl hydrogen atoms with fluorine atoms affords.¹⁴⁶

Introducing perfluoroalkyl chains can also affect the solubility of compounds, in that it affords solubility in fluorinated solvents such as perfluorohexanes and perfluoroethers. This can allow for materials functionalised with perfluoroalkyl chains to be implemented in orthogonal processing, by solution processing from fluorinated solvents.

The Skabara group has previously published work on oligofluorene-functionalised truxenes,¹⁴⁷ and it was in our interest to observe changes in the optical and electrochemical properties by introducing perfluorohexylthiophene units at the terminal positions of the of the oligofluorene arms. Planarity of the backbone is an important concept in conjugated organic oligomers and polymers, as any twist in the dihedral angle between aromatic repeat units can lessen the p-orbital overlap, breaking the effective conjugation length.¹⁴⁸ The steric effects of substituents attached to the hetero- or carbocycles in the conjugated backbone can induce twisting of the repeat units relative to the plane of the backbone. Therefore in order to observe if the position of the perfluorohexyl chains would have an effect, two molecules that are structural isomers were synthesised and studied to compare their optical and electrochemical properties. Furthermore, a significantly larger molecule was synthesised to observe how a molecule with longer conjugated arms would also be affected by the perfluorohexylthiophene units. The solubility of these compounds in highly fluoruous solvents, namely perfluorohexanes and perfluoroethers, was also tested.

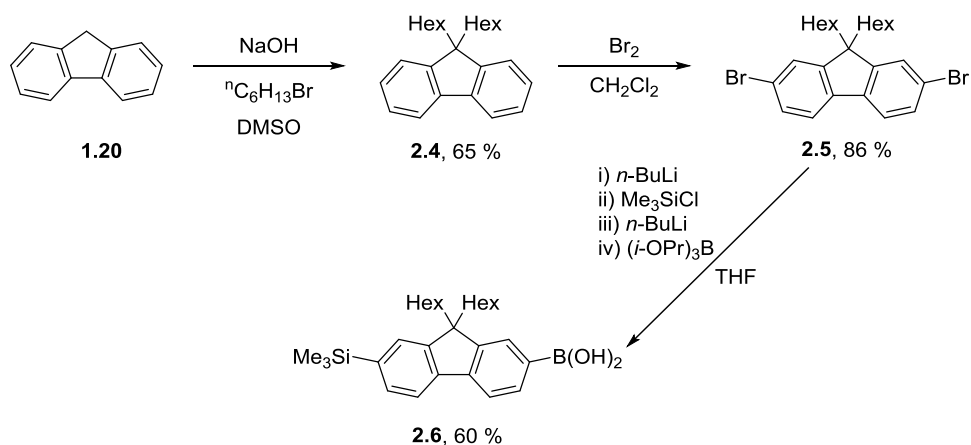
2.2 Synthesis

The original synthetic route selected was to produce oligofluorene-truxenes, using the convergent approach, and to couple them with perfluorohexyl thiophene units at the terminal positions of the oligofluorene arms. The synthesis of the truxene core is presented in scheme 2.1.¹⁴⁷ A condensation reaction of 1-indanone produced the unfunctionalised truxene, **1.44**, which has poor solubility. Alkylation by successive treatment with *n*-butyllithium and the addition of 1-bromohexane is required to improve solubility before bromination with bromine in CH₂Cl₂ to afford the functionalised core **2.3**.



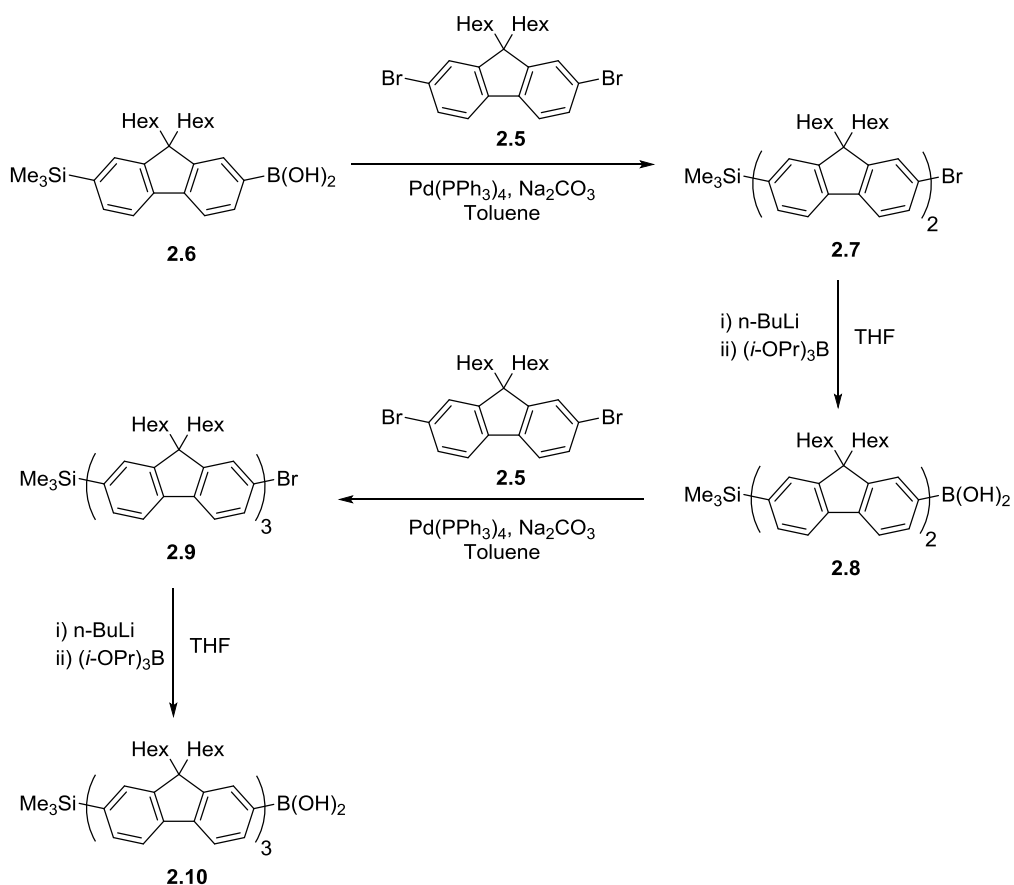
Scheme 2.1 Synthesis and functionalization of truxene core.

The synthesis of the oligofluorene arms is shown in schemes 2.2 and 2.3. 2,7-Dibromo-9,9-dihexylfluorene **2.5** was obtained from the dialkylation and dibromination of fluorene **1.20**. Compound **2.5** is converted to the boronic acid **2.6** by substitution of one bromine with a trimethylsilyl group and the conversion of the other to a boronic acid. This one pot reaction afforded compound **2.6** in good yield (scheme 2.2).



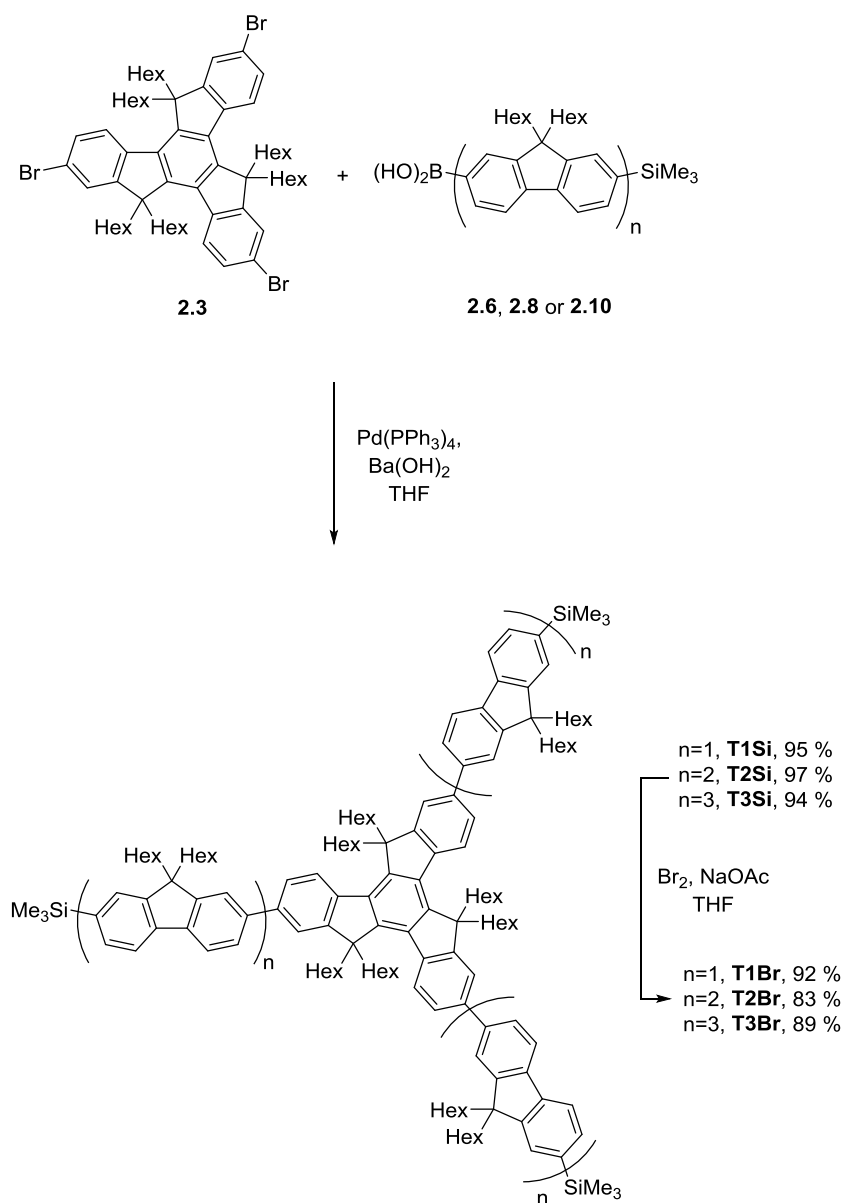
Scheme 2.2 Functionalization of fluorene.

Compound **2.6** was then used as a starting block for the oligofluorene arms. The bifluorene, **2.7**, was synthesised by Suzuki-Miyaura coupling of the boronic acid **2.6** with the dibromide **2.5**. In order to diminish formation of the terfluorene by twofold coupling of **2.5** with **2.6**, 3 equivalents of **2.5** were used in the reaction. These conditions afforded compound **2.7** in good yield, while a significant portion of unreacted dibromide **2.5** can be isolated and recovered during the purification process. Treatment of **2.7** with *n*-butyllithium followed by the addition of triisopropyl borate afforded the bifluorenyl boronic acid **2.8**. Using the same conditions as those which produced compound **2.8**, compound **2.10** was then prepared.



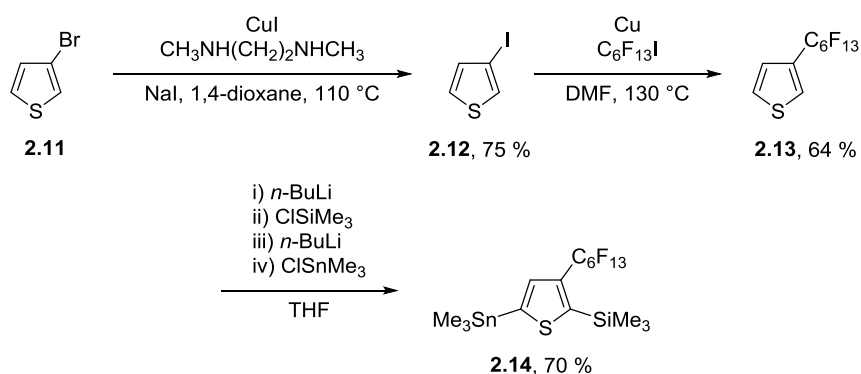
Scheme 2.3 Synthesis of oligofluorene arms.

The trimethylsilyl terminated oligofluorene truxenes were then synthesised by reaction of either compounds **2.6**, **2.8** or **2.10** with functionalised truxene **2.3**. For these reactions, a stronger base, barium hydroxide, was employed, affording the **TXSi** compounds in high yields, where X refers to the number of fluorene units in each arm. Reaction of these compounds with bromine in a basic solution of THF afforded the brominated compounds **TXBr**.¹⁴⁹



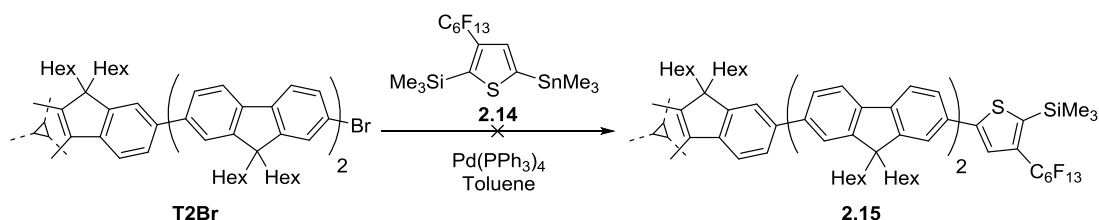
Scheme 2.4 Coupling of oligofluorene arms to truxene core.

3-Perfluorohexylthiophene **2.13** was synthesised from 3-bromothiophene **2.11** via initial halogen exchange, using the method described by Buchwald *et al.*,¹⁵⁰ to afford 3-iodothiophene **2.12**, which then underwent a copper mediated coupling reaction with perfluorohexyl iodide (Scheme 2.5). A one-pot, two-step reaction was then used to functionalise the thiophene with a trimethylsilyl group at the C2 position, and a trimethyltin group at the C5 position.



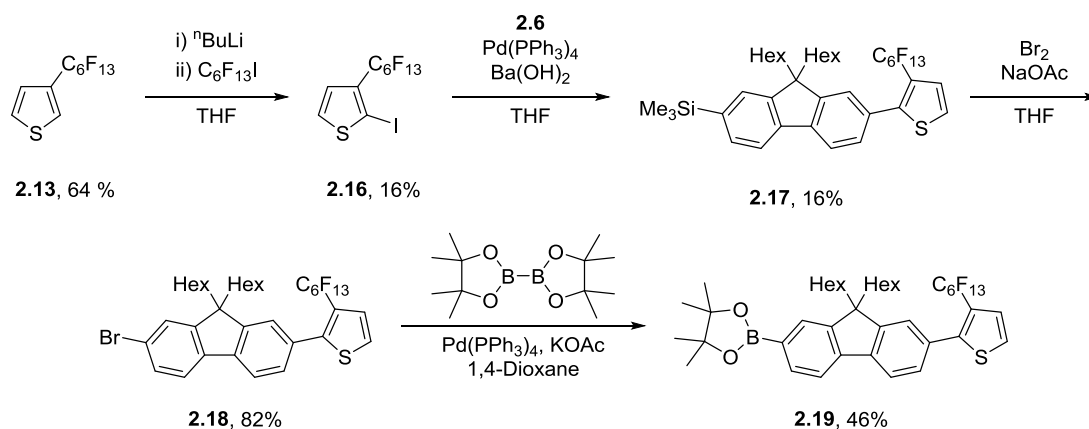
Scheme 2.5 Preparation of compound **2.14**.

Attempts to couple compound **2.14** to **T2Br** afforded an inseparable mixture of products from incomplete coupling. This synthetic step requires three reactions on the one molecule, and if these reactions are not sufficiently high yielding then it is likely that mixtures from partial coupling will be observed. It was therefore clear that a different synthetic route was required in order to afford the target molecules.



Scheme 2.6 Attempted coupling of perfluorohexyl thiophene to **T2Br**.

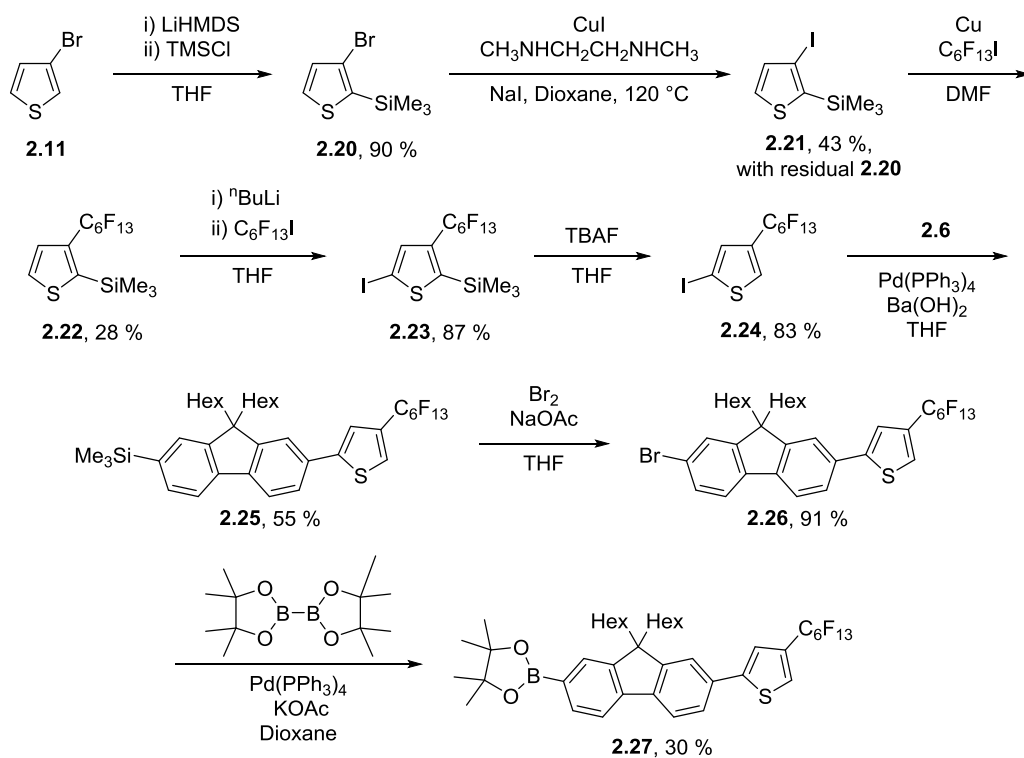
Since the coupling reaction of fluorenyl boronic acids with the tribromotruxene core are almost quantitative in yield (see Scheme 2.4), the new synthetic route selected involved the coupling of 3-perfluorohexylthiophene with one fluorene unit. The resulting fluorene-thiophene substrate could then be functionalised and coupled to the truxene core. Lithiation of 3-perfluorohexylthiophene, **2.13**, and treatment with perfluorohexyl iodide gave the product 2-iodo-3-perfluorohexylthiophene **2.16**. The regioselectivity of this reaction was poor, and the product was obtained as a mixture with its isomer, 2-iodo-4-perfluorohexylthiophene, which was separated by column chromatography. Compound **2.16** then underwent Suzuki-Miyaura coupling with **2.6**, and the product obtained, **2.17**, was deprotected by bromination and then reacted with bis(pinacolato)diboron to afford boronic ester **2.19**.



Scheme 2.7 Synthesis of thiophene-fluorene arm for 3-isomer.

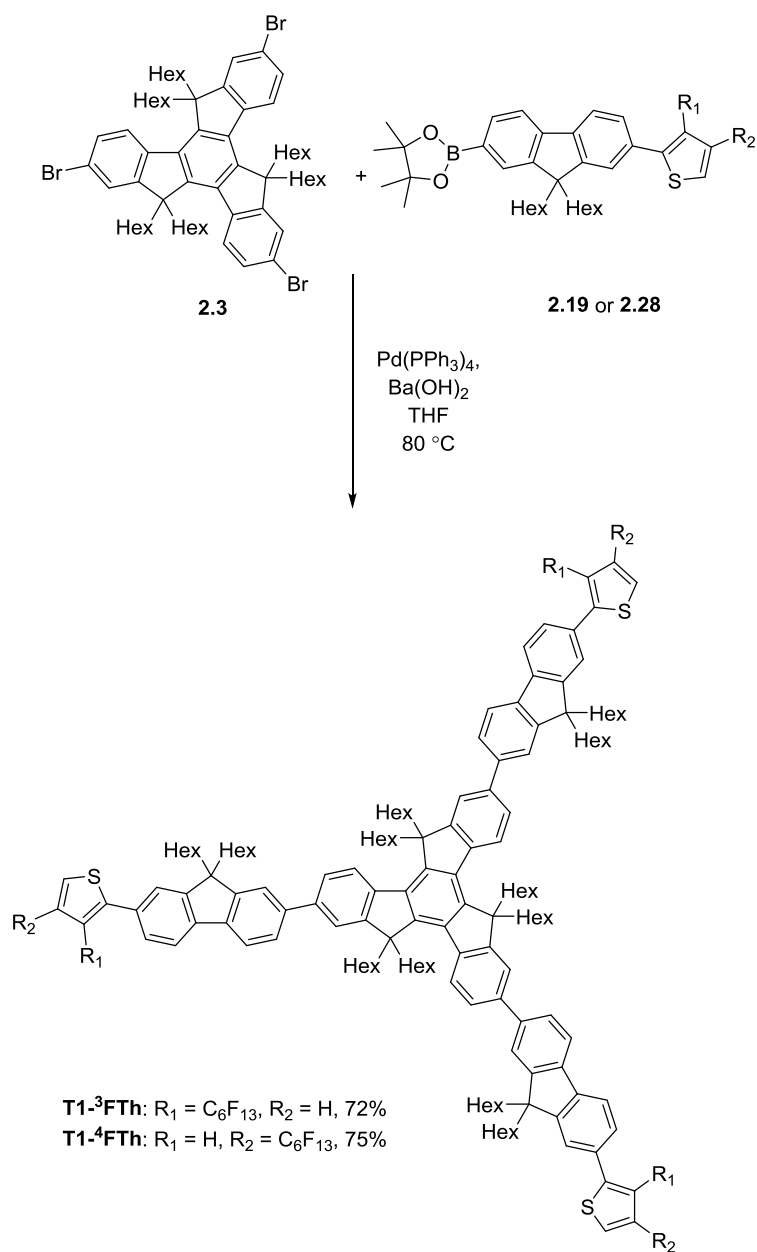
While Scheme 2.7 shows the synthetic route that afforded the target material where the perfluorohexyl chain is attached to the C3-position of the thiophene, Scheme 2.8 shows the synthetic route that affords perfluorohexyl chain at the C4-position of the thiophene. The synthesis of 2-iodo-4-perfluorohexylthiophene, **2.24**, began with treatment of 3-bromothiophene, **2.11**, with lithium bis(trimethylsilyl)amide and

chlorotrimethylsilane to afford 2-trimethylsilyl-3-bromothiophene, **2.20**. However, although conditions were unchanged, the halogen exchange reaction used to afford **2.21** was poorer yielding than that which produced **2.12**. A ^1H NMR spectra of a sample from the reaction mixture showed that this was due to incomplete conversion from the bromide to the iodide. The poorer conversion is attributed to the increased steric bulk provided by the trimethylsilyl group at the neighbouring carbon inhibiting insertion of the copper iodide into the carbon-bromine bond. The inability to separate **2.20** and **2.21** meant that this mixture was not further purified, and the mixture was taken forward. The subsequent copper mediated coupling reaction to afford **2.22** was also poor yielding and a mixture of **2.20**, **2.21** and **2.22** was obtained, which was determined again by a ^1H NMR of a sample of the reaction mixture. Compound **2.22** was recovered pure by a fluorinous extraction from a 5 % water/ethanol solution. Lithiation and treatment with perfluorohexyliodide afforded **2.23**, which was then deprotected using TBAF to afford **2.24**. The boronic ester **2.27** was then synthesized using the same steps as compound **2.19**.



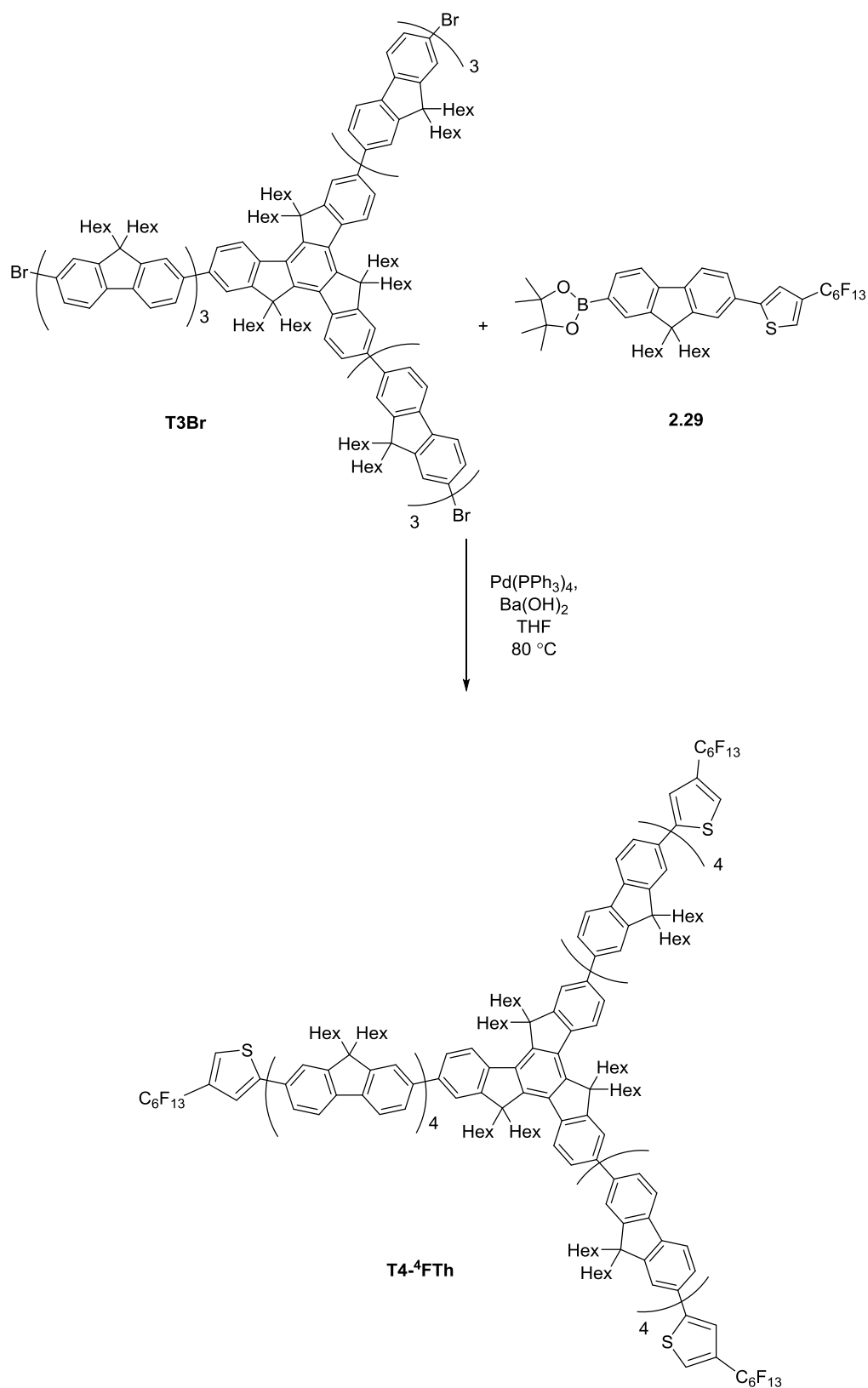
Scheme 2.8 Synthesis of thiophene-fluorene arm for 4-isomer.

T1-³FTh and **T1-⁴FTh** were then synthesized by Suzuki-Miyaura coupling of **2.3** and the relevant boronate ester, **2.19** or **2.28** (Scheme 2.9).



Scheme 2.9 Coupling of arms to truxene core.

T4-⁴FTh (Scheme 2.10) was synthesized by coupling **2.28** with **T3Br**.



Scheme 2.10 Synthesis of **T4-4FTh**.

2.3 Results and Discussion

In comparison to the corresponding spectra of **T1** and **T4**, the introduction of perfluorohexyl thiophene units to the terminal positions on the arms leads to a red shift in absorption (Table 2.1). The red shift observed within the **4FTh** – substituted series (**T1-4FTh** and **T4-4FTh**) increases with increasing chain length. The absorption of the oligomers in solution (dichloromethane), shown in Figure 2.1, all exhibit strong $\pi\text{-}\pi^*$ transitions. The maximum absorption band was observed at 349 nm for **T1-3FTh**, 362 nm for **T1-4FTh**, and 380 nm for **T4-4FTh**. Using the onset of absorption, the optical HOMO-LUMO gaps were estimated to be 3.22, 3.18 and 3.05 eV for **T1-3FTh**, **T1-4FTh** and **T4-4FTh**, respectively. In comparison to the HOMO-LUMO gap for **T1**, the gaps for **T1-3FTh** and **T1-4FTh** are slightly narrower. With regards to the HOMO-LUMO gap of **T4-4FTh**, there is no observed difference between itself and that of **T4**.

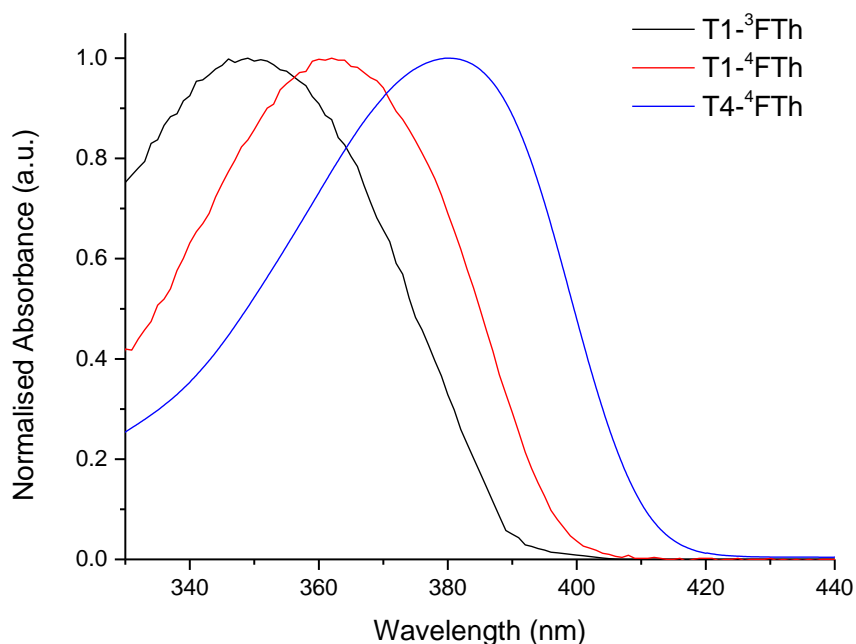


Figure 2.1 Normalised absorbance of **TX-^YFTh** materials in solution (CH_2Cl_2 , 1×10^{-6} M).

Compound	λ_{\max} (nm) Absorption (CH ₂ Cl ₂)	Onset (nm)	ϵ (mM ⁻¹ cm ⁻¹)	HOMO-LUMO Gap (eV)
T1-³FTh	349	387	306	3.22
T1-⁴FTh	362	392	323	3.18
T4-⁴FTh	380	409	385	3.05
T1^a	343	-	-	3.29
T4^a	374	-	-	3.05

^a Values obtained from the literature¹⁴⁷

Table 2.1 Absorbance Data for **TX-YFTh** and **TX** materials.

The emission spectra for the oligomers are shown in Figure 2.2. The maximum wavelength of emission was observed at 412 nm for **T1-³FTh**, 402 nm for **T1-⁴FTh**, and 421 nm for **T4-⁴FTh**. Comparison of the spectra for **T1-³FTh** and **T1-⁴FTh** shows a pronounced vibronic feature at 418 nm in the spectrum for **T1-⁴FTh**, that is not observed in the spectrum of **T1-³FTh**. This is an indication of the planarity of the **T1-⁴FTh** molecule's ground state in comparison to that of its isomer. While the emission spectrum of **T4-⁴FTh** also reveals the vibronic structure, it is less pronounced, with a shoulder at 440 nm. The Stokes shift for **T1-⁴FTh** and **T4-⁴FTh** are 40 and 41 nm respectively; however the shift for **T1-³FTh** is larger, at around 63 nm. This is an indication that the excited state of **T1-³FTh** undergoes a greater conformational change before emission than that of **T1-⁴FTh**, which is further evidence of the greater planarity in the **T1-⁴FTh** ground state compared to that of its isomer. The photoluminescence quantum yield of **T1-⁴FTh** and **T4-⁴FTh** was estimated by measuring the absorbance and emission at varying concentrations and plotting the value of the integrated emission against $1 \cdot 10^{-\text{Abs}}$, affording a straight line relationship. Similar studies were also carried out on 9,10-diphenylanthracene, which was used as a standard with a known quantum yield.¹⁵¹ These gave PLQY values of 0.86 and 0.93 for **T1-⁴FTh** and **T4-⁴FTh** compounds respectively.

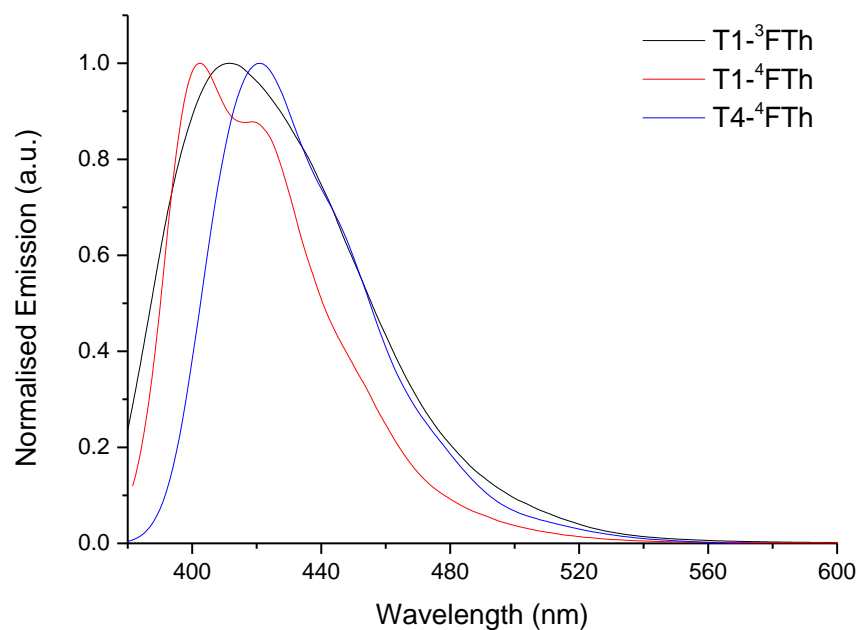


Figure 2.2 Normalised emission of **TX-YFTh** materials materials in solution (CH_2Cl_2 , 5×10^{-7} M).

Compound	λ_{max} (nm) Emission (CH_2Cl_2)	Φ_{PL} (CH_2Cl_2)
T1-³FTh	412	-
T1-⁴FTh	402, 418	0.86
T4-⁴FTh	421, 440sh	0.93
T1^a	375sh, 396, 416sh	-
T4^a	411, 436, 460sh	-

Table 2.2 Emission Data for **TX-YFTh** and **TX** materials.

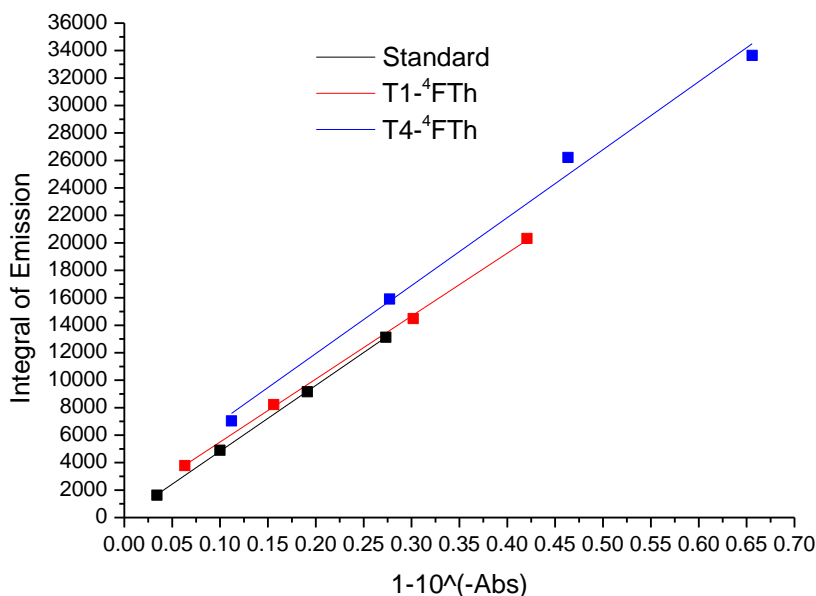


Figure 2.3 Plot of absorbance vs integral of emission.

The cyclic voltammograms for the oxidation and reduction of the oligomers are shown in Figures 2.4-2.6. **T1-³FTh** showed one irreversible oxidation peak at +1.09 V, and a reduction peak was found at -2.22 V. From the onset of the oxidation and reduction peaks the HOMO level was estimated to be -5.72 eV, and the LUMO -2.74 eV, using data referenced to the ferrocene/ferrocenium redox couple, which has a known value of -4.8 eV.^{152, 153} In comparison to the HOMO and LUMO values for **T1** (-5.6 and -2.2 eV),¹⁴⁷ there is a decrease in the HOMO and a large decrease in the LUMO, resulting in a contraction of the HOMO-LUMO gap. For **T1-⁴FTh**, quasi-reversible oxidation peaks were found at +0.86 and +1.03 V, while irreversible peaks were found at +1.26 and +1.44 V. A reduction peak was observed at -2.84 V. From the onset of the oxidation and reduction peaks the HOMO level was estimated to be -5.55 eV, and the LUMO -2.39 eV. In comparison to the values of **T1**, there is no significant difference in the HOMO value, while the LUMO decreased, resulting in a narrowed electrochemical HOMO-LUMO gap. A similar effect is observed for **T4-⁴FTh** in comparison with **T4**,¹⁴⁷ where the HOMO is -5.53 eV

compared to -5.5 eV for **T4** and the LUMO is lower (-2.35 eV for **T4-4FTh** and -2.3 eV for **T4**). While there is good agreement between the values of electrochemical and optical HOMO-LUMO gap for **T1-4FTh** and **T4-4FTh** oligomers, for **T1-3FTh** there is a difference of 0.24 eV.

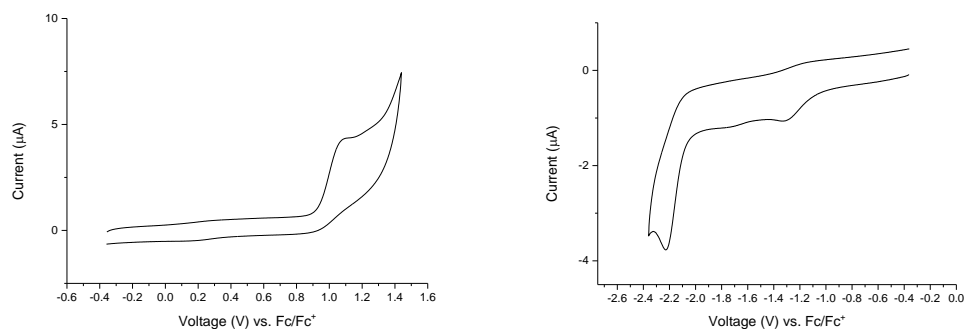


Figure 2.4 Oxidation (left) and reduction (right) waves from cyclic voltammetry of **T1-3FTh** in dichloromethane, electrolyte 0.1 M Bu_4NPF_6 , glassy carbon electrode, scan rate 100 mVs^{-1} .

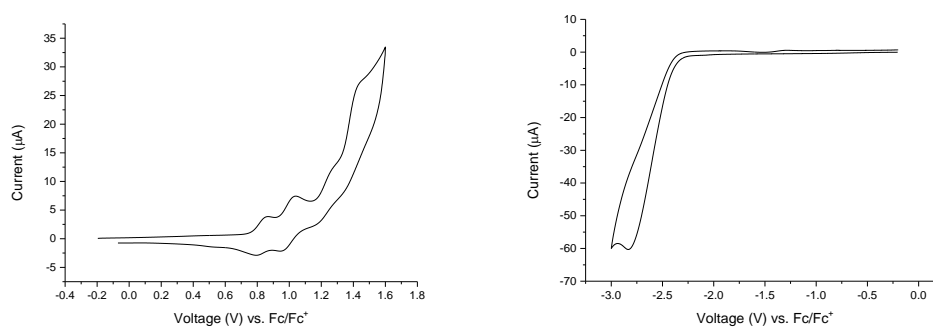


Figure 2.5 Oxidation (left) and reduction (right) waves from cyclic voltammetry of **T1-4FTh** in tetrahydrofuran, electrolyte 0.1 M Bu_4NPF_6 , glassy carbon electrode, scan rate 100 mVs^{-1} .

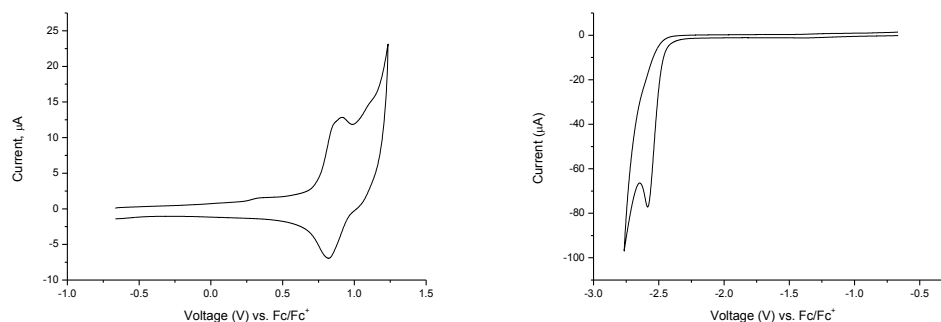


Figure 2.6 Oxidation (left) and reduction (right) waves from cyclic voltammetry of **T4-4FTh** in 1:1 acetonitrile/benzene, electrolyte 0.1 M Bu_4NPF_6 , glassy carbon electrode, scan rate 100 mVs^{-1} .

Compound	E_{ox} (V) Peaks $E_{\text{Pa}}/E_{\text{Pc}}$ or E_{Pa}^a	HOMO	E_{red} (V) Peaks E_{P}	LUMO	HOMO-LUMO Gap (eV)
T1-3FTh	+1.09	-5.72	-2.22	-2.74	2.98
T1-4FTh	+0.86/0.79 +1.03/0.96 +1.26 ^b +1.44 ^b	-5.55	-2.84	-2.39	3.16
T4-4FTh	+0.91/+0.82 ^c +1.11 ^c	-5.53	-2.59	-2.35	3.18
T1^d	-	-5.6	-	-2.2	3.4
T4^d	-	-5.5	-	-2.3	3.2

^aNo cathodic peak is reported where the wave is irreversible, ^bPeak exists as a shoulder, ^cTwo unresolved single electron peaks, ^dValues obtained from the literature.¹⁴⁷

Table 2.3 Electrochemical Data for **TX-YFTh** and **TX**.

In order to rationalise the difference in optical and structural properties between the two isomers, DFT calculations were performed on the smaller truxenes (Figures 2.7 and 2.8). The **T1-3FTh** and **T1-4FTh** structures were optimised in the gas-phase using the BP86-D functional,¹⁵⁴⁻¹⁵⁶ with the def2-TZVP basis set,¹⁵⁷ implemented in TURBOMOLE 6.3.1.¹⁵⁸ The optimisations were carried out using the RI-J

approximation.¹⁵⁹ The hexyl chains on the fluorene units were shortened to methyl groups in the model in order to decrease the computational cost of the simulation.

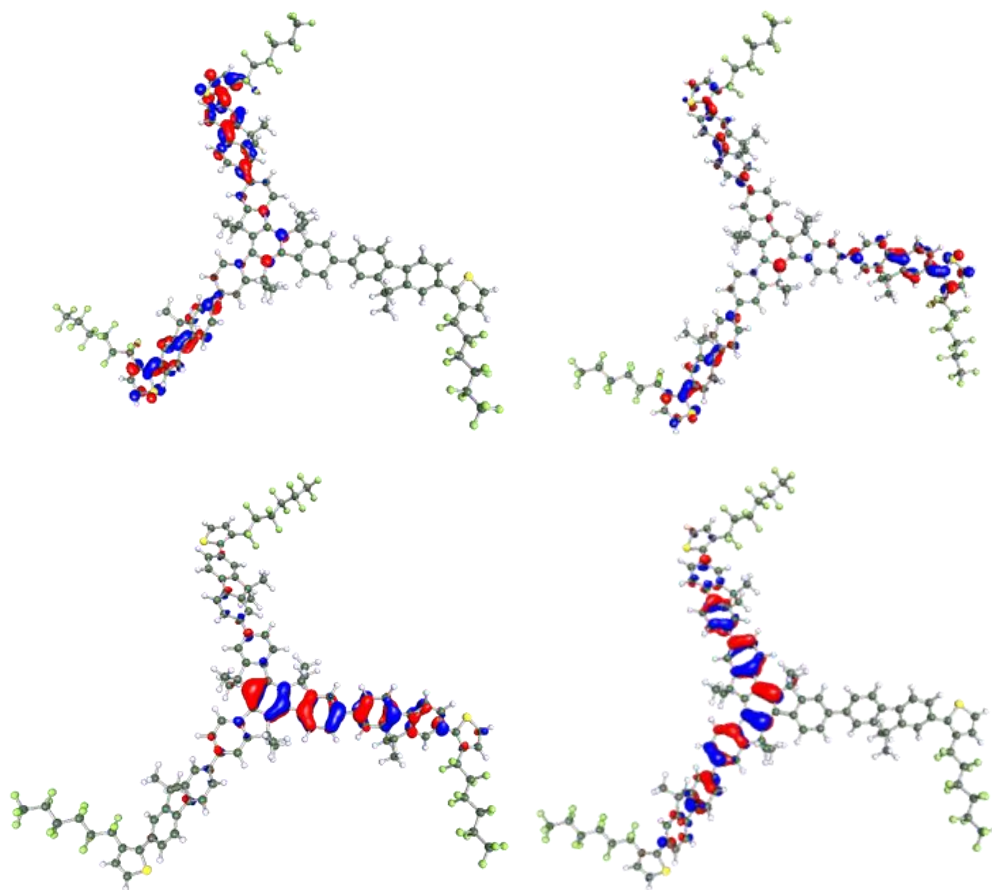


Figure 2.7 HOMO-1 (bottom, left), HOMO (bottom, right), LUMO (top, left) and LUMO+1 (top, right) of **T1-3FTh**. Coloured regions indicate the different phases within the molecular orbitals.

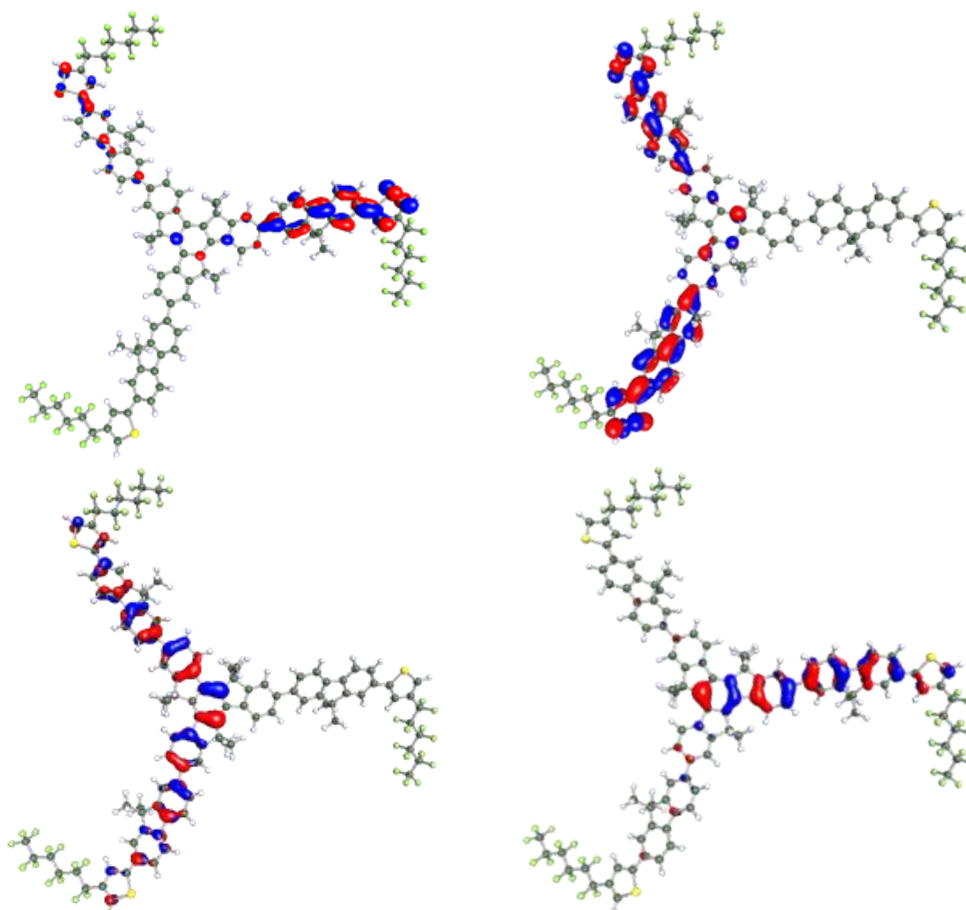


Figure 2.8 HOMO-1 (bottom, left), HOMO (bottom, right), LUMO (top, left) and LUMO+1 (top, right) of **T1-4FTh**. Coloured regions indicate the different phases within the molecular orbitals.

The main structural difference observed is the degree of twisting between the fluorene and thiophene in the two structures. The average dihedral angle in **T1-3FTh** is 40.9° whilst there is a much smaller twist of 6.4° in **T1-4FTh**. The frontier orbitals of the isomers were also compared and are shown below (Figures 2.7 and 2.8). The HOMO-1 and HOMO for both molecules ($\Delta E[\mathbf{T1-3FTh}] = 0.0054$ eV and $\Delta E[\mathbf{T1-4FTh}] = 0.0030$ eV) are essentially degenerate and show a splitting due to a slight break in symmetry. This is also the case for the LUMO and LUMO+1 of each isomer ($\Delta E[\mathbf{T1-3FTh}] = 0.013$ eV and $\Delta E[\mathbf{T1-4FTh}] = 0.0047$ eV). The HOMO-1 and HOMO of the compounds show there to be a larger contribution of

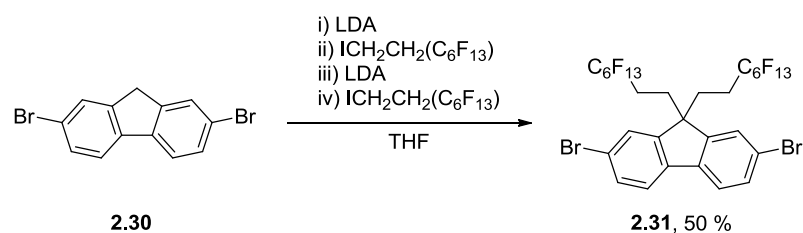
the thiophene unit to the conjugation of the molecule in **T1-4FTh** compared to **T1-3FTh**. This reaffirms that the thiophene unit of **T1-3FTh** is too twisted to contribute significantly to the conjugation of the molecule.

2.4 Conclusions and Future Work

In conclusion, three new star-shaped oligomers, namely **T1-3FTh**, **T1-4FTh**, **T4-4FTh**, have been synthesised. For the smaller molecules, the presence of the powerfully electron withdrawing perfluorohexyl chain within the molecules leads to a more stabilised LUMO, in comparison to the non-substituted analogue **T1**. The optical and electrochemical properties of the molecules with shorter oligofluorene arms are altered to a much greater extent than the conjugated system containing longer oligofluorene arms, where HOMO and LUMO levels as well as the optical HOMO-LUMO gaps remain essentially the same for the substituted and the parent systems. The electrochemical properties of **T1-3FTh** are more affected by the presence of the perfluoroalkyl thiophene substituent than those of **T1-4FTh**.

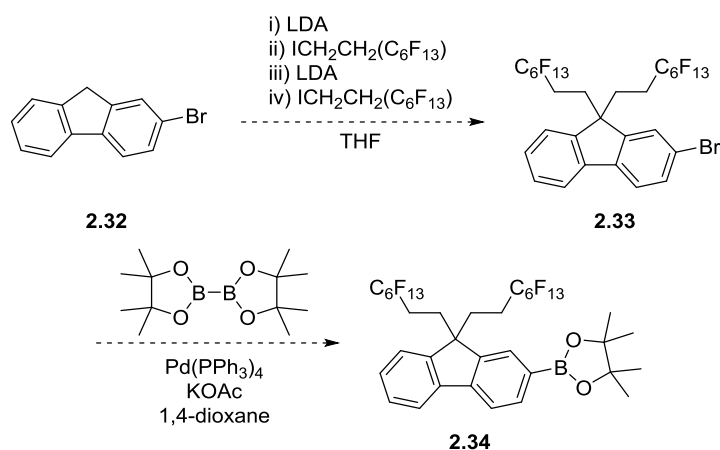
Unfortunately, the materials were found to have poor solubility in fluorinated solvents such as perfluorohexanes and perfluoroethers. We believe that greater fluorine content is required within the molecules for them to be soluble in such solvents. One way to achieve this would be to alter the alkyl chains attached to the fluorenes throughout the molecule with perfluoroalkyl chains. However, perfluoroalkyl chains do not undergo S_N2 type reactions and therefore there is no way to readily alkylate the fluorene units. One solution to this challenge is to employ short alkyl spacer groups, such as methylene and ethylene groups. While this allows for easy alkylation of carbocyclic and heterocyclic units, it places the perfluorohexyl chain further away from the conjugated unit and therefore lessens the electronic effects. Ober *et al.* have demonstrated the

synthesis of semiperfluoroalkyl polyfluorenes, with both $(\text{CH}_2)_2$ and $(\text{CH}_2)_4$ spacer units, reporting good solubility in fluorinated solvents.¹⁴⁴ Optical and electrochemical studies of these materials showed that, in comparison to alkylated polyfluorenes the HOMO and LUMO levels were reduced with a widening on the band gap. The alkylation of the fluorene monomers with $(\text{CH}_2)_2$ spacer groups required *n*-butyllithium as the base, followed by bromination under harsh conditions. The resulting dibromide was not reactive towards lithium-halogen exchange, and therefore it would not be possible to asymmetrically functionalise the fluorene unit. However, in the course of these studies we have demonstrated the semiperfluoroalkylation of 2,7-dibromofluorene using lithium diisopropylamine as base to afford compound **2.31** (Scheme 2.11), with yields consistent with those reported by Ober *et al.*

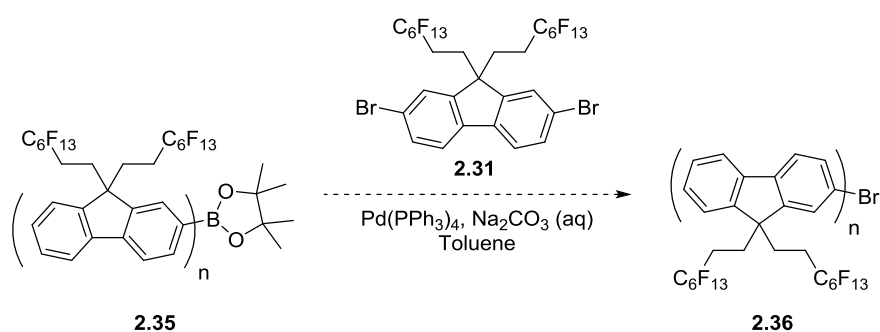


Scheme 2.11 Semi-perfluoroalkylation of fluorene.

Using these conditions, a monobromo-semiperfluoroalkyl-fluorene, **2.33**, could be synthesised (Scheme 2.12). Through reaction of **2.33** with bispinacolatodiboron under Suzuki-Miyaura conditions, compound **2.34** can be synthesised, and used as a starting block to afford oligo(fluorenes) containing semiperfluoroalkyl chains (Scheme 2.13), which to date have not been investigated. This could then lead to a route towards starshaped semiperfluoroalkyl oligofluorenes.



Scheme 2.12 Functionalisation of semiperfluoroalkyl-fluorene.



Scheme 2.13 Coupling of semiperfluoroalkyl-fluorene.

While having longer alkyl spacers would allow for easier synthesis of such compounds, as demonstrated by Ober *et al.*, they would also inhibit π - π stacking of the oligomers in the bulk material due to longer chain length. A further downside would also be in the increased molecular weight of material without any increase in fluorophore units, which is undesirable. One alternative to this would be to employ longer alkyl spacer groups with shorter perfluoroalkyl chain length. However, the length of the perfluoroalkyl chain will have an effect on solubility in fluorinated solvents, and therefore the length of alkyl/perfluoro alkyl chain must be carefully selected.

3 Tri(ethylene glycol) substituted oligofluorene-functionalised truxenes

3.1 Introduction

As stated previously within this report, the alkyl chains present at the 9-positions of the fluorene unit have a dual purpose; protecting the position against oxidation whilst also providing solubility. By applying alkyl chains with varying polarity, the solubility of the overall fluorene unit can be manipulated. The most common substituents reported are linear alkyl chains, which provide solubility in non-polar solvents and, depending on length, inhibit aggregation. For the purpose of orthogonal processing it was in our interest to develop fluorene based materials that are soluble in polar solvents. To obtain solubility in polar solvents such as methanol, acetonitrile and even water there are two approaches: covalent and non covalent.

The covalent approach involves the introduction of alkyl chains which are covalent in nature whilst affording polar solubility. The most common examples are those employing ethylene glycol chains **3.1**,^{104, 160-165} and other examples include alkyl chains terminated with diethanol-amino **3.2**,¹⁶⁶ and phosphonate functionalities, **3.3**.¹⁶⁷

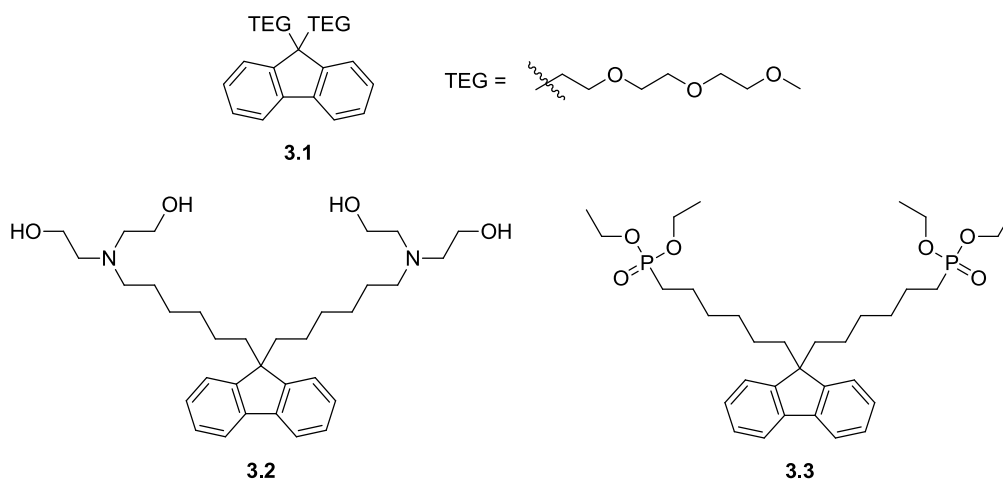


Figure 3.1 Examples of covalent polar fluorenes.

The HOMO-LUMO levels of polymers and co-polymers of these units are such that they have been applied as ETLs,^{167, 168} some of which also show effective hole blocking properties. In each case excellent electron injection was observed, which is rationalised by the ability of lone pairs on the heteroatoms of the side chains to coordinate to metal cathodes, such as aluminium.¹⁶⁹ This creates an interfacial layer which facilitates efficient electron injection from the electrode.

The non covalent approach involves alkyl chains with ionic terminal groups, which usually results in high solubility in water/alcohol mixtures. By far the most common examples are ammonium terminated alkyl chains, with a range of counterions possible.^{64, 170-173} The selection of the counterion is an important one, as different counterions influence the optical and electrochemical properties of the overall polymer or oligomer to varying degrees, which allows for the tuning of these properties. Yang *et al.* investigated the effect of counterion on a benzothiadiazole and fluorene copolymer.¹⁷⁴

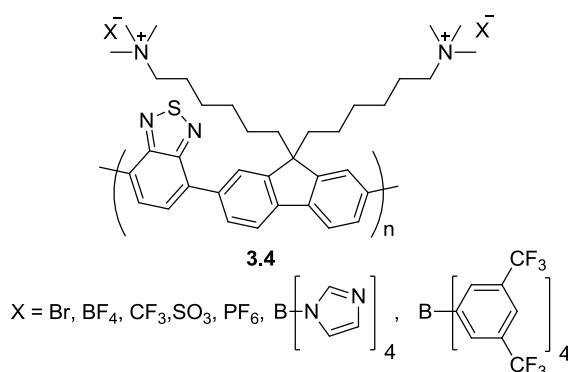


Figure 3.2 Fluorene with ionic side chains with varying counterions.

The authors found a general trend where the quantum yield of photoluminescence increased with increasing size of counterion in the solid state and in water, whereas the same trend was not observed for solvents including DMSO. This trend was attributed to the greater inter-

chain distance with increasing counterion size, which is believed to directly decrease the level of photoluminescence self quenching.

Recently, Lonergan *et al.* have reported poly(fluorene-co-alt-fluorene)s polyelectrolytes based on repeat units of **3.1** and a fluorene unit substituted with alkyl chains containing a sodium sulfonate group (Figure 3.3). By varying the monomer ratios, the ionic character of the polymer (the ratio of ionic functional groups to aromatic rings) could be controlled.¹⁷⁵

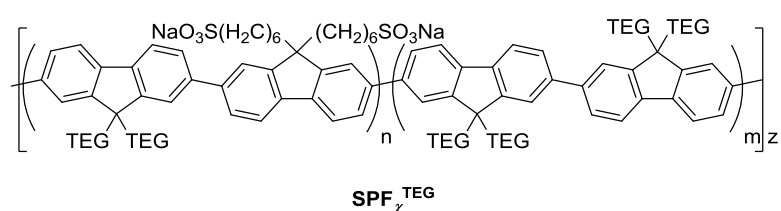


Figure 3.3 Structure of $\text{SPF}_x^{\text{TEG}}$.

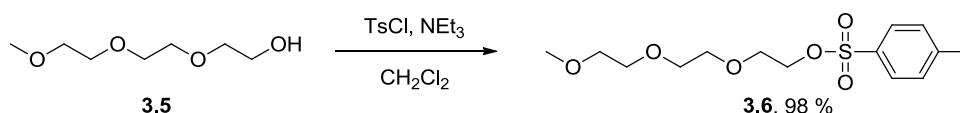
One drawback of using ionic species in conducting polymers is their instability towards doping. Sax *et al.* have demonstrated that an OLED device employing a poly(fluorene) substituted with the sodium salt of an alkyl sulfonic acid chain, which afforded the polymer good solubility in water, as an electron transport layer gave evidence of increasing onset voltages and smaller electroluminescence efficiency over time when a bias was applied.¹⁷⁶ The authors attributed this phenomenon to the fact that the cation counterions moved under bias towards the cathode, while the anions remain fixed in place on the side chains of the polymer. This effectively resulted in *n*-doped and *p*-doped areas within the material in the device, leading to a change in the device performance over time.

The approach taken within this research was to alter the side chains of the previously published oligofluorene-functionalised truxenes such that the resulting analogues were soluble in polar solvents for the purpose of

orthogonal processing. Due to the instability of ionic based materials towards doping, the covalent approach was selected.

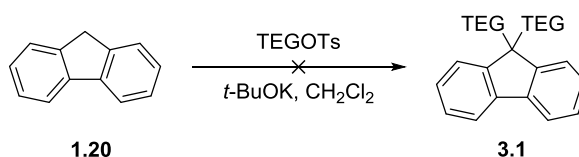
3.2 Synthesis

At the time of conducting the research no direct route to compound **3.1** had been reported directly from commercially available material. Therefore a synthetic route to compound **3.8**, which would be the repeat unit within the oligomers, was required. Triethylene glycol mono methyl ether **3.5** was selected due to its wide availability at low cost, and is converted to the tosylate derivative, TEGOTs **3.6**, in almost quantitative yield.



Scheme 3.1 Preparation of TEGOTs, **3.6**.

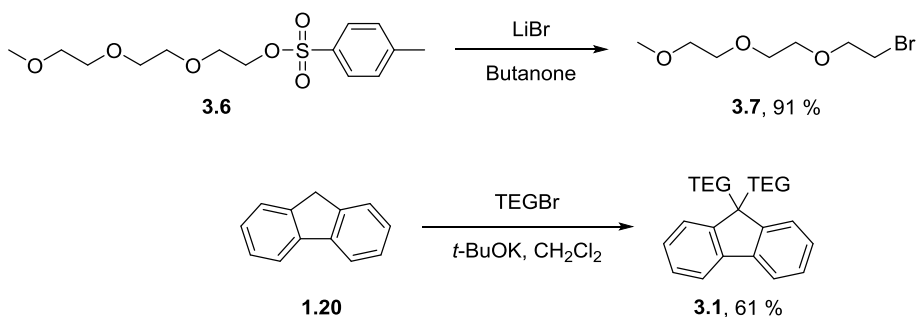
However, using the tosylate **3.6** as the alkylating reagent with fluorene did not afford the target material (Scheme 3.2), and instead a mixture of partially alkylated material and starting materials was obtained.



Scheme 3.2 Unsuccessful alkylation of fluorene with TEG chains.

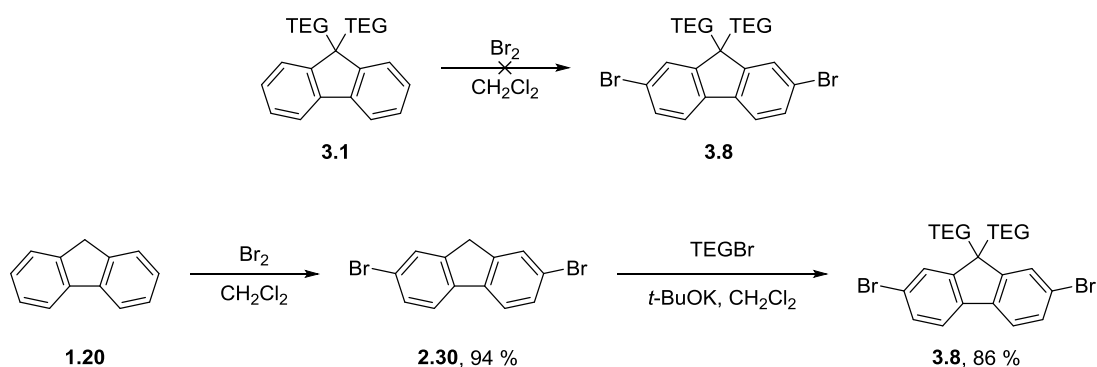
The tosylate **3.6** was then converted to the bromide derivative under Finkelstein conditions similar to those reported by Swager *et al.*¹⁷⁷ In this instance, by using lithium bromide as the salt, the bromide derivative, **3.7** TEGBr, was obtained pure after distillation. Recently, Turner *et al.* have reported a very similar route to convert **3.6** to **3.7**, using sodium bromide

as the salt and acetone as the solvent, albeit with a poorer yield.¹⁷⁸ By using the bromide as the alkylating reagent the di-TEG-fluorene, **3.1**, was obtained (Scheme 3.3).



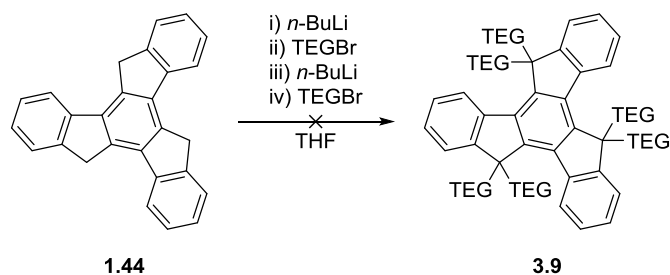
Scheme 3.3 Successful alkylation of fluorene with TEG chains.

In order to further functionalise the fluorene unit halogenation was first required. However, bromination under the conditions reported for that of 2,7-dibromo-9,9-dihexylfluorene, **2.5**, did not afford the desired product. ¹H NMR of the crude reaction mixture displayed a complex array of peaks between 3 and 4 ppm, where the -CH₂- peaks for the TEG chains normally appear. It was assumed that the TEG chains were not stable under the conditions for bromination. Therefore, in order to circumvent this problem bromination of fluorene was performed first, followed by alkylation, in order to form compound **3.8** (Scheme 3.4).



Scheme 3.4 Alkylation of 2,7-dibromofluorene with TEG chains.

Attempts to synthesise a truxene core with TEG alkyl chains were unsuccessful (Scheme 3.5). The sequential process of deprotonation and addition of electrophile, then a second deprotonation and addition of excess electrophile gave multiple inseparable products which were, as determined from ^1H NMR analysis, the products of incomplete alkylation.

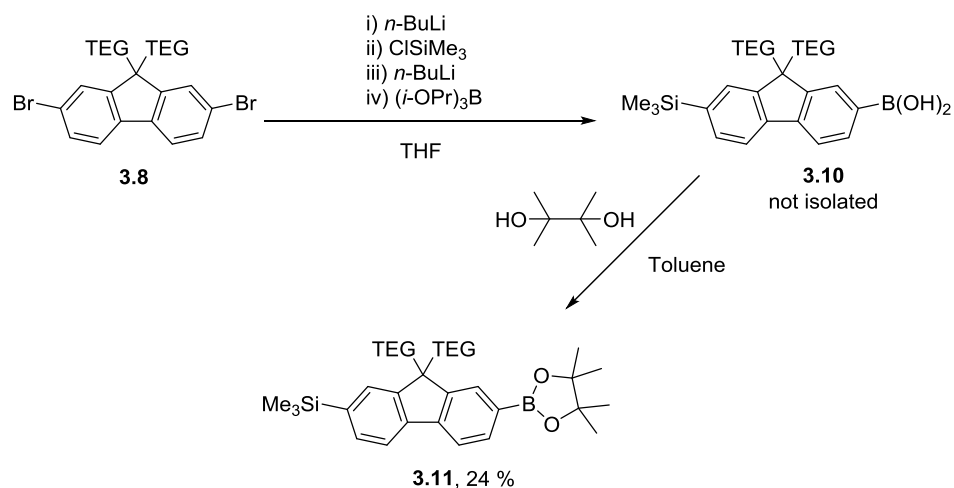


Scheme 3.5 Unsuccessful alkylation of truxene with TEG chains.

Therefore, the hexahexyltruxene **2.3** was selected as the core. It was hoped that the chains on the truxene core, being at the centre of the star shaped oligomers, would not contribute greatly in comparison to that of the oligofluorene arms to the overall solubility of the oligomer. While shorter alkyl chains would ensure no contribution to the solubility, in order to completely suppress aggregation in the bulk material of oligo-fluorenyl truxenes, which is centred at the truxene core, hexyl chains have been selected.

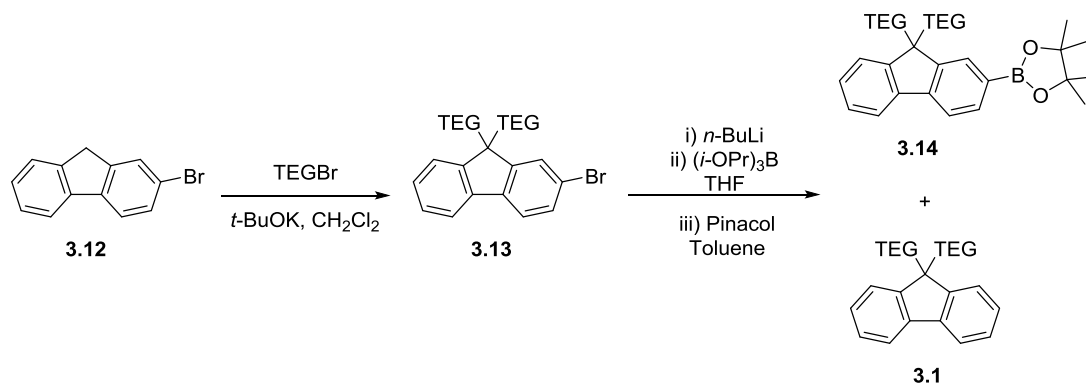
The original synthetic pathway towards polar oligofluorenes was identical to that of the non-polar oligofluorenes previously published and also present within chapter 2 of this report. The first step was the one-pot, two-step asymmetric functionalisation to afford fluorene with trimethylsilyl and boronic acid functional groups. However, compound **3.10** was not recovered from the silica gel column during purification. It was assumed that the acid was not stable on silica, and the reaction was repeated, but in this instance the crude material was instead dissolved in a solution of toluene and pinacol to afford the boronate ester. In this

instance the functionalised fluorene compound, **3.11**, was obtained from the column, albeit with slight impurities present. However the yield was very poor, and was not improved upon reattempts.



Scheme 3.6 Preparation of **3.11**.

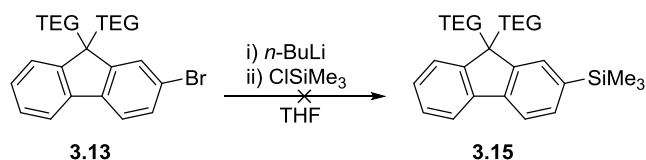
To investigate why such a poor yield of compound **3.11** was observed, the monobromofluorene **3.13** was synthesised using alkylation conditions identical to those which produced **3.8** (Scheme 3.7).



Scheme 3.7 Investigation of side products formed during the preparation of **3.14**.

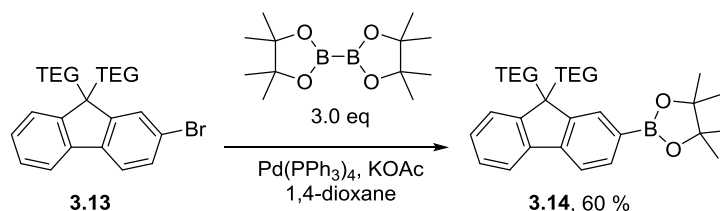
Attempts to functionalise **3.13** with a boronate ester group by lithiation afforded the desired product, but low yields and small quantities of

inseparable impurities were again observed. In addition, a single by-product from the reaction mixture was also isolated during purification, the ^1H NMR of which was consistent with the unfunctionalised di-TEG-fluorene **3.1**. The combined number of moles of compounds **3.14** and **3.1** were close to that of the number of moles of **3.13** used in the reaction (approx. 94 %). It can be assumed therefore that the lithium halogen exchange goes to completion, however reaction with the electrophile did not and compound **3.1** was produced during aqueous workup. To confirm that the poor yields observed were not dependent upon the electrophile an attempt was made to synthesise 2-trimethylsilyl-di-TEG-fluorene by using trimethylsilyl chloride as the electrophile after lithiation of the bromo fluorene **3.13**. In this case, after workup, multiple inseparable products were obtained. This confirms that the poor yields observed during functionalisation of diTEG-fluorenes by lithiation are not dependent on the electrophile.



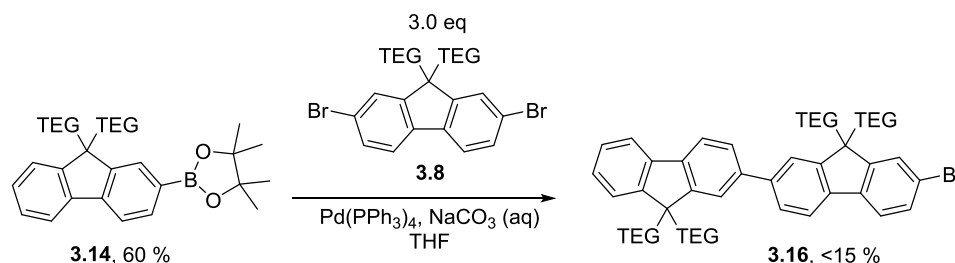
Scheme 3.8 Attempted synthesis of **3.15** *via* Li-halogen exchange of **3.13**.

It therefore became evident that functionalisation utilising alkyl lithium reagents were not suitable for fluorenes with ethylene glycol chains. To address this issue, a palladium catalysed cross-coupling reaction with excess bispinacolatodiboron afforded the boronate ester **3.14** in good yield without impurities after precipitation from diethyl ether.



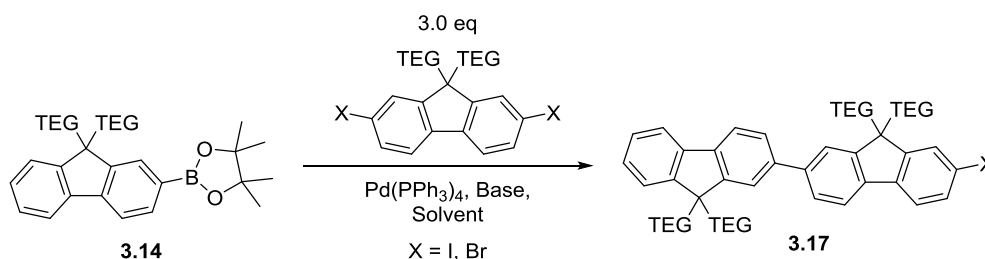
Scheme 3.9 Synthesis of compound **3.14**.

Since compound **3.14** is asymmetrically functionalised it is a suitable starting material to build oligomers by the same synthetic route as planned. The next step is the Suzuki-Miyaura cross-coupling reaction of **3.14** with excess of the dibromo-diTEG-fluorene, **3.8** (Scheme 3.10).



Scheme 3.10 Suzuki-Miyaura cross-coupling of **3.14** with **3.8**.

This reaction again was low yielding and the desired compound was not separable by silica gel chromatography from some side-products. A range of conditions were tried in an attempt to improve the yield, as detailed below in Table 3.1. The general conditions are shown in Scheme 3.11.



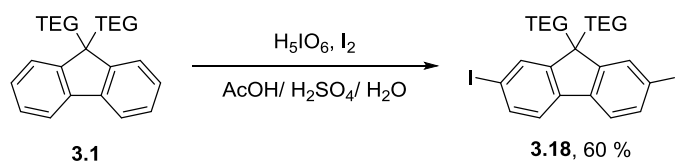
Scheme 3.11 General conditions for attempted preparation of bifluorene **3.17**.

Ent.	Halogen X	Base	Solvent	Reaction Time (h)	Temp (°C)	Yield
1	Br	Na ₂ CO ₃ (aq)	Toluene	18	80	S.M. only
2	Br	Na ₂ CO ₃ (aq)	THF	18	70	Poor (<25 %)
3	Br	Na ₂ CO ₃ (aq)	1,4-dioxane	18	90	Poor (<25 %)
4	Br	Na ₂ CO ₃ (aq)	DME	18	90	Poor (<25 %)
5	Br	Na ₂ CO ₃ (aq)	DMF	18	90	Poor (<25 %)
6	Br	Na ₂ CO ₃ (aq)	DME	72	90	Poor (<25 %)
7	Br	NaHCO ₃ (aq)	1,4-dioxane	18	90	S.M. only
8	Br	Ba(OH) ₂ (aq)	THF	18	70	Poor (<25 %)
9	Br	NaOAc	THF	18	70	S.M. only
10	Br	K ₃ PO ₄	DMF	18	90	Poor (<25 %)
11	I	Na ₂ CO ₃ (aq)	THF	18	70	Poor (<25 %)
12	I	CsF	DMF	18	90	Poor (<25 %)

Table 3.1 Conditions for Scheme 3.11.

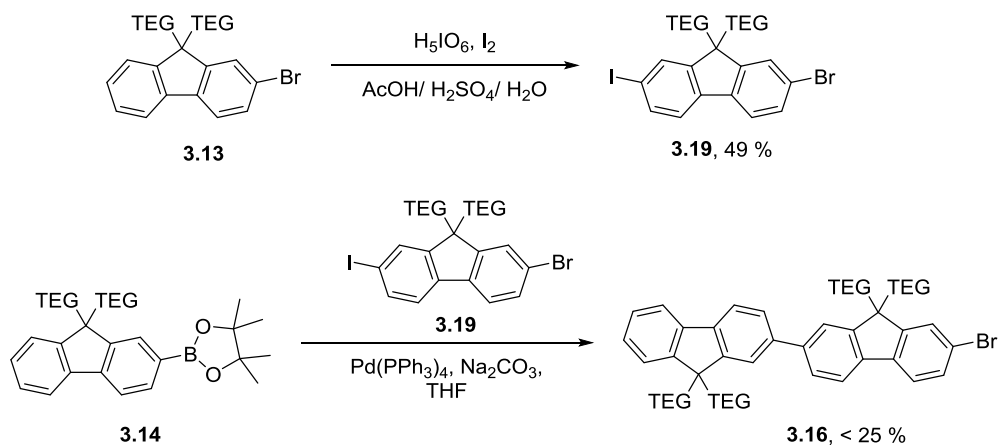
Entry 1 matches the conditions used in the successful synthesis for oligofluorenes in chapter 2, however only starting materials were observed in the ¹H NMR in this attempt. To probe the effect of solvent on the reaction, entries 2-5 were attempted with differing solvents, using firstly ethereal solvents such as THF, 1,4-dioxane and dimethoxyethane (DME) due to the good solubility of the starting materials in ethereal solvents, and then moving to DMF. In entry 2, using THF as the solvent, the compound was isolated with slight inseparable impurities as a yellow oil at approximately 25 % yield. In all other cases, the crude product was isolated and the ¹H NMR was compared to that of the crude mixture of entry 2, using the ratio of peaks corresponding to the terminal CH₃ group of the TEG chains of both the dibromo-diTEG-fluorene starting material and the product to estimate conversion to the product. In entry 3, 4 and 5, no improvement in the yield was observed by changing the solvent. To determine if the poor yields observed were a result of slow reaction kinetics, entry 6 describes a trial reaction which was allowed to stir at high temperature for 72 h, but no improvement upon yield was observed. Entry 7 matches the conditions reported by Sax *et al.* which successfully afforded a copolymer of fluorene units alkylated with tetra-ethylene glycol and poly-ethylene glycol chains.¹⁶⁴ However, under these conditions

only both fluorenyl starting materials were recovered. For entry 8 a strong base, barium hydroxide, was employed with poor yield again observed. In the previous 8 attempts the base was either added as an aqueous solution, or water was added to the reaction mixture to help solublise the base. The next two entries involved dry conditions, employing sodium acetate with THF and tribasic potassium phosphate with DMF. Since no improvement with these conditions was observed it can be inferred that the presence of water was not detrimental to the reaction. In entry 11, instead of the dibromo-fluorene, diiodo-diTEG-fluorene, **3.18**, was employed. Compound **3.18** was synthesised by iodination of **3.1**, shown in scheme 3.12. Using the same reaction conditions as entry 2, no improvement in reaction conversion was observed. Another attempt with **3.18** using yet untried conditions, employing caesium fluoride as the base in a DMF solution, again did not improve yields above the 25 % mark.



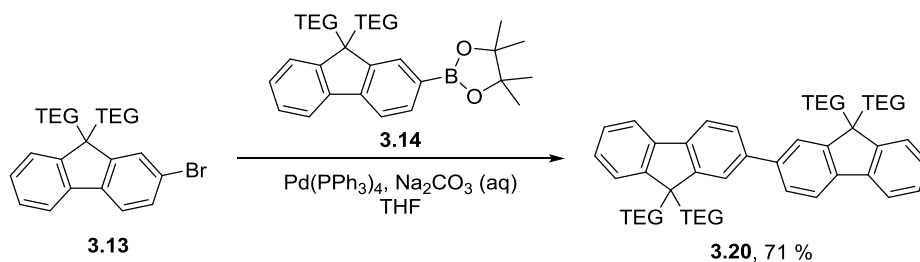
Scheme 3.12 Iodination of diTEG-fluorene.

Finally, a thirteenth attempt was made, in this case using 2-bromo-7-iodo-9,9-bis(2-(2-(2-methoxyethoxy)ethoxy)ethyl)-9H-fluorene **3.19** as the dihalogen (only 1.2 eq. employed). By using a fluorene with one bromide and one iodide, palladium insertion should take place selectively at the iodide, thus minimising the opportunity for formation of a terfluorene by-product. In this case however, poor yields were again observed, with inseparable impurities.



Scheme 3.13 Attempted coupling of **3.14** with **3.19**.

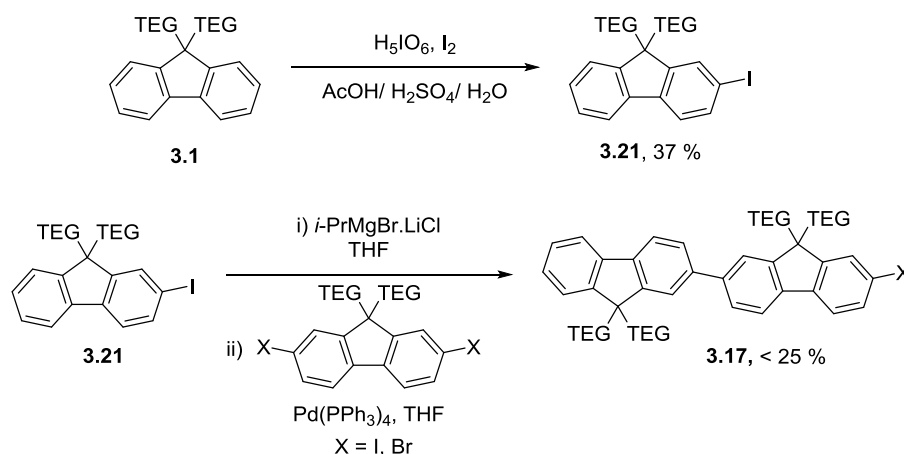
To attempt to understand the poor yields the reaction was simplified by reacting 1.2 eq of **3.14** with 1.0 eq of the monobromo-fluorene, **3.13** (Scheme 3.14). In this instance the bi-fluorene **3.20** was obtained without impurities, in good yield, after column chromatography.



Scheme 3.14 Successful preparation of bifluorene **3.20**.

In order to ascertain whether the poor yields observed were restricted to Suzuki-Miyaura coupling, it was within our interest to attempt the synthesis of oligofluorenes using a different coupling reaction. Geng *et al.* have published conditions which afforded oligofluorenes by way of Kumada coupling,¹⁰⁵ and Bazan *et al.* have successfully employed these conditions to afford a polyfluorene with PEG side chains of 7 repeat units in length.¹⁶³

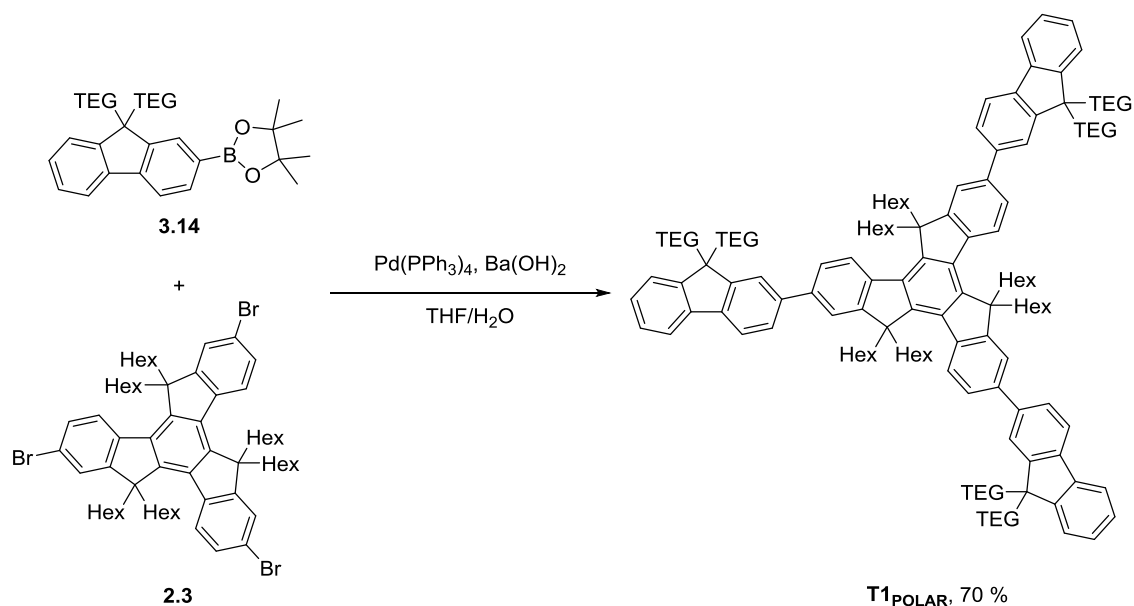
Bazan *et al.* have stated that the reaction of turbo Grignard reagents with bromo-fluorenes requires approximately 8 hours reaction time in order to achieve completion, but the reaction with iodo-fluorenyl compounds take as little as 1 h to achieve completion.¹⁰⁵ Therefore, iodo-diTEG-fluorene, **3.21**, was required, which was synthesised by mono-iodination of compound **3.1**. Compound **3.21** was treated with the turbo Grignard isopropylmagnesium chloride: lithium chloride complex and stirred for 1h, then transferred to a pre-stirred solution of dibromo-diTEG-fluorene and *tetrakis*(triphenylphosphine)palladium(0) and stirred at room temperature overnight. However, poor conversion to the desired product was observed. A second attempt with these conditions was made using instead diiodo-diTEG-fluorene, but once again poor yields, which were estimated from ¹H NMRs, were observed. Interestingly, yields were consistent with those observed from Suzuki-Miyaura coupling (Table 1). This shows that the poor yields observed in the coupling of diTEG-fluorenes is not limited to the Suzuki-Miyaura coupling reaction.



Scheme 3.15 Attempted synthesis of **3.17** by Kumada coupling.

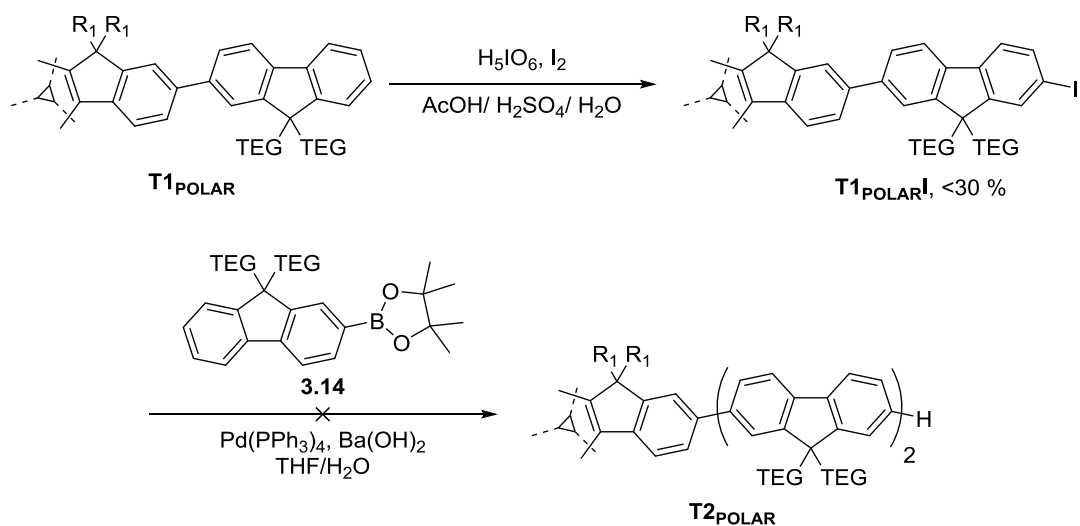
While reaction of **3.14** with dihalogenated fluorenes failed to afford bifluorenes in acceptable yields, coupling **3.14** with the tribromohexahexyltruxene **2.3** afforded the polar analogue of **T1**, **T1_{POLAR}**,

in good yield (Scheme 3.16), under conditions previously used to produce the **TX** compounds.¹⁴⁹



Scheme 3.16 Preparation of **T1_{POLAR}**.

Since no conditions could be found to prepare oligofluorenes an attempt was made to synthesise **T2_{POLAR}** by the divergent approach, since at such short arm length the separation problems, discussed in chapter 1.6, figure 1.49, should not be as great. As stated above, TEG chains are not stable under the conditions required for bromination, therefore **T1_{POLAR}** was iodinated using the conditions for iodination of truxene reported by Pei *et al.*¹⁷⁹ This transformation was poor yielding and after purification by silica gel chromatography some slight impurities were present that could not be separated, however the compound was taken forward for cross-coupling with **3.14** regardless. This reaction afforded a complex mixture of inseparable products, none of which could be attributed to the desired product.



Scheme 3.17 Unsuccessful preparation of **T2POLAR**.

3.3 Results and Discussion

An explanation for the poor reactivity observed when treating **3.9** and **3.15** with *n*-butyllithium followed by addition of an electrophile can be explored when considering the TEG chains in full (Figure 3.4). The lone pairs from the oxygen atoms in the chain are available to coordinate with the aryl-lithium compound formed during the reaction. It is well known that crown ethers are excellent ligands for alkali metals,^{180, 181} and ethylene glycol chains can be envisioned as linear crown ethers. Holmes *et al.* have reported a hole transport material with a fluorene unit substituted with tetraethylene glycol chains that was used to solvate lithium ions.¹⁸² It can therefore be inferred that the TEG chains present on the fluorene units are coordinating to the lithium centre after initial lithium-halogen exchange, as demonstrated in Figure 3.1. This could lower the reactivity of the fluorenyl-lithium complex towards electrophiles, and explain the poor yields observed. Quenching this intermediate with water would lead to the formation of compound **3.1**, which is the only side product observed in these reactions.

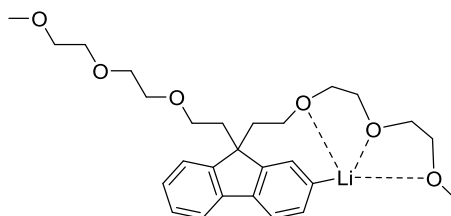


Figure 3.4 Interaction of TEG chains within the lithium intermediate.

A similar coordinating effect towards intermediate palladium complexes could also explain the poor yields observed from fluorene-fluorene coupling to afford bi-fluorene **3.17** (Figure 3.5). Once the oxidative insertion of the active palladium species into the carbon-bromide bond takes place, the lone pairs on the oxygen atoms within the TEG chains could ligate to the palladium and hinder the reaction.

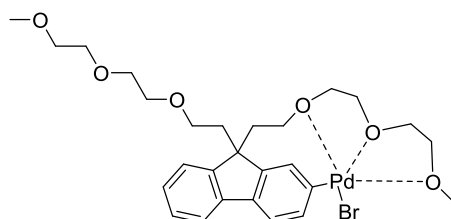


Figure 3.5 Interaction of TEG chains with palladium.

No such effect would take place during the formation of **T1polar** since the alkyl chains present on the truxene core are saturated carbon chains without any lone pairs available to act as a ligand. This would explain why good yields for this reaction are observed, while poor yields are observed when attempting the fluorene-fluorene coupling where the bromo-fluorenes are substituted with TEG chains.

This reasoning however does not sufficiently explain the good yield observed with the coupling reaction of monobromo-fluorene **3.15** and fluorenyl boronate ester **3.17** (Scheme 3.10). In this reaction, a slight excess of boronate ester **3.17** (1.2 eq) was employed. The only other successful coupling reaction for a bromo-diTEG-fluorene compound was

that of the formation of compound **3.14**, where a large excess of the boronate ester species was used. From these observations it can be inferred that successful coupling requires an excess of boronate ester, and therefore coupling with an excess of dibromofluorene in the conditions shown in Scheme 1.1 is not suitable for the preparation of oligofluorenes. The effect of the TEG chains shown in Figure 3.5 could mean that after insertion of the palladium into the carbon-bromine bond, which is the first step in the catalytic cycle of the Suzuki-Miyaura coupling reaction (Figure 3.6),¹⁸³ the intermediate complex is poorly reactive, requiring excess boronate ester to afford good yields. Interestingly, in the reaction to form **T1POLAR** (Scheme 3.16) the bromo-fluorenyl moiety is substituted with hexyl chains, and good yields were observed, with easy separation of the product by silica gel chromatography. While this observation provides support for the proposals made that the catalytic intermediate after oxidative addition is poorly reactive towards the boronate ester species, further work is required to fully investigate the poor yields of TEG substituted fluorene-fluorene coupling.

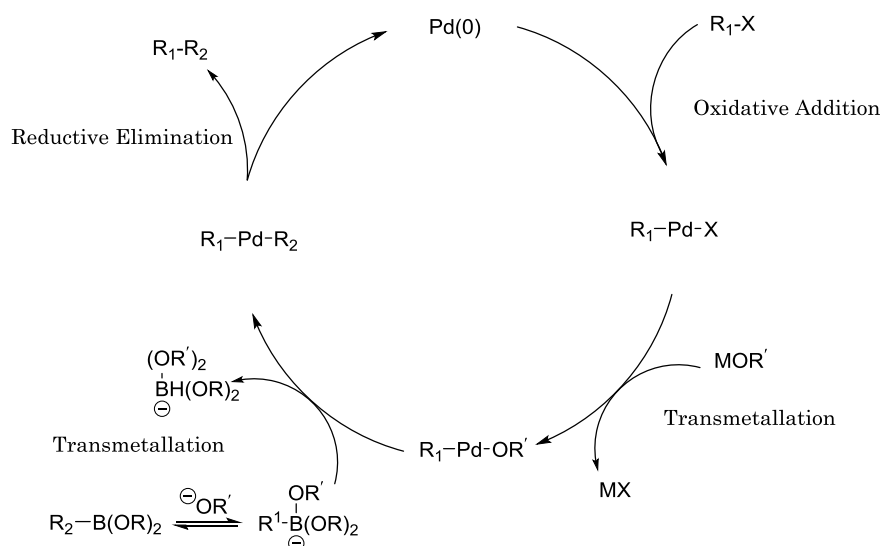


Figure 3.6 Catalytic cycle of Suzuki-Miyaura coupling.

These complex problems would severely limit the synthesis of oligo(fluorenes) substituted with TEG chains, and may explain the lack of examples in the literature of such compounds.

While it was not possible to prepare diTEG-substituted oligofluorenes, the successful preparation of **T1_{POLAR}** required further investigation. The compound, although containing only one polar fluorene unit, had good solubility in methanol and acetonitrile, which is in contrast to the poor solubility of the non-polar **TX** compounds in those solvents. The normalised absorption and emission spectra in solution (acetonitrile) is shown in Figures 3.8 and 3.9 respectively.

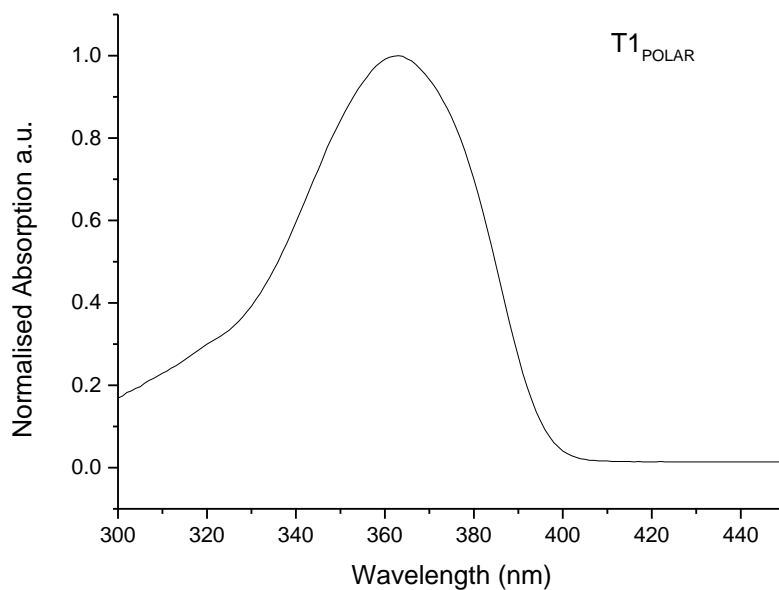


Figure 3.7 Absorption spectrum of **T1_{POLAR}** materials in solution (CH_2Cl_2 , 1×10^{-6} M).

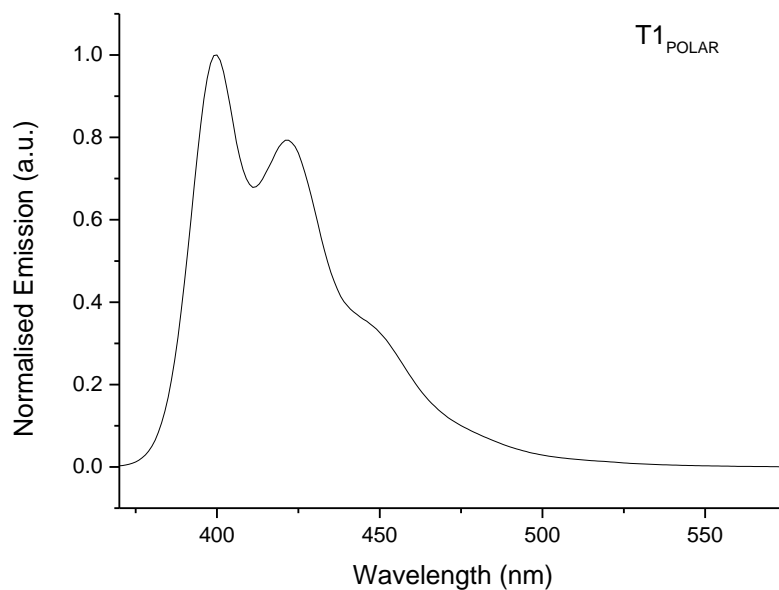


Figure 3.8 Emission spectrum of **T1_{POLAR}** materials in solution (CH_2Cl_2 , 5×10^{-7} M).

The absorption spectrum of **T1_{POLAR}** shows an absorption maximum at 363 nm, which is a 20 nm red shift in comparison to **T1**. The optical HOMO-LUMO gap, which was estimated from the onset, was found to be 3.15 eV. This is slightly narrower to that observed for **T1**. The wavelength maximum for the emission spectrum was observed at 400 nm. A peak was also observed at 422 nm and a shoulder at 446 nm, which are attributed to well resolved vibronic features of the molecules, which indicates good planarity within the molecular structure. The Stokes shift for **T1_{POLAR}** was estimated to be 37 nm and is similar to that of **T1**.

Compound	λ_{max} (nm) absorption (MeCN)	Onset (nm)	ϵ ($\text{mM}^{-1} \text{cm}^{-1}$)	HOMO-LUMO Gap (eV)	λ_{max} (nm) emission (MeCN)
T1_{POLAR}	363	395	79.4	3.15	400, 422, 446sh
T1^a	343	-	-	3.29	375sh, 396, 416sh

Table 3.2 Optical Data for **T1_{POLAR}**.

The cyclic voltammograms for **T1_{POLAR}** are shown in Figure 3.9. The oxidation curve shows two quasireversible oxidation waves, at 0.86 and 1.06 V. The reduction curve shows two irreversible reduction peaks at -2.57 and -2.74. The electrochemical HOMO and LUMO values were determined from the onsets of the first oxidation peak and the reduction wave respectively, and were estimated to be -5.57 and -2.38, respectively, with reference to ferrocene. The HOMO value is essentially the same as that for **T1**, however the LUMO has been lowered, which results in a narrower HOMO-LUMO gap in comparison to **T1**. The value of the electrochemical HOMO-LUMO gap, estimated to be 3.19 eV, is narrower to that of **T1** and correlates very well with the optical HOMO-LUMO gap.

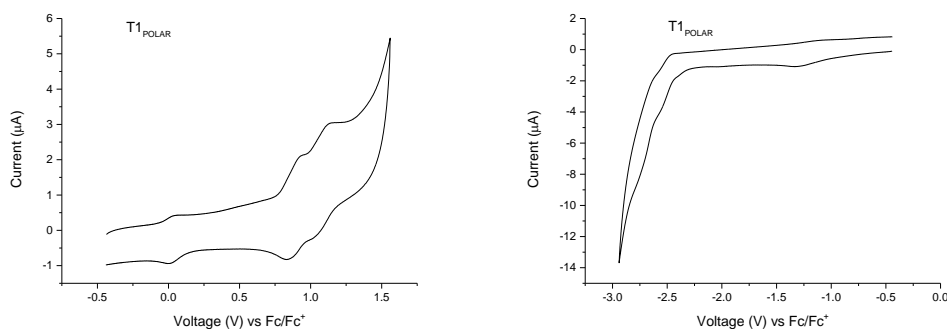


Figure 3.9 Oxidation (left) and reduction (right) waves from cyclic voltammetry of **T1_{POLAR}** in dichloromethane, electrolyte 0.1 M Bu₄NPF₆, glassy carbon working electrode, scan rate 100 mVs⁻¹.

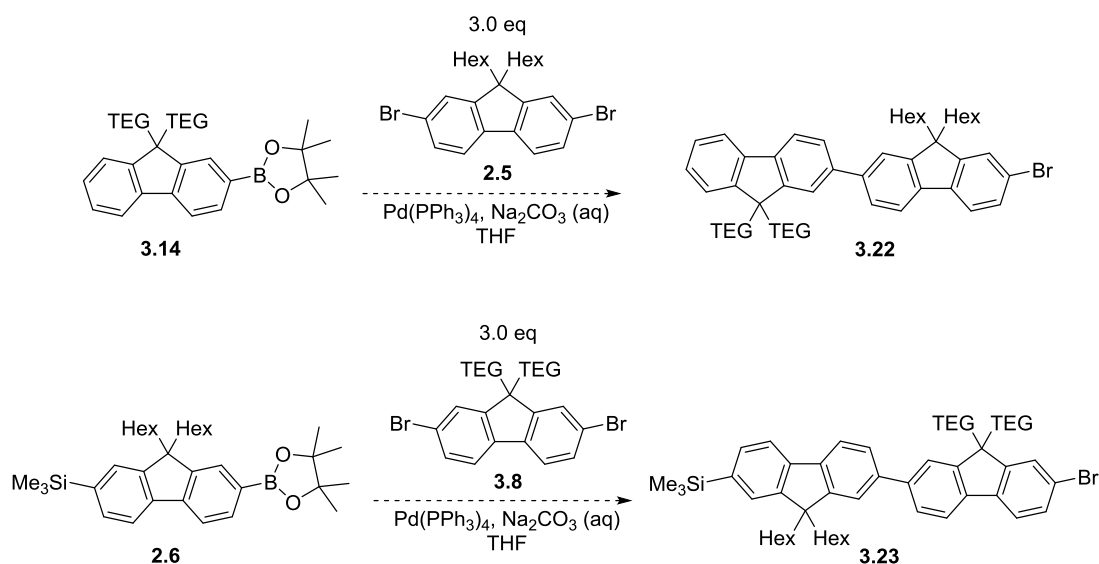
Compound	E _{ox} (V) Peaks E _{ox} ^{1/2}	HOMO	E _{red} (V) Peaks E _P	LUMO	HOMO-LUMO Gap (eV)
T1-³FTh	0.86, 1.06	-5.57	-2.57, -2.74	-2.38	3.19
T1	-	-5.60	-	-2.20	3.4

Table 3.3 Electrochemical data for **T1_{POLAR}**.

3.4 Conclusions and Future work

A polar analogue of **T1** has been presented, which had good solubility in methanol and acetonitrile, and the optical and electrochemical properties have been investigated. In comparison to **T1**, **T1_{POLAR}** has a similar HOMO level but a more stabilised LUMO, affording a slightly narrower band gap. Unfortunately, it was not possible to synthesise the larger polar analogues due to problems encountered when trying to produce oligo(fluorenes) substituted with TEG chains.

A reason for the poor yields observed under a variety of conditions for the coupling reactions of TEG substituted fluorenes has been proposed. In order to support the postulations made to explain the poor results observed for the cross-coupling of TEG substituted fluorenes (Scheme 3.11, Table 1) a series of further reactions should be conducted. The coupling of dibromo-dihexyl-fluorene **2.5** with diTEG-fluorenyl boronic ester **3.14**, while also, under the same reaction conditions, the coupling of dibromo-diTEG-fluorene **3.8** with the di-hexyl-fluorenyl boronic acid **2.6** should be made. A comparison of the yields and starting material recovered would be sufficient to either support or dispute the reasoning made for the poor yields observed. Should the yield of **3.22** be significantly greater than that of **3.23**, this would support the proposals made that the TEG chains affect the aryl-palladium-bromine intermediates. However, should the yield of **3.23** be greater than that of **3.22**, or there is no significant difference between the yields, then this would show that the TEG chains do not interfere with the intermediate compound and that the poor yields are the result of another factor.



Scheme 3.18 Proposed further reactions to explain poor yields of TEG alkylated fluorenes.

It would also be of interest to repeat the reaction shown in scheme 3.14, where the symmetrical TEG-substituted bifluorene **3.20** was prepared, but with a slight change in conditions. By using an excess of **3.13** (1.5-2.0 eq), any drop in observed yield would again support the postulations for the poor yield of TEG-substituted fluorene-fluorene coupling that have been proposed. While using an excess of boronate ester **3.14** would also in theory be of interest, any homo-coupling of the boronate esters within the reaction mixture would lead to an artificially increased yield, since the desired product of hetero-coupling is identical to the homo-coupled product.

4 Attempted formation of alkyl amine end capped oligofluorene-functionalised truxenes.

4.1 Introduction

Oligofluorene-functionalised truxenes **T3** and **T4** (Figure 4.1) have previously been investigated as gain material in organic DFB lasers.^{184, 185} Samuel *et al.* have measured the amplified spontaneous emission (ASE) of **T4** thin films, reporting a ASE threshold of 4 kWcm^{-2} ,¹⁸⁴ which is significantly lower than that of polyfluorene (58 kWcm^{-2}), one of the blue-emitting gain material benchmarks.¹⁸⁶ A low optical loss coefficient of 2.3 cm^{-1} was also recorded, a reduction of more than one third in comparison to polyfluorene, indicating that few losses occur from scattering or self-quenching. When **T4** was applied as the gain material in a DFB laser a low lasing threshold of 270 Wcm^{-2} was observed. Samuel *et al.* have also reported a DFB laser with **T3** as the gain material which demonstrated a tuning range as broad as 51 nm .¹⁸⁵

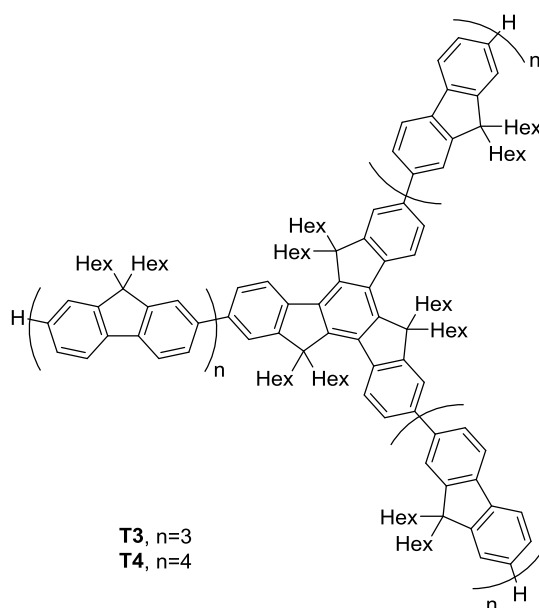


Figure 4.1 Structure of **T3** and **T4**.

Organic gain materials have the advantage over inorganic materials in that they can be further functionalised, which affords the opportunity to introduce functional groups such that probes can be bound directly to the gain material without the need for an added electrolyte, which simplifies

the design of the DFB laser. By careful introduction of cavities in the thin film of the gain material the surface area can be increased, which could lead to improved sensitivity of the overall device.

We have sought to introduce functional groups at the terminal positions of the oligofluorene arms such that the new compounds will also have electrolyte characteristics. In order to mimic the properties of poly(allyl amine) (Figure 4.2), the hydrochloride salt of which is commonly used as a polyelectrolyte in functional thin films,^{83, 85} alkyl primary amines were selected as the functional groups.

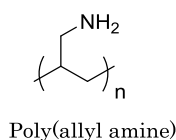
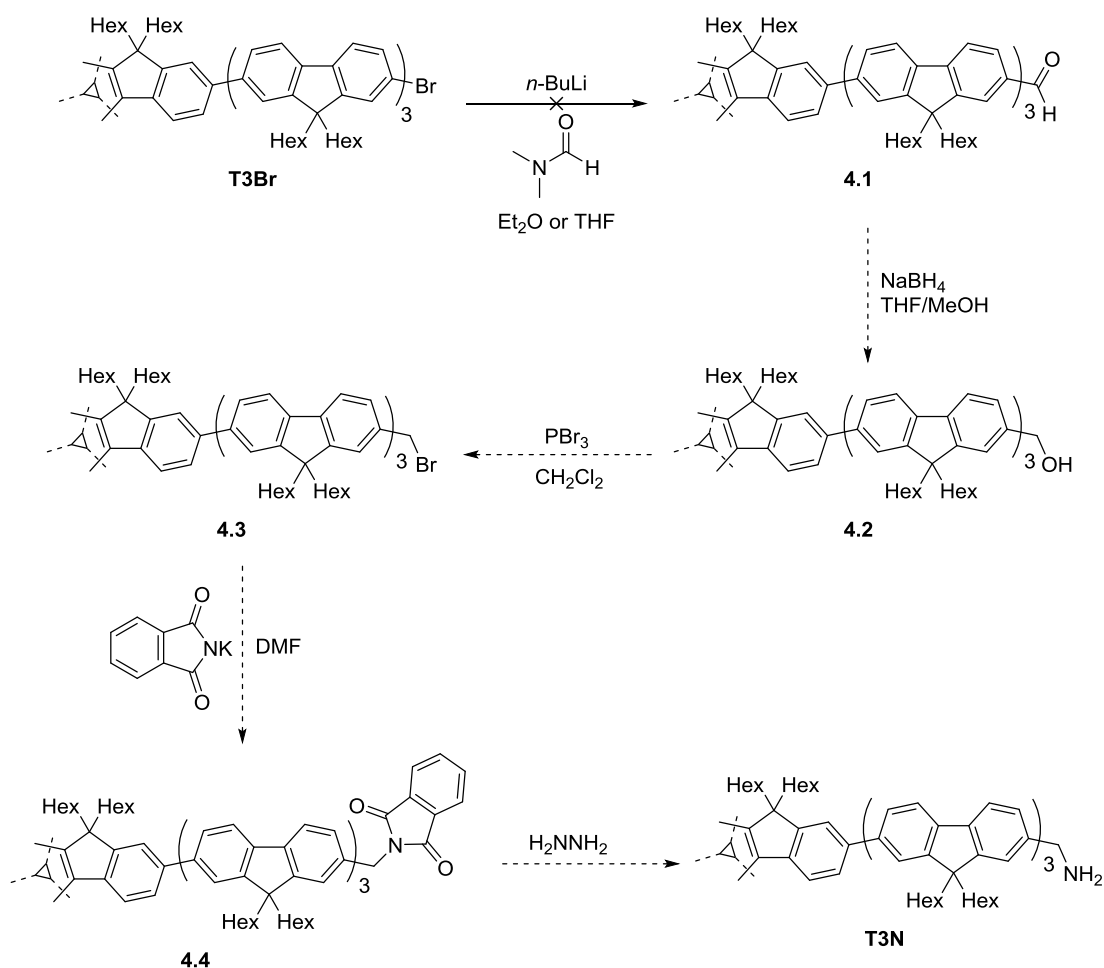


Figure 4.2 Structure of poly(allyl amine).

4.2 Synthesis

In order to end functionalise oligofluorene-functionalised truxenes with alkyl primary amine groups the synthetic route selected involved the reaction of potassium phthalimide with a methylene bromide functionality to form a protected primary amine (Scheme 4.1). Introduction of the methylene bromide to the terminal position of the oligofluorene arms could be achieved in relatively few steps by initial lithium halogen exchange then conversion of the nucleophilic centre formed to a formyl functionality by quenching with a suitable electrophile, such as DMF. Reduction to the alcohol and subsequent treatment with PBr₃ would generate the desired -CH₂Br group. After reaction with phthalimide salt, deprotection of the phthalimide with a suitably strong nucleophile would then afford the target amine compound.



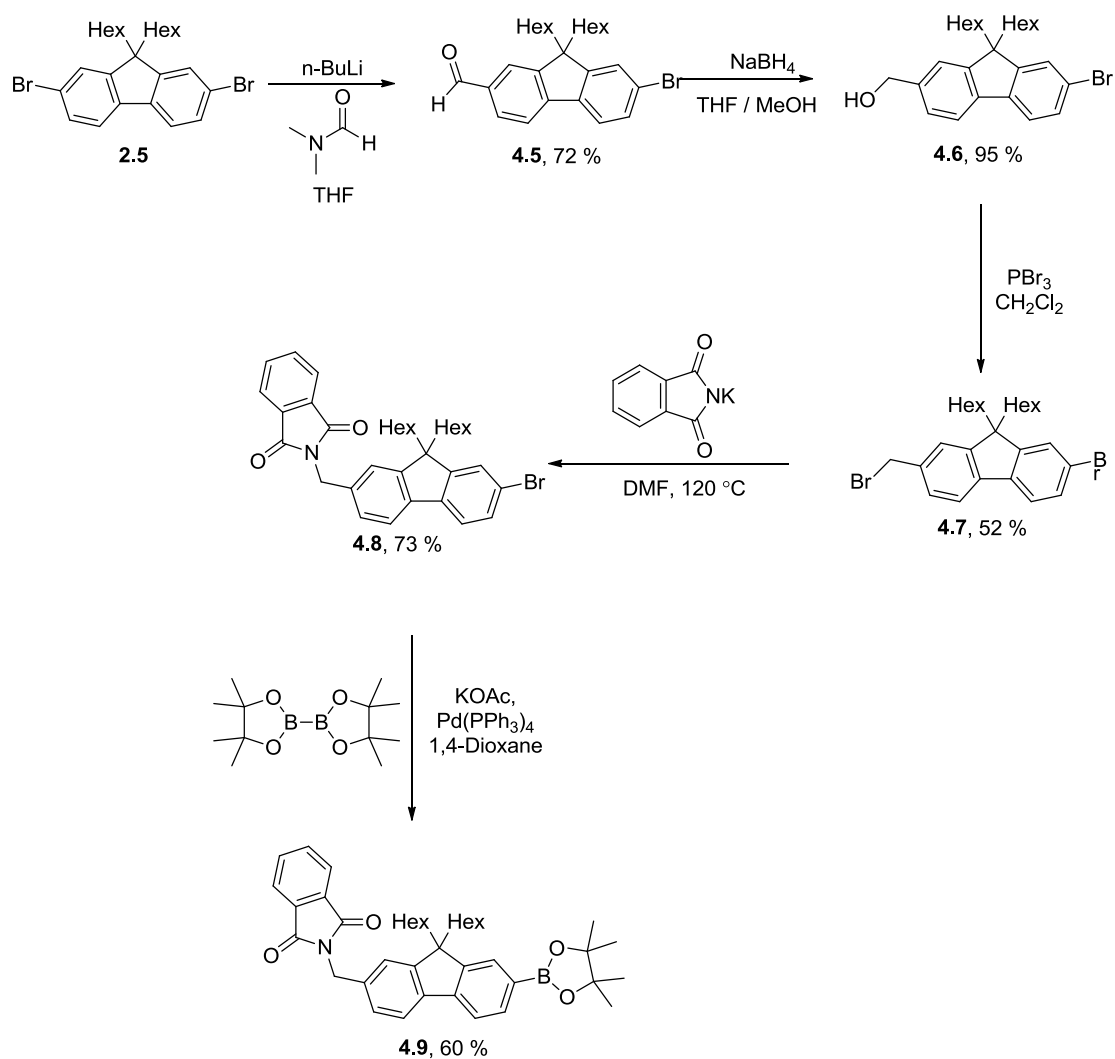
Scheme 4.1 Initially proposed synthesis of **T3N**.

Initial attempts to tri-functionalise **T3Br** with formyl groups to afford compound **4.1** proved to be difficult due to the poor solubility of the **T3**-lithium intermediate in ethereal solvents. In both THF and Et_2O , precipitate was observed after addition of the alkyllithium reagent, which proved insoluble even after warming to room temperature. After addition of the electrophile and allowing for a sufficient reaction time, TLC analysis of the reaction mixture showed multiple products present with poor separation. ^1H NMR analysis of the crude mixture after workup showed that poor conversion to the aldehyde had taken place in both instances, and TLC analysis showed multiple, inseparable products. From

these results it was clear that tri-functionalisation of oligofluorene-functionalised truxenes was not a suitable synthetic route.

A new route was proposed where a single fluorene unit with a methylene phthalimide functionality would be coupled to **T3Br**, the deprotection of which would afford the desired **T4** analogue (Scheme 4.2 and 4.3). The functionalisation of the single fluorene unit would be identical to that proposed for functionalisation of **T3Br** (Scheme 4.1), with two additional synthetic steps (introduction of boronic ester functionality and cross coupling) required to produce the target material. While additional steps is undesirable, the methodology is simplified since each reaction is only one-fold, rather than three-fold, and it was hoped that this would lead to improved yields of the target compound.

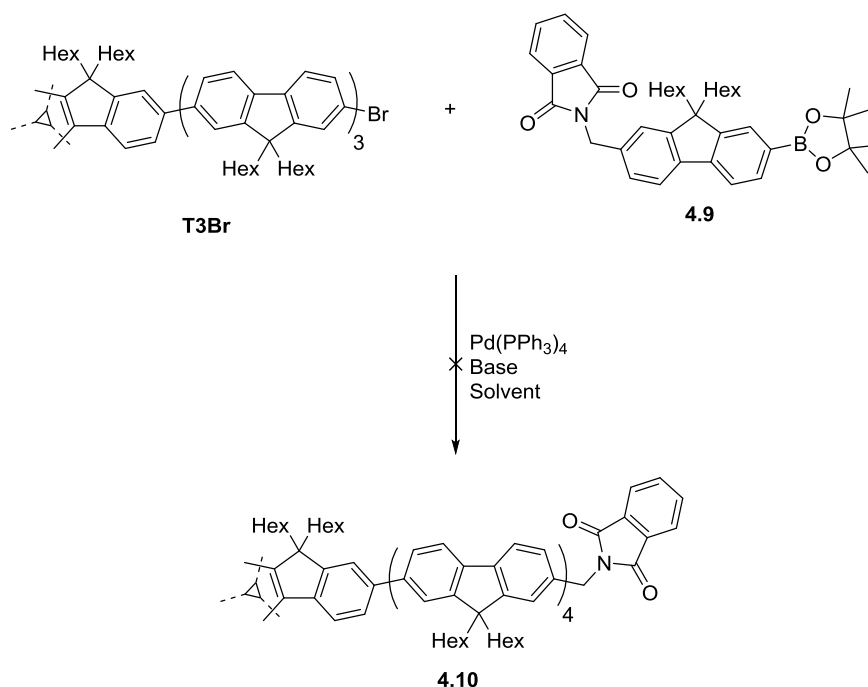
Treatment of **2.5** with 1.0 eq of *n*-butyllithium, followed by addition of excess DMF afforded the aldehyde **4.5**, which was reduced to the alcohol **4.6** by treatment with NaBH₄ in the presence of MeOH. Conversion of the alcohol functionality to a bromide was achieved by reaction of PBr₃, and treatment with potassium phthalimide at high temp was sufficient to prepare the desired fluorenyl methylene phthalimide intermediate **4.8**. In order to couple this unit to **T3Br** under Suzuki-Miyaura conditions, **4.8** was converted to the boronic ester **4.9** by coupling with bispinacolatodiboron.



Scheme 4.2 Synthesis of compound 4.9.

The next step in the synthetic route was the coupling of **4.9** to **T3Br** (Scheme 4.3), which was first attempted with the condition which produced the **TXSi** compounds in chapter 2, scheme 2.4. However, after aqueous workup TLC analysis gave only a single spot which would not move from the baseline under any eluent mixtures. ^1H NMR analysis of the crude mixture was too complex for any structural information to be ascertained. It was proposed that the barium hydroxide, used as the base for the Suzuki-Miyaura coupling, was reacting with the phthalimide functionality, leading to the formation of side products. A second attempt employing a less nucleophilic base, caesium fluoride, gave the same

result. A third attempt was then made employing tribasic potassium phosphate, which is a very poor nucleophile. In this instance however, only starting materials were recovered from the reaction. Another attempt with caesium fluoride, this time as a microwave reaction, was made in order to control reaction times and temperatures. After 1h at 120 °C only starting materials were observed, which was also the case after 1h at 140 °C. However, after 1h at 160 °C, the strongly fluorescent baseline spot was again observed. A final attempt was made, again in the microwave, with tribasic potassium phosphate for 1h at 160 °C, where unfortunately only starting materials were observed.

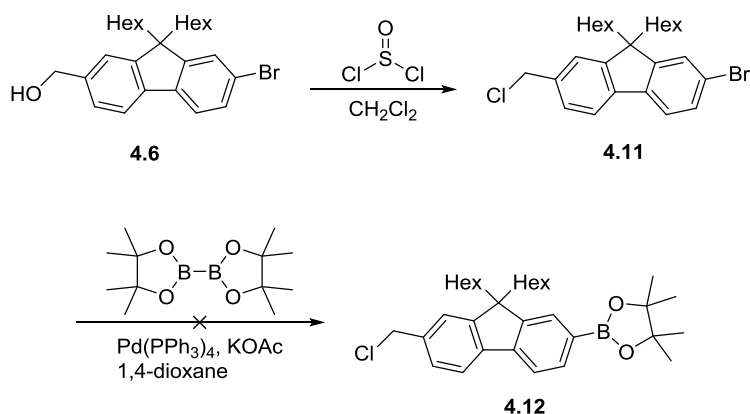


Scheme 4.3 Attempted coupling of **4.9** with **T3Br**.

It was proposed that the phthalimide group was not stable under the harsh conditions required for efficient coupling of arms to core, and that the phthalimide group would need to be introduced to the oligofluorene functionalised truxenes after coupling. This would require a leaving group which would be stable, or poorly reactive, towards the coupling conditions. To this end, chlorides and tosylates were both identified,

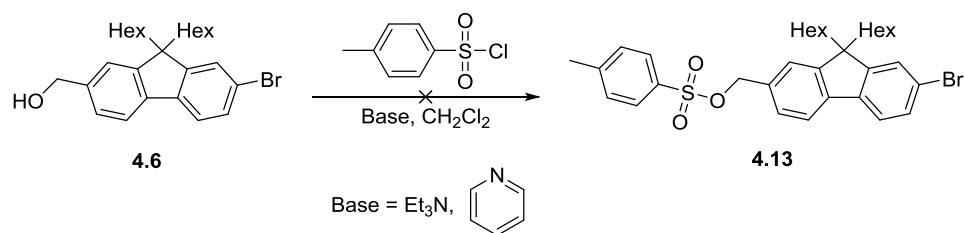
since alkyl halides and pseudo-halides are less reactive than aryl halides and pseudo-halides towards coupling.¹⁸⁷

Treatment of the alcohol **4.6** with thionyl chloride afforded **4.11** in good yield. However, the coupling reaction with bispinacolatodiboron gave multiple products, suggesting that the methylene chloride was not as poorly reactive as first presumed.



Scheme 4.4 Attempted synthesis of compound **4.12**.

An attempt to synthesise the methylene tosylate **4.13** from the alcohol **4.6** under the same conditions as those which produced **3.6** (scheme 3.1) did not afford the desired product. TLC analysis showed a small quantity of tosyl chloride present with the main component of the crude mixture appearing as a spot which would not move from the baseline regardless of eluent. A similar result was observed in a second attempt which employed a stronger base.



Scheme 4.5 Attempted synthesis of compound **4.13**.

4.3 Results and Discussion

We propose that during the cross coupling of **4.9** with **T3Br** the strong base caused deprotection of the phthalimide group, affording a primary amine functionality. Under cross-coupling condition, alkyl amines react with aryl halides in what is known as the Buchwald-Hartwig amination.¹⁸⁸ In this reaction primary and secondary amines undergo cross-coupling with aryl halides to form new arylamine compounds (Figure 4.3)

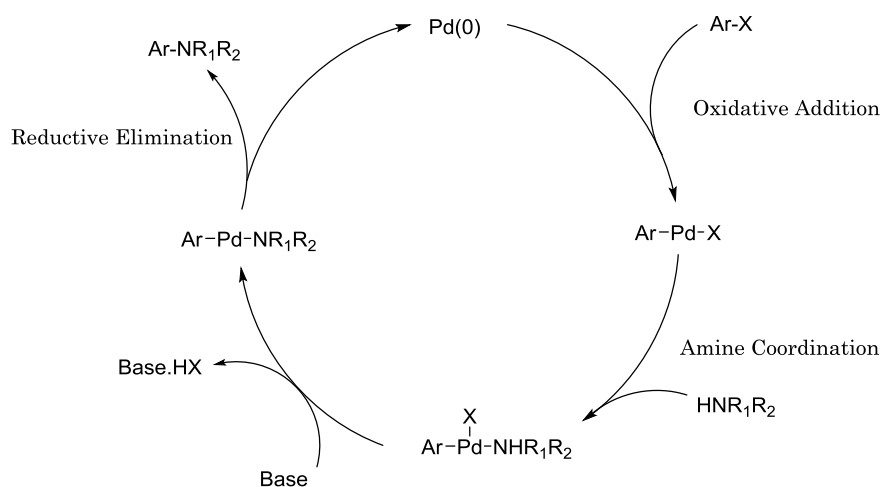


Figure 4.3 Catalytic cycle of Buchwald-Hartwig amination.

A Buchwald-Hartwig coupling of undesirable by-products formed in the reaction shown in scheme 4.3 would afford a complex cross-linked polymer, which is believed to be the large fluorescent spot observed on the baseline under TLC analysis. In order to form the target material **4.10**, a

strong base is necessary for efficient, 3-fold cross coupling, and attempts to find a strong base with poor nucleophilic character, to inhibit the deprotection, was not successful.

The fluorenyl methylene chloride compound **4.11** was synthesised in good yield from the alcohol **4.6** (scheme 4.4). However, subsequent coupling with bispinacolatodiboron was shown to give multiple products. In this reaction, both coupling of the methylene chloride functionality with bispinacolatodiboron and coupling of compound **4.12** with itself would lead to undesirable by-products. Since many of the components of the crude material were not separable it was not possible to determine which by-products had formed.

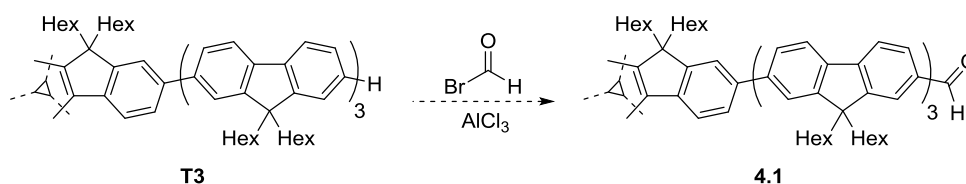
Attempted formation of the tosylate **4.13** afforded a crude mixture which gave only two spots by TLC analysis. The major spot would not move from the baseline regardless of eluent mixture, while the second, faint spot corresponded to tosyl chloride, which had been used in a slight excess. A ^1H NMR of the crude mixture was not sufficient to determine whether the desired compound **4.13** or a different compound had been formed.

4.4 Conclusions and Future Work

While a simple route to introduce a methylene phthalimide functionality to a fluorene unit has been developed, successful synthesis of the target compounds was not achieved. Attempts to synthesise a fluorene unit functionalised with a methyl chloride group was successful, but this compound did not show selective coupling of the aryl bromide over the methyl chloride functionality. Finally, attempts to synthesise a fluorene unit functionalised with a methylene tosylate group were unsuccessful.

The successful preparation of compound **4.9** in a good yield indicates that the phthalimide group is stable towards weak bases, which are often sufficient for the preparation of polymers and dendrimers, both of which have seen applications as gain material in lasers.⁷⁶⁻⁸⁰ Therefore, the synthetic methodology outlined in this chapter could be applicable for compounds of a similar nature with similar applications. The limitations discovered in this work may also prove useful for the attempted synthesis of related compounds in future work by others.

Another route towards compound **4.1** could be achieved by using the unfunctionalised **T3** in a Friedel-Crafts reaction with formyl bromide (scheme 4.6), similar to conditions which Pei *et al.* have reported for the introduction of an acetyl group to truxene, **1.42**.¹²⁴ The poor stability of formyl bromide, which would require to be made *in situ*, may lead to poor yields. This step could also be accomplished using Vilsmeier-Haack conditions (POCl₃, DMF), but selectivity and achieving complete reaction on all three arms could be problematic.



5 Experimental

General Experimental

^1H NMR were collected on either a Bruker DPX 400 or AV 500 spectrometer at 400 MHz or 500 MHz respectively, while ^{13}C NMR were run on either a Bruker DPX 400 or AV 500 spectrometer at 100 MHz or 125 MHz respectively. ^{19}F NMR were run on a Bruker AV 400 spectrometer at 376 MHz. Chemical shifts are in parts per million (ppm) and were measured in deuterated chloroform, the peak for which was corrected to 7.60 ppm.¹⁸⁹

Low resolution mass spectroscopy was carried out at the University of Strathclyde using a Finnigan LCQ duo ESI, while high resolution mass spectroscopy was carried out at the University of Glasgow on a JEOL High Resolution Mass Spectrometer using FAB or at the EPSRC National Mass Spectrometry Service Centre, Swansea using a LTQ Orbitrap XL.

All reagents were obtained from commercial suppliers. Solvents were purified using a Pure-Solv 400 Solvent Purification system. 1,4-Dioxane was purified by distillation over sodium metal at atmospheric pressure.

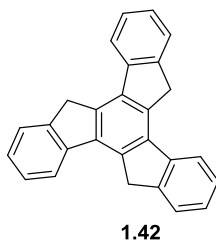
All glassware was oven dried to remove traces of moisture before use.

Cyclic Voltammetry (CV) measurements of oxidation and reduction potentials were performed on a CHI660A Electrochemical Workstation with iR compensation at 100 mV s⁻¹. Dichloromethane was used as the solvent, aqueous Ag/AgCl as the reference electrode, with platinum wire and a glassy carbon disk ($\text{Ø} = 3$ mm) as the counter and working electrodes, respectively. The solutions contained the substrate in a concentration of 5×10^{-4} M, together with $n\text{-Bu}_4\text{NPF}_6$ (0.1 M) as the supporting electrolyte. All CV experiments were referred to the Fc/Fc⁺

couple which was measured before and after the measurement of the target compounds of used as an internal standard.

Absorption spectra were recorded using a ThermoSpectronic Unicam UV 300, whilst emission spectra were recorded using a Perkin Elmer LS45 Luminescence Spectrometer, where the excitation wavelength for each compound was the wavelength corresponding to the compounds' maximum absorption.

Truxene (1.42)¹⁴⁷



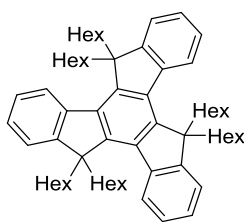
1-Indanone **2.1** (13.6 g, 0.1 mol, 1.0 eq) was dissolved in a mixture of acetic acid (60 ml) and conc. hydrochloric acid (30 ml). This solution was then heated at 100 °C for 16 h with stirring, affording a yellow suspension. The suspension was poured into a beaker of ice, and the precipitate was isolated by filtration before being washed with water, acetone and CH₂Cl₂. The resulting powder was then dried in a dessicator to afford the title product as an off-white powder (10.15 g, 88 %).

The ¹H NMR spectrum was recorded;

δ_{H} (400 MHz, CDCl₃): 7.98 (3H, d, *J* 8.0 Hz, CH), 7.72 (3H, d, *J* 7.6 Hz, CH), 7.52 (3H, t, *J* 7.4 Hz, CH), 7.41 (3H, t, *J* 7.1 Hz, CH), 4.31 (6H, s, CH₂).

This was consistent with the previously published data.¹⁴⁷

Hexahexyltruxene (2.2)¹⁴⁷



2.2

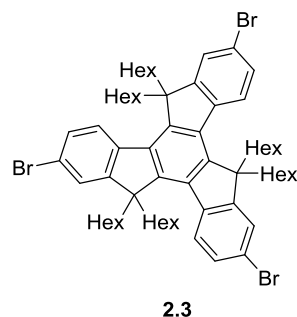
Truxene **1.42** (3.18 g, 9.29 mmol, 1.0 eq) was suspended in dry THF (50 ml) under N₂, and the suspension was chilled in an ice bath. *n*-Butyllithium (2.2 M in hexane, 16 ml, 35 mmol, 3.75 eq) was added dropwise over 15 mins, affording a deep-red coloured solution, which was stirred at rt for 30 mins. 1-Bromohexane (5 ml, 35 mmol, 3.75 eq) was added dropwise to the solution over 10 mins, which was then stirred for 4 h. The solution was then chilled again in an ice bath, *n*-butyllithium (16 ml, 35 mmol, 3.75 eq) was added dropwise over 15 mins, and the solution stirred for a further 30 mins. 1-Bromohexane (5 ml, 35 mmol, 3.75 eq) was added dropwise over 10 mins, and the solution was stirred at rt for 18 h under N₂. Thin layer chromatography (eluting with petroleum ether) was used to ensure the reaction was complete before the reaction mixture was quenched with a solution of saturated ammonium chloride in water (100 ml) and extracted with petroleum ether (4 × 25 ml). The organic portions were combined and the solvent was evaporated to afford the crude product as a yellow oil. This was purified by silica gel chromatography eluting with petroleum ether to afford the title product as a yellow solid (6.79 g, 88%).

The ¹H NMR spectrum was recorded;

δ_{H} (400 MHz, CDCl₃): 8.37 (3H, d, *J* 7.2 Hz, CH), 7.46 (3H, d, *J* 5.2 Hz, CH), 7.40-7.36 (6H, m, CH), 2.98-2.93 (6H, m, CH₂), 2.11-2.04 (6H, m, CH₂), 0.94-0.83 (36H, m, CH₂), 0.62-0.58 (18H, m, CH₃), 0.56-0.44 (12H, m, CH₂).

This was consistent with the previously published data.¹⁴⁷

Tribromohexahexyltruxene (2.3)¹⁴⁷



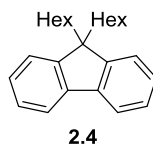
Hexahexyltruxene **2.3** (6.63 g, 7.82 mmol, 1.0 eq) was dissolved in CH₂Cl₂ (50 ml), to which bromine (2.0 ml, 38.8 mmol, 5.0 eq) was added dropwise over 5 mins, with minimum exposure to light. The reaction mixture was stirred at rt for 18 h. After this time it was washed with an aqueous solution of sodium sulphite (50 ml) and extracted with CH₂Cl₂ (3 × 50 ml). The organic layers were combined and washed with a saturated aqueous solution of sodium hydrogen carbonate (50 ml), dried over magnesium sulphate, and the solvent was evaporated. The crude product was recrystallised from hexane, and filtration afforded the title product as yellow crystals (5.81 g, 68 %).

The ¹H NMR spectrum was recorded;

δ_{H} (400 MHz, CDCl₃): 8.18 (3H, d, *J* 7.8 Hz, CH), 7.54 (3H, d, *J* 2.0 Hz, CH), 7.54-7.51 (3H, m, CH), 2.85-2.81 (6H, m, CH₂), 2.06-1.98 (6H, m, CH₂), 1.01-0.78 (36H, m, CH₂), 0.65-0.61 (18H, m, CH₃), 0.51-0.42 (12H, m, CH₂).

This was consistent with the previously published data.¹⁴⁷

9,9-Dihexylfluorene (2.4)¹⁴⁷



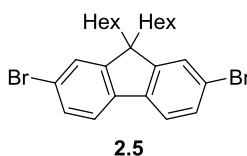
9*H*-Flourene **1.20** (39.9 g, 0.24 mol, 1.0 eq) was suspended in DMSO (400 ml) and stirred by mechanical stirrer until fully dissolved. Benzyltriethylammomium chloride (3.42 g, 0.015 mol, 0.06 eq) and 1-bromohexane (90 ml, 0.64 mol, 2.67 eq) were then added. The solution was chilled in an ice bath, and a 50 % solution of NaOH in water (96 ml) was added over 2 h. The solution was then left to warm to rt and was stirred for 18 h. The resulting purple solution was quenched with water (200 ml), and extracted with petroleum ether (5 × 200 ml). The organic portions were combined, dried over magnesium sulfate, and the solvent was removed by rotary evaporation to afford a yellow oil, which was recrystallised from methanol. Filtration afforded the product (**2.4**) as white crystals (52.0 g, 65 %).

The ¹H NMR spectrum was recorded;

δ_{H} (400 MHz, CDCl₃): 7.71-7.70 (2H, m, CH), 7.35-7.27 (6H, m, CH), 1.98-1.95 (4H, m, CH₂), 1.13-1.02 (12H, m, CH₂), 0.78-0.77 (6H, m, CH₃), 0.64-0.62 (4H, m, CH₂).

This was consistent with the previously published data.¹⁴⁷

2,7-Dibromo-9,9-dihexylfluorene (2.5)¹⁴⁷



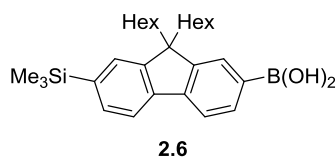
9,9-Dihexylfluorene **2.4** (30 g, 0.09 mol, 1.0 eq) was dissolved in dry CH₂Cl₂ (180 ml), to which I₂ (220 mg, 0.86 mmol, 0.01 eq) was added. The reaction vessel was equipped with a drying tube containing CaCl₂, followed by a NaOH trap. Bromine (10.6 ml, 0.21 mol, 2.3 eq) was then added dropwise over 1 h. The solution was left to stir for 18 h at rt, under N₂, with minimum exposure to light. The solution was then cooled in an ice bath for 10 mins, then added to a solution of sodium sulfite in water (300ml) and cooled by adding ice. The solution was then extracted with CH₂Cl₂ (2 x 300 ml), washed with a saturated solution of sodium hydrogen carbonate in water (300 ml) and then washed with water until the pH was neutral (2 x 300 ml). The organic layers were dried over magnesium sulfate and the solvent was evaporated to afford a yellow oil, which was recrystallised in hot methanol with added charcoal to afford white crystals. These crystals were recrystallised in hexane and dried in a dessicator to afford the title product as white crystals (25.4 g, 86 %).

The ¹H NMR spectrum was recorded;

δ_{H} (400 MHz, CDCl₃): 7.58 (2H, d, *J* 8.8 Hz, CH), 7.47-7.45 (4H, m, CH), 1.94-1.90 (4H, m, CH₂), 1.16-1.02 (12H, m, CH₂), 0.81-0.77 (6H, m, CH₃), 0.61-0.57 (4H, m, CH₂).

This was consistent with the previously published data.¹⁴⁷

9,9-Dihexyl-7-trimethylsilylfluorene-2-ylboronic acid (**2.6**)¹⁹⁰



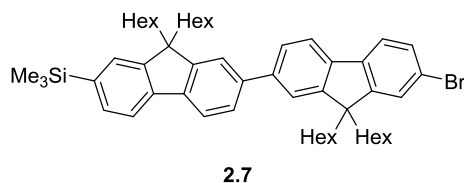
2,7-Dibromo-9,9-dihexylfluorene **2.6** (6.77 g, 0.014 mol, 1.0 eq) was dissolved in dry THF (100 ml) under N₂. The temperature of the solution was lowered to -80 °C using a petroleum ether/liquid N₂ bath, and *n*-butyllithium (2.0 M in hexane, 6.8 ml, 0.014 mol, 1.0 eq) was added

dropwise over 30 mins. The solution was stirred for 5 mins, cooled to -95 °C and chlorotrimethylsilane (1.8 ml, 0.014 mol, 1.0 eq) was added. The solution was then allowed to warm to r.t. over 30 mins, then cooled back to -80 °C and *n*-butyllithium (2.0 M in hexane, 8.2 ml, 0.017 mol, 1.2 eq) was added dropwise. The solution was then cooled further to -100 °C, triisopropylborate (10 ml, 0.043 mol, 3.0 eq) was added dropwise, and the solution was warmed to rt and stirred under N₂ for 18 h. Distilled water (500 ml) was used to quench the solution, which was then extracted with diethyl ether (3 × 100 ml). The organic layers were combined and washed with distilled water (500 ml), dried over magnesium sulfate, and the solvent was evaporated. The product was purified by silica gel chromatography, eluting first with toluene, followed by diethyl ether to afford the product as a white powder (3.75 g, 60 %).

¹H NMR (400 MHz, CDCl₃): δ_H 8.32-8.30 (1H, m, CH), 8.23 (1H, s, CH), 7.90 (1H, d, *J* 8.0 Hz, CH), 7.80 (1H, d, *J* 7.6 Hz, CH), 7.55 (2H, d, *J* 6.4 Hz, CH), 2.14-2.00 (4H, m, CH₂), 1.13-1.04 (12H, m, CH₂), 0.79-0.73 (6H, m, CH₃), 0.73-0.6 (4H, m, CH₂), 0.36-0.32 (9H, m, CH₃); ¹³C NMR (125 MHz, CDCl₃): δ_C 150.8, 150.4, 145.6, 141.4, 140.2, 134.6, 131.9, 129.8, 127.8, 119.7, 119.4, 55.0, 40.2, 31.4, 29.6, 23.8, 22.5, 14.0, -0.9.

This was consistent with the previously published data.¹⁹⁰

(7'-Bromo-9,9,9',9'-tetrahexyl-9H,9'H-[2,2'-bifluoren]-7-yl)trimethylsilane (2.7)¹⁹⁰



A solution of 9,9-dihexyl-7-trimethylsilylfluoren-2-ylboronic acid **2.6** (8.0 g, 17.76 mmol, 1.0 eq) in dry toluene (20 ml) was added *via cannula* to a

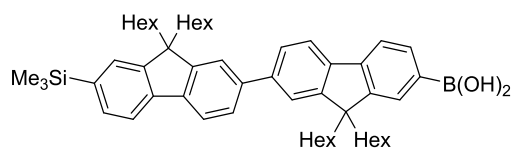
solution of 2,7-dibromo-9,9-dihexylfluorene **2.5** (26.24 g, 53.29 mmol, 3.0 eq) and *tetrakis*(triphenylphosphine) palladium(0) (0.61 g, 0.53 mmol, 0.03 eq) in dry toluene (55 ml), which had previously been stirred at rt for 20 mins. An aqueous solution of sodium carbonate (2M, 20.40 ml, 40.85 mmol, 2.3 eq) was added to the reaction mixture, which was heated at 80 °C under Ar for 18 h. The reaction mixture was then allowed to cool to rt and added to distilled water (300 ml). The organic layer was removed and the aqueous layer was extracted with CH₂Cl₂ (4 x 300 ml). The organic layers were combined, washed with distilled water (2 x 600 ml), dried over MgSO₄ and the solvent was evaporated. The product was purified by silica gel chromatography, eluting with pre-distilled pet. ether to afford a clear oil. The product was isolated as a white powder by precipitation from acetone (12.0 g, 83 %).

The ¹H NMR spectrum was recorded;

δ_{H} (400 MHz, CDCl₃): 7.78 (1H, d, *J* 6.0 Hz, CH), 7.74 (1H, d, *J* 6.0 Hz, CH), 7.72 (1H, d, *J* 5.8 Hz, CH), 7.65-7.59 (5H, m, CH), 7.52-7.47 (4H, m, CH), 2.05-2.01 (8H, m, CH₂), 1.16-1.08 (24H, m, CH₂), 0.80-0.71 (20H, m, CH₂/CH₃), 0.33 (9H, s, CH₃).

This was consistent with the previously published data.¹⁹⁰

(9,9,9',9'-Tetrahexyl-7'-(trimethylsilyl)-9H,9'H-[2,2'-bifluoren]-7-yl)boronic acid (2.8)¹⁴⁹



2.8

n-Butyllithium (2.24 M in hexane, 7.8 ml, 17.46 mmol, 1.2 eq) was added dropwise to a solution of (7'-bromo-9,9,9',9'-tetrahexyl-9H,9'H-[2,2'-bifluoren]-7-yl)trimethylsilane **2.7** (12.0 g, 14.7 mmol, 1.0 eq) in dry THF (200 ml) at -80 °C, which was allowed to stir for 10 mins then cooled to -

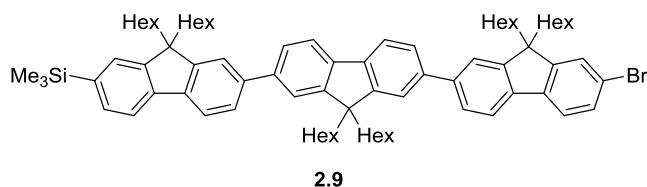
90 °C. Triisopropylborate (10.2 ml, 44.1 mmol, 3.0 eq) was added dropwise, then the reaction mixture was allowed to warm to rt and stir for 18 h under Ar. The reaction mixture was quenched with distilled water (500 ml), and the aqueous mixture was extracted with Et₂O (4 x 200 ml). The organic layers were washed with distilled water (500 ml), dried over MgSO₄ and the solvent was evaporated. The product was purified by silica gel chromatography eluting first with toluene, and then with Et₂O to isolate the product as an off-white powder (9.0 g, 79 %).

The ¹H NMR spectrum was recorded;

δ_{H} (400 MHz, CDCl₃): 8.38 (1H, d, *J* 8.0 Hz, CH), 8.30 (1H, s, CH), 7.96 (1H, d, *J* 8.0 Hz, CH), 7.93 (1H, d, *J* 8.0 Hz, CH), 7.84-7.63 (6H, m, CH), 7.58-7.55, (2H, m, CH), 2.22-2.03 (8H, m, CH₂), 1.17-1.09 (24H, m, CH₂), 0.83-0.77 (20H, m, CH₂/CH₃), 0.36 (9H, s, CH₃).

This was consistent with the previously published data.¹⁴⁹

(7''-Bromo-9,9,9',9',9'',9''-hexahexyl-9H,9'H,9''H-[2,2':7',2''-terfluoren]-7-yl)trimethylsilane(2.9)¹⁴⁹



A solution of (9,9,9',9'-tetrahexyl-7'-(trimethylsilyl)-9H,9'H-[2,2'-bifluoren]-7-yl)boronic acid **2.8** (7.68 g, 9.81 mmol, 1.0 eq) in dry toluene (40 ml) was added *via cannula* to a solution of 2,7-dibromo-9,9-dihexylfluorene **2.5** (14.50 g, 29.43 mmol, 3.0 eq) and *tetrakis*(triphenylphosphine) palladium(0) (0.33 g, 0.29 mmol, 0.03 eq) in dry toluene (40 ml), which had previously been stirred at rt for 20 mins. An aqueous solution of sodium carbonate (2M, 11.28 ml, 22.56 mmol, 2.3 eq) was added to the reaction mixture, which was heated at 80 °C under

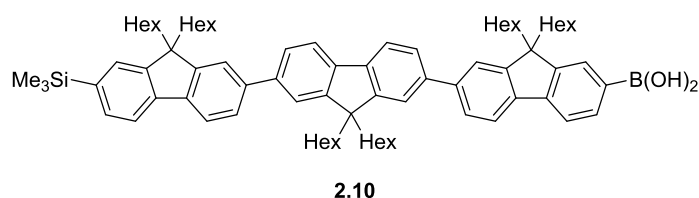
Ar for 18 h. The reaction mixture was then allowed to cool to rt and added to distilled water (300 ml). The organic layer was removed and the aqueous layer was extracted with CH₂Cl₂ (6 x 200 ml). The organic layers were combined, washed with distilled water (2 x 400 ml), dried over MgSO₄ and the solvent was evaporated. The product was purified by silica gel chromatography, eluting first with pre-distilled pet. ether, then with a pet. ether/toluene 20:1 mixture to afford a clear oil. The product was isolated as a white powder by precipitation from acetone (5.07 g, 45 %).

The ¹H NMR spectrum was recorded;

δ_{H} (400 MHz, CDCl₃): 7.83-7.72 (5H, m, CH), 7.68-7.60 (9H, m, CH), 7.53-7.48 (4H, m, CH), 2.12-2.03 (12H, m, CH₂), 1.16-1.09 (36H, m, CH₂), 0.83-0.76 (30H, m, CH₂/CH₃), 0.34 (9H, s, CH₃).

This was consistent with the previously published data.¹⁴⁹

(9,9,9',9',9'',9''-Hexahexyl-7''-(trimethylsilyl)-9H,9'H,9''H-[2,2':7',2''-terfluoren]-7-yl)boronic acid (2.10)¹⁴⁹



n-Butyllithium (2.35 M, 1.55 ml, 3.15 mmol, 1.2 eq) was added dropwise to a solution of (7''-bromo-9,9,9',9',9'',9''-hexahexyl-9H,9'H,9''H-[2,2':7',2''-terfluoren]-7-yl)trimethylsilane **2.9** (3.50 g, 3.04 mmol, 1.0 eq) in dry THF (50 ml) at -80 °C, which was allowed to stir for 10 mins then cooled to -90 °C. Triisopropylborate (2.10 ml, 9.12 mmol, 3.0 eq) was added dropwise, then the reaction mixture was then allowed to warm to rt and stir for 18 h under Ar. The reaction mixture was quenched with distilled water (200 ml), and the aqueous mixture was extracted with Et₂O (5 x 150 ml). The

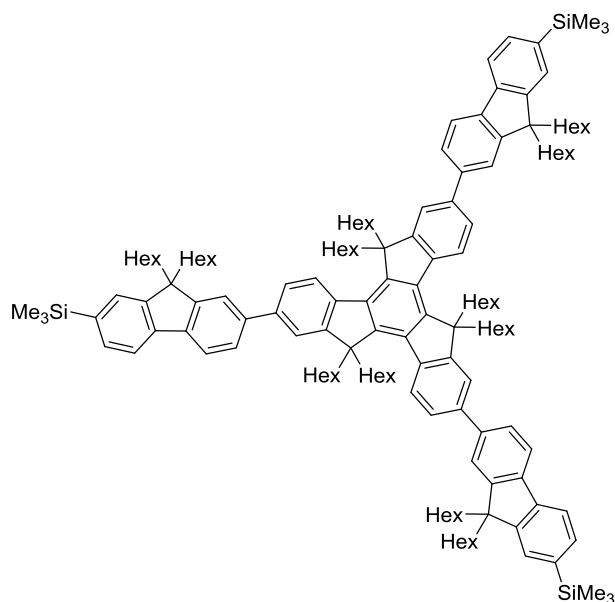
organic layers were washed with distilled water (500 ml), dried over MgSO_4 and the solvent was evaporated. The product was purified by silica gel chromatography eluting first with toluene, and then with Et_2O to isolate the product as an off-white powder (2.61 g, 77 %).

The ^1H NMR spectrum was recorded;

δ_{H} (400 MHz, CDCl_3): 8.37 (1H, d, J 7.6 Hz, CH), 8.30 (1H, s, CH), 7.98-7.65 (12H, m, CH), 7.54-7.51 (4H, m, CH), 2.22-2.04 (12H, m, CH_2), 1.18-1.11 (36H, m, CH_2), 0.84-0.76 (30H, m, CH_2/CH_3), 0.34 (9H, s, CH_3).

This was consistent with the previously published data.¹⁴⁹

T1Si¹⁴⁹



T1Si

9,9-Dihexyl-7-trimethylsilylfluoren-2-ylboronic acid **2.6** (1.29 g, 2.86 mmol, 4.77 eq), tribromohexahexyltruxene **2.3** (0.65 g, 0.60 mmol, 1.0 eq), *tetrakis*(triphenylphosphine)palladium(0) (0.18 g, 0.16 mmol, 0.26 eq) and barium hydroxide octahydrate (1.38 g, 4.38 mmol, 7.3 eq) were suspended in dry DME (20 ml) under Ar, to which degassed distilled water (2.6 ml) was added. The reaction mixture was then heated at 80 °C for 18 h, then

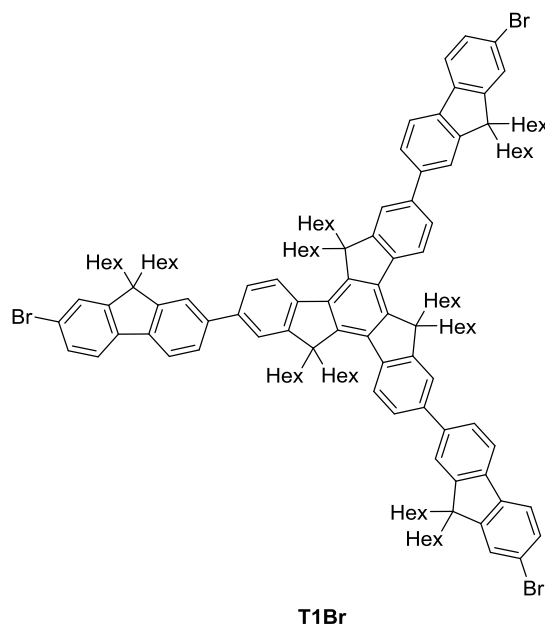
cooled to rt and quenched with a saturated aqueous solution of ammonium chloride (100 ml). The crude product was extracted with CH₂Cl₂ (6 x 100 ml), the organic layers were combined, dried over MgSO₄, the solvent was evaporated and the crude product was placed under vacuum overnight. The product was purified by silica gel chromatography, eluting with a petroleum ether/toluene 15:1 mixture to afford the product as a white powder (1.17 g, 95 %).

The ¹H NMR spectrum was recorded;

δ_{H} (400 MHz, CDCl₃): 8.50 (3H, d, *J* 6.4 Hz, CH), 7.84 (3H, d, *J* 6.0 Hz, CH), 7.79-7.75 (15H, m, CH), 7.56 (3H, d, *J* 6.0 Hz, CH₂), 7.54 (3H, s, CH), 3.10-3.05 (6H, m, CH₂), 2.28-2.22 (6H, m, CH₂), 2.08 (12H, t, *J* 6.0 Hz, CH₂) 1.10-0.91 (72H, m, CH₂), 0.88-0.71 (30H, m, CH₂ & CH₃), 0.70-0.62 (30H, m, CH₂ & CH₃), 0.35 (27H, s, CH₃).

This was consistent with the previously published data.¹⁴⁹

T1Br¹⁴⁹



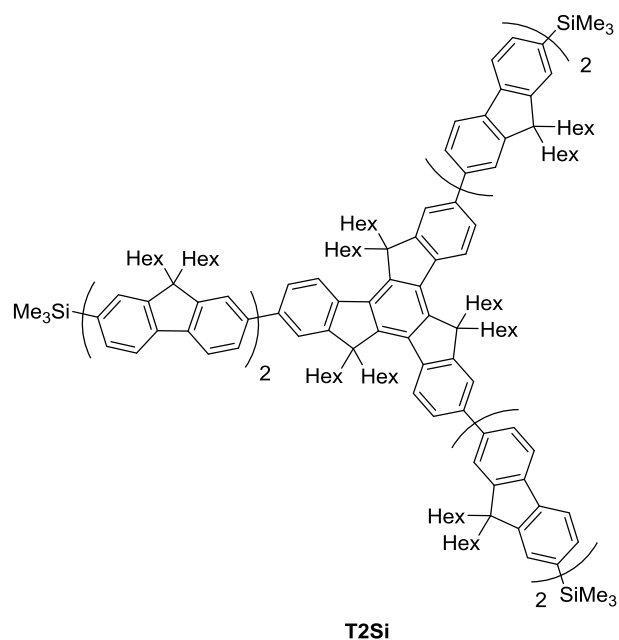
T1Si (1.17 g, 0.57 mmol, 1.0 eq) and sodium acetate (0.14 g, 1.71mmol, 3.0 eq) were dissolved in dry THF (35 ml) under Ar, and cooled to 0 °C.

Bromine (0.21 ml, 3.97 mmol, 7.0 eq) was added dropwise to the reaction mixture, which was stirred at 0 °C for 30 mins with minimum exposure to light. The reaction was quenched by addition of triethylamine (1 ml) followed by addition of an aqueous solution of sodium sulfite (1M, 40 ml). The aqueous mixture was diluted with distilled water (100 ml) and extracted with CH₂Cl₂ (5 x 200 ml). The organic layers were then washed with a saturated aqueous solution of sodium hydrogen carbonate (200 ml), dried over MgSO₄ and the solvent was evaporated. The crude product was filtered through a silica plug, washing with copious amounts of toluene. The solvent was then evaporated and the resulting oil was dissolved in the minimum volume of CH₂Cl₂. The addition of excess methanol resulted in a white precipitate, which was isolated by filtration to afford the title compound as a white powder (1.08 g, 92 %).

The ¹H NMR spectrum was recorded;

δ_{H} (400 MHz, CDCl₃): 8.50 (3H, d, *J* 8.8 Hz, CH), 7.80 (3H, d, *J* 6.0 Hz, CH), 7.79-7.76 (9H, m, CH), 7.72 (3H, s, CH₂), 7.63 (3H, d, *J* 8.0 Hz, CH), 7.52-7.50 (6H, m, CH), 3.09-3.06 (6H, m, CH₂), 2.27-2.24 (6H, m, CH₂), 2.11-2.03 (12H, m, CH₂) 1.18-0.82 (72H, m, CH₂), 0.84-0.71 (30H, m, CH₂ & CH₃), 0.70-0.62 (30H, m, CH₂ & CH₃).

This was consistent with the previously published data.¹⁴⁹

T2Si¹⁴⁹

(9,9,9',9'-Tetrahexyl-7'-(trimethylsilyl)-9H,9'H-[2,2'-bifluorene]-7-yl)boronic acid **2.8** (6.0 g, 7.66 mmol, 4.77 eq), tribromohexahexyltruxene **2.3** (1.73 g, 1.60 mmol, 1.0 eq), *tetrakis*(triphenylphosphine)palladium(0) (0.48 g, 0.42 mmol, 0.26 eq) and barium hydroxide octahydrate (3.69 g, 11.68 mmol, 7.3 eq) were suspended in dry THF (40 ml) under Ar, to which degassed distilled water (7.15 ml) was added. The reaction mixture was then heated at 80 °C for 18 h, then cooled to rt and quenched with a saturated aqueous solution of ammonium chloride (200 ml). The crude product was extracted with CH₂Cl₂ (8 x 200 ml), the organic layers were combined, dried over MgSO₄, the solvent was evaporated and the crude product was placed under vacuum overnight. The product was purified by silica gel chromatography, eluting with a petroleum ether/toluene 7:1 mixture, to afford the product as a white powder (4.47 g, 97%).

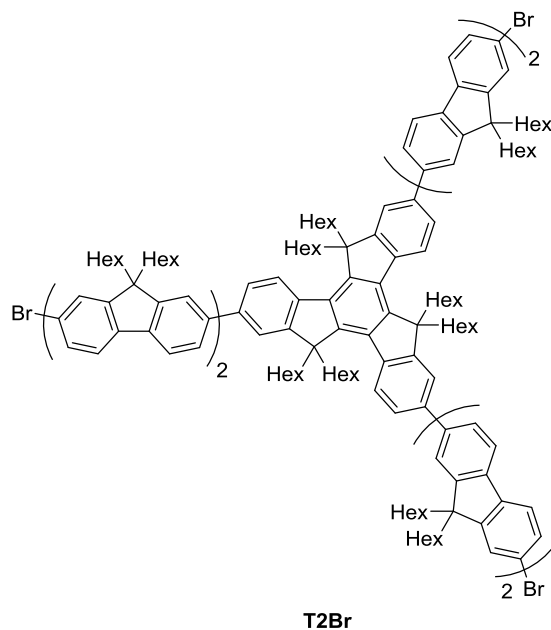
The ¹H NMR spectrum was recorded;

δ_{H} (400 MHz, CDCl₃): 8.53 (3H, d, *J* 8.0 Hz, CH), 7.88 (3H, d, *J* 7.6 Hz, CH), 7.86-7.50 (33H, m, CH), 7.21-7.18 (6H, m, CH), 3.10-3.05 (6H, m, m,

CH₂), 2.37-2.00 (30H, m, CH₂), 1.17-0.64 (198H, m, CH₂ & CH₃), 0.35 (27H, s, CH₃).

This was consistent with the previously published data.¹⁴⁹

T2Br¹⁴⁹



T2Si (0.30 g, 0.10 mmol, 1.0 eq) and sodium acetate (0.024 g, 0.29 mmol, 3.0 eq) were dissolved in dry THF (10 ml) under Ar, and cooled to 0 °C. Bromine (0.035 ml, 0.68 mmol, 7.0 eq) was added dropwise to the reaction mixture, which was stirred at 0 °C for 30 mins with minimum exposure to light. The reaction was quenched by addition of triethylamine (0.25 ml) followed by addition of an aqueous solution of sodium sulfite (1M, 10 ml). The aqueous mixture was diluted with distilled water (30 ml) and extracted with CH₂Cl₂ (5 x 50 ml). The organic layers were then washed with a saturated aqueous solution of sodium hydrogen carbonate (50 ml), dried over MgSO₄ and the solvent was evaporated. The crude product was filtered through a silica plug, washing with copious amounts of toluene. The solvent was then evaporated and the resulting oil was dissolved in the minimum volume of CH₂Cl₂. The addition of excess methanol resulted

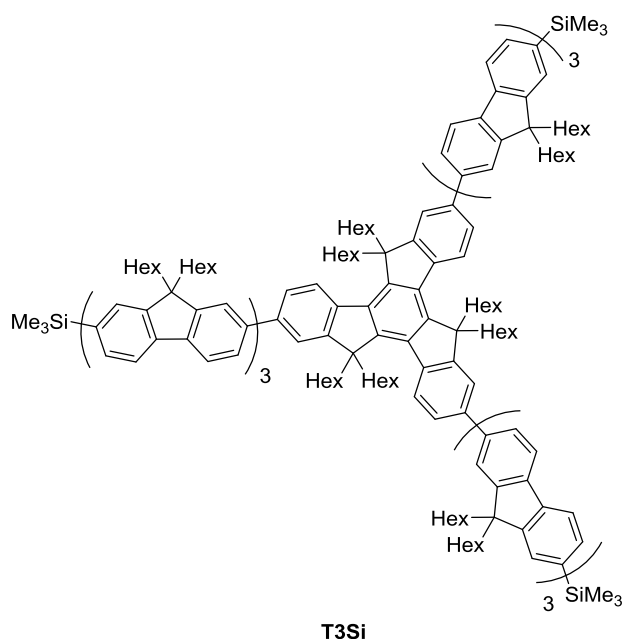
in a white precipitate, which was isolated by filtration to afford the title compound as a white powder (0.25 g, 83 %).

The ^1H NMR spectrum was recorded;

δ_{H} (400 MHz, CDCl_3): 8.53g (3H, d, J 8.0 Hz, CH), 7.80-7.61 (36H, m, CH), 7.52-7.49 (6H, m, CH), 3.09-3.06 (6H, m, CH_2), 2.28-2.02 (30H, m, CH_2), 1.20-0.63 (198H, m, CH_2 & CH_3).

This was consistent with the previously published data.¹⁴⁹

T3Si¹⁴⁹



(9,9,9',9',9'',9''-Hexahexyl-7''-(trimethylsilyl)-9H,9'H,9''H-[2,2':7',2''-terfluoren]-7-yl)boronic acid **2.10** (1.50 g, 1.34 mmol, 4.77 eq), tribromohexahexyltruxene **2.3** (0.31 g, 0.28 mmol, 1.0 eq), *tetrakis*(triphenylphosphine)palladium(0) (0.08 g, 0.07 mmol, 0.26 eq) and barium hydroxide octahydrate (0.65 g, 2.06 mmol, 7.3 eq) were suspended in dry THF (10 ml) under Ar, to which degassed distilled water (1.3 ml) was added. The reaction mixture was then heated at 80 °C for 18 h, cooled to rt and quenched with a saturated aqueous solution of

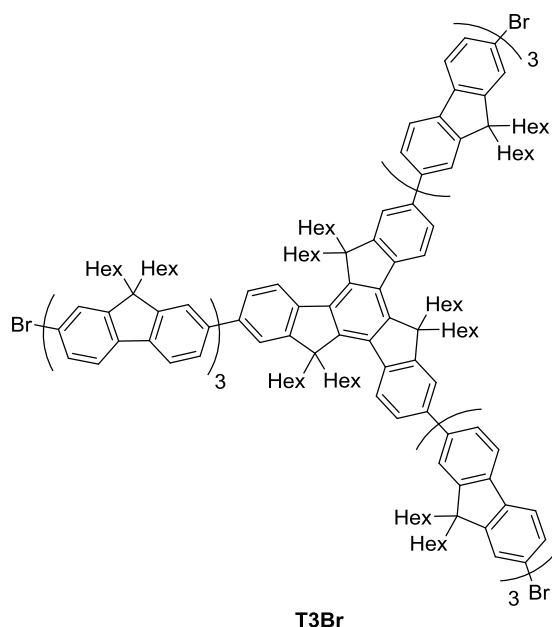
ammonium chloride (100 ml). The crude product was extracted with CH_2Cl_2 (8 x 100 ml), the organic layers were combined, dried over MgSO_4 , the solvent was evaporated and the crude product was placed under vacuum overnight. The product was purified by silica gel chromatography, eluting with a petroleum ether/toluene 10:1 mixture, to afford the product as a white powder (1.07 g, 94 %).

The ^1H NMR spectrum was recorded;

δ_{H} (400 MHz, CDCl_3): 8.54 (3H, d, J 6.4 Hz, CH), 7.91-7.80 (27H, m, CH), 7.75-7.65 (27H, m, CH), 7.54-7.52 (6H, m, CH), 3.12-3.07 (6H, m, CH_2), 2.30-2.00 (42H, m, CH_2), 1.02-0.65 (264H, m, CH_2 & CH_3), 0.35 (27H, s, CH_3).

This was consistent with the previously published data.¹⁴⁹

T3Br¹⁴⁹



T3Si (1.25 g, 0.31 mmol, 1.0 eq) and sodium acetate (0.076 g, 0.93 mmol, 3.0 eq) were dissolved in dry THF (10 ml) under Ar, and cooled to 0 °C. Bromine (0.11 ml, 2.15 mmol, 7.0 eq) was added dropwise to the reaction mixture, which was stirred at 0 °C for 30 mins with minimum exposure to

light. The reaction was quenched by addition of triethylamine (1 ml), followed by addition of an aqueous solution of sodium sulfite (1M, 40 ml). The aqueous mixture was diluted with distilled water (100 ml) and extracted with CH₂Cl₂ (5 x 200 ml). The organic layers were then washed with a saturated aqueous solution of sodium hydrogen carbonate (200 ml), dried over MgSO₄ and the solvent was evaporated. The crude product was filtered through a silica plug, washing with copious amounts of toluene. The solvent was then evaporated and the resulting oil was dissolved in the minimum volume of CH₂Cl₂. The addition of excess methanol resulted in a white precipitate, which was isolated by filtration to afford the title compound as a white powder (1.11 g, 89 %).

The ¹H NMR spectrum was recorded;

δ_{H} (400 MHz, CDCl₃): 8.53 (3H, d, *J* 6.0 Hz, CH), 7.82-7.61 (54H, m, CH), 7.51-7.49 (6H, m, CH), 3.12-3.06 (6H, m, CH₂), 2.28-1.98 (42H, m, CH₂), 1.18-0.64 (264H, m, CH₂ & CH₃).

This was consistent with the previously published data.¹⁴⁹

3-Iodothiophene (2.12)



2.12

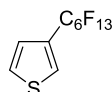
Copper iodide (0.71 g, 3.75 mmol, 0.05 eq) and sodium iodide (22.5 g, 150 mmol, 2.0 eq) were charged to the reaction vessel, which was backfilled with Ar. 3-Bromothiophene **2.11** (7 ml, 75.05 mmol, 1.0 eq), *N,N'*-dimethylethylenediamine (0.74 ml, 7.5 mmol, 0.1 eq) and 1,4-dioxane (80 ml) were added and the suspension heated at 110 °C, under Ar, for 24 h. The suspension was cooled to rt, diluted with hexane and filtered through silica gel (4 cm deep), eluting with diethyl ether. The solvent was then removed to afford the title product as a yellow liquid (11.5 g, 75 %).

The ^1H NMR of spectrum was recorded;

δ_{H} (400 MHz, CDCl_3): 7.42-7.41 (1H, dd, J 3.0, 1.0 Hz, CH), 7.22-7.20 (1H, dd, J 2.0, 3.0 Hz, CH), 7.13-7.11 (1H, dd, J 5.0, 1.0 Hz, CH).

This is consistent with the previously published data.¹⁹¹

3-Perfluorohexylthiophene (2.13)¹⁹²



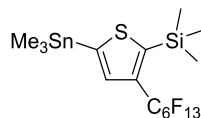
2.13

Copper powder (14.4 g, 228 mmol, 3.2 eq) was suspended in dry DMF (100 ml) under Ar, to which 3-iodothiophene **2.12** (15 g, 71.4 mmol, 1.0 eq) and perfluorohexyl iodide (23.2 ml, 107.1 mmol, 1.5 eq) were added. The reaction mixture was heated at 130 °C for 20 h, after which time it was cooled and filtered through celite to afford a purple solution. The solution was poured into chilled conc. hydrochloric acid (75 ml acid, 75 g ice) and decanted. The solution was then extracted with hexane (4 × 250 ml). The organic layers were combined, washed with sodium sulphite solution (250 ml, 0.1 M) and water (250 ml), dried over magnesium sulphate and the solvent evaporated. The product was purified by silica gel chromatography eluting with hexane to afford the title product as a yellow liquid (18.5 g, 64 %).

^1H NMR (400 MHz, CDCl_3): δ_{H} 7.75-7.74 (1H, m, CH), 7.47-7.44 (1H, m, CH), 7.26-7.24 (1H, m, CH); ^{19}F NMR (376 MHz, CDCl_3): δ_{F} -80.81 (3F), -106.07 (2F), -121.61 (2F), -122.26 (2F), -122.82 (2F), -126.12 (2F). HRMS (ED): calcd for $\text{C}_{10}\text{H}_3\text{F}_{13}\text{S}$, 401.9748, found m/z 401.9752 (M^+).

This was consistent with the previously published data.¹⁹²

**Trimethyl-(3-(perfluorohexyl)-5-(trimethylstannyl)thiophen-2-yl)silane
(2.14)**

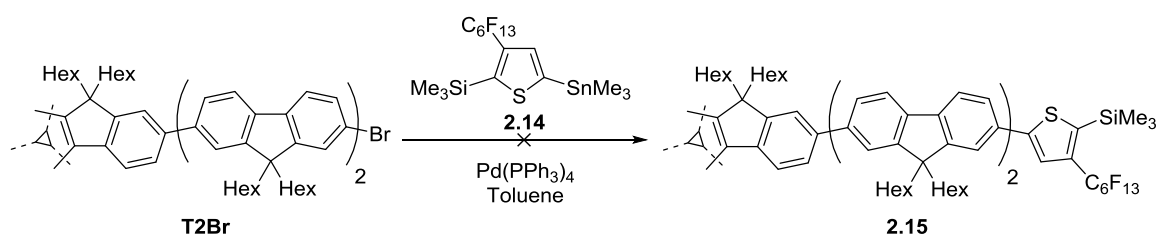


2.14

n-Butyllithium (2.15 M in hexane, 0.58 ml, 1.24 mmol, 1.0 eq) was added dropwise to a solution of 3-perfluorohexylthiophene **2.13** (0.5 g, 1.24 mmol, 1.0 eq) in dry THF (15 ml) at -80 °C, which was allowed to warm to rt, then cooled to -90 °C and chlorotrimethylsilane (0.15 ml, 1.24 mmol, 1.0 eq) was added dropwise. The reaction mixture was allowed to warm to rt and stir for 30 mins before cooling to -80 °C. *n*-Butyllithium (2.15 M in hexane, 0.68 ml, 1.49 mmol, 1.2 eq) was added dropwise, and the reaction mixture was allowed to warm to rt before cooling to -80 °C followed by the addition of trimethyltin chloride (1M in THF, 1.86 ml, 1.86 mmol, 1.5 eq). The reaction mixture was then allowed to warm to rt and stirred for 18 h under Ar. The reaction mixture was diluted with Et₂O (85 ml) and quenched with a saturated aqueous ammonium chloride solution (100 ml). The organic layer was separated, washed with brine (100 ml) and distilled water (100 ml), dried over MgSO₄ and the solvent was evaporated to afford a brown oil. The ¹H NMR was recorded and the title compound was used without further purification.

¹H NMR (400 MHz, CDCl₃): δ_H 7.43 (1H, s, CH), 0.41 (9H, s, CH₃), 0.34 (9H, s, CH₃).

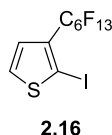
Attempted Synthesis of 2.15



Trimethyl(3-(perfluorohexyl)-5-(trimethylstannyl)thiophen-2-yl)silane

2.14 (76 mg, 0.12 mmol, 3.6 eq), **T2Br** (100 mg, 0.033 mmol, 1.0 eq) and *tetrakis*(triphenylphosphine)palladium(0) (2 mg, 0.0017 mmol, 0.05 eq) were dissolved in dry toluene (8 ml) under Ar and heated at 80 °C overnight. After cooling to rt the reaction mixture was diluted with Et₂O (100 ml), washed with a saturated aqueous solution of ammonium chloride (100ml) and distilled water (100 ml), dried over MgSO₄ and the solvent was evaporated. ¹H NMR and TLC analysis showed only starting materials present.

2-Iodo-3-perfluorohexylthiophene (2.16)

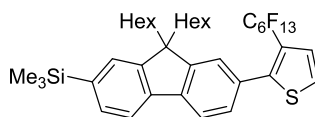


3-Perfluorohexylthiophene **2.13** (0.5 g, 1.24 mmol, 1.0 eq) was dissolved in THF (40 ml) under Ar and cooled to -80 °C, to which *n*-butyllithium (2.4 M in hexane, 0.57 ml, 1.36 mmol, 1.1 eq) was added dropwise. The reaction mixture was allowed to warm to rt over 30 mins, then cooled again to -80 °C where perfluorohexyliodide (0.32 ml, 1.49 mmol, 1.2 eq) was added, then allowed to warm to rt and stirred overnight under Ar. The reaction mixture was quenched with distilled water (100 ml) and the product was extracted with Et₂O (3 x 100 ml). The organic layers were

combined, washed with sodium sulfite solution (1 M, 100 ml) and distilled water (100 ml), dried over MgSO_4 , and the solvent was evaporated. Kugelrohr distillation (ca. 80 °C) removed starting material, and the product was purified by silica gel chromatography eluting with hexane to afford the product as a yellow oil (0.105 g, 16 %) with starting material impurities. The compound was used without further purification.

^1H NMR (400 MHz, CDCl_3): δ_{H} 7.53 (1H, d, J 5.6 Hz, CH), 6.99 (1H, d, J 5.6 Hz, CH); ^{13}C NMR (100 MHz, CDCl_3): δ_{C} 133.5, 133.2, 128.5; ^{19}F NMR (376 MHz, CDCl_3): δ_{F} -80.76 (3F), -105.85 (2F), -120.66 (2F), -121.65 (2F), -122.74 (2F), -126.05 (2F).

(9,9-Dihexyl-7-(3-(perfluorohexyl)thiophen-2-yl)-fluoren-2-yl)trimethylsilane (2.17)

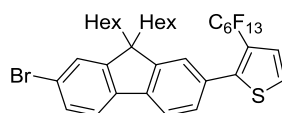


2.17

9,9-Dihexyl-7-trimethylsilylfluoren-2-ylboronic acid **2.6** (90 mg, 0.20 mmol, 1.05 eq), 2-iodo-3-perfluorohexylthiophene **2.16** (100 mg, 0.19 mmol, 1.0 eq), *tetrakis*(triphenylphosphine) palladium(0) (12 mg, 0.01 mmol, 0.05 eq) and barium hydroxide octahydrate (100 mg, 0.32 mmol, 1.6 eq) were suspended in THF (8 ml) and distilled water (0.3 ml) under Ar, and heated at 80 °C for 20 h. The reaction mixture was cooled to rt, then quenched with saturated ammonium chloride solution (50 ml) and the product was extracted with CH_2Cl_2 (4 x 50 ml). The organic layers were combined, dried over MgSO_4 and the solvent was evaporated. The residue was purified by silica gel chromatography eluting with distilled petroleum ether and the product was isolated as a yellow oil (0.12 g, 80 %).

^1H NMR (400 MHz, CDCl_3): δ_{H} 7.71 (2H, d, J 7.6 Hz, CH), 7.51 (1H, d, J 7.6 Hz, CH), 7.48 (1H, s, CH), 7.40-7.37 (3H, m, CH), 7.22 (1H, d, J 5.6 Hz, CH), 1.97-1.91 (4H, m, CH_2), 1.12-1.03 (12H, m, CH_2), 0.78-0.74 (6H, m, CH_3), 0.67-0.63 (4H, m, CH_2), 0.327 (9H, s, CH_3); ^{13}C NMR (100 MHz, CDCl_3): δ_{C} 150.8, 150.6, 149.2, 142.2, 141.3, 140.1, 132.2, 130.9, 129.3, 127.9, 127.6, 125.6, 125.2, 125.0, 119.6, 119.4, 119.3, 55.5, 40.5, 31.7, 31.7, 31.6, 29.9, 23.9, 22.81, 22.78, 22.75, 14.3, 14.21, 14.18; ^{19}F NMR (376 MHz, CDCl_3): δ_{F} -80.85 (3F), -102.05 (2F), -120.94 (2F), -121.80 (2F), -122.85 (2F), -126.16 (2F) ; m/z (ESI) 805.85 ($[\text{M}]^+$, 100 %). HRMS (ED): calcd for $\text{C}_{38}\text{H}_{43}\text{F}_{13}\text{SSi}$, 806.2647, found m/z 806.2642 (M^+).

2-(7-Bromo-9,9-dihexylfluoren-2-yl)-3-(perfluorohexyl)thiophene (2.18)



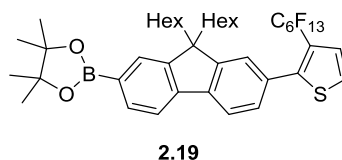
2.18

(9,9-Dihexyl-7-(3-(perfluorohexyl)thiophen-2-yl)-fluoren-2-yl)trimethylsilane **2.17** (112 mg, 0.14 mmol, 1.0 eq) and sodium acetate (11.5 mg, 0.14 mmol, 1.0 eq) were dissolved in THF (7 ml) under Ar. The reaction vessel was covered in tin foil and cooled to 0 °C using an ice bath. Bromine (0.014 ml, 0.28 mmol, 2.30 eq) was added to the reaction mixture dropwise, which was then stirred at 0 °C under Ar for 30 mins. The reaction mixture was quenched with triethylamine (0.1 ml) followed by a sodium sulfite solution (1 M, 4 ml). The mixture was diluted with distilled water (10 ml) and the product was extracted with CH_2Cl_2 (5 x 20 ml). The organic layers were combined, washed with saturated sodium hydrogen carbonate solution (20 ml), then dried over MgSO_4 and the solvent was evaporated. The crude product was dissolved in toluene and filtered through a silica plug, eluting with more toluene. The solvent was then

evaporated to afford the product as a yellow oil (0.094g, 82 %). This was used immediately without further purification.

^1H NMR (400 MHz, CDCl_3): δ_{H} 7.67 (1H, d, J 8.4 Hz, CH), 7.59 (1H, d, J 8.4 Hz, CH), 7.48 (2H, m, CH), 7.40-7.37 (3H, m, CH), 7.22 (1H, d, J 5.6 Hz, CH), 1.97-1.93 (4H, m, CH_2), 1.12-1.03 (12H, m, CH_2), 0.78-0.75 (6H, m, CH_3), 0.67-0.63 (4H, m, CH_2); ^{13}C NMR (100 MHz, CDCl_3): δ_{C} 153.7, 150.3, 141.1, 139.8, 131.3, 130.5, 129.6, 127.7, 126.6, 125.7, 125.1, 122.0, 121.7, 119.5, 55.9, 40.7, 31.8, 29.9, 24.0, 22.9, 14.2; ^{19}F NMR (376 MHz, CDCl_3): δ_{F} -80.85 (3F), -102.05 (2F), -120.94 (2F), -121.77 (2F), -122.83 (2F), -126.14 (2F).

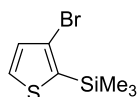
2-(9,9-Dihexyl-7-(3-(perfluorohexyl)thiophen-2-yl)-fluoren-2-yl)-4,4,5,5-tetramethyl-1,3,2-dioxaborolane (2.19)



2-(7-Bromo-9,9-dihexylfluoren-2-yl)-3-(perfluorohexyl)thiophene **2.18** (550 mg, 0.68 mmol, 1.0 eq), bis(pinacolato)diboron (208 mg, 0.82 mmol, 1.2 eq), *tetrakis*(triphenylphosphine)palladium(0) (38 mg, 0.03 mmol, 0.05 eq) and potassium acetate (186 mg, 1.90 mmol, 2.8 eq) were dissolved in dry 1,4-dioxane (7ml) under Ar, and heated at 110 °C for 20 h. The reaction mixture was cooled to rt and quenched with distilled water (50 ml), then the product was extracted with Et_2O (4 x 40 ml). The organic layers were combined, washed with brine (50 ml), dried over MgSO_4 and the solvent was evaporated. The product was purified by silica gel chromatography, eluting first with ethyl acetate/hexane (1:50) to remove impurities, then with ethyl acetate/hexane (1:20) to afford the product as an orange semi-solid (0.272 g, 46 %).

^1H NMR (400 MHz, CDCl_3): δ_{H} 7.84-7.81 (1H, m, CH), 7.76-7.72 (2H, m, CH), 7.49-7.47 (1H, m, CH), 7.40-7.37 (3H, m, CH), 7.22 (1H, d, J 5.6 Hz), 2.01-1.93 (4H, m, CH_2), 1.36 (12H, s, CH_3), 1.11-1.02 (12H, m, CH_2), 0.77-0.73 (6H, m, CH_3), 0.68-0.5 (4H, m, CH_2); ^{13}C NMR (100 MHz, CDCl_3): δ_{C} 150.2, 150.6, 149.1, 143.7, 142.0, 135.1, 134.2, 131.3, 139.3, 139.2, 128.1, 127.6, 125.6, 125.2, 119.8, 119.6, 84.1, 55.6, 40.6, 31.8, 30.0, 25.3, 25.2, 24.0, 22.9, 14.2; ^{19}F NMR (376 MHz, CDCl_3): δ_{F} -80.83 (3F), -102.08 (2F), -120.94 (2F), -121.79 (2F), -122.82 (2F), -126.14 (2F). m/z (ESI) 860.35 ($[\text{M}]^+$, 100 %). HRMS (EI): calcd for $\text{C}_{41}\text{H}_{46}\text{F}_{13}\text{O}_2\text{S}$ 860.3116, found m/z 860.3104 (M^+).

2-Trimethylsilyl-3-bromothiophene (2.20)¹⁹³



2.20

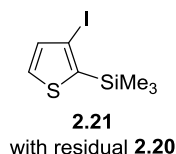
3-Bromothiophene **2.11** (5 ml, 53.4 mmol, 1.0 eq) was dissolved in dry THF (50ml) under Ar and cooled in an ice-bath, to which lithium bis(trimethylsilyl) amide (1.0 M in THF, 58.7 ml, 58.7 mmol, 1.1 eq) was added dropwise. The reaction mixture was stirred for 1 h, after which time chlorotrimethylsilane (13.5 ml, 106.8 mmol, 2.0 eq) was added dropwise and stirred for 2 h. The reaction mixture was quenched with sat. aq. ammonium chloride solution (200 ml) and distilled water (200 ml). The aqueous layer was extracted with Et_2O (350 ml), and the organic layer was washed with water (200 ml), dried over MgSO_4 and the solvent was evaporated. Kugelrohr distillation removed trace amounts of starting material **2.11** and the crude product was purified by silica gel chromatography, eluting with hexane, to afford the product as a colourless oil (11.54 g, 90 %).

The ^1H NMR spectrum was recorded;

^1H NMR (400 MHz, CDCl_3): δ_{H} 7.45 (1H, d, J 4.8 Hz, CH), 7.11 (1H, d, J 5.2 Hz, CH), 0.48 (9H, s, CH_3).

This was consistent with the previously published data.¹⁹³

2-Trimethylsilyl-3-iodothiophene (2.21)

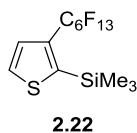


Copper iodide (0.45 g, 2.4 mmol, 0.05 eq) and sodium iodide (14.65 g, 97.8 mmol, 2.0 eq) were suspended in freshly distilled dioxane (75 ml) under Ar, to which 2-trimethylsilyl-3-bromothiophene **2.20** (11.5 g, 48.9 mmol, 1.0 eq) and N,N' -dimethylethylenediamine (0.48 ml, 4.89 mmol, 0.1 eq) were added. The reaction mixture was heated at reflux for 12 h, then cooled to rt, and filtered through a silica plug, washing with Et_2O . The solvent was removed to afford a mixture of the product and starting material. The crude material was used without further purification (6.5 g product, estimated by ^1H NMR integrals).

The ^1H NMR spectrum for **2.21** is as follows:

^1H NMR (400 MHz, CDCl_3): δ_{H} 7.39 (1H, d, J 5.0 Hz, CH), 7.23 (1H, d, J 4.5 Hz, CH), 0.48 (9H, s, CH_3).

2-Trimethylsilyl-3-perfluorohexylthiophene (2.22)

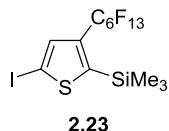


Copper powder (4.29 g, 68.03 mmol, 3.2 eq) and a mixture of **2.21** and **2.20** (6.0 g, 21.26 mmol, 1.0 eq of **2.21** assumed) were suspended in dry

DMF (50 ml) under Ar, to which perfluorohexyliodide (6.9 ml, 31.89 mmol, 1.5 eq) was added. The reaction mixture was heated at 130 °C for 72 h, then cooled to rt, filtered over Celite and diluted with distilled water (100 ml). The aqueous layer was extracted with hexane (3 x 200 ml), then the organic layers were combined and washed with aq. sodium sulphite solution (1.0 M, 200 ml) and distilled water (100 ml), dried over MgSO₄ and the solvent was evaporated. The crude product was suspended in a 5 % H₂O/EtOH solution (30 ml), which was extracted with perfluorohexanes (2 x 25 ml). The fluorinated layer was dried over MgSO₄ and the solvent was evaporated to afford the product as a yellow oil (2.85 g, 28 %).

¹H NMR (400 MHz, CDCl₃): δ_H 7.63-7.61 (1H, m, CH), 7.34-7.32 (1H, m, CH), 0.38 (9H, s, CH₃); ¹³C NMR (100 MHz, CDCl₃): δ_C 145.0, 134.7, 134.4, 131.3, 129.1, 0.57; ¹⁹F NMR (376 MHz, CDCl₃): δ_F -80.85 (3F), -102.08 (2F), -120.21 (2F), -121.58 (2F), -122.80 (2F), -126.06 (2F); HRMS (ED): calcd for C₁₃H₁₁F₁₃SSi, 474.0143, found m/z 474.0145 (M⁺).

2-Trimethylsilyl-3-perfluorohexyl-5-iodothiophene (2.23)

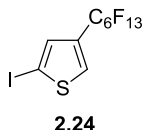


2-Trimethylsilyl-3-perfluorohexylthiophene **2.22** (2.5 g, 5.27 mmol, 1.0 eq) was dissolved in dry THF (100ml) under Ar and cooled to -80 °C, to which *n*-butyllithium (2.37M in hexane, 2.44 ml, 5.80 mmol, 1.1 eq) was added dropwise and stirred for 15 mins at -80 °C, after which perfluorohexyliodide (1.37 ml, 6.32 mmol, 1.2 eq) was added dropwise. The reaction mixture was allowed to warm to rt and stir for 18 h, then quenched with sat. sodium hydrogen carbonate solution (100 ml) and diluted with distilled water (100 ml). The aqueous layer was extracted

with Et₂O (3 x 150 ml) and the organic layers were combined, dried over MgSO₄ and the solvent was evaporated. The product was purified by filtering through a silica plug, eluting with hexane, to afford the product as a golden oil (2.75 g, 87 %).

¹H NMR (400 MHz, CDCl₃): δ_H 7.41 (1H, t, *J* 1.6 Hz, CH), 0.37 (9H, s, CH₃); ¹³C NMR (100 MHz, CDCl₃): δ_C 152.6, 138.3, 136.1, 79.0, 0.4; ¹⁹F NMR (376 MHz, CDCl₃): δ_F -80.80 (3F), -102.77 (2F), -120.13 (2F), -121.55 (2F), -122.76 (2F), -126.04 (2F); HRMS (EI): calcd for C₁₀H₁₀F₁₃ISSi, 599.9110, found m/z 599.9107 (M⁺)

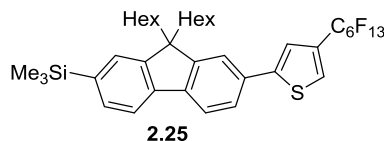
2-Iodo-4-perfluorohexylthiophene (2.24)



2-Trimethylsilyl-3-perfluorohexyl-5-iodothiophene **2.23** (2.75 g, 4.58 mmol, 1.0 eq) was dissolved in dry (THF) under Ar, to which tetrabutylammonium fluoride (1.0 M in THF, 4.81 ml, 4.81 mmol, 1.05 eq) was added dropwise and stirred at rt for 4 h. The reaction mixture was quenched with distilled water (100 ml) and the aqueous layer was extracted with Et₂O (2 x 100 ml). The organic layers were combined, dried over MgSO₄ and the solvent was evaporated to afford a black oil. The crude product was filtered through a silica plug eluting with Et₂O to afford the product as a brown oil (2.01 g, 83 %).

¹H NMR (400 MHz, CDCl₃): δ_H 7.74 (1H, s, CH), 7.37 (1H, s, CH); ¹³C NMR (100 MHz, CDCl₃): δ_C 135.0, 134.4, 132.1, 75.6; ¹⁹F NMR (376 MHz, CDCl₃): δ_F -80.78 (3F), -106.68 (2F), -12.54 (2F), -121.07 (2F), -122.78 (2F), -126.02 (2F); HRMS (EI): calcd for C₁₀H₂F₁₃IS, 527.8714, found m/z 527.8710 (M⁺),.

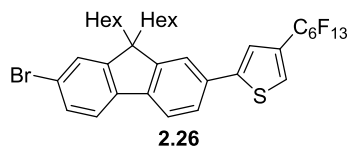
(9,9-Dihexyl-7-(4-(perfluorohexyl)thiophen-2-yl)-9H-fluoren-2-yl)trimethylsilane (2.25)



9,9-Dihexyl-7-trimethylsilylfluoren-2-ylboronic acid **2.6** (1.34 g, 2.98 mmol, 1.05 eq), 2-iodo-4-perfluorohexylthiophene **2.24** (1.5 g, 2.84 mmol, 1.0 eq), *tetrakis*(triphenylphosphine) palladium(0) (0.16 g, 0.14 mmol, 0.05 eq) and barium hydroxide octahydrate (1.46 g, 4.54 mmol, 1.6 eq) were suspended in dry THF (120 ml) and distilled water (5 ml) under Ar, and heated at 80 °C for 20 h. The reaction mixture was cooled to rt, then quenched with saturated ammonium chloride solution (200 ml) and the product was extracted with CH₂Cl₂ (4 x 200 ml). The organic layers were combined, dried over MgSO₄ and the solvent was evaporated. The product was purified by silica gel chromatography eluting with distilled petroleum ether and the product was isolated as a yellow oil (1.25 g, 55 %).

¹H NMR (400 MHz, CDCl₃): δ_H 7.74-7.69 (2H, m, CH), 7.66 (1H, s, CH), 7.59-7.57 (1H, m, CH), 7.54-7.50 (2H, m, CH), 7.48 (1H, s, CH), 7.44 (1H, s, CH), 2.03-1.99 (4H, m, CH₂), 1.14-1.07 (12H, m, CH₂), 0.78-0.75 (6H, t, *J* 6.8 Hz, CH₃), 0.70-0.66 (4H, m, CH₂), 0.33 (9H, s, CH₃); ¹³C NMR (100 MHz, CDCl₃): δ_C 152.4, 150.4, 147.9, 142.1, 141.2, 140.1, 132.3, 132.2, 131.1, 128.0, 127.0, 125.4, 120.9, 120.7, 119.5, 55.6, 40.4, 31.7, 29.9, 24.0, 22.8, 14.3; ¹⁹F NMR (376 MHz, CDCl₃): δ_F -80.75 (3F), -106.57 (2F), -121.46 (2F), -121.91 (2F), -122.72 (2F), -126.02 (2F); HRMS (EI): calcd for C₃₈H₄₂F₁₃SSi, 806.2647, found *m/z* 806.2646 (M⁺),.

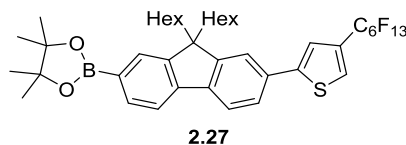
2-(7-Bromo-9,9-dihexyl-9H-fluoren-2-yl)-4-(perfluorohexyl)thiophene
(2.26)



(9,9-Dihexyl-7-(4-(perfluorohexyl)thiophen-2-yl)-9H-fluoren-2-yl)trimethylsilane **2.25** (1.25 g, 1.55 mmol, 1.0 eq) and sodium acetate (0.127 g, 1.55 mmol, 1.0 eq) were dissolved in dry THF (50 ml) under Ar. The reaction vessel was covered in tin foil and cooled to 0 °C using an ice bath. Bromine (0.15 ml, 3.10 mmol, 2.0 eq) was added to the reaction mixture dropwise, which was then stirred at 0 °C under Ar for 30 mins. The reaction mixture was quenched with triethylamine (1 ml) followed by a sodium sulfite solution (1 M, 50 ml). The mixture was diluted with distilled water (100 ml) and the product was extracted with CH₂Cl₂ (4 x 200 ml). The organic layers were combined, washed with saturated sodium hydrogen carbonate solution (100 ml), then dried over MgSO₄ and the solvent was evaporated. The crude product was dissolved in toluene and filtered through a silica plug, eluting with more toluene. The solvent was then evaporated to afford the product as a yellow oil (1.15 g, 91 %).

¹H NMR (400 MHz, CDCl₃): δ_H 7.70-7.67 (2H, m, CH), 7.61-7.57 (2H, m, CH), 7.52 (1H, d, *J* 1.2 Hz, CH), 7.50-7.48 (2H, m, CH), 7.44 (1H, s, CH), 2.02-1.97 (4H, m, CH₂), 1.16-1.04 (12H, m, CH₂), 0.80-0.76 (6H, t, *J* 6.8 Hz, CH₃), 0.68-0.62 (4H, m, CH₂); ¹³C NMR (100 MHz, CDCl₃): δ_C 153.5, 151.8, 147.5, 141.0, 139.7, 132.5, 131.1, 130.5, 129.4, 128.6, 127.1, 126.6, 125.6, 121.9, 121.6, 121.1, 120.7, 120.6, 56.0, 40.6, 31.8, 30.0, 24.0, 22.9, 14.3; ¹⁹F NMR (376 MHz, CDCl₃): δ_F -80.77 (3F), -106.58 (2F), -121.46 (2F), -121.90 (2F), -122.74 (2F), -126.00 (2F); HRMS (EI): calcd for C₃₅H₃₄BrF₁₃S, 812.1357, found *m/z* 812.1347 (M⁺).

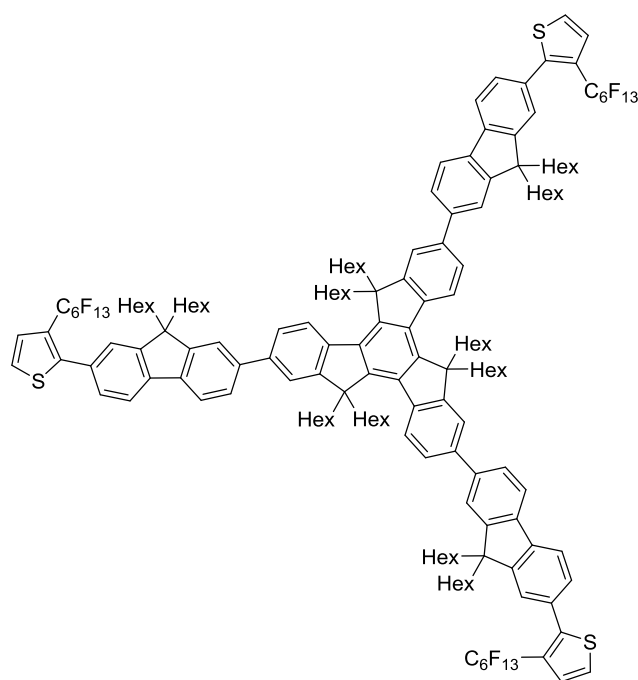
2-(9,9-Dihexyl-7-(4-(perfluorohexyl)thiophen-2-yl)-9H-fluoren-2-yl)-4,4,5,5-tetramethyl-1,3,2-dioxaborolane (2.27)



2-(7-bromo-9,9-dihexyl-9H-fluoren-2-yl)-4-(perfluorohexyl)thiophene thiophene **2.26** (1.15 g, 1.41 mmol, 1.0 eq), bis(pinacolato)diboron (0.43 g, 1.69 mmol, 1.2 eq), *tetrakis*(triphenylphosphine)palladium(0) (81 mg, 0.07 mmol, 0.05 eq) and potassium acetate (0.39 g, 3.95 mmol, 2.8 eq) were dissolved in dry dioxane (14 ml) under Ar, and heated at 110 °C for 20 h. The reaction mixture was cooled to rt and quenched with distilled water (100 ml), then the product was extracted with Et₂O (4 x 100 ml). The organic layers layers combined, washed with brine (100 ml), dried over MgSO₄ and the solvent was evaporated. The product was purified by silica gel chromatography, eluting first with ethyl acetate/hexane (1:50) to remove impurities then with ethyl acetate/hexane (1:20) to afford the product as a brown oil (0.35 g, 30 %).

¹H NMR (400 MHz, CDCl₃): δ_H 7.86-7.84 (1H, d, *J* 7.6 Hz, CH), 7.79-7.71 (3H, m, CH), 7.67 (1H, d, *J* 7.6 Hz, CH), 7.61-7.59 (1H, m, CH), 7.53 (1H, s, CH), 7.46 (1H, s, CH), 2.08-2.01 (4H, m, CH₂), 1.41 (12H, s, CH₃) 1.14-1.02 (12H, m, CH₂), 0.78-0.75 (6H, t, *J* 6.8 Hz, CH₃), 0.69-0.62 (4H, m, CH₂); ¹³C NMR (100 MHz, CDCl₃): δ_C 152.8, 150.48, 147.8, 143.6, 142.0, 134.3, 132.5, 131.1, 129.3, 129.2, 127.1, 125.4, 121.0, 120.6, 119.6, 84.2, 55.7, 41.6, 31.8, 30.0, 25.3, 24.0, 22.9, 14.3; ¹⁹F NMR (376 MHz, CDCl₃): δ_F -80.79 (3F), -106.58 (2F), -121.47 (2F), -121.91 (2F), -122.74 (2F), -126.05 (2F); HRMS (EI): calcd for C₄₁H₄₆BF₁₃O₂S, 860.3116, found m/z 860.3099 (M⁺).

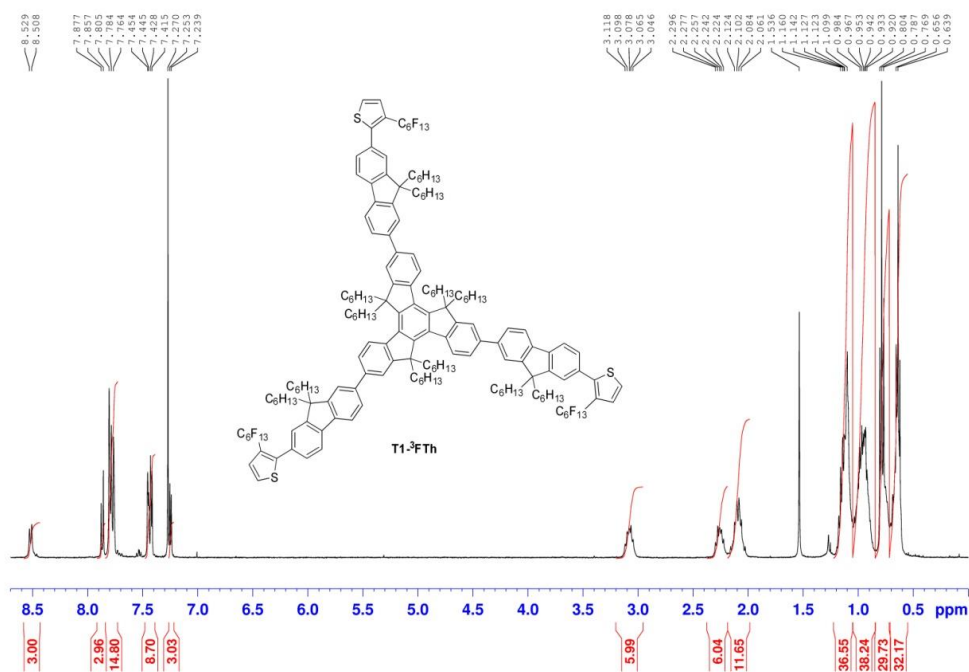
T1-³FTh



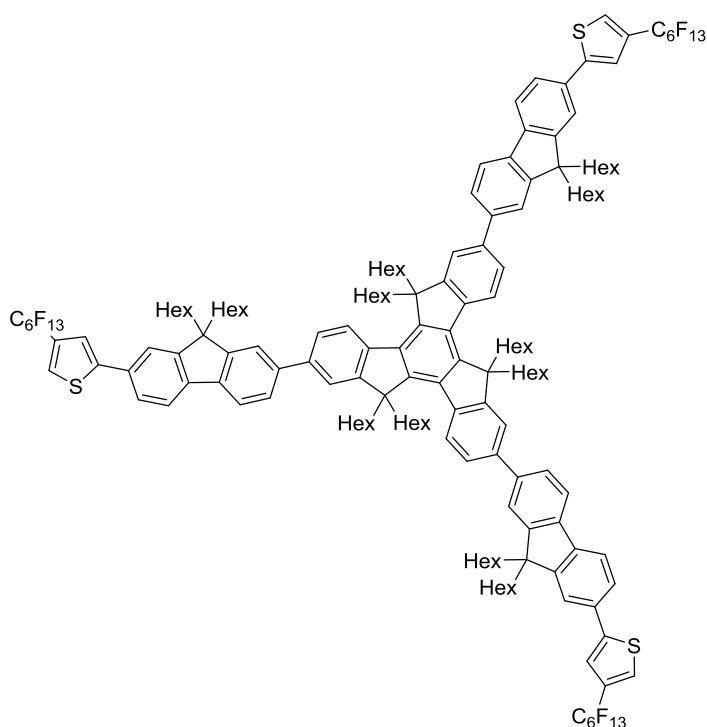
T1-³FTh

2-(9,9-Dihexyl-7-(3-(perfluorohexyl)thiophen-2-yl)-fluoren-2-yl)-4,4,5,5-tetramethyl-1,3,2-dioxaborolane **2.19** (210 mg, 0.24 mmol, 4.77 eq), tribromohexahexyltruxene **2.3** (54.2 mg, 0.05 mmol, 1.0 eq), *tetrakis*(triphenylphosphine)palladium(0) (17.3 mg, 0.015 mmol, 0.3 eq) and barium hydroxide octahydrate (115 mg, 0.37 mmol, 7.3 eq) were suspended in THF (5 ml) under Ar, to which degassed distilled water (0.65 ml) was added. The reaction mixture was then heated at 80 °C for 18 h, then cooled to rt and quenched with a saturated aqueous solution of ammonium chloride (50 ml). The crude product was extracted with CH₂Cl₂ (6 x 50 ml), the organic layers were combined, dried over MgSO₄, the solvent was evaporated and the crude product was placed under vacuum overnight. The product was loaded onto silica and eluted with a petroleum ether/toluene (10:1) mixture to afford the product as a white powder (110 mg, 72%).

^1H NMR (400 MHz, CDCl_3): δ_{H} 8.52 (3H, s, CH), 7.87 (3H, d, J 7.6 Hz, CH), 7.81-7.76 (12H, m, CH), 7.53 (3H, d, J 8.0 Hz, CH), 7.50-7.41 (9H, m, CH), 7.25 (3H, d, J 5.2 Hz, CH) 3.08-3.07 (6H, m, CH_2) 2.28-2.26 (6H, m, CH_2), 2.10-2.08 (12H, m, CH_2), 1.14-1.07 (36H, m, CH_3), 0.98-0.87 (36H, m, CH_3), 0.80-0.77 (30H, m, CH_2), 0.66-0.62 (30H, m, CH_2); ^{13}C NMR (100 MHz, CDCl_3): δ_{C} 154.8, 152.3, 150.9, 149.2, 145.6, 142.0, 141.1, 140.1, 140.0, 139.8, 138.5, 130.8, 129.5, 127.7, 126.5, 125.6, 125.3, 125.2, 125.0, 121.6, 120.9, 120.7, 119.4, 56.3, 55.8, 40.9, 37.5, 31.9, 31.8, 30.0, 29.9, 24.4, 24.1, 22.9, 22.7, 14.2; ^{19}F NMR (376 MHz, CDCl_3): δ_{F} -80.83 (9F), -102.00 (6F), -120.889 (6F), -121.75 (6F), -122.81 (6F), -126.15 (6F); MALDI-TOF MS : m/z 2959.39 ($[\text{M}-\text{C}_6\text{H}_{13}]^+$, 100 %), 2981.01 ($[\text{M}-\text{C}_6\text{H}_{13}+\text{Na}]$, 70 %), 3044.50 ($[\text{M}]^+$, 35 %).



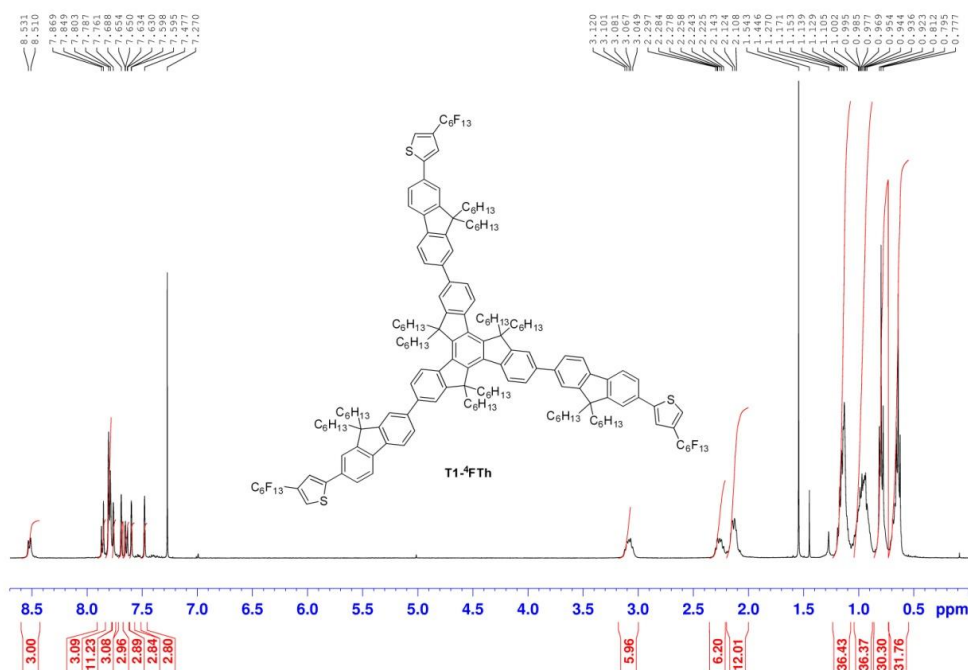
T1-4FTh



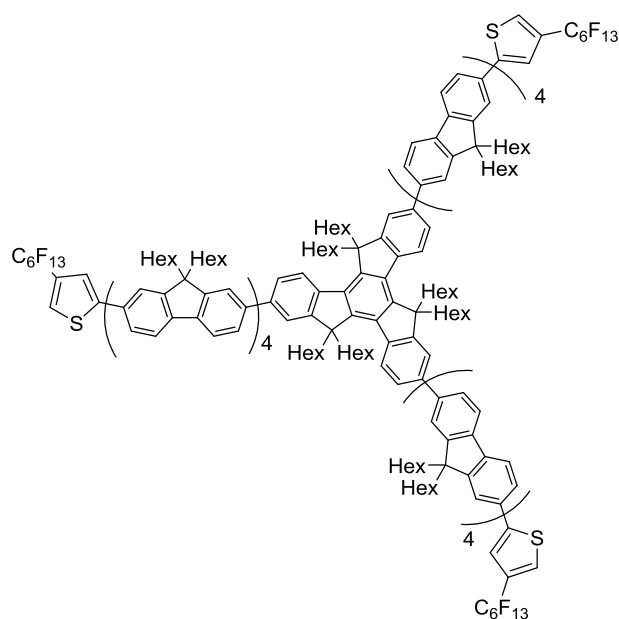
T1-4FTh

2-(9,9-Dihexyl-7-(4-(perfluorohexyl)thiophen-2-yl)-9H-fluoren-2-yl)-4,4,5,5-tetramethyl-1,3,2-dioxaborolane **2.27** (350 mg, 0.407 mmol, 4.77 eq), tribromohexahexyltruxene **2.3** (92 mg, 0.085 mmol, 1.0 eq), *tetrakis*(triphenylphosphine)palladium(0) (29 mg, 0.0255 mmol, 0.3 eq) and barium hydroxide octahydrate (196 mg, 0.62 mmol, 7.3 eq) were suspended in THF (8 ml) under Ar, to which degassed distilled water (1 ml) was added. The reaction mixture was then heated at 80 °C for 18 h, then cooled to rt and quenched with a saturated aqueous solution of ammonium chloride (50 ml). The crude product was extracted with CH₂Cl₂ (6 x 50 ml), the organic layers were combined, dried over MgSO₄, the solvent was evaporated and the crude product was placed under vacuum overnight. The product was loaded onto silica and eluted with a petroleum ether/toluene (15:1) mixture to afford the product as a sticky yellow solid (195 mg, 75 %).

^1H NMR (400 MHz, CDCl_3): δ_{H} 8.52 (3H, d, J 8.4 Hz, CH), 7.86 (3H, d, J 8.0 Hz, CH), 7.80 (12H, d, J 6.4 Hz, CH), 7.76 (3H, s, CH), 7.69 (3H, s, CH), 7.64 (3H, d, J 8.0 Hz, CH), 7.60 (3H, s, CH), 7.48 (3H, s, CH), 3.10-3.08 (6H, m, CH_2), 2.27-2.24 (6H, m, CH_2), 2.14-2.11 (12H, m, CH_2), 1.17-1.11 (36H, m, CH_2), 1.00-0.92 (36H, m, CH_3), 0.81-0.78 (30H, m, CH_2), 0.69-0.62 (30H, m, CH_2); ^{13}C NMR (100 MHz, CDCl_3): δ_{C} 154.8, 152.5, 152.1, 147.8, 145.6, 141.9, 141.0, 140.1, 140.0, 139.8, 138.5, 132.1, 131.1, 127.0, 126.6, 125.6, 125.3, 121., 121.0, 120.6, 56.3, 55.9, 40.8, 37.5, 31.9, 31.8, 30.0, 29.9, 24.4, 24.2, 22.86, 22.69, 22.7, 14.32, 14.27, 14.2; ^{19}F NMR (376 MHz, CDCl_3): δ_{F} -80.73 (3F), -106.57 (2F), -121.46 (2F), -121.90 (2F), -122.73 (2F), -126.03 (2F); MALDI-TOF MS: m/z 2959.39 ($[\text{M}-\text{C}_6\text{H}_{13}]^+$, 100 %), 2981.01 ($[\text{M}-\text{C}_6\text{H}_{13}+\text{Na}]$, 70 %), 3044.50 ($[\text{M}]^+$, 35 %).



T4-⁴FTh

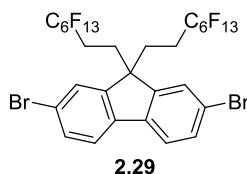


T4-⁴FTh

2-(9,9-Dihexyl-7-(4-(perfluorohexyl)thiophen-2-yl)-9H-fluoren-2-yl)-4,4,5,5-tetramethyl-1,3,2-dioxaborolane **2.27** (54 mg, 0.063 mmol, 6.0 eq), **T3Br** (46 mg, 0.011 mmol, 1.0 eq), *tetrakis*(triphenylphosphine)-palladium(0) (16 mg, 0.014 mmol, 1.2 eq) and barium hydroxide octahydrate (59 mg, 0.19 mmol, 17.0 eq) were suspended in THF (5 ml) under Ar, to which degassed distilled water (0.12 ml) was added. The reaction mixture was then heated at 80 °C for 24 h, then cooled to rt and quenched with a saturated aqueous solution of ammonium chloride (50 ml). The crude product was extracted with CH₂Cl₂ (6 x 50 ml), the organic layers were combined, dried over MgSO₄, the solvent was evaporated and the crude product was placed under vacuum overnight. The product was loaded onto silica and eluted with a petroleum ether/dichloromethane (7:1) mixture to afford a yellow solid. The product was precipitated from the minimum volume of CH₂Cl₂ by the addition of methanol to afford the title product as an off white solid (57.9 mg, 85 %).

^1H NMR (400 MHz, CDCl_3) δ_{H} , 8.70-8.40 (1H, d, broad), 8.00-7.56 (27H, m, CH), 7.47 (1H, s, CH), 3.30-2.90 (2H, s, broad, CH_2), 2.48-1.90 (18H, m, CH_2), 1.30-0.60 (110H, m, CH_2 and CH_3); ^{13}C NMR (CDCl_3 , δ , 100 MHz) 154.6, 152.3, 152.0, 151.9, 147.6, 145.4, 141.6, 141.2, 140.8, 140.7, 140.5, 140.3, 140.3, 140.2, 140.13, 139.8, 139.7, 139.6, 138.4, 131.8, 130.9, 126.5, 126.4, 125.4, 121.7, 121.5, 120.7, 120.4, 56., 55.61, 55.55, 55.51, 40.5, 31.4, 31.7, 31.66, 31.63, 29.9, 29.8, 29.7, 24.2, 24.0, 23.9, 22.8, 22.7, 22.5, 14.2, 14.12, 14.10; ^{19}F NMR (376 MHz, CDCl_3): δ_{F} -80.73 (3F), -106.56 (2F), -121.45 (2F), -121.88 (2F), -122.71 (2F), -126.01 (2F); MALDI-TOF MS: m/z 6037(M^+), 5952($[\text{M}-\text{C}_6\text{H}_{13}]^+$). Anal. Calcd for $\text{C}_{393}\text{H}_{477}\text{F}_{39}\text{S}_3$: C, 78.17; H, 7.96. Found: C, 77.92; H, 7.85.

2,7-Dibromo-9,9-bis(3,3,4,4,5,5,6,6,7,7,8,8,8-tridecafluorooctyl)-fluorene (2.29)

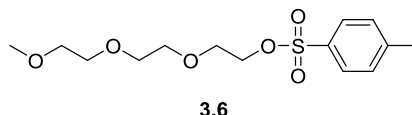


Lithium diisopropyl amide (1.7M in hexane, 1 ml, 1.7 mmol, 1.1 eq) was added dropwise to a solution of 2,7-dibromo-9H-fluorene (0.5 g, 1.55 mmol, 1.0 eq) in dry THF (20 ml) under Ar at -60 °C, which was allowed to warm to rt, then cooled to -60 °C and a solution of 1H,1H,2H,2H-perfluorooctylidide (0.73 g, 1.55 mmol, 1.0 eq) in dry THF (5 ml) was added dropwise. The reaction mixture was allowed to warm to rt and stirred at this temperature for 1.5 h, then cooled to -60 °C and lithium diisopropyl amide (1.7M in hexane, 1 ml, 1.7 mmol, 1.1 eq) added dropwise. The reaction mixture was allowed to warm to rt then cooled again to -60 °C where a solution of 1H,1H,2H,2H-perfluorooctylidide (0.88 g, 1.86 mmol, 1.2 eq) in dry THF (5 ml) was added dropwise.

Finally, the reaction mixture was allowed to warm to rt and stirred overnight under Ar. The mixture was filtered through a silica plug, eluting with copious amounts of THF, and the solvent was then evaporated. The crude mixture was purified by silica gel chromatography eluting with 5 % CH₂Cl₂/hexane to afford a white powder, which was dissolved in the minimum amount of hot hexane and placed in a freezer overnight. The product was then obtained as white crystals by precipitation (0.79 g, 50 %).

¹H NMR (400 MHz, CDCl₃) δ_H, 7.62-7.57 (4H, m, CH), 7.51-7.50 (2H, m, CH), 2.36-2.32 (4H, m, CH₂), 1.36-1.22 (4H, m, CH₂); ¹³C NMR (CDCl₃, δ, 100 MHz): δ_C 148.4, 139.4, 132.4, 126.2, 123.0, 122.3, 53.6, 30.7, 26.3, 26.1; ¹⁹F NMR (376 MHz, CDCl₃): δ_F -80.83 (6F), -113.75 (4F), -122.12 (24), -122.92 (8F), -126.15 (4F), -126.05 (2F); MALDI-TOF MS: *m/z* MALDI-TOF MS: *m/z* 1015.25 ([M]⁺, 100 %), 1870.97 ([M-Br]₂⁺, 74 %), 668.41 ([M-C₂H₄(C₆F₁₃)]⁺). HRMS (EI): calcd for C₂₉H₁₄Br₂F₂₆, 1015.9027, found *m/z* 1015.9029 (M⁺).

2-(2-(2-Methoxyethoxy)ethoxy)ethyl 4-methylbenzenesulfonate (3.6)¹⁹⁴



A solution of *p*-toluenesulfonyl chloride (47.66 g, 250 mmol, 1.0 eq) in dry CH₂Cl₂ (200 ml) was added *via cannula* to a solution of triethylene glycol monomethyl ether (40 ml, 250 mmol, 1.0 eq) and triethylamine (70 ml, 500 mmol, 2.0 eq) in dry CH₂Cl₂ at 0 °C under Ar. The solution was allowed to warm to rt and stir for 18h, where a precipitate was observed. The reaction mixture was then quenched with distilled water (500 ml). The organic fraction was removed and the aqueous fraction was extracted with CH₂Cl₂ (2 x 250 ml). The organic fractions were combined, washed

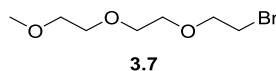
with distilled water (250 ml), dried over MgSO_4 and the solvent was evaporated to afford a pale yellow oil (77.96g, 98 %). The product was used without further purification.

The ^1H NMR spectrum was recorded;

^1H NMR (400 MHz, CDCl_3): δ_{H} 7.79 (2H, d, J 8.0 Hz, CH), 7.34 (2H, d, J 8.0 Hz, CH), 4.16 (2H, t, J 4.8 Hz, CH_2), 3.68 (2H, t, J 4.8 Hz, CH_2), 3.62-3.59 (6H, m, CH_2), 3.54-3.51 (2H, m, CH_2), 3.37 (3H, s, CH_3), 2.44 (3H, s, CH_3).

This was consistent with the previously published data.¹⁹⁴

1-Bromo-2-(2-(2-methoxyethoxy)ethoxy)ethane (3.7)



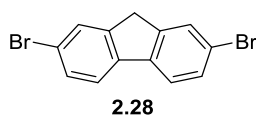
2-(2-(2-Methoxyethoxy)ethoxy)ethyl 4-methylbenzenesulfonate **3.6** (8.82 g, 27.7 mmol, 1.0 eq) and lithium bromide (6.01 g, 69.25 mmol, 2.5 eq) were dissolved in butanone (80 ml) and heated at 80 °C for 18 h, over which time a precipitate was formed. The reaction mixture was cooled to rt and filtered to remove the precipitate. The solvent was evaporated from the filtrate, which was dissolved in CH_2Cl_2 (1 L) and washed with distilled water (2 x 500 ml) and sodium thiosulfate (500 ml). The organic fraction was dried over MgSO_4 and the solvent was evaporated. Kugelrohr distillation at 85 °C afforded the product as a colourless oil (5.75 g, 91 %).

The ^1H NMR spectrum was recorded;

^1H NMR (400 MHz, CDCl_3): δ_{H} 3.82 (2H, t, J 6.4 Hz, CH_2), 3.70-3.65 (6H, m, CH_2), 3.57-3.55 (2H, m, CH_2), 3.48 (2H, t, J 6.4 Hz, CH_2), 3.39 (3H, s, CH_3).

This was consistent with the previously published data.¹⁹⁵

2,7-Dibromo-9H-fluorene (2.28)



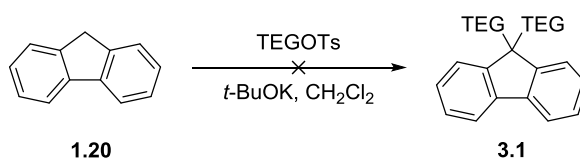
9H-Fluorene (22.75g, 136.9 mmol, 1.0 eq) and iodine (0.39 g, 1.54 mmol, 0.01 eq) were dissolved in CH₂Cl₂ and cooled to 0 °C, to which a solution of bromine (15.8 ml, 306.4 mmol, 2.3 eq) in CH₂Cl₂ (20 ml) was added dropwise over 1 h, after which the solution was allowed to warm to rt and stirred with the minimum exposure to light for 18h. The reaction mixture was quenched with an aqueous solution of sodium sulfite (1 M, 100 ml) and diluted with CH₂Cl₂ (200 ml). The organic fraction was removed and the aqueous layer was extracted with CH₂Cl₂ (2 x 100 ml). The organic layers were combined, washed with distilled water (150 ml), dried over MgSO₄ and the solvent was evaporated to afford the product as an off-white solid (41.68 g, 94 %).

The ¹H NMR spectrum was recorded;

¹H NMR (400 MHz, CDCl₃): δ_H 7.66 (2H, s, CH), 7.59 (2H, d, *J* 8.4 Hz, CH), 7.50 (2H, 8.0 Hz, CH), 3.85 (2H, s, CH₂).

This was consistent with the previously published data.¹⁹⁶

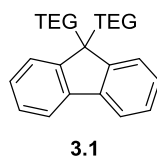
Attempted Synthesis of 9,9-Bis(2-(2-(2-methoxyethoxy)ethoxy)ethyl)-9H-fluorene (3.1)



A suspension of potassium *tert*-butoxide (1.68 g, 15 mmol, 2.5 eq) in dry THF (10 ml) was added dropwise to a solution of 9H-

fluorene **1.20** (1.0 g, 6 mmol, 1.0 eq) and 2-(2-(2-Methoxyethoxy)ethoxy)ethyl 4-methylbenzenesulfonate (7.26 g, 22.8 mmol, 3.8 eq) in dry THF (15 ml) under Ar. The reaction mixture was allowed to warm to rt and stirred under Ar for 4 h, then filtered through a silica plug washing with copious amounts of THF. ^1H NMR of the crude mixture showed evidence of compounds from incomplete alkylation only.

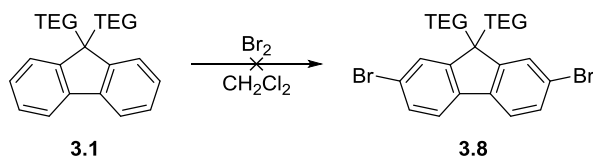
9,9-Bis(2-(2-(2-methoxyethoxy)ethoxy)ethyl)-9H-fluorene (**3.1**)



A suspension of potassium *tert*-butoxide (8.4 g, 75 mmol, 2.5 eq) in dry THF (65 ml) was added dropwise to a solution of 9H-fluorene **1.20** (5 g, 30 mmol, 1.0 eq) and 1-bromo-2-(2-(2-methoxyethoxy)ethoxy)ethane (25.9 g, 114 mmol, 3.8 eq) in dry THF (60 ml) under Ar. The reaction mixture was allowed to warm to rt and stirred under Ar for 4 h, then filtered through a silica plug washing with copious amounts of THF. The solvent was evaporated and Kugelrohr distillation at 85 °C removed excess 1-bromo-2-(2-(2-methoxyethoxy)ethoxy)ethane. The compound was purified by silica gel chromatography to afford the compound as a yellow oil (8.41 g, 61 %).

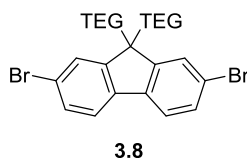
^1H NMR (400 MHz, CDCl_3): δ_{H} 7.68 (2H, d, J 6.4 Hz, CH), 7.41 (2H, d, J 6.4 Hz, CH), 7.36-7.27 (4H, m, CH), 3.56-3.51 (4H, m, CH_2), 3.49-3.46 (4H, m, CH_2), 3.42-3.39 (4H, m, CH_2), 3.34 (6H, s, CH_3), 3.23-3.21 (4H, m, CH_2), 2.76 (4H, t, J 7.2 Hz, CH_2), 2.39 (4H, t, J 7.2 Hz, CH_2). ^{13}C NMR (100 MHz, CDCl_3): δ_{C} 149.1, 140.7, 127.7, 127.6, 123.4, 120.1, 72.2, 70.8, 70.7, 70.2, 67.4, 59.3, 51.4, 40.0, 39.9; MALDI-TOF MS: m/z 458.27 ($[\text{M}]^+$, 100 %). 481.20 ($[\text{M}+\text{Na}]^+$, 48 %).

Attempted synthesis of 2,7-Dibromo-9,9-bis(2-(2-(2-methoxyethoxy)ethoxy)ethyl)-9H-fluorene (3.8)



9,9-Bis(2-(2-(2-methoxyethoxy)ethoxy)ethyl)-9H-fluorene **3.1** (1.0 g, 2.18 mmol, 1.0 eq) was dissolved in dry CH₂Cl₂ (10 ml), to which I₂ (5.6 mg, 0.02 mmol, 0.01 eq) was added. The reaction vessel was equipped with a drying tube containing CaCl₂, followed by a NaOH trap. Bromine (0.26 ml, 5.01 mmol, 2.3 eq) was then added dropwise over 1 h. The solution was left to stir for 18 h at rt, under N₂, with minimum exposure to light. The solution was then cooled in an ice bath for 10 mins, then added to a solution of sodium sulfite in water (50 ml) and cooled by adding ice. The solution was then extracted with CH₂Cl₂ (2 x 100 ml), washed with a saturated solution of sodium hydrogen carbonate in water (50 ml) and then washed with water until the pH was neutral (2 x 50 ml). The organic layers were dried over magnesium sulfate and the solvent was evaporated. The ¹H NMR spectrum of the crude material showed no evidence of the title compound.

2,7-Dibromo-9,9-bis(2-(2-(2-methoxyethoxy)ethoxy)ethyl)-9H-fluorene (3.8)



A suspension of potassium *tert*-butoxide (17.31 g, 154.3 mmol, 2.5 eq) in dry THF (200 ml) was added dropwise to a solution of

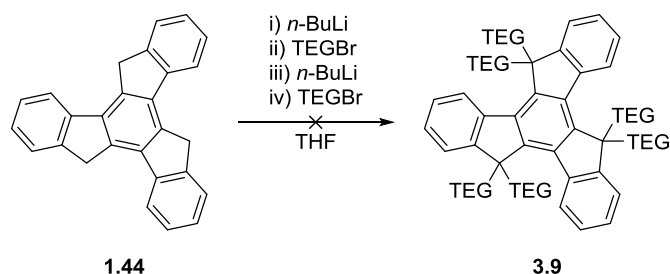
2,7-dibromo-9*H*-fluorene **2.38** (20 g, 61.7 mmol, 1.0 eq) and 1-bromo-2-(2-(2-methoxyethoxy)ethoxy)ethane **3.7** (53.26 g, 234.5 mmol, 3.8 eq) in dry THF (300 ml) under Ar. The reaction mixture was allowed to warm to rt and stirred under Ar for 4 h, then filtered through a silica plug washing with copious amounts of THF. The solvent was evaporated and Kugelrohr distillation at 85 °C removed impurities. The residual yellow oil was dissolved in the minimum volume of Et₂O and cooled to -20 °C to precipitate the product, which was isolated as a white powder by filtration (32.47 g, 86 %).

The ¹H NMR spectrum was recorded;

¹H NMR (400 MHz, CDCl₃): δ_H 7.54-7.46 (6H, m, CH), 3.56-3.52 (4H, m, CH₂), 3.50-3.46 (4H, m, CH₂), 3.40 (4H, dd, *J* 5.2, 4.8 Hz, CH₂), 3.35 (6H, s, CH₃), 3.22 (4H, dd, *J* 5.2, 4.8 Hz, CH₂), 2.79 (4H, t, *J* 7.3 Hz, CH₂), 2.34 (4H, t, *J* 7.3 Hz, CH₂).

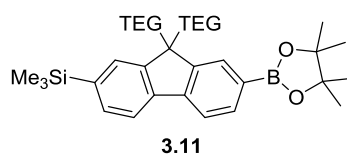
This was consistent with the previously published data.¹⁷⁰

Attempted synthesis of Hexa-TEG-truxene (**3.9**)



in an ice bath, *n*-butyllithium (2.0 M in hexane, 9.1 ml, 18.15 mmol, 3.75 eq) was added dropwise over 15 mins, and the solution stirred for a further 30 mins. 1-Bromo-2-(2-(2-methoxyethoxy)ethoxy)ethane (4.12 g, 18.15 mmol, 3.75 eq) was added dropwise over 10 mins, and the solution was stirred at rt for 18 h under N₂. TLC and ¹H NMR analysis showed multiple products from incomplete alkylation.

(9,9-bis(2-(2-(2-methoxyethoxy)ethoxy)ethyl)-7-(4,4,5,5-tetramethyl-1,3,2-dioxaborolan-2-yl)-9H-fluoren-2-yl)trimethylsilane (3.11)

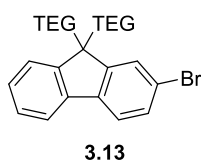


n-Butyllithium (2.4 M in hexane, 0.68 ml, 1.63 mmol, 1.0 eq) was added dropwise to a solution of 2,7-dibromo-9,9-bis(2-(2-(2-methoxyethoxy)ethoxy)ethyl)-9H-fluorene **3.8** (1.0 g, 1.63 mmol, 1.0 eq) in dry THF (15 ml) at -80 °C, which was allowed to stir for 10 mins then cooled to -90 °C and chlorotrimethylsilane (0.21 ml, 1.63 mmol, 1.0 eq) was added. The solution was then allowed to warm to r.t. over 30 mins, then cooled back to -80 °C and *n*-butyllithium (2.4 M in hexane, 0.82 ml, 1.96 mmol, 1.2 eq) was added dropwise. The solution was then cooled further to -100 °C, triisopropylborate (1.31 ml, 4.89 mmol, 3.0 eq) was added dropwise, and the solution was warmed to rt and stirred under N₂ for 18 h. Distilled water (500 ml) was used to quench the solution, which was then extracted with diethyl ether (3 × 100 ml). The organic layers were combined and washed with distilled water (500 ml), dried over magnesium sulfate, and the solvent was evaporated. The crude product was dissolved in dry toluene (50 ml) under Ar, to which pinacol (230 mg 1.96 mmol, 1.2 eq) was added. The reaction mixture was stirred at rt overnight, then washed with distilled water (3 x 50 ml). The aqueous

fractions were combined and washed with CH_2Cl_2 (3 50 ml). The organic fractions were then combined, washed with distilled water (100 ml), dried over MgSO_4 and the solvent was evaporated. Silica gel chromatography eluting with a 30 % hexane in EtOAc mixture afforded the product as a pale yellow oil with slight impurities (257 mg, 24 %). This compound was not purified further.

^1H NMR (500 MHz, CDCl_3): δ_{H} 7.84 (1H, s, CH), 7.81 (1H, d, J 7.5 Hz, CH), 7.68 (1H, d, J 7.5 Hz, CH), 7.54 (1H, s, CH), 7.50 (1H, d, J 7.5 Hz, CH), 3.55-3.50 (4H, m, CH_2), 3.49-3.45 (4H, m, CH_2), 3.40 (4H, t, 4.0 Hz, CH_2), 3.34 (6H, s, CH_3), 3.20 (4H, m, CH_2), 2.73 (4H, m, CH_2), 2.40 (4H, m, CH_2), 1.36 (12H, s, CH_3), 0.32 (9H, s, CH_3)

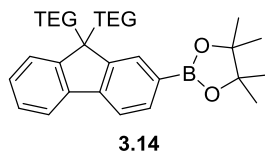
2-Bromo-9,9-bis(2-(2-(2-methoxyethoxy)ethoxy)ethyl)-9H-fluorene (3.13)



A suspension of potassium *tert*-butoxide (6.23 g, 51.0 mmol, 2.5 eq) in dry THF (60 ml) was added dropwise to a solution of 2-bromo-9H-fluorene (5.0 g, 20.40 mmol, 1.0 eq) and 1-bromo-2-(2-(2-methoxyethoxy)ethoxy)ethane **3.6** (12.97 g, 12.97 mmol, 3.8 eq) in dry THF (65 ml) under Ar. The reaction mixture was allowed to warm to rt and stirred under Ar for 4 h, then filtered through a silica plug washing with copious amounts of THF. The solvent was evaporated and Kugelrohr distillation at 85 °C removed impurities. The residual yellow oil was dissolved in the minimum volume of Et_2O and cooled to -20 °C to precipitate the product, which was isolated as a white powder by filtration (8.35 g, 75 %).

^1H NMR (400 MHz, CDCl_3): δ_{H} 7.66-7.64 (1H, m, CH), 7.55 (1H, s, CH), 7.54 (1H, d, J 10.0 Hz, CH), 7.46 (1H, dd, J 8.0 Hz 1.6 Hz, CH), 7.41-7.38

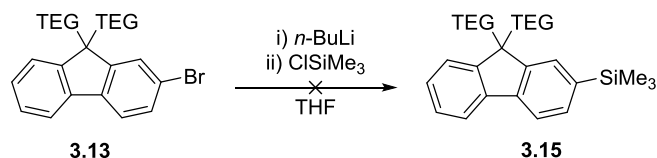
2-(9,9-Bis(2-(2-(2-methoxyethoxy)ethoxy)ethyl)-9H-fluoren-2-yl)-4,4,5,5-tetramethyl-1,3,2-dioxaborolane (3.14)



2,7-Dibromo-9,9-bis(2-(2-(2-methoxyethoxy)ethoxy)ethyl)-9H-fluorene **3.13** (250 mg, 0.47 mmol, 1.0 eq), bis(pinacolato)diboron (295 mg, 1.16 mmol, 2.5 eq), *tetrakis*(triphenylphosphine)palladium(0) (26 mg, 0.023 mmol, 0.05 eq) and potassium acetate (160 mg, 1.63 mmol, 3.5 eq) were dissolved in dry 1,4-dioxane (5 ml) under Ar and heated at 90 °C for 18 h. The reaction was then cooled to rt, and diluted with water (30 ml). After extraction with Et₂O (3 x 30 ml) the organic layers were combined, washed with water (30 ml), dried over MgSO₄ and the solvent was evaporated. The crude product was purified by silica gel chromatography eluting with 2 % MeOH in Et₂O to afford a white solid (170 mg, 60 %).

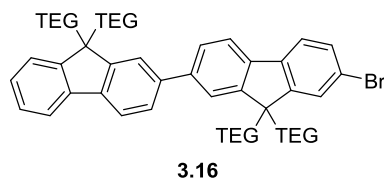
¹H NMR (400 MHz, CDCl₃): δ_H 7.84 (1H, s, CH), 7.81 (1H, d, *J* 7.2 Hz, CH), 7.72-7.67 (2H, m, CH), 7.44-7.72 (1H, m, CH), 7.35-7.32 (2H, m, CH), 3.53-3.50 (4H, m, CH₂), 3.50-3.47 (4H, m, CH₂), 3.40 (4H, dd, *J* 6.0, 5.2 Hz, CH₂), 3.39 (6H, s, CH₃), 3.20 (4H, dd, *J* 6.0, 5.2 Hz, CH₂), 2.79-2.67 (4H, m, CH₂), 2.48-2.39 (4H, t, *J* 7.3 Hz, CH₂); ¹³C NMR (100 MHz, CDCl₃): δ_C 149.8, 148.3, 143.7, 140.6, 134.4, 129.5, 128.2, 127.6, 123.5, 120.6, 119.4, 84.1, 72.2, 70.8, 70.3, 67.3, 59.3, 51.4, 39.9, 25.3; MALDI-TOF MS: *m/z* 607.19 ([M+Na]⁺, 100 %); Anal. Calcd for C₃₃H₄₉BO₈: C, 67.81; H, 8.45 Found: C, 67.64; H, 8.70.

Attempted synthesis of (9,9-bis(2-(2-(2-methoxyethoxy)ethoxy)ethyl)-9H-fluoren-2-yl)trimethylsilane (3.15)



n-Butyllithium (2.38 M in hexane, 0.23 ml, 0.55 mmol, 1.2 eq) was added dropwise to a solution of 2-bromo-9,9-bis(2-(2-(2-methoxyethoxy)ethoxy)ethyl)-9H-fluorene **3.13** (250 mg, 0.46 mmol, 1.0 eq) in dry THF (10 ml) at -80 °C, which was allowed to stirred for 10 mins then cooled to -90 °C. Chlorotrimethylsilane (0.07 ml, 0.55 mmol, 1.2 eq) was added dropwise, then the reaction mixture was then allowed to warm to rt and stir for 18 h under Ar. The reaction mixture was quenched with distilled water (50 ml), and the aqueous mixture was extracted with Et₂O (3 x 50 ml). The organic layers were washed with distilled water (50 ml), dried over MgSO₄ and the solvent was evaporated. Analysis by TLC and ¹H NMR of crude mixture gave evidence of multiple, inseparable products.

Attempted synthesis of 7-bromo-9,9,9',9'-tetrakis(2-(2-(2-methoxyethoxy)ethoxy)ethyl)-9H,9'H-2,2'-bifluorene (3.16)



General method by Suzuki-Miyaura Coupling:

2-(9,9-Bis(2-(2-(2-methoxyethoxy)ethoxy)ethyl)-9H-fluoren-2-yl)-4,4,5,5-tetramethyl-1,3,2-dioxaborolane, 2,7-dihalo-9,9-bis(2-(2-(2-methoxy-

ethoxy)ethoxy)ethyl)-9H-fluorene, *tetrakis*(triphenylphosphine)palladium (0) and base were dissolved in solvent and heated at reflux. The reaction mixture was then cooled to rt and added to water. The aqueous suspension was extracted with EtOAc until the extractions were no longer fluorescent under long wave UV light, then the organic layers were dried over MgSO₄ and the solvent was evaporated. TLC and ¹H NMR analysis were used and compared to starting material to determine whether the reaction had gone to completion.

Attempt 1:

2-(9,9-Bis(2-(2-(2-methoxyethoxy)ethoxy)ethyl)-9H-fluoren-2-yl)-4,4,5,5-tetramethyl-1,3,2-dioxaborolane **3.14** (250 mg, 0.43 mmol, 1.0 eq), 2,7-dibromo-9,9-bis(2-(2-(2-methoxyethoxy)ethoxy)ethyl)-9H-fluorene **3.8** (786 mg, 1.28 mmol, 3.0 eq), *tetrakis*(triphenylphosphine)palladium(0) (15 mg, 0.013 mmol, 0.03 eq) and an aqueous solution of sodium carbonate (2M, 1.1 ml, 2.15 mmol, 5.0 eq) were dissolved in dry toluene (10 ml) and heated at 80 °C for 18 h under Ar. Analysis gave no evidence of product, showing only starting materials present.

Attempt 2:

2-(9,9-Bis(2-(2-(2-methoxyethoxy)ethoxy)ethyl)-9H-fluoren-2-yl)-4,4,5,5-tetramethyl-1,3,2-dioxaborolane **3.14** (462 mg, 0.79 mmol, 1.0 eq), 2,7-dibromo-9,9-bis(2-(2-(2-methoxyethoxy)ethoxy)ethyl)-9H-fluorene **3.8** (1.45 g, 2.37 mmol, 3.0 eq), *tetrakis*(triphenylphosphine)palladium(0) (27 mg, 0.024 mmol, 0.03 eq) and an aqueous solution of sodium carbonate (2M, 0.88 ml, 1.75 mmol, 2.3 eq) were dissolved in dry THF (10 ml) and heated at 70 °C for 18 h under Ar. Analysis showed poor conversion to the product and the crude mixture contained mainly starting materials with other impurities, from which the desired product was inseparable. From ¹H NMR peak the yield of desired product was approximately 25 %.

Attempt 3:

2-(9,9-Bis(2-(2-(2-methoxyethoxy)ethoxy)ethyl)-9H-fluoren-2-yl)-4,4,5,5-tetramethyl-1,3,2-dioxaborolane **3.14** (366 mg, 0.63 mmol, 1.0 eq), 2,7-dibromo-9,9-bis(2-(2-(2-methoxyethoxy)ethoxy)ethyl)-9H-fluorene **3.8** (1.16 g, 1.89 mmol, 3.0 eq), *tetrakis*(triphenylphosphine)palladium(0) (22 mg, 0.019 mmol, 0.03 eq) and an aqueous solution of sodium carbonate (2M, 0.73 ml, 1.45 mmol, 2.3 eq) were dissolved in dry 1,4-dioxane (10 ml) and heated at 90 °C for 18 h under Ar. Analysis showed poor conversion to the product and the crude mixture contained mainly starting materials with other impurities, from which the desired product was inseparable. From ¹H NMR peak the yield of desired product was approximately 25 %.

Attempt 4:

2-(9,9-Bis(2-(2-(2-methoxyethoxy)ethoxy)ethyl)-9H-fluoren-2-yl)-4,4,5,5-tetramethyl-1,3,2-dioxaborolane **3.14** (250 mg, 0.43 mmol, 1.0 eq), 2,7-dibromo-9,9-bis(2-(2-(2-methoxyethoxy)ethoxy)ethyl)-9H-fluorene **3.8** (786 mg, 1.28 mmol, 3.0 eq), *tetrakis*(triphenylphosphine)palladium(0) (15 mg, 0.013 mmol, 0.03 eq) and an aqueous solution of sodium carbonate (2M, 4.3 ml, 8.60 mmol, 20 eq) were dissolved in dry DME (10 ml) and heated at 90 °C for 18 h under Ar. Analysis showed poor conversion to the product and the crude mixture contained mainly starting materials with other impurities, from which the desired product was inseparable. From ¹H NMR peak the yield of desired product was approximately 25 %.

Attempt 5:

2-(9,9-Bis(2-(2-(2-methoxyethoxy)ethoxy)ethyl)-9H-fluoren-2-yl)-4,4,5,5-tetramethyl-1,3,2-dioxaborolane **3.14** (500 mg, 0.86 mmol, 1.0 eq), 2,7-dibromo-9,9-bis(2-(2-(2-methoxyethoxy)ethoxy)ethyl)-9H-fluorene **3.8** (1.58 g, 2.58 mmol, 3.0 eq), *tetrakis*(triphenylphosphine)palladium(0) (30 mg, 0.025 mmol, 0.03 eq) and an aqueous solution of sodium carbonate (2M, 0.99 ml, 1.98 mmol, 2.3 eq) were dissolved in dry DMF (10 ml) and

heated at 90 °C for 18 h under Ar. Analysis showed poor conversion to the product and the crude mixture contained mainly starting materials with other impurities, from which the desired product was inseparable. From ¹H NMR peak the yield of desired product was approximately 25 %.

Attempt 6:

2-(9,9-Bis(2-(2-(2-methoxyethoxy)ethoxy)ethyl)-9H-fluoren-2-yl)-4,4,5,5-tetramethyl-1,3,2-dioxaborolane **3.14** (250 mg, 0.43 mmol, 1.0 eq), 2,7-dibromo-9,9-bis(2-(2-(2-methoxyethoxy)ethoxy)ethyl)-9H-fluorene **3.8** (786 mg, 1.28 mmol, 3.0 eq), *tetrakis*(triphenylphosphine)palladium(0) (15 mg, 0.013 mmol, 0.03 eq) and an aqueous solution of sodium carbonate (2M, 1.1 ml, 2.15 mmol, 5.0 eq) were dissolved in dry DME (10 ml) and heated at 90 °C for 72 h under Ar. Analysis showed poor conversion to the product and the crude mixture contained mainly starting materials with other impurities, from which the desired product was inseparable. From ¹H NMR peak the yield of desired product was approximately 25 %.

Attempt 7:

2-(9,9-Bis(2-(2-(2-methoxyethoxy)ethoxy)ethyl)-9H-fluoren-2-yl)-4,4,5,5-tetramethyl-1,3,2-dioxaborolane **3.14** (250 mg, 0.43 mmol, 1.0 eq), 2,7-dibromo-9,9-bis(2-(2-(2-methoxyethoxy)ethoxy)ethyl)-9H-fluorene **3.8** (786 mg, 1.28 mmol, 3.0 eq), *tetrakis*(triphenylphosphine)palladium(0) (15 mg, 0.013 mmol, 0.03 eq) and an aqueous solution of sodium hydrogen carbonate (1M, 8.56 ml, 8.56 mmol, 20 eq) were dissolved in dry 1,4-dioxane (10 ml) and heated at 90 °C for 18 h under Ar. Analysis gave no evidence of product, showing only starting materials present.

Attempt 8:

2-(9,9-Bis(2-(2-(2-methoxyethoxy)ethoxy)ethyl)-9H-fluoren-2-yl)-4,4,5,5-tetramethyl-1,3,2-dioxaborolane **3.14** (257 mg, 0.44 mmol, 1.0 eq), 2,7-dibromo-9,9-bis(2-(2-(2-methoxyethoxy)ethoxy)ethyl)-9H-fluorene **3.8** (811

mg, 1.32 mmol, 3.0 eq), *tetrakis*(triphenylphosphine)palladium(0) (15 mg, 0.013 mmol, 0.03 eq) and barium hydroxide (208 mg, 0.66 mmol, 1.5 eq) were dissolved in dry THF (8 ml) and water (1 ml) and heated at 70 °C for 18 h under Ar. Analysis showed poor conversion to the product and the crude mixture contained mainly starting materials with other impurities, from which the desired product was inseparable. From ¹H NMR peak the yield of desired product was approximately 25 %.

Attempt 9:

2-(9,9-Bis(2-(2-(2-methoxyethoxy)ethoxy)ethyl)-9H-fluoren-2-yl)-4,4,5,5-tetramethyl-1,3,2-dioxaborolane **3.14** (250 mg, 0.43 mmol, 1.0 eq), 2,7-dibromo-9,9-bis(2-(2-(2-methoxyethoxy)ethoxy)ethyl)-9H-fluorene **3.8** (786 mg, 1.28 mmol, 3.0 eq), *tetrakis*(triphenylphosphine)palladium(0) (15 mg, 0.013 mmol, 0.03 eq) and sodium acetate (105 mg, 1.28 mmol, 3.0 eq) were dissolved in dry THF (10 ml) and heated at 70 °C for 18 h under Ar. Analysis gave no evidence of product, showing only starting materials present.

Attempt 10:

2-(9,9-Bis(2-(2-(2-methoxyethoxy)ethoxy)ethyl)-9H-fluoren-2-yl)-4,4,5,5-tetramethyl-1,3,2-dioxaborolane **3.14** (300 mg, 0.51 mmol, 1.0 eq), 2,7-dibromo-9,9-bis(2-(2-(2-methoxyethoxy)ethoxy)ethyl)-9H-fluorene **3.8** (940 mg, 1.53 mmol, 3.0 eq), *tetrakis*(triphenylphosphine)palladium(0) (23 mg, 0.022 mmol, 0.03 eq) and tribasic potassium phosphate (248 mg, 1.17 mmol, 2.3 eq) were dissolved in dry DMF (10 ml) and heated at 90 °C for 18 h under Ar. Analysis showed poor conversion to the product and the crude mixture contained mainly starting materials with other impurities, from which the desired product was inseparable. From ¹H NMR peak the yield of desired product was approximately 25 %.

Attempt 11:

2-(9,9-Bis(2-(2-(2-methoxyethoxy)ethoxy)ethyl)-9H-fluoren-2-yl)-4,4,5,5-tetramethyl-1,3,2-dioxaborolane **3.14** (220 mg, 0.38 mmol, 1.0 eq), 2,7-diiodo-9,9-bis(2-(2-(2-methoxyethoxy)ethoxy)ethyl)-9H-fluorene **3.18** (803 mg, 1.13 mmol, 3.0 eq), *tetrakis*(triphenylphosphine)palladium(0) (12.7 mg, 0.011 mmol, 0.03 eq) and an aqueous solution of sodium carbonate (2M, 0.44 ml, 0.87 mmol, 2.3 eq) were dissolved in dry THF (5 ml) and heated at 70 °C for 18 h under Ar. Analysis showed poor conversion to the product and the crude mixture contained mainly starting materials with other impurities, from which the desired product was inseparable. From ¹H NMR peak the yield of desired product was approximately 25 %.

Attempt 12:

2-(9,9-Bis(2-(2-(2-methoxyethoxy)ethoxy)ethyl)-9H-fluoren-2-yl)-4,4,5,5-tetramethyl-1,3,2-dioxaborolane **3.14** (150 mg, 0.26 mmol, 1.0 eq), 2,7-diiodo-9,9-bis(2-(2-(2-methoxyethoxy)ethoxy)ethyl)-9H-fluorene **3.18** (470 mg, 0.78 mmol, 3.0 eq), *tetrakis*(triphenylphosphine)palladium(0) (9.4 mg, 0.008 mmol, 0.03 eq) and caesium fluoride (79.0 mg, 0.52 mmol, 2.0 eq) were dissolved in dry DMF (5 ml) and heated at 90 °C for 18 h under Ar. Analysis showed poor conversion to the product and the crude mixture contained mainly starting materials with other impurities, from which the desired product was inseparable. From ¹H NMR peak the yield of desired product was approximately 25 %.

Attempt 13:

2-(9,9-Bis(2-(2-(2-methoxyethoxy)ethoxy)ethyl)-9H-fluoren-2-yl)-4,4,5,5-tetramethyl-1,3,2-dioxaborolane (193 mg, 0.33 mmol, 1.0 eq), 2-bromo-7-iodo-9,9-bis(2-(2-(2-methoxyethoxy)ethoxy)ethyl)-9H-fluorene (268 mg, 0.40 mmol, 1.2 eq), *tetrakis*(triphenylphosphine)palladium(0) (12 mg, 0.01 mmol, 0.03 eq) and an aqueous solution of sodium carbonate (2M, 0.38 ml, 0.76 mmol, 2.3 eq) were dissolved in dry THF (10 ml) and heated at 70 °C

for 18 h under Ar. Analysis showed poor conversion to the product and the crude mixture contained mainly starting materials with other impurities, from which the desired product was inseparable. From ^1H NMR peak the yield of desired product was approximately 25 %.

Attempt by Kumada coupling 1:

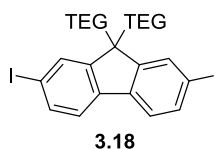
Isopropyl magnesium chloride.lithium chloride complex (1.3M in THF, 0.33 ml, 0.43 mmol, 1.0 eq) was added dropwise to a solution of 2-iodo-9,9-bis(2-(2-(2-methoxyethoxy)ethoxy)ethyl)-9H-fluorene **3.21** (250 mg, 0.43 mmol, 1.0 eq) in dry THF (3 ml) under Ar at -20 °C and stirred for 1 h. The reaction mixture was then added to a solution of 2,7-dibromo-9,9-bis(2-(2-(2-methoxyethoxy)ethoxy)ethyl)-9H-fluorene **3.8** (792 mg, 1.29 mmol, 3.0 eq) and [1,3-bis(diphenylphosphino)propane]dichloronickel(II) (12 mg, 0.02 mmol, 0.05 eq) in dry THF (2 ml) under Ar at -20°C. The reaction mixture was allowed to warm to rt then and stir for 18 h, then added to distilled water (50 ml). The aqueous mixture was extracted with CH_2Cl_2 (4 x 50 ml), and the organic layers were washed with distilled water (50 ml), dried over MgSO_4 and the solvent was evaporated. Analysis showed poor conversion to the product and the crude mixture contained mainly starting materials with other impurities, from which the desired product was inseparable. From ^1H NMR peak the yield of desired product was approximately 25 %.

Attempt by Kumada coupling 2:

Isopropyl magnesium chloride.lithium chloride complex (1.3M in THF, 0.33 ml, 0.43 mmol, 1.0 eq) was added dropwise to a solution of 2-iodo-9,9-bis(2-(2-(2-methoxyethoxy)ethoxy)ethyl)-9H-fluorene **3.21** (250 mg, 0.43 mmol, 1.0 eq) in dry THF (3 ml) under Ar at -20 °C and stirred for 1 h. The reaction mixture was then added to a solution of 2,7-diiodo-9,9-bis(2-(2-(2-methoxyethoxy)ethoxy)ethyl)-9H-fluorene **3.18** (916 mg, 1.29 mmol, 3.0 eq) and [1,3-bis(diphenylphosphino)propane]dichloronickel(II) (12 mg,

0.02 mmol, 0.05 eq) in dry THF (2 ml) under Ar at -20°C. The reaction mixture was allowed to warm to rt then and stir for 18 h, then added to distilled water (50 ml). The aqueous mixture was extracted with CH₂Cl₂ (4 x 50 ml), and the organic layers were washed with distilled water (50 ml), dried over MgSO₄ and the solvent was evaporated. Analysis showed poor conversion to the product and the crude mixture contained mainly starting materials with other impurities, from which the desired product was inseparable. From ¹H NMR peak the yield of desired product was approximately 25 %.

2,7-Diiodo-9,9-bis(2-(2-(2-methoxyethoxy)ethoxy)ethyl)-9H-fluorene (3.18)

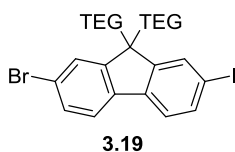


Iodine (0.91 mg, 3.46 mmol, 0.8 eq) and periodic acid (0.40 mg, 1.74 mmol, 0.4 eq) were added to a solution of 9,9-bis(2-(2-(2-methoxyethoxy)ethoxy)ethyl)-9H-fluorene **3.1** (2.0 g, 1.86 mmol, 1.0 eq) in a mixture of acetic acid (10 ml), sulfuric acid (0.3 ml) and water (1 ml), which was then heated at 55 °C overnight. The reaction mixture was diluted with an aqueous solution of sodium sulfite (1 M, 100 ml) and extracted with CH₂Cl₂ (4 x 100 ml). The organic layers were dried over MgSO₄ and the solvent was evaporated. The crude product was purified by silica gel chromatography, eluting first with CH₂Cl₂, then with Et₂O to afford a yellow oil, which was precipitated from Et₂O at -15 °C to afford the product as a white powder (1.82g, 60 %).

¹H NMR (400 MHz, CDCl₃): δ_H 7.74 (2H, d, *J* 1.2 Hz, CH), 7.67 (2H, dd, *J* 8.0, 1.2 Hz, CH), 7.40 (2H, d, *J* 8.0 Hz, CH), 3.57-3.53 (4H, m, CH₂), 3.51-3.47 (4H, m, CH₂), 3.41 (4H, dd, *J* 5.2, 4.8 Hz, CH₂), 3.36 (6H, s, CH₃), 3.23 (4H, dd, *J* 5.2, 4.8 Hz, CH₂), 2.79 (4H, t, *J* 7.6 Hz, CH₂), 2.33 (4H, t, *J*

7.6 Hz, CH₂). ¹³C NMR (100 MHz, CDCl₃): δ_C 151.1, 139.4, 136.8, 132.8, 121.9, 93.56, 72.2, 70.81, 70.77, 70.3, 67.1, 59.3, 52.0, 39.8; MALDI-TOF MS: *m/z* 733.06 ([M+Na]⁺, 100 %), 749.05 ([M +K]⁺, 40 %); HRMS (EI): calcd for C₂₇H₃₆I₂O₆ ([M+NH₄]⁺), 728.0940, found *m/z* 728.0930 ([M+NH₄]⁺),

2-Bromo-7-iodo-9,9-bis(2-(2-(2-methoxyethoxy)ethoxy)ethyl)-9H-fluorene (3.19)

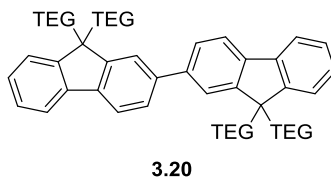


Iodine (228 mg, 0.88 mmol, 0.8 eq) and periodic acid (100 mg, 0.44 mmol, 0.4 eq) were added to a solution of 2-bromo-9,9-bis(2-(2-(2-methoxyethoxy)ethoxy)ethyl)-9H-fluorene **3.13** (1 g, 1.86 mmol, 1.0 eq) in a mixture of acetic acid (5 ml), sulfuric acid (0.15 ml) and water (0.5 ml), which was then heated at 55 °C overnight. The reaction mixture was diluted with an aqueous solution of sodium sulfite (1 M, 50 ml) and extracted with CH₂Cl₂ (4 x 50 ml). The organic layers were dried over MgSO₄ and the solvent was evaporated. The crude product was purified by silica gel chromatography, eluting with Et₂O, to afford the product as a yellow oil (600 mg, 49 %). The compound was placed under vacuum and used without precipitation or further purification.

The ¹H NMR spectrum was recorded;

¹H NMR (400 MHz, CDCl₃): δ_H 7.73 (1H, d, *J* 1.2 Hz, CH), 7.67 (1H, dd, *J* 8.0, 1.6 Hz, CH), 7.56-7.45 (3H, m, CH), 7.40 (1H, d, *J* 7.6 Hz, CH), 3.71-3.51 (4H, m, CH₂), 3.49-3.47 (4H, m, CH₂), 3.40-3.37 (4H, m, CH₂) 3.35 (6H, s, CH₃), 3.22-3.20 (4H, m, CH₂), 2.78 (4H, t, *J* 7.2 Hz, CH₂), 2.33 (4H, t, *J* 7.2 Hz, CH₂).

9,9,9',9'-Tetrakis(2-(2-(2-methoxyethoxy)ethoxy)ethyl)-9H,9'H-2,2'-bifluorene (3.20)

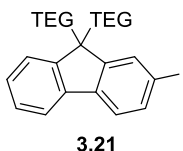


2-Bromo-9,9-bis(2-(2-(2-methoxyethoxy)ethoxy)ethyl)-9H-fluorene **3.13** (250 mg, 0.46 mmol, 1.0 eq), 2-(9,9-bis(2-(2-(2-methoxyethoxy)ethoxy)ethyl)-9H-fluoren-2-yl)-4,4,5,5-tetramethyl-1,3,2-dioxaborolane **3.14** (321 mg, 0.55 mmol, 1.2 eq) and *tetrakis*(triphenylphosphine)palladium(0) (23 mg, 0.02 mmol, 0.05 eq) were dissolved in dry THF (5 ml), to which an aqueous solution of sodium carbonate (2M, 0.65 ml, 1.29 mmol, 2.8 eq) was added. The reaction mixture was heated at 70 °C overnight, then cooled to rt and added to brine (50 ml). The aqueous fraction was extracted with EtOAc (5 x 30 ml), then the organic layers were washed with brine (50 ml), dried over MgSO₄ and the solvent was evaporated. The crude product was purified by silica gel chromatography, eluting first with 5 % MeOH/Et₂O, then 10 % MeOH/Et₂O to afford the product as a yellow powder. Precipitation from Et₂O at -20 °C then gave the product as a white powder (299 mg, 71 %).

¹H NMR (400 MHz, CDCl₃): δ_H 7.78-7.72 (4H, m, CH), 7.68-7.64 (4H, m, CH), 7.46 (2H, d, *J* 7.2 Hz, CH), 7.39-7.33 (4H, m, CH), 3.55-3.51 (8H, m, CH₂), 3.47-3.45 (8H, m, CH₂), 3.43-3.41 (8H, m, CH₂) 3.32 (12H, s, CH₃), 3.27-3.23 (8H, m, CH₂), 2.90-2.76 (8H, m, CH₂), 2.50-2.46 (8H, m, CH₂):
¹³C NMR (100 MHz, CDCl₃): δ_C 149.9, 149.4, 140.8, 140.4, 140.0, 127.71, 127.67, 126.9, 123.5, 121.8, 120.5, 120.2, 72.1, 70.79, 70.76, 70.72, 70.3, 67.4, 59.3, 51.6, 40.1; MALDI-TOF MS: *m/z* 914.58 ([M]⁺, 100 %); HRMS

(ED): calcd for C₅₄H₇₄O₁₂ [M+NH₄]⁺ 932.5519, found m/z 932.5510 ([M+NH₄]⁺).

2-Iodo-9,9-bis(2-(2-(2-methoxyethoxy)ethoxy)ethyl)-9H-fluorene (3.21)

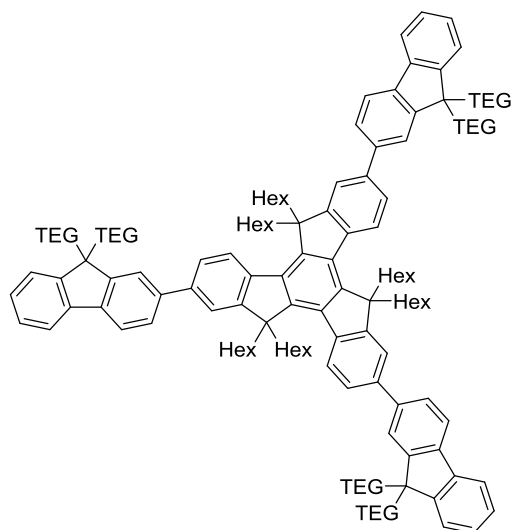


Iodine (374 mg, 1.44 mmol, 0.33 eq) and periodic acid (169 mg, 0.74 mmol, 0.17 eq) were added to a solution of 9,9-bis(2-(2-(2-methoxyethoxy)ethoxy)ethyl)-9H-fluorene **3.1** (2.0 g, 4.36 mmol, 1.0 eq) in a mixture of acetic acid (10 ml), sulfuric acid (0.3 ml) and water (2 ml) and heated at 55 °C for 4 h. After cooling to rt, the reaction mixture was added to an aqueous solution of sodium sulfite (1M, 50 ml) and extracted with CH₂Cl₂ (4 x 50 ml). The organic layers were washed with a saturated aqueous solution of sodium hydrogen carbonate (50 ml) and distilled water (50 ml), dried over MgSO₄ and the solvent was evaporated. The product was purified by silica gel chromatography, eluting with 10 % EtOAc/Et₂O, to afford a yellow oil, which was dissolved in Et₂O and cooled to -20 °C to precipitate the title product as a white powder, which was isolated by filtration (1.01 g, 37 %).

¹H NMR (400 MHz, CDCl₃): δ_H 7.75 (1H, d, *J* 1.2, CH), 7.68-7.64 (2H, m, CH), 7.43 (1H, d, *J* 6.4 Hz, CH), 7.40-7.38 (1H, m, CH), 7.36-7.33 (2H, m, CH), 3.57-3.52 (4H, m, CH₂), 3.50-3.47 (4H, m, CH₂), 3.40 (4H, t, *J* 4.0 Hz, CH₂), 3.35 (6H, s, CH₃), 3.25-3.18 (4H, m, CH₂), 2.76 (4H, t, *J* 6.0 Hz, CH₂), 2.37-2.34 (4H, m, CH₂); ¹³C NMR (100 MHz, CDCl₃): δ_C 151.6, 148.63, 140.4, 139.8, 136.6, 132.8, 128.3, 127.8, 123.4, 121.8, 120.3, 92.9, 72.2, 70.8, , 70.3, 67.2, 59.3, 51.7, 39.9; MALDI-TOF MS: *m/z* 607.05 ([M+Na]⁺, 100 %), 623.03 ([M+K]⁺, 35 %) 482.18 ([M-

$(\text{CH}_2\text{CH}_2\text{O})_2\text{Me}]^+$, 10 %). Anal. Calcd for $\text{C}_{27}\text{H}_{37}\text{IO}_6$: C, 55.48; H, 6.38
Found: C, 55.39; H, 6.45.

T1^{Polar}

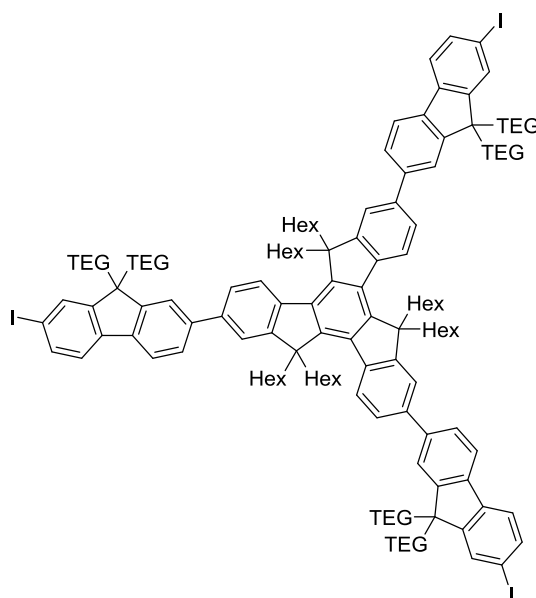


T1^{POLAR}

2-(9,9-Bis(2-(2-(2-methoxyethoxy)ethoxy)ethyl)-9H-fluoren-2-yl)-4,4,5,5-tetramethyl-1,3,2-dioxaborolane **3.14** (1.50 g, 2.57 mmol, 4.77 eq), tribromohexahexyltruxene **2.3** (0.58 g, 0.54 mmol, 1.0 eq), *tetrakis*(triphenylphosphine)palladium(0) (0.16 g, 0.14 mmol, 0.3 eq) and barium hydroxide octahydrate (1.2 g, 3.94 mmol, 7.3 eq) were suspended in THF (8 ml) under Ar, to which degassed distilled water (1 ml) was added. The reaction mixture was then heated at 70 °C for 18 h, then cooled to rt and quenched with a saturated aqueous solution of ammonium chloride (100 ml). The crude product was extracted with CH_2Cl_2 (8 x 100 ml), the organic layers were combined, dried over MgSO_4 , the solvent was evaporated and the crude product was placed under vacuum overnight. The product was loaded onto silica and eluted with a 2% MeOH/ Et_2O mixture to afford the product as a sticky white solid (850 mg, 70 %).

^1H NMR (400 MHz, CDCl_3): δ_{H} 8.52 (3H, d, J 8.8 Hz, CH), 7.84-7.75 (18H, m, CH), 7.48 (3H, d, J 6.8 Hz, CH), 7.41-7.38 (6H, m, CH), 3.55-3.53 (12H, m, CH_2), 3.49-3.44 (24H, m, CH_2), 3.34 (18H, s, CH_3), 3.28 (12H, t, J 4.8 Hz, CH_2), 3.10-3.07 (6H, m, CH_2), 2.93-2.83 (12H, m, CH_2), 2.52 (12H, t, J 7.8 Hz, CH_2), 2.30-2.20 (6H, m, CH_2), 1.03-0.90 (36H, m, CH_2), 0.65-0.61 (30H, m, CH_2 & CH_3); ^{13}C NMR (100 MHz, CDCl_3): δ_{C} 154.7, 149.9, 149.3, 145.5, 140.8, 140.5, 140.1, 139.3, 138.4, 127.6, 126.8, 125.6, 125.2, 123.4, 121.6, 120.6, 120.4, 120.1, 70.7, 76.9, 67.4, 59.2, 56.2, 51.5, 29.9, 24.3, 22.6, 14.2; MALDI-TOF MS: m/z 2152.65 ($[\text{M}-\text{C}_6\text{H}_{13}+\text{Na}]^+$, 100 %), 2131.00 ($[\text{M}-\text{C}_6\text{H}_{13}]^+$, 64 %), 2217.04 ($[\text{M}]^+$, 40 %); Anal. Calcd for $\text{C}_{144}\text{H}_{198}\text{O}_{18}$: C, 78.01; H, 9.00 Found: C, 78.27; H, 8.92.

T1_{polar}I



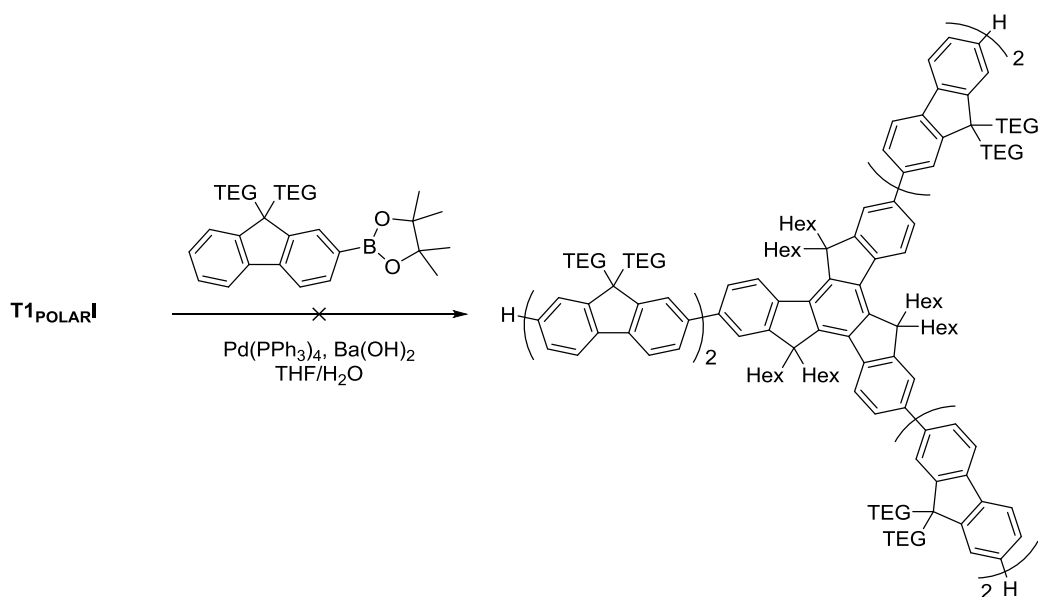
T1_{POLAR}I

T1_{Polar} (475 mg, 0.21 mmol, 1.0 eq) was dissolved in a mixture of acetic acid (4.1 ml), sulfuric acid (0.12 ml) and water (0.81 ml) and heated to 60 °C, then iodine (53 mg, 0.21 mmol, 1.0 eq) and periodic acid (48 mg, 0.21 mmol, 1.0 eq) were added and the reaction mixture was heated at 60 °C

for 18 h. The reaction mixture was cooled to rt and diluted with brine (50 ml) then extracted with EtOAc (8 x 30 ml). The organic layers were washed with water (2 x 50 ml) and brine (50 ml), dried over MgSO₄ and the solvent was evaporated. The product was purified by silica gel chromatography eluting with Et₂O, resulting in a yellow oil which was dissolved in the minimum volume of THF. The solution was added dropwise to hexane, cooled at -40 °C, to afford a white suspension. The suspension was placed in a freezer overnight, then the title compound was isolated as a white powder, with slight impurities from incomplete iodination, by filtration (172 mg, < 30 %).

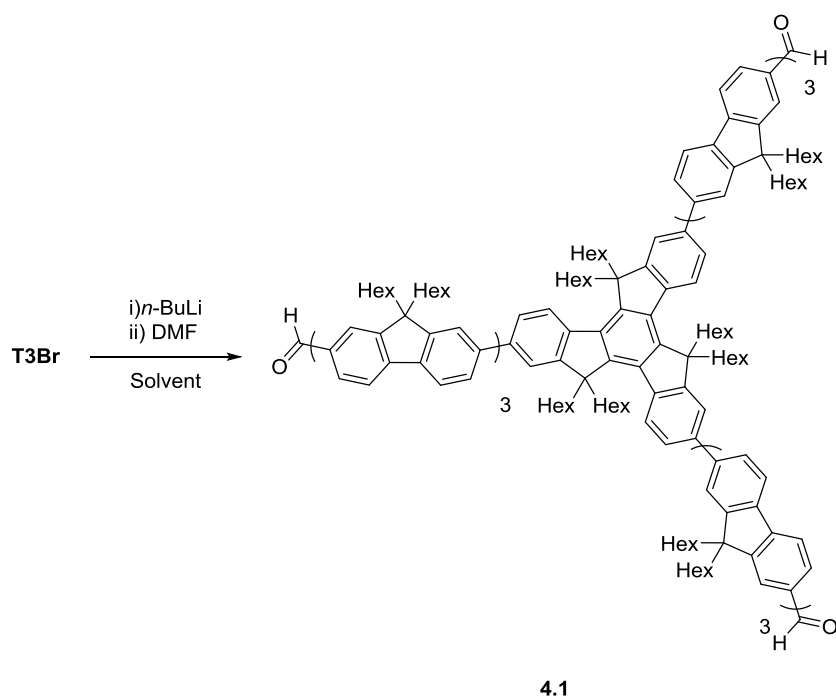
¹H NMR (400 MHz, CDCl₃): δ_H 8.51 (3H, d, *J* 8.8 Hz, CH), 7.82-7.62 (18H, m, CH), 7.72 (3H, d, *J* 6.4 Hz, CH), 7.50 (3H, d, *J* 8.0 Hz, CH), 3.57-3.53 (12H, m, CH₂), 3.51-3.49 (12H, m, CH₂), 3.45 (12H, t, *J* 4.8 Hz, CH₂), 3.34 (18H, s, CH₃), 3.30-3.27 (12H, m, CH₂), 3.11-3.06 (6H, m, CH₂), 2.94-2.84 (12H, m, CH₂), 2.48 (12H, t, *J* 7.8 Hz, CH₂), 2.31-2.21 (6H, m, CH₂), 1.01-0.91 (36H, m, CH₂), 0.68-0.61 (30H, m, CH₂ & CH₃); MALDI-TOF MS: *m/z* 2530.11 ([M-C₆H₁₃+Na]⁺, 100 %), 2593.75 ([M]⁺, 60 %), 2404.15 ([M-C₆H₁₃-I+Na]⁺, 42 %), 2467.78 ([M-I]⁺, 36 %).

Attempted Synthesis of T_{polar2}



2-(9,9-Bis(2-(2-(2-methoxyethoxy)ethoxy)ethyl)-9H-fluoren-2-yl)-4,4,5,5-tetramethyl-1,3,2-dioxaborolane **3.14** (111 mg, 0.19 mmol, 4.77 eq), **T_{1POLAR1}** (100 mg, 0.039 mmol, 1.0 eq), *tetrakis*(triphenylphosphine)palladium(0) (11.6 mg, 0.01 mmol, 0.3 eq) and barium hydroxide octahydrate (88.4 mg, 0.28 mmol, 7.3 eq) were suspended in dry THF (5 ml) under Ar, to which degassed distilled water (0.65 ml) was added. The reaction mixture was then heated at 70 °C for 18 h, then cooled to rt and quenched with a saturated aqueous solution of ammonium chloride (50 ml). The crude product was extracted with CH₂Cl₂ (8 x 30 ml), the organic layers were combined, dried over MgSO₄, the solvent was evaporated and the crude product was placed under vacuum overnight. TLC analysis showed multiple inseparable products were present, which was also observed by ¹H NMR of the crude product, which were attributed to incomplete coupling. Attempted purification by silica gel chromatography did not afford the title compound free from by-products.

Attempted Synthesis of T3-tricarbaldehyde (4.1)



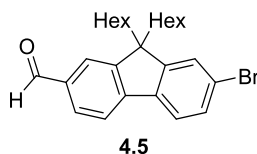
Attempt 1:

n-Butyllithium (2.35 M in hexane, 0.14 ml, 0.33 mmol, 9.0 eq) was added dropwise to a solution of **T3Br** (150 mg, 0.037 mmol, 1.0 eq) in dry Et₂O (15 ml) under Ar at -80 °C, which was then stirred for 30 mins before allowing to warm to rt. The reaction mixture was then cooled back to -80 °C and *N,N*-dimethylformamide (0.035 ml, 0.44 mmol, 12.0 eq) was added dropwise. The reaction mixture was then allowed to warm to rt and stirred under Ar for 18 h. The reaction was quenched by addition of distilled water (50 ml), and the resulting suspension was extracted with Et₂O (4 x 50 ml). The organic layers were washed with water (50 ml), dried over MgSO₄ and the solvent was evaporated. TLC analysis showed multiple inseparable products present and comparison of the aldehyde peak in the ¹H NMR with that of aromatic peaks showed that poor conversion had taken place.

Attempt 2:

n-Butyllithium (2.35 M in hexane, 0.14 ml, 0.33 mmol, 9.0 eq) was added dropwise to a solution of **T3-3Br** (150 mg, 0.037 mmol, 1.0 eq) in dry Et₂O (5 ml) under Ar at -80 °C, which was then stirred for 30 mins before allowing to warm to rt. The reaction mixture was then cooled back to -80 °C and *N,N*-dimethylformamide (0.035 ml, 0.44 mmol, 12.0 eq) was added dropwise. The reaction mixture was then allowed to warm to rt and stirred under Ar for 18 h. The reaction was quenched by addition of distilled water (50 ml), and the resulting suspension was extracted with Et₂O (4 x 50 ml). The organic layers were washed with water (50 ml), dried over MgSO₄ and the solvent was evaporated. TLC analysis showed multiple inseparable products present and comparison of the aldehyde peak in the ¹H NMR with that of aromatic peaks showed that poor conversion had taken place.

7-Bromo-9,9-dihexyl-9H-fluorene-2-carbaldehyde (4.5)



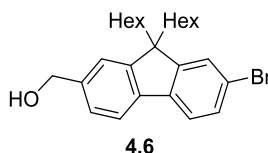
n-Butyllithium (2.27 M in hexane, 4.72 ml, 10.71 mmol, 1.05 eq) was added dropwise to a solution of 2,7-dibromo-9,9-dihexylfluorene **2.5** (5.0 g, 10.2 mmol, 1.0 eq) in dry THF (100 ml) under Ar at -80 °C. After stirring at -80 °C for 1 h, *N,N*-dimethylformamide (1.12 ml, 15.3 mmol, 1.5 eq) was added to the reaction mixture, which was then allowed to warm to rt and stirred for 18 h under Ar. The reaction mixture was quenched with distilled water (100 ml) and the organic phase was separated. The aqueous phase was extracted with Et₂O (2 x 100 ml), and the organic phases were combined and washed with brine (2 x 100 ml), dried over

MgSO₄ and the solvent was evaporated. Purification by silica gel chromatography, eluting with 25 % CH₂Cl₂/hexane, afforded the product as a yellow oil (3.26 g, 72 %). The ¹H NMR spectrum was recorded;

¹H NMR (400 MHz, CDCl₃): δ_H 10.07 (1H, s, CHO), 7.88-7.80 (1H, m, CH), 7.65 (2H, d, *J* 8.8 Hz, CH), 7.53-7.51 (2H, m, CH), 2.03-1.93 (4H, m, CH₂), 1.14-1.00 (12H, m, CH₂), 0.77 (6H, t, *J* 7.2 Hz, CH₃), 0.60-0.54 (4H, m, CH₂).

This was consistent with the previously published data.¹⁹⁷

(7-Bromo-9,9-dihexyl-9H-fluoren-2-yl)methanol (4.6)

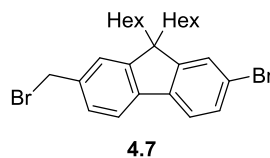


7-Bromo-9,9-dihexyl-9H-fluorene-2-carbaldehyde **4.5** (2.0 g, 4.53 mmol, 1.0 eq) was dissolved in THF (20 ml) and diluted with MeOH (30 ml), to which sodium borohydride (363 mg, 9.06 mmol, 2.0 eq) was added in portions. The reaction mixture was stirred for 18 h at rt, then quenched with water (100 ml) and extracted with Et₂O (4 x 100 ml). The organic layers were washed with water (100 ml), dried over MgSO₄ and the solvent was evaporated to afford the product as a yellow oil (1.9 g, 95 %). The product was used without further purification. The ¹H NMR spectrum was recorded;

¹H NMR (400 MHz, CDCl₃): δ_H 7.65 (1H, d, *J* 8.0 Hz, CH), 7.55 (1H, d, *J* 7.2 Hz, CH), 7.46-7.44 (2H, m, CH), 7.34-7.32 (2H, m, CH), 4.78 (2H, s, CH₂), 2.01-1.92 (4H, m, CH₂), 1.15-1.03 (12H, m, CH₂), 0.78 (6H, t, *J* 7.2 Hz, CH₃), 0.65-0.55 (4H, m, CH₂).

This was consistent with the previously published data.¹⁹⁸

2-Bromo-7-(bromomethyl)-9,9-dihexyl-9H-fluorene (4.7)

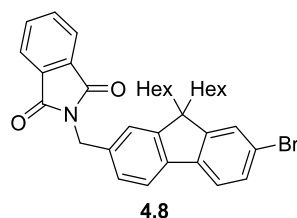


(7-Bromo-9,9-dihexyl-9H-fluoren-2-yl)methanol **4.6** (2.0 g, 4.51 mmol, 1.0 eq) was dissolved in dry THF (60 ml) under Ar and cooled to 0 °C, to which phosphorus tribromide (0.47 ml, 4.96 mmol, 1.1 eq) was added dropwise. The reaction mixture was allowed to warm to rt and stirred for 18 h. The reaction mixture was then quenched with distilled water (100 ml) and extracted with Et₂O (4 x 100 ml). The organic layers were washed with distilled water (100 ml), dried over MgSO₄ and the solvent was evaporated. The crude product was purified by silica gel chromatography eluting with 10 % CH₂Cl₂/hexane to afford the product as a colourless oil (1.20 g, 52 %). The ¹H NMR spectrum was recorded;

¹H NMR (400 MHz, CDCl₃): δ_H 7.62 (1H, d, *J* 7.6 Hz, CH), 7.55 (1H, d, *J* 8.8 Hz, CH), 7.47-7.45 (2H, m, CH), 7.38-7.34 (2H, m, CH), 4.60 (2H, s, CH₂), 2.00-1.88 (4H, m, CH₂), 1.15-1.05 (12H, m, CH₂), 0.78 (6H, t, *J* 7.2 Hz, CH₃), 0.66-0.56 (4H, m, CH₂).

This was consistent with the previously published data.¹⁹⁹

2-((7-Bromo-9,9-dihexyl-9H-fluoren-2-yl)methyl)isoindoline-1,3-dione (4.8)

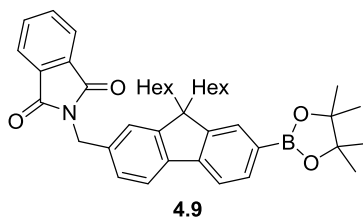


2-Bromo-7-(bromomethyl)-9,9-dihexyl-9H-fluorene **4.7** (1.2 g, 2.37 mmol, 1.0 eq) and potassium phthalimide (0.46 g, 2.49 mmol, 1.05 eq) were

dissolved in dry DMF under Ar, which was heated at 120 °C for 18 h. The reaction mixture was cooled to 0 °C and added slowly to a mixture of ice and water (100 ml). The aqueous suspension was extracted with Et₂O (3 x 50 ml), and the organic layers were washed with distilled water (2 x 50 ml), dried over MgSO₄ and the solvent was evaporated. The product was purified by silica gel chromatography, eluting with 30 % Et₂O/hexane, to afford the title compound as an off-white solid (0.99 g, 73 %).

¹H NMR (400 MHz, CDCl₃): δ_H 7.87-7.84 (2H, m, CH), 7.72-7.70 (2H, m, CH), 7.60 (1H, d, *J* 8.4 Hz, CH), 7.51 (1H, d, *J* 8.0 Hz, CH), 7.44-7.40 (4H, m, CH), 4.91 (2H, s, CH₂), 1.96-1.84 (4H, m, CH₂), 1.10-0.97 (12H, m, CH₂), 0.74 (6H, t, *J* 7.2 Hz, CH₃), 0.63-0.54 (4H, m, CH₂); ¹³C NMR (100 MHz, CDCl₃): δ_C 168.3, 153.6, 151.3, 140.1, 140.0, 136.0, 134.3, 132.5, 130.3, 128.0, 126.5, 124.0, 123.7, 121.4, 120.2, 55.7, 42.3, 40.4, 31.7, 29.9, 24.0, 22.8, 14.3; MALDI-TOF MS: *m/z* 571.02 ([M]⁻, 100 %); HRMS (EI): calcd for C₃₄H₃₈BrNO₂ ([M+H]⁺) 572.2159, found *m/z* 572.2152 ([M+H]⁺).

2-((9,9-Dihexyl-7-(4,4,5,5-tetramethyl-1,3,2-dioxaborolan-2-yl)-9H-fluoren-2-yl)methyl)isoindoline-1,3-dione (4.9)

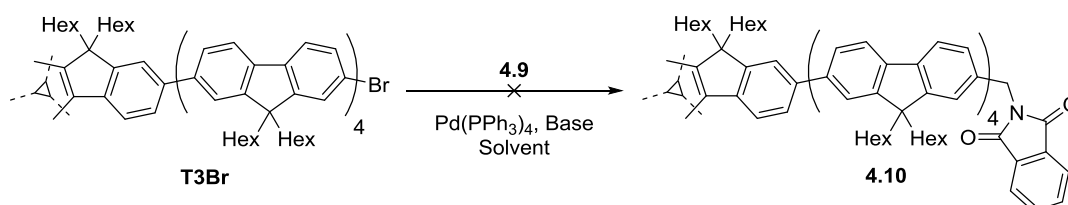


2-((7-Bromo-9,9-dihexyl-9H-fluoren-2-yl)methyl)isoindoline-1,3-dione **4.8** (800 mg, 1.40 mmol, 1.0 eq), bis(pinacolatodiboron) (889 mg, 3.5 mmol, 2.5 eq), tetrakis(triphenylphosphine) palladium(0) (81 mg, 0.07 mmol, 0.05 eq) and potassium acetate (1.37 g, 14.0 mmol, 10 eq) were suspended in dry 1,4-dioxane (15 ml) under Ar and heated at 90 °C for 24 h. After cooling to rt the reaction mixture was added to distilled water (100 ml) and the aqueous suspension was extracted with Et₂O (4 x 100 ml). The

organic fractions were washed with water, dried over MgSO₄ and the solvent was evaporated. The crude product was purified by silica gel chromatography, eluting with 30 % Et₂O/hexane, affording an off-white powder which was precipitated from CH₂Cl₂ by adding MeOH to afford the target compound as a white powder which was isolated by filtration (520 mg, 60 %).

¹H NMR (400 MHz, CDCl₃): δ_H 7.87-7.84 (2H, m, CH), 7.78 (1H, d, *J* 7.2 Hz, CH), 7.73 (1H, s, CH), 7.72-7.67 (2H, m, CH), 7.66 (2H, d, *J* 8.0 Hz CH), 7.44 (1H, s, CH) 7.41 (1H, d, *J* 8.4 Hz) 4.92 (2H, s, CH₂), 1.96 (4H, t, *J* 8.0 Hz, CH₂), 1.38 (12H, s, CH₃), 1.12-0.99 (12H, m, CH₂), 0.72 (6H, t, *J* 7.0 Hz, CH₃), 0.62-0.55 (4H, m, CH₂); ¹³C NMR (100 MHz, CDCl₃): δ_C 152.2, 150.6, 143.9, 141.0, 136.0, 134.3, 134.0, 123.6, 129.2, 127.8, 124.0, 123.6, 120.6, 119.3, 84.0, 55.4, 42.4, 40.3, 31.7, 29.9, 25.3, 24.0, 22.8, 14.3; MALDI-TOF MS: *m/z* 619.28 ([M]⁻, 100 %); HRMS (EI): calcd for C₄₀H₅₀BNO₄.NH₄ ([M+NH₄]⁺) 637.4178, found *m/z* 637.4168 ([M+NH₄]⁺).

Attempted synthesis of T4-trimethylenephthalimide (4.10)



Attempt 1:

2-((9,9-Dihexyl-7-(4,4,5,5-tetramethyl-1,3,2-dioxaborolan-2-yl)-9H-fluoren-2-yl)methyl)isoindoline-1,3-dione **4.x** (100 mg, 0.16 mmol, 4.77 eq), **T3-3Br** (130 mg, 0.032 mmol, 1.0 eq), *tetrakis*(triphenylphosphine)palladium(0) (11.5 mg, 0.01 mmol, 0.3 eq) and barium hydroxide octahydrate (75.7 mg, 0.24 mmol, 7.5 eq) were suspended in THF (5 ml) under Ar, to which degassed distilled water (0.15 ml) was added. The reaction mixture was then heated at 70 °C for

18 h, then cooled to rt and quenched with a saturated aqueous solution of ammonium chloride (50 ml). The crude product was extracted with CH₂Cl₂ (6 x 50 ml), the organic layers were combined, dried over MgSO₄, the solvent was evaporated and the crude product was placed under vacuum overnight. Attempts to purify the product by silica gel chromatography eluting with 20 % CH₂Cl₂/hexane afforded small quantities of starting materials only. TLC and ¹H NMR analysis showed evidence of by-products not consistent with the title product.

Attempt 2:

2-((9,9-Dihexyl-7-(4,4,5,5-tetramethyl-1,3,2-dioxaborolan-2-yl)-9H-fluoren-2-yl)methyl)isoindoline-1,3-dione (100 mg, 0.16 mmol, 4.77 eq), **T3-3Br** (130 mg, 0.032 mmol, 1.0 eq), *tetrakis*(triphenylphosphine)palladium(0) (11.5 mg, 0.01 mmol, 0.3 eq) and caesium fluoride (36 mg, 0.24 mmol, 7.5 eq) were dissolved in THF (5 ml) under Ar. The reaction mixture was then heated at 70 °C for 18 h, then cooled to rt and quenched with a saturated aqueous solution of ammonium chloride (50 ml). The crude product was extracted with CH₂Cl₂ (6 x 50 ml), the organic layers were combined, dried over MgSO₄, the solvent was evaporated and the crude product was placed under vacuum overnight. TLC and ¹H NMR analysis showed evidence of by-products not consistent with the title product.

Attempt 3:

2-((9,9-Dihexyl-7-(4,4,5,5-tetramethyl-1,3,2-dioxaborolan-2-yl)-9H-fluoren-2-yl)methyl)isoindoline-1,3-dione (100 mg, 0.16 mmol, 4.77 eq), **T3-3Br** (130 mg, 0.032 mmol, 1.0 eq), *tetrakis*(triphenylphosphine)palladium(0) (11.5 mg, 0.01 mmol, 0.3 eq) and tribasic potassium phosphate (51 mg, 0.24 mmol, 7.5 eq) were dissolved in THF (5 ml) under Ar. The reaction mixture was then heated at 70 °C for 18 h, then cooled to rt and quenched with a saturated

aqueous solution of ammonium chloride (50 ml). The crude product was extracted with CH₂Cl₂ (6 x 50 ml), the organic layers were combined, dried over MgSO₄, the solvent was evaporated and the crude product was placed under vacuum overnight. TLC and ¹H NMR analysis showed only starting materials present.

Attempt 4:

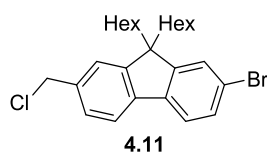
2-((9,9-Dihexyl-7-(4,4,5,5-tetramethyl-1,3,2-dioxaborolan-2-yl)-9H-fluoren-2-yl)methyl)isoindoline-1,3-dione (50 mg, 0.08 mmol, 4.77 eq), **T3-3Br** (65 mg, 0.016 mmol, 1.0 eq), *tetrakis*(triphenylphosphine)palladium(0) (6 mg, 0.005 mmol, 0.3 eq) and caesium fluoride (18 mg, 0.12 mmol, 7.5 eq) were dissolved in THF (5 ml) under Ar. The reaction mixture was then heated in a microwave reactor at 120 °C for 1 h. TLC and ¹H NMR of a sample of the reaction mixture showed only starting material present. The reaction was heated in the microwave at 140 °C, again for 1 h. TLC and ¹H NMR of a sample of the reaction mixture again showed only starting material present. The reaction mixture was heated in a microwave reactor at 160 °C for a further 1 h, after which TLC and ¹H NMR of a sample of the reaction mixture showed evidence of by-products not consistent with the title product.

Attempt 5:

2-((9,9-Dihexyl-7-(4,4,5,5-tetramethyl-1,3,2-dioxaborolan-2-yl)-9H-fluoren-2-yl)methyl)isoindoline-1,3-dione (50 mg, 0.08 mmol, 4.77 eq), **T3-3Br** (65 mg, 0.016 mmol, 1.0 eq), *tetrakis*(triphenylphosphine)palladium(0) (6 mg, 0.005 mmol, 0.3 eq) and tribasic potassium phosphate (25 mg, 0.12 mmol, 7.5 eq) were dissolved in THF (5 ml) under Ar. The reaction mixture was then heated in a microwave reactor at 120 °C for 1 h. TLC and ¹H NMR of a sample of the reaction mixture showed only starting material present. The reaction was

heated in the microwave at 140 °C, again for 1 h. TLC and ^1H NMR of a sample of the reaction mixture again showed only starting material present. The reaction mixture was heated in a microwave reactor at 160 °C for a further 1 h, after which TLC and ^1H NMR of a sample of the reaction mixture showed only starting materials present.

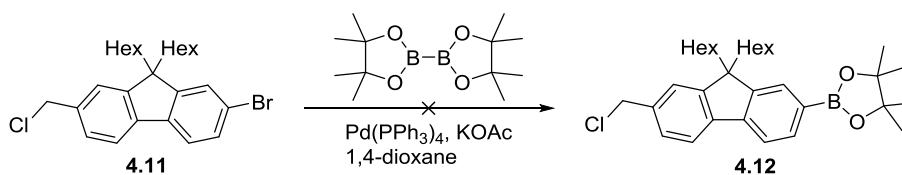
2-Bromo-7-(chloromethyl)-9,9-dihexyl-9H-fluorene (4.11)



Thionyl chloride (0.57 ml, 7.88 mmol, 3.5eq) was added dropwise to a solution of (7-bromo-9,9-dihexyl-9H-fluoren-2-yl)methanol **4.6** (1.0 g, 2.25 mmol, 1.0 eq) and dry DMF (1 drop) in dry CH_2Cl_2 (15 ml) under Ar, and stirred for 18 h. The reaction was quenched with a saturated aqueous solution of NaHCO_3 (50 ml), and the resulting aqueous suspension was extracted with CH_2Cl_2 (3 x 50 ml). The organic layers were washed with distilled water (50 ml), dried over MgSO_4 and the solvent was evaporated. Purification by silica gel chromatography, eluting with 10 % CH_2Cl_2 /hexane afforded the target compound as a yellow oil (850 mg, 82 %).

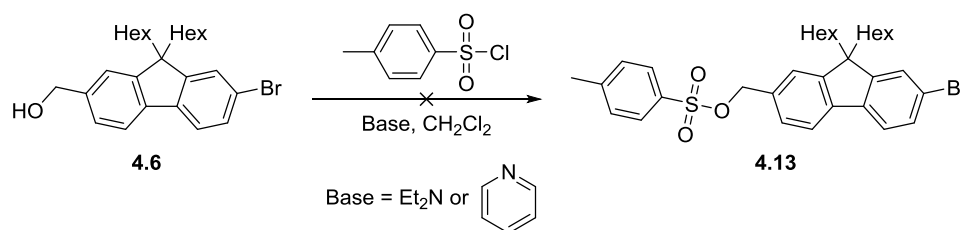
^1H NMR (400 MHz, CDCl_3): δ_{H} 7.65 (1H, d, J 7.6 Hz, CH), 7.56 (1H, d, J 8.8 Hz, CH), 7.48-7.45 (2H, m, CH), 7.38-7.35 (2H, m, CH), 4.69 (2H, s, CH_2), 2.00-1.91 (4H, m, CH_2), 1.16-1.05 (12H, m, CH_2), 0.79 (6H, t, J 7.2 Hz, CH_3), 0.66-0.58 (4H, m, CH_2); ^{13}C NMR (100 MHz, CDCl_3): δ_{C} 153.6, 151.3, 140.7, 139.8, 137.1, 130.4, 128.0, 126.6, 123.5, 121.7, 121.5, 120.3, 55.8, 47.1, 40.5, 31.8, 29.9, 24.0, 22.9, 14.3; MALDI-TOF MS: m/z 425.7 ($[\text{M}-\text{Cl}]^+$, 100 %) 418.45 ($[\text{M}-\text{Br}+\text{K}]^+$, 66 %). HRMS (EI): calcd for $\text{C}_{26}\text{H}_{34}\text{BrCl}$ ($[\text{M}+\text{H}]^+$) 460.1527, found m/z 460.1518 ($[\text{M}+\text{H}]^+$).

Attempted synthesis of (7-bromo-9,9-dihexyl-9H-fluoren-2-yl)methyl 4-methylbenzenesulfonate (4.12)



2-Bromo-7-(chloromethyl)-9,9-dihexyl-9H-fluorene **4.11** (650 mg, 1.41 mmol, 1.0 eq), bis(pinacolatodiboron) (447 mg, 1.76 mmol, 1.25 eq), tetrakis(triphenylphosphine) palladium(0) (81 mg, 0.07 mmol, 0.05 eq) and potassium acetate (702 mg, 7.05 mmol, 5 eq) were suspended in dry 1,4-dioxane (15 ml) under Ar and heated at 90 °C for 24 h. After cooling to rt the reaction mixture was added to distilled water (50 ml) and the aqueous suspension was extracted with Et₂O (3 x 50 ml). The organic fractions were washed with water, dried over MgSO₄ and the solvent was evaporated. TLC and ¹H NMR analysis gave evidence of multiple products present, most of which were inseparable from each other.

Attempted synthesis of (7-bromo-9,9-dihexyl-9H-fluoren-2-yl)methyl 4-methylbenzenesulfonate (4.13)



Attempt 1:

A solution of *p*-toluenesulfonyl chloride (0.65 g, 3.38 mmol, 1.5 eq) in dry CH₂Cl₂ (5 ml) was added dropwise to a solution of triethylamine (0.62 ml, 4.50 mmol, 2.0 eq) and (7-bromo-9,9-dihexyl-9H-fluoren-2-yl)methanol **4.6**

(1.0 g, 2.25 mmol, 1.0 eq) in dry CH_2Cl_2 (5 ml) under Ar, which was cooled in an ice bath. The reaction mixture was allowed to warm to rt and stirred for 18 h. The reaction was quenched by addition of distilled water (50 ml), and extracted with CH_2Cl_2 (3 x 50 ml). The organic layers were dried over MgSO_4 and the solvent was evaporated. TLC analysis in a range of solvents showed that the main spot would not move from the baseline and silica gel chromatography, eluting with 25 % Et_2O /hexane afforded only small amounts of starting material.

Attempt 2

A solution of *p*-toluenesulfonyl chloride (448 mg, 2.35 mmol, 1.1 eq) in dry CH_2Cl_2 (5 ml) was added dropwise to a solution of pyridine (0.35 ml, 4.28 mmol, 2.0 eq) and (7-bromo-9,9-dihexyl-9H-fluoren-2-yl)methanol **4.x** (950 mg, 2.14 mmol, 1.0 eq) in dry CH_2Cl_2 (5 ml) under Ar, which was cooled in an ice bath. The reaction mixture was allowed to warm to rt and stirred for 18 h. The reaction was quenched by addition of distilled water (50 ml), and extracted with CH_2Cl_2 (3 x 50 ml). The organic layers were dried over MgSO_4 and the solvent was evaporated. TLC analysis in a range of solvents showed that the main spot would not move from the baseline and silica gel chromatography, eluting with 25 % Et_2O /hexane afforded only small amounts of starting material.

Tetrakis(triphenylphosphine) palladium(0)

Palladium dichloride (0.50 g, 2.8 mmol, 1.0 eq) and triphenylphosphine (3.70 g, 14.10 mmol, 5.0 eq) were suspended in dry DMSO (40 mL) under Ar, and were heated until complete dissolution occurred, ca. 130 °C. Hydrazine monohydrate (0.55 ml, 11.28 mmol, 4.0 eq) was then added rapidly to afford a dark solution which was allowed to cool to rt, where precipitation was observed. The reaction mixture was filtered under Ar and the precipitate was washed with dry MeOH (2 x 20 mL) and dry Et_2O

(2 × 20 mL) to afford the product as a bright yellow solid (3.03g, 93%).
This compound was routinely used without analysis.

6 References

1. Atkins, P.; De Paula, J. *Physical Chemistry*. 8th ed.; Oxford University Press, Oxford, 2006.
2. Heeger, A. J., *Chem. Soc. Rev.* **2010**, *39*, 2354-2371.
3. Roncali, J., *Chem. Rev.* **1997**, *97*, 173-206.
4. Bredas, J. L., *J. Chem. Phys.* **1985**, *82*, 3808-3811.
5. Hoogmartens, I.; Adriaensens, P.; Vanderzande, D.; Gelan, J.; Quattrocchi, C.; Lazzaroni, R.; Bredas, J. L., *Macromolecules* **1992**, *25*, 7347-7356.
6. Chiang, C. K.; Fincher, C. R., Jr.; Park, Y. W.; Heeger, A. J.; Shirakawa, H.; Louis, E. J.; Gau, S. C.; MacDiarmid, A. G., *Phys. Rev. Lett.* **1977**, *39*, 1098-1101.
7. Bredas, J. L.; Street, G. B., *Acc. Chem. Res.* **1985**, *18*, 309-315.
8. Singh, M.; Haverinen, H. M.; Dhagat, P.; Jabbour, G. E., *Adv. Mater.* **2010**, *22*, n/a-n/a.
9. Toolan, D. T. W.; Howse, J. R., *J. Mater. Chem. C* **2013**, *1*, 603-616.
10. Krebs, F. C., *Org. Electron.* **2009**, *10*, 761-768.
11. Zaumseil, J.; Sirringhaus, H., *Chem. Rev.* **2007**, *107*, 1296-1323.
12. Guo, Y.; Yu, G.; Liu, Y., *Adv. Mater.* **2010**, *22*, 4427-4447.
13. Yoshiro, Y., *Sci. Tech, Adv. Mater.* **2009**, *10*, 024313.
14. Allard, S.; Forster, M.; Souharce, B.; Thiem, H.; Scherf, U., *Angew. Chem. Int. Ed.* **2008**, *47*, 4070-4098.
15. Anthony, J. E.; Brooks, J. S.; Eaton, D. L.; Parkin, S. R., *J. Am. Chem. Soc.* **2001**, *123*, 9482-9483.
16. Ando, S.; Nishida, J.-i.; Fujiwara, E.; Tada, H.; Inoue, Y.; Tokito, S.; Yamashita, Y., *Chem. Mater.* **2005**, *17*, 1261-1264.
17. Afzali, A.; Dimitrakopoulos, C. D.; Breen, T. L., *J. Am. Chem. Soc.* **2002**, *124*, 8812-8813.
18. Anthony, J. E., *Chem. Rev.* **2006**, *106*, 5028-5048.
19. Acton, O.; Dubey, M.; Weidner, T.; O'Malley, K. M.; Kim, T.-W.; Ting, G. G.; Hutchins, D.; Baio, J. E.; Lovejoy, T. C.; Gage, A. H.;

- Castner, D. G.; Ma, H.; Jen, A. K. Y., *Adv. Funct. Mater.* **2011**, *21*, 1476-1488.
20. Sangchul, L.; Seok-Ju, K.; Gunho, J.; Minhyeok, C.; Woojin, P.; Jongwon, Y.; Taehyeon, K.; Yung Ho, K.; Dong-Yu, K.; Byoung Hun, L.; Takhee, L., *Appl. Phys. Lett.* **2011**, *99*, 083306.
21. Hutchins, D. O.; Weidner, T.; Baio, J.; Polishak, B.; Acton, O.; Cernetic, N.; Ma, H.; Jen, A. K. Y., *J. Mater. Chem. C* **2013**, *1*, 101-113.
22. Garnier, F.; Yassar, A.; Hajlaoui, R.; Horowitz, G.; Deloffre, F.; Servet, B.; Ries, S.; Alnot, P., *J. Am. Chem. Soc.* **1993**, *115*, 8716-8721.
23. Sirringhaus, H.; Brown, P. J.; Friend, R. H.; Nielsen, M. M.; Bechgaard, K.; Langeveld-Voss, B. M. W.; Spiering, A. J. H.; Janssen, R. A. J.; Meijer, E. W.; Herwig, P.; de Leeuw, D. M., *Nature* **1999**, *401*, 685-688.
24. Nunzi, J.-M., *C. R. Phys.* **2002**, *3*, 523-542.
25. Cao, Y.; Yu, G.; Zhang, C.; Menon, R.; Heeger, A. J., *Synth. Met.* **1997**, *87*, 171-174.
26. Padinger, F.; Rittberger, R. S.; Sariciftci, N. S., *Adv. Funct. Mater.* **2003**, *13*, 85-88.
27. Tang, C. W., *Appl. Phys. Lett.* **1986**, *48*, 183-185.
28. Yu, G.; Gao, J.; Hummelen, J. C.; Wudl, F.; Heeger, A. J., *Science* **1995**, *270*, 1789-1791.
29. Günes, S.; Neugebauer, H.; Sariciftci, N. S., *Chem. Rev.* **2007**, *107*, 1324-1338.
30. Allemand, P. M.; Koch, A.; Wudl, F.; Rubin, Y.; Diederich, F.; Alvarez, M. M.; Anz, S. J.; Whetten, R. L., *J. Am. Chem. Soc.* **1991**, *113*, 1050-1051.
31. Sariciftci, N. S.; Smilowitz, L.; Heeger, A. J.; Wudl, F., *Science* **1992**, *258*, 1474-1476.

32. Brabec, C. J.; Gowrisanker, S.; Halls, J. J. M.; Laird, D.; Jia, S.; Williams, S. P., *Adv. Mater.* **2010**, *22*, 3839-3856.
33. Wudl, F., *Acc. Chem. Res.* **1992**, *25*, 157-161.
34. Woo, C. H.; Thompson, B. C.; Kim, B. J.; Toney, M. F.; Fréchet, J. M. J., *J. Am. Chem. Soc.* **2008**, *130*, 16324-16329.
35. Ballantyne, A. M.; Chen, L.; Nelson, J.; Bradley, D. D. C.; Astuti, Y.; Maurano, A.; Shuttle, C. G.; Durrant, J. R.; Heeney, M.; Duffy, W.; McCulloch, I., *Adv. Mater.* **2007**, *19*, 4544-4547.
36. Cheng, Y.-J.; Yang, S.-H.; Hsu, C.-S., *Chem. Rev.* **2009**, *109*, 5868-5923.
37. Moulé, A. J.; Meerholz, K., *Adv. Mater.* **2008**, *20*, 240-245.
38. Li, G.; Shrotriya, V.; Huang, J.; Yao, Y.; Moriarty, T.; Emery, K.; Yang, Y., *Nat. Mater.* **2005**, *4*, 864-868.
39. Chih-Wei, C.; Hoichang, Y.; Wei-Jen, H.; Jinsong, H.; Gang, L.; Yang, Y., *Appl. Phys. Lett.* **2008**, *92*, 103306.
40. Ma, W.; Yang, C.; Gong, X.; Lee, K.; Heeger, A. J., *Adv. Funct. Mater.* **2005**, *15*, 1617-1622.
41. Ayzner, A. L.; Wanger, D. D.; Tassone, C. J.; Tolbert, S. H.; Schwartz, B. J., *J. Phys. Chem. C* **2008**, *112*, 18711-18716.
42. Hou, J.; Park, M.-H.; Zhang, S.; Yao, Y.; Chen, L.-M.; Li, J.-H.; Yang, Y., *Macromolecules* **2008**, *41*, 6012-6018.
43. Liang, Y.; Xiao, S.; Feng, D.; Yu, L., *J. Phys. Chem. C* **2008**, *112*, 7866-7871.
44. Schulz, G. L.; Chen, X.; Holdcroft, S., *Appl. Phys. Lett.* **2009**, *94*, 023302.
45. Loser, S.; Bruns, C. J.; Miyauchi, H.; Ortiz, R. P.; Facchetti, A.; Stupp, S. I.; Marks, T. J., *J. Am. Chem. Soc.* **2011**, *133*, 8142-8145.
46. Ku, S.-Y.; Liman, C. D.; Burke, D. J.; Treat, N. D.; Cochran, J. E.; Amir, E.; Perez, L. A.; Chabynyc, M. L.; Hawker, C. J., *Macromolecules* **2011**, *44*, 9533-9538.

47. Owczarczyk, Z. R.; Braunecker, W. A.; Garcia, A.; Larsen, R.; Nardes, A. M.; Kopidakis, N.; Ginley, D. S.; Olson, D. C., *Macromolecules* **2013**, *46*, 1350-1360.
48. Polander, L. E.; Pandey, L.; Barlow, S.; Tiwari, S. P.; Risko, C.; Kippelen, B.; Brédas, J.-L.; Marder, S. R., *J. Phys. Chem. C* **2011**, *115*, 23149-23163.
49. Kraft, A.; Grimsdale, A. C.; Holmes, A. B., *Angew. Chem. Int. Ed.* **1998**, *37*, 402-428.
50. Wayne, C. E.; Wayne, R. P. *Photochemistry*. Oxford University Press, Oxford, 1996.
51. Friend, R. H.; Gymer, R. W.; Holmes, A. B.; Burroughes, J. H.; Marks, R. N.; Taliani, C.; Bradley, D. D. C.; Santos, D. A. D.; Bredas, J. L.; Logdlund, M.; Salaneck, W. R., *Nature* **1999**, *397*, 121-128.
52. Burroughes, J. H.; Bradley, D. D. C.; Brown, A. R.; Marks, R. N.; Mackay, K.; Friend, R. H.; Burns, P. L.; Holmes, A. B., *Nature* **1990**, *347*, 539-541.
53. Kido, J.; Kimura, M.; Nagai, K., *Science* **1995**, *267*, 1332-1334.
54. Yang, J. P.; Jin, Y. D.; Heremans, P. L.; Hoefnagels, R.; Dieltiens, P.; Blockhuys, F.; Geise, H. J.; Van der Auweraer, M.; Borghs, G., *Chem. Phys. Lett.* **2000**, *325*, 251-256.
55. Wang, H.; Xu, Y.; Tsuboi, T.; Xu, H.; Wu, Y.; Zhang, Z.; Miao, Y.; Hao, Y.; Liu, X.; Xu, B.; Huang, W., *Org. Electron.* **2013**, *14*, 827-838.
56. Kulkarni, A. P.; Tonzola, C. J.; Babel, A.; Jenekhe, S. A., *Chem. Mater.* **2004**, *16*, 4556-4573.
57. Tang, C. W.; VanSlyke, S. A., *Appl. Phys. Lett.* **1987**, *51*, 913-915.
58. Chen, C. H.; Shi, J., *Coord. Chem. Rev.* **1998**, *171*, 161-174.
59. Higginson, K. A.; Zhang, X.-M.; Papadimitrakopoulos, F., *Chem. Mater.* **1998**, *10*, 1017-1020.

60. Brown, A. R.; Bradley, D. D. C.; Burroughes, J. H.; Friend, R. H.; Greenham, N. C.; Burn, P. L.; Holmes, A. B.; Kraft, A., *Appl. Phys. Lett.* **1992**, *61*, 2793-2795.
61. Kraft, A., *Chem. Commun.* **1996**, *0*, 77-79.
62. Brien, D. O.; Weaver, M. S.; Lidzey, D. G.; Bradley, D. D. C., *Appl. Phys. Lett.* **1996**, *69*, 881-883.
63. Masamichi, I.; Shizuo, T.; Youichi, S.; Toshiyasu, S.; Yasunori, T., *Appl. Phys. Lett.* **2001**, *79*, 156-158.
64. Ma, W.; Iyer, P. K.; Gong, X.; Liu, B.; Moses, D.; Bazan, G. C.; Heeger, A. J., *Adv. Mater.* **2005**, *17*, 274-277.
65. Shirota, Y., *J. Mater. Chem.* **2000**, *10*, 1-25.
66. Slyke, S. A. V.; Chen, C. H.; Tang, C. W., *Appl. Phys. Lett.* **1996**, *69*, 2160-2162.
67. Brien, D. F. O.; Baldo, M. A.; Thompson, M. E.; Forrest, S. R., *Appl. Phys. Lett.* **1999**, *74*, 442-444.
68. Saragi, T. P. I.; Fuhrmann-Lieker, T.; Salbeck, J., *Adv. Funct. Mater.* **2006**, *16*, 966-974.
69. Salbeck, J.; Yu, N.; Bauer, J.; Weissörtel, F.; Bestgen, H., *Synth. Met.* **1997**, *91*, 209-215.
70. Inada, H.; Shirota, Y., *J. Mater. Chem.* **1993**, *3*, 319-320.
71. Shirota, Y.; Kobata, T.; Noma, N., *Chem. Lett.* **1989**, *18*, 1145-1148.
72. Zou, Y.; Ye, T.; Ma, D.; Qin, J.; Yang, C., *J. Mater. Chem.* **2012**, *22*, 23485-23491.
73. Maiman, T. H., *Nature* **1960**, *187*, 493-494.
74. Samuel, I. D. W.; Turnbull, G. A., *Chem. Rev.* **2007**, *107*, 1272-1295.
75. Avanesjan, O. S.; Benderskii, V. A.; Brikenstein, V. K.; Broude, V. L.; Korshunov, L. I.; Lavrushko, A. G.; Tartakovskii, I. I., *Mol. Cryst. Liq. Cryst.* **1974**, *29*, 165-174.
76. Tessler, N.; Denton, G. J.; Friend, R. H., *Nature* **1996**, *382*, 695-697.

77. Gupta, R.; Stevenson, M.; Dogariu, A.; McGehee, M. D.; Park, J. Y.; Srdanov, V.; Heeger, A. J.; Wang, H., *Appl. Phys. Lett.* **1998**, *73*, 3492-3494.
78. Heliotis, G.; Xia, R.; Bradley, D. D. C.; Turnbull, G. A.; Samuel, I. D. W.; Andrew, P.; Barnes, W. L., *Appl. Phys. Lett.* **2003**, *83*, 2118-2120.
79. Theander, M.; Granlund, T.; Johanson, D. M.; Ruseckas, A.; Sundström, V.; Andersson, M. R.; Inganäs, O., *Adv. Mater.* **2001**, *13*, 323-327.
80. Lawrence, J. R.; Turnbull, G. A.; Samuel, I. D. W.; Richards, G. J.; Burn, P. L., *Opt. Lett.* **2004**, *29*, 869-871.
81. Spehr, T.; Siebert, A.; Fuhrmann-Lieker, T.; Salbeck, J.; Rabe, T.; Riedl, T.; Johannes, H. H.; Kowalsky, W.; Wang, J.; Weimann, T.; Hinze, P., *Appl. Phys. Lett.* **2005**, *87*, 161103.
82. Duarte, F. J.; Liao, L. S.; Vaeth, K. M., *Opt. Lett.* **2005**, *30*, 3072-3074.
83. Haughey, A. M.; Guilhabert, B.; Kanibolotsky, A. L.; Skabara, P. J.; Burley, G. A.; Dawson, M. D.; Laurand, N., *Sens. Actuators, B* **2013**, *185*, 132-139.
84. Lu, M.; Choi, S. S.; Wagner, C. J.; Eden, J. G.; Cunningham, B. T., *Appl. Phys. Lett.* **2008**, *92*, 261502.
85. Lu, M.; Choi, S. S.; Irfan, U.; Cunningham, B. T., *Appl. Phys. Lett.* **2008**, *93*, 111113.
86. Yafang, T.; Chun, G.; Chu, A.; Meng, L.; Goldschlag, W.; Cheng-Sheng, H.; Pokhriyal, A.; George, S.; Cunningham, B. T., *Sensors Journal, IEEE* **2012**, *12*, 1174-1180.
87. Murphy, A. R.; Fréchet, J. M. J., *Chem. Rev.* **2007**, *107*, 1066-1096.
88. Heekyung, K.; Younghun, B.; Rupasree Ragini, D.; Byoung-Ki, C.; Pil-Soo, A., *Appl. Phys. Lett.* **2007**, *91*, 093512.
89. Duan, L.; Hou, L.; Lee, T.-W.; Qiao, J.; Zhang, D.; Dong, G.; Wang, L.; Qiu, Y., *J. Mater. Chem.* **2010**, *20*, 6392-6407.

90. Solomeshch, O.; Medvedev, V.; Mackie, P. R.; Cupertino, D.; Razin, A.; Tessler, N., *Adv. Funct. Mater.* **2006**, *16*, 2095-2102.
91. Muller, C. D.; Falcou, A.; Reckefuss, N.; Rojahn, M.; Wiederhirn, V.; Rudati, P.; Frohne, H.; Nuyken, O.; Becker, H.; Meerholz, K., *Nature* **2003**, *421*, 829-833.
92. Elschner, A.; Heuer, H. W.; Jonas, F.; Kirchmeyer, S.; Wehrmann, R.; Wussow, K., *Adv. Mater.* **2001**, *13*, 1811-1814.
93. Huang, F.; Wu, H.; Cao, Y., *Chem. Soc. Rev.* **2010**, *39*, 2500-2521.
94. Zakhidov, A. A.; Lee, J.-K.; Fong, H. H.; DeFranco, J. A.; Chatzichristidi, M.; Taylor, P. G.; Ober, C. K.; Malliaras, G. G., *Adv. Mater.* **2008**, *20*, 3481-3484.
95. Yu, M. S.; Curran, D. P.; Nagashima, T., *Org. Lett.* **2005**, *7*, 3677-3680.
96. Fong, H. H.; Lee, J.-K.; Lim, Y.-F.; Zakhidov, A. A.; Wong, W. W. H.; Holmes, A. B.; Ober, C. K.; Malliaras, G. G., *Adv. Mater.* **2011**, *23*, 735-739.
97. Grimsdale, A. C.; Müllen, K., *Macromol. Rapid Commun.* **2007**, *28*, 1676-1702.
98. Jiao, H.; Schleyer, P. v. R.; Mo, Y.; McAllister, M. A.; Tidwell, T. T., *J. Am. Chem. Soc.* **1997**, *119*, 7075-7083.
99. Abbel, R.; Schenning, A. P. H. J.; Meijer, E. W., *J. Polym. Sci., Part A: Polym. Chem.* **2009**, *47*, 4215-4233.
100. Ranger, M.; Rondeau, D.; Leclerc, M., *Macromolecules* **1997**, *30*, 7686-7691.
101. Janietz, S.; Bradley, D. D. C.; Grell, M.; Giebeler, C.; Inbasekaran, M.; Woo, E. P., *Appl. Phys. Lett.* **1998**, *73*, 2453-2455.
102. Cho, S. Y.; Grimsdale, A. C.; Jones, D. J.; Watkins, S. E.; Holmes, A. B., *J. Am. Chem. Soc.* **2007**, *129*, 11910-11911.
103. Setayesh, S.; Grimsdale, A. C.; Weil, T.; Enkelmann, V.; Müllen, K.; Meghdadi, F.; List, E. J. W.; Leising, G., *J. Am. Chem. Soc.* **2001**, *123*, 946-953.

104. Pei, Q.; Yang, *J. Am. Chem. Soc.* **1996**, *118*, 7416-7417.
105. Huang, L.; Wu, S.; Qu, Y.; Geng, Y.; Wang, F., *Macromolecules* **2008**, *41*, 8944-8947.
106. Bernius, M. T.; Inbasekaran, M.; O'Brien, J.; Wu, W., *Adv. Mater.* **2000**, *12*, 1737-1750.
107. Yasuda, T.; Fujita, K.; Tsutsui, T.; Geng, Y.; Culligan, S. W.; Chen, S. H., *Chem. Mater.* **2004**, *17*, 264-268.
108. Geng, Y.; Trajkovska, A.; Katsis, D.; Ou, J. J.; Culligan, S. W.; Chen, S. H., *J. Am. Chem. Soc.* **2002**, *124*, 8337-8347.
109. Heeney, M.; Bailey, C.; Giles, M.; Shkunov, M.; Sparrowe, D.; Tierney, S.; Zhang, W.; McCulloch, I., *Macromolecules* **2004**, *37*, 5250-5256.
110. Ohmori, Y.; Uchida, M.; Muro, K.; Yoshino, K., *Jpn. J. Appl. Phys., Part 2* **1991**, *30*, 1941 - 1943.
111. Tang, W.; Ke, L.; Tan, L.; Lin, T.; Kietzke, T.; Chen, Z.-K., *Macromolecules* **2007**, *40*, 6164-6171.
112. Okamoto, T.; Jiang, Y.; Qu, F.; Mayer, A. C.; Parmer, J. E.; McGehee, M. D.; Bao, Z., *Macromolecules* **2008**, *41*, 6977-6980.
113. Herguth, P.; Jiang, X.; Liu, M. S.; Jen, A. K. Y., *Macromolecules* **2002**, *35*, 6094-6100.
114. Campbell, A. J.; Bradley, D., D. C.; Antoniadis, H., *Appl. Phys. Lett.* **2001**, *79*, 2133-2135.
115. Perepichka, D. F.; Rosei, F., *Science* **2009**, *323*, 216-217.
116. Kanibolotsky, A. L.; Perepichka, I. F.; Skabara, P. J., *Chem. Soc. Rev.* **2010**, *39*, 2695-2728.
117. Jia, W.-L.; Song, D.; Wang, S., *J. Org. Chem.* **2002**, *68*, 701-705.
118. Liu, X.-M.; He, C.; Huang, J.; Xu, J., *Chem. Mater.* **2004**, *17*, 434-441.
119. Sakamoto, Y.; Suzuki, T.; Miura, A.; Fujikawa, H.; Tokito, S.; Taga, Y., *J. Am. Chem. Soc.* **2000**, *122*, 1832-1833.
120. Li, Z. H.; Wong, M. S.; Tao, Y., *Tetrahedron* **2005**, *61*, 5277-5285.

121. Bauer, T.; Schlüter, A. D.; Sakamoto, J., *Synlett* **2010**, *2010*, 877-880.
122. Sun, X. B.; Liu, Y. Q.; Chen, S. Y.; Qiu, W. F.; Yu, G.; Ma, Y. Q.; Qi, T.; Zhang, H. J.; Xu, X. J.; Zhu, D. B., *Adv. Funct. Mater.* **2006**, *16*, 917-925.
123. Kim, S.; Kalbitz, H.; Hillmann, S.; Meier, H., *Eur. J. Org. Chem.* **2009**, *2009*, 1976-1983.
124. Cao, X.-Y.; Zhang, W.-B.; Wang, J.-L.; Zhou, X.-H.; Lu, H.; Pei, J., *J. Am. Chem. Soc.* **2003**, *125*, 12430-12431.
125. Simpson, C. D.; Wu, J.; Watson, M. D.; Mullen, K., *J. Mater. Chem.* **2004**, *14*, 494-504.
126. Pei, J.; Wang, J.-L.; Cao, X.-Y.; Zhou, X.-H.; Zhang, W.-B., *J. Am. Chem. Soc.* **2003**, *125*, 9944-9945.
127. Gómez-Lor, B.; Frutos, Óscar d.; Ceballos, Plácido A.; Granier, T.; Echavarren, Antonio M., *Eur. J. Org. Chem.* **2001**, *2001*, 2107-2114.
128. Gómez-Lor, B.; González-Cantalapiedra, E.; Ruiz, M.; de Frutos, Ó.; Cárdenas, D. J.; Santos, A.; Echavarren, A. M., *Chem. Eur. J.* **2004**, *10*, 2601-2608.
129. Zhao, K.-Q.; Chen, C.; Monobe, H.; Hu, P.; Wang, B.-Q.; Shimizu, Y., *Chem. Commun.* **2011**, *47*, 6290-6292.
130. Tseng, K.-P.; Kao, M.-T.; Tsai, T. W. T.; Hsu, C.-H.; Chan, J. C. C.; Shyue, J.-J.; Sun, S.-S.; Wong, K.-T., *Chem. Commun.* **2012**, *48*, 3515-3517.
131. González-Cantalapiedra, E.; Ruiz, M.; Gómez-Lor, B.; Alonso, B.; García-Cuadrado, D.; Cárdenas, D. J.; Echavarren, A. M., *Eur. J. Org. Chem.* **2005**, *2005*, 4127-4140.
132. Kao, M.-T.; Chen, J.-H.; Chu, Y.-Y.; Tseng, K.-P.; Hsu, C.-H.; Wong, K.-T.; Chang, C.-W.; Hsu, C.-P.; Liu, Y.-H., *Org. Lett.* **2011**, *13*, 1714-1717.

133. Sun, Y. M.; Xiao, K.; Liu, Y. Q.; Wang, J. L.; Pei, J.; Yu, G.; Zhu, D. B., *Adv. Funct. Mater.* **2005**, *15*, 818-822.
134. de Frutos, Ó.; Gómez-Lor, B.; Granier, T.; Monge, M. Á.; Gutiérrez-Puebla, E.; Echavarren, A. M., *Angew. Chem. Int. Ed.* **1999**, *38*, 204-207.
135. de Frutos, Ó.; Granier, T.; Gómez-Lor, B.; Jiménez-Barbero, J.; Monge, Á.; Gutiérrez-Puebla, E.; Echavarren, A. M., *Chem. Eur. J.* **2002**, *8*, 2879-2890.
136. Zhang, W.-B.; Jin, W.-H.; Zhou, X.-H.; Pei, J., *Tetrahedron* **2007**, *63*, 2907-2914.
137. Kimura, M.; Kuwano, S.; Sawaki, Y.; Fujikawa, H.; Noda, K.; Taga, Y.; Takagi, K., *J. Mater. Chem.* **2005**, *15*, 2393-2398.
138. Diring, S. p.; Puntoriero, F.; Nastasi, F.; Campagna, S.; Ziesel, R., *J. Am. Chem. Soc.* **2009**, *131*, 6108-6110.
139. Cao, X.-Y.; Zhang, W.; Zi, H.; Pei, J., *Org. Lett.* **2004**, *6*, 4845-4848.
140. Wang, J.-L.; Yan, J.; Tang, Z.-M.; Xiao, Q.; Ma, Y.; Pei, J., *J. Am. Chem. Soc.* **2008**, *130*, 9952-9962.
141. Yang, Z.; Xu, B.; He, J.; Xue, L.; Guo, Q.; Xia, H.; Tian, W., *Org. Electron.* **2009**, *10*, 954-959.
142. Lai, W.-Y.; He, Q.-Y.; Ma, Z.; Huang, W., *Chem. Lett.* **2009**, *38*, 286-287.
143. Casado, J.; Pappenfus, T. M.; Miller, L. L.; Mann, K. R.; Ortí, E.; Viruela, P. M.; Pou-Amérigo, R.; Hernández, V.; López Navarrete, J. T., *J. Am. Chem. Soc.* **2003**, *125*, 2524-2534.
144. Lee, J.-K.; Fong, H. H.; Zakhidov, A. A.; McCluskey, G. E.; Taylor, P. G.; Santiago-Berrios, M. e.; Abruña, H. c. D.; Holmes, A. B.; Malliaras, G. G.; Ober, C. K., *Macromolecules* **2010**, *43*, 1195-1198.
145. Facchetti, A.; Yoon, M.-H.; Stern, C. L.; Hutchison, G. R.; Ratner, M. A.; Marks, T. J., *J. Am. Chem. Soc.* **2004**, *126*, 13480-13501.
146. Endo, T.; Takeoka, Y.; Rikukawa, M.; Sanui, K., *Synth. Met.* **2003**, *135-136*, 333-334.

147. Kanibolotsky, A. L.; Berridge, R.; Skabara, P. J.; Perepichka, I. F.; Bradley, D. D. C.; Koeberg, M., *J. Am. Chem. Soc.* **2004**, *126*, 13695-13702.
148. Tsao, H. N.; Mullen, K., *Chem. Soc. Rev.* **2010**, *39*, 2372-2386.
149. Belton, C. R.; Kanibolotsky, A. L.; Kirkpatrick, J.; Orofino, C.; Elmasly, S. E. T.; Stavrinou, P. N.; Skabara, P. J.; Bradley, D. D. C., *Adv. Funct. Mater.* **2013**, *23*, 2792-2804.
150. Klapars, A.; Buchwald, S. L., *J. Am. Chem. Soc.* **2002**, *124*, 14844-14845.
151. Hamai, S.; Hirayama, F., *J. Phys. Chem.* **1983**, *87*, 83-89.
152. Pommerehne, J.; Vestweber, H.; Guss, W.; Mahrt, R. F.; Bässler, H.; Porsch, M.; Daub, J., *Adv. Mater.* **1995**, *7*, 551-554.
153. Heeney, M.; Zhang, W.; Crouch, D. J.; Chabynyc, M. L.; Gordeyev, S.; Hamilton, R.; Higgins, S. J.; McCulloch, I.; Skabara, P. J.; Sparrowe, D.; Tierney, S., *Chem. Commun.* **2007**, 5061-5063.
154. Becke, A. D., *Physical Review A* **1988**, *38*, 3098-3100.
155. Perdew, J. P., *Physical Review B* **1986**, *33*, 8822-8824.
156. Grimme, S., *J. Comput. Chem.* **2006**, *27*, 1787-1799.
157. Weigend, F.; Ahlrichs, R., *PCCP* **2005**, *7*, 3297-3305.
158. Ahlrichs, R.; Bär, M.; Häser, M.; Horn, H.; Kölmel, C., *Chem. Phys. Lett.* **1989**, *162*, 165-169.
159. Feyereisen, M.; Fitzgerald, G.; Komornicki, A., *Chem. Phys. Lett.* **1993**, *208*, 359-363.
160. Kervella, Y.; Armand, M.; Stéphan, O., *J. Electrochem. Soc.* **2001**, *148*, H155-H160.
161. Xue, C.; Velayudham, S.; Johnson, S.; Saha, R.; Smith, A.; Brewer, W.; Murthy, P.; Bagley, S. T.; Liu, H., *Chem. Eur. J.* **2009**, *15*, 2289-2295.
162. Lu, H.-H.; Ma, Y.-S.; Yang, N.-J.; Lin, G.-H.; Wu, Y.-C.; Chen, S.-A., *J. Am. Chem. Soc.* **2011**, *133*, 9634-9637.

163. Traina, C. A.; Bakus Ii, R. C.; Bazan, G. C., *J. Am. Chem. Soc.* **2011**, *133*, 12600-12607.
164. Sax, S.; Rugen-Penkalla, N.; Neuhold, A.; Schuh, S.; Zojer, E.; List, E. J. W.; Müllen, K., *Adv. Mater.* **2010**, *22*, 2087-2091.
165. Sun, M.-l.; Zhong, C.-m.; Li, F.; Pei, Q.-b., *Chin. J. Polym. Sci.* **2012**, *30*, 503-510.
166. Huang, F.; Niu, Y. H.; Zhang, Y.; Ka, J. W.; Liu, M. S.; Jen, A. K. Y., *Adv. Mater.* **2007**, *19*, 2010-2014.
167. Zhou, G.; Qian, G.; Ma, L.; Cheng, Y.; Xie, Z.; Wang, L.; Jing, X.; Wang, F., *Macromolecules* **2005**, *38*, 5416-5424.
168. Huang, F.; Zhang, Y.; Liu, M. S.; Jen, A. K. Y., *Adv. Funct. Mater.* **2009**, *19*, 2457-2466.
169. Niu, Y.-H.; Ma, H.; Xu, Q.; Jen, A. K. Y., *Appl. Phys. Lett.* **2005**, *86*, 083504.
170. Pu, K.-Y.; Fang, Z.; Liu, B., *Adv. Funct. Mater.* **2008**, *18*, 1321-1328.
171. Oh, S.-H.; Vak, D.; Na, S.-I.; Lee, T.-W.; Kim, D.-Y., *Adv. Mater.* **2008**, *20*, 1624-1629.
172. Oh, S.-H.; Na, S.-I.; Jo, J.; Lim, B.; Vak, D.; Kim, D.-Y., *Adv. Funct. Mater.* **2010**, *20*, 1977-1983.
173. Seo, J. H.; Gutacker, A.; Walker, B.; Cho, S.; Garcia, A.; Yang, R.; Nguyen, T.-Q.; Heeger, A. J.; Bazan, G. C., *J. Am. Chem. Soc.* **2009**, *131*, 18220-18221.
174. Yang, R.; Garcia, A.; Korystov, D.; Mikhailovsky, A.; Bazan, G. C.; Nguyen, T.-Q., *J. Am. Chem. Soc.* **2006**, *128*, 16532-16539.
175. Stay, D.; Lonergan, M. C., *Macromolecules* **2013**, *46*, 4361-4369.
176. Sax, S.; Mauthner, G.; Piok, T.; Pradhan, S.; Scherf, U.; List, E. J. W., *Org. Electron.* **2007**, *8*, 791-795.
177. Kouwer, P. H. J.; Swager, T. M., *J. Am. Chem. Soc.* **2007**, *129*, 14042-14052.

178. Behrendt, J. M.; Wang, Y.; Willcock, H.; Wall, L.; McCairn, M. C.; O'Reilly, R. K.; Turner, M. L., *Polym. Chem.* **2013**, *4*, 1333-1336.
179. Cao, X.-Y.; Zi, H.; Zhang, W.; Lu, H.; Pei, J., *J. Org. Chem.* **2005**, *70*, 3645-3653.
180. Pedersen, C. J., *J. Am. Chem. Soc.* **1967**, *89*, 7017-7036.
181. Gokel, G. W.; Leevy, W. M.; Weber, M. E., *Chem. Rev.* **2004**, *104*, 2723-2750.
182. Park, T.; Haque, S. A.; Potter, R. J.; Holmes, A. B.; Durrant, J. R., *Chem. Commun.* **2003**, *0*, 2878-2879.
183. Suzuki, A., *J. Organomet. Chem.* **1999**, *576*, 147-168.
184. Tsiminis, G.; Wang, Y.; Shaw, P. E.; Kanibolotsky, A. L.; Perepichka, I. F.; Dawson, M. D.; Skabara, P. J.; Turnbull, G. A.; Samuel, I. D. W., *Appl. Phys. Lett.* **2009**, *94*, 243304.
185. Wang, Y.; Tsiminis, G.; Yang, Y.; Ruseckas, A.; Kanibolotsky, A. L.; Perepichka, I. F.; Skabara, P. J.; Turnbull, G. A.; Samuel, I. D. W., *Synth. Met.* **2010**, *160*, 1397-1400.
186. Heliotis, G.; Bradley, D. D. C.; Turnbull, G. A.; Samuel, I. D. W., *Appl. Phys. Lett.* **2002**, *81*, 415-417.
187. González-Bobes, F.; Fu, G. C., *J. Am. Chem. Soc.* **2006**, *128*, 5360-5361.
188. Hartwig, J. F., *Angew. Chem. Int. Ed.* **1998**, *37*, 2046-2067.
189. Fulmer, G. R.; Miller, A. J. M.; Sherden, N. H.; Gottlieb, H. E.; Nudelman, A.; Stoltz, B. M.; Bercaw, J. E.; Goldberg, K. I., *Organometallics* **2010**, *29*, 2176-2179.
190. Tavasli, M.; Bettington, S.; Bryce, M. R.; Attar, H. A. A.; Dias, F. B.; King, S.; Monkman, A. P., *J. Mater. Chem.* **2005**, *15*, 4963-4970.
191. Wu, X.; Chen, T.-A.; Zhu, L.; Rieke, R. D., *Tetrahedron Lett.* **1994**, *35*, 3673-3674.
192. Leroy, J.; Rubinstein, M.; Wakselman, C., *J. Fluorine Chem.* **1985**, *27*, 291-298.

193. Devarie-Baez, N. O.; Shuhler, B. J.; Wang, H.; Xian, M., *Org. Lett.* **2007**, *9*, 4655-4658.
194. Hao, J.; Servello, J.; Sista, P.; Biewer, M. C.; Stefan, M. C., *J. Mater. Chem.* **2011**, *21*, 10623-10628.
195. Wakim, S.; Bouchard, J.; Blouin, N.; Michaud, A.; Leclerc, M., *Org. Lett.* **2004**, *6*, 3413-3416.
196. Li, Q.; Guo, H.; Ma, L.; Wu, W.; Liu, Y.; Zhao, J., *J. Mater. Chem.* **2012**, *22*, 5319-5329.
197. Goudreault, T.; He, Z.; Guo, Y.; Ho, C.-L.; Zhan, H.; Wang, Q.; Ho, K. Y.-F.; Wong, K.-L.; Fortin, D.; Yao, B.; Xie, Z.; Wang, L.; Kwok, W.-M.; Harvey, P. D.; Wong, W.-Y., *Macromolecules* **2010**, *43*, 7936-7949.
198. Chen, C.-H.; Hsu, Y.-C.; Chou, H.-H.; Thomas, K. R. J.; Lin, J. T.; Hsu, C.-P., *Chem. Eur. J.* **2010**, *16*, 3184-3193.
199. Tsai, L.-R.; Chen, Y., *J. Polym. Sci., Part A: Polym. Chem.* **2008**, *46*, 70-84.